ABSTRACT

Title of Dissertation: Cosmological Probes of Physics Beyond the Standard Model

Soubhik Kumar
Doctor of Philosophy, 2020

Dissertation Directed by: Professor Raman Sundrum
Department of Physics

The Standard Model (SM) of particle physics can explain a diverse variety of experimental observations. However, there remain multiple compelling reasons why we believe that the SM is not the final theory of the universe. In this thesis, we first briefly discuss some of those shortcomings of the SM, and then focus on ways in which cosmological observations can be used to probe theories beyond the SM. The primary probe we consider for this purpose is primordial non-Gaussianity (NG) of cosmological perturbations. We show that by precise studies of NG we can probe ultra-high energy gauge theories that might otherwise be energetically completely inaccessible to terrestrial experiments, by focusing first on (i) generic spontaneously broken Higgsed gauge theories, and then on, (ii) higher-dimensional Grand Unified Theories (GUTs). Building upon this, we also discuss a simple curvaton extension of the standard inflationary paradigm where strength of various NG signals can be orders of magnitude larger, and thus be easily accessible via observations in the coming decade.

Cosmological Probes of Physics Beyond the Standard Model

by

Soubhik Kumar

Dissertation submitted to the Faculty of the Graduate School of the
University of Maryland, College Park in partial fulfillment
of the requirements for the degree of
Doctor of Philosophy
2020

Advisory Committee:
Professor Raman Sundrum, Chair/Advisor
Professor Kaustubh Agashe
Professor Zackaria Chacko
Professor Anson Hook
Professor Richard Wentworth

Dedication

To Ma, Baba and Titas.

Acknowledgments

My Ph.D. journey has been far from a solo one, and this is a great opportunity to thank all the friends, family, teachers, and collaborators whose support made this thesis possible.

I would like to start by thanking my advisor, Prof. Raman Sundrum. His deep insights, vast knowledge, and clarity of thought are only some of the many other qualities that have continually inspired me. I especially want to thank him for spending countless hours discussing physics with me, and his willingness to patiently listen to my thoughts, even when they were ill-formed. I also greatly admire his willingness and infectious enthusiasm to jump into less familiar but exciting areas of research and this is something I will take with me as I continue in my research career. Away from academic life, he has been an exemplary human being showing empathy and care for my personal life as well. I hope to have him as a mentor and collaborator in the years to come.

I would also like to thank Prof. Kaustubh Agashe. I have been fortunate enough to regularly interact with him over these years and collaborate on ideas related to extra dimensions. His enthusiasm and thoroughness have been very inspiring as well. I will always appreciate his willingness to answer questions, often in a very careful and detailed manner. At the same time, his probing questions often forced me to think more carefully about seemingly simple ideas, and in the end, enriched my understanding.

Prof. Zackaria Chacko has been very influential right from the start of my

graduate school. His Quantum Field Theory lectures were the ones through which I got introduced to some of the core ideas of the subject, and I deeply appreciate the clarity of his lectures. Although he was not my official advisor, he regularly cared about my progress. His advice on various aspects of academic life, both pertaining to research and more general aspects, has been very valuable.

Prof. Anson Hook has been a continual source of exciting new ideas that made many lunches and other informal discussions so much fun. I had the chance of collaborating with him on axion physics and hope to continue that in the future. His way of simplifying problems and quick back-of-the-envelope estimations have been an inspiration.

I would also like to thank Prof. Paulo Bedaque, Prof. Alessandra Buonanno, Prof. Thomas Cohen, Prof. Zohreh Davoudi, Prof. Bei-Lok Hu, Prof. Ted Jacobson, Prof. Xiangdong Ji and Prof. Rabi Mohapatra for enjoyable discussions during these years. I am also greatly indebted to Prof. Richard Wentworth along with Profs. Sundrum, Agashe, Chacko, and Hook for agreeing to serve on my thesis committee and spending their invaluable time to review this thesis.

I have been very fortunate to have wonderful collaborators from whom I learned a lot. I thank Arushi Bodas, Kaustubh Deshpande, Peizhi Du, Majid Ekhterachian, Zhen Liu, Yuhsin Tsai for their time, discussions and continued collaborations.

Enormous thanks are also due to past and present students and post-docs at Maryland for lots of fun discussions. They include Stefano Antonini, Dawid Brzeminski, Dan Carney, Jack Collins, David Curtin, Saurav Das, Abhish Dev,

Sanket Doshi, Reza Ebadi, Anton de la Fuente, Michael Geller, Sungwoo Hong, Chang Hun Lee, Rashmish Mishra, Arif Mohd, Simon Riquelme, Prashant Saraswat, Antony Speranza, Gustavo Marques Tavares, Christopher Verhaaren, Yixu Wang among others. I would also like to thank all the participants of TASI 2018 for making it so memorable.

I would also like to thank everyone at IISER-Kolkata for all their help during my undergraduate days, and especially, my undegraduate thesis guide Prof. Ritesh K. Singh for his kind mentoring and many insightful physics discussions.

Thanks are also due to Heather Markle and Melanie Knouse for making various administrative processes so smooth at Maryland Center for Fundamental Physics (MCFP).

My friends Sabyasachi, Sarthak, Tamoghna, Subhojit, Subhayan along with others made life at College Park super enjoyable. Special thanks goes to Sabyasachi for tolerating me as a housemate for this entire duration. My old friends Abhijit and Suvadip were, as usual, omnipresent and responsible for lots of fun whenever I had the chance to visit India.

None of this would have been possible without the generous support, love, and care of my parents. They were the first ones to encourage me to pursue physics and no words are enough to express my gratitude towards them. They will always remain two of the strongest pillars of my life.

Titas has been a constant ray of sunshine ever since she came into my life. Although often she was physically a few hundred miles away, her encouragement, love, and care became only closer as the days passed. I owe so much of my well-being

to her.

I would also like to acknowledge the help and financial support from MCFP, National Science Foundation (NSF), University Fellowship, Dean's Fellowship, Monroe H. Martin Graduate Research Fellowship, and Professor C H Woo Award in Nuclear and Particle Theory during my graduate study.

It is impossible to remember everyone and any omission reflects my sloppiness, not your deeply-valued friendship. Thank you!

Table of Contents

List of Tables

List of Figures

Chapter 1: Introduction

1.1 The Standard Model and the need to go beyond it

The Standard Model (SM) of particle physics (for a review see [1]) has been a crowning achievement in all of physics, and perhaps, in all of science. SM can explain a variety of experimental observations spanning across more than 40 orders of magnitude in scales, from hundredths of a femtometer to tens of Gigaparsecs. However, there are compelling reasons to believe that this is not the end of the story.

Various gravitational observations, including the Cosmic Microwave Background (CMB), suggest that around 85 percent of all matter and around 26 percent of all energy density in the present Universe, consists of the so called Dark Matter (DM), see e.g. [2]. The SM does not give us any clue about what constitutes the DM and whether/how it interacts non-gravitationally with the rest of the SM. Similarly mysterious is the nature of Dark Energy which constitutes, an even bigger, 68 percent of the energy density of the present Universe, see e.g. [2]. At the same time, the SM does not explain the origin of the observed tiny neutrino masses [3]. Furthermore, in the Universe around us, we see more matter than antimatter. The SM does not provide a dynamical mechanism by which such a matter-antimatter

asymmetry could have been generated starting from a symmetric initial state.

Apart from these observational puzzles, there remain some striking conceptual puzzles about the SM as well. In 2012, we discovered the Higgs boson at the Large Hadron Collider (LHC) [4, 5]. Through the mechanism of spontaneous symmetry breaking, the Higgs boson plays a crucial role in SM by giving masses to almost all the elementary particles of the SM. Although we have measured the mass of the Higgs boson to be around 125 GeV, we do not know the fundamental origin of the Higgs boson and where its mass and self-coupling comes from. Thus, a theory beyond the SM that *dynamically* explains the mass and the coupling of the Higgs boson is required to truly understand the masses of elementary particles around us. In fact, various beyond the SM theories, where we can *calculate* the Higgs mass from first principles, often predict a Higgs mass hierarchically larger than its observed value of 125 GeV, giving rise to the so called Higgs Hierarchy Problem.

Another conceptual puzzle is related to the strength of observed coupling parameters in the strong, weak and electromagnetic interactions. According to the SM, these three coupling parameters seem to "unify" around a very high energy scale of 10^{13-14} GeV. Just as how Maxwell's theory unified electricity and magnetism, and the electroweak theory unified electromagnetism with weak interactions, SM does give hints that the electroweak and the strong interactions might also get unified into a Grand Unified Theory (GUT) at those very high scales [6]. While we do not know the possibility of such a grand unification for certainty as of now, an answer is very much desirable.

The set of exciting questions above gives us strong reasons to believe that there

is physics beyond the SM (BSM). The important question that we can then ask is: what are the most theoretically plausible BSM scenarios that are also experimentally testable in the near future? The LHC, starting more than a decade ago, has been playing a driving role in this regard since it is probing physics at multi-TeV scales, particularly relevant for the Hierarchy Problem. While it has not given us any strong hints of BSM physics as yet, with its various detector upgrades for its "High-Luminosity" phase [7], it will be able to gather more than 10 times the data it has obtained till now with much more precision. Thus it is very much possible that exciting discoveries could be around the corner. Apart from that, in recent years a variety of novel experimental ideas probing physics at energies much lower than the TeV scale, has emerged, especially in the context of DM, and more generally, Dark Sectors, that very weakly interact with the SM, but can share many of its complexities.

While the progress to understand the physics at TeV scales or below has been phenomenal, we can also wonder about how to experimentally/observationally probe BSM physics operating at scales much bigger than a TeV. There are indeed several well-motivated BSM theories that are believed to operate at such high scales, one example being GUTs mentioned above. Since such GUTs can easily exist at energies 10 orders of magnitude above that accessible by the LHC — the highest energy particle collider build to date — at first sight it seems impossible that we can probe such very high-scale theories.

The primary focus of this thesis is to demonstrate how we can use cosmological observables, especially Primordial Non-Gaussianity (NG), to *directly* probe precisely

those high-scales theories. We will make a crucial use of the fact that currently, our best developed theory, that explains the structure of the Universe at large scales, strongly suggests an early period of Cosmic Inflation during which the early Universe underwent a very energetic expansion. In general, the expansion of the Universe can be characterized by the Hubble parameter, H, as will be described below. Current CMB observations indicate that Hubble scale during inflation could have been as big as 5×10^{13} GeV [8]. With the aid of this large energy scale H, the rapidly expanding Universe could have cosmologically produced ultra-heavy particles with masses $\sim H$. Once produced, these particles, via their decay into inflationary field(s) that determine density perturbations, can leave their distinctive features, such as their masses and spins, in the NG of CMB and in the distribution of galaxies forming Large Scale Structure (LSS) — giving us a unique probe of BSM physics operating at very high scales. While at present, the observed spectrum of primordial perturbations is purely Gaussian, in the coming decade, we will have significant improvement in NG measurements, most notably using LSS (see e.g. [9]), and perhaps also from 21-cm cosmology experiments probing cosmic dark ages, spanning redshifts of $z \sim 30-100$ (see e.g. [10, 11]). Therefore by studying CMB, LSS and 21-cm cosmology, we can do *on-shell spectroscopy* of ultra-heavy particles that are otherwise inaccessible. Before getting on to main part of the thesis, let us briefly review some of the essential concepts.

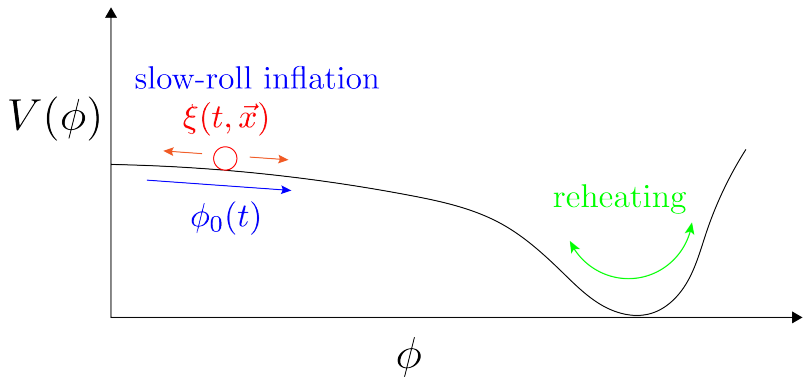

Figure 1.1: The motion of the inflaton field ϕ on an inflationary potential $V(\phi)$. After slowly rolling in the region labelled as "slow-roll inflation", the inflaton field reaches the region labelled as "reheating" where it oscillates around the minima of the potential and decays into SM radiation bath giving rise to a radiation dominated Universe. The classical dynamics of this evolution is controlled by the homogeneous part $\phi_0(t)$ of the inflaton field. The observed density perturbations in the reheated Universe, on the other hand, comes from its quantum mechanical fluctuations, $\xi(t,\vec{x})$.

1.2 Cosmic inflation

The observed Universe is extremely homogeneous and isotropic on large scales. However on smaller scales, we also observe inhomogeneities and anisotropies via CMB and LSS. An era of cosmic inflation in the very early Universe is the leading paradigm to explain both these features of the observed Universe on large and small scales [12, 13, 14]. For a review of cosmic inflation, see [15]. The simplest models of inflation postulate a scalar field, the inflaton ϕ, that slowly rolls along its almost-flat potential during inflation as shown in fig. 1.1. While this slow-roll takes place, the potential energy density of the inflaton remains almost constant at a positive value, and consequently, the Universe undergoes a rapid expansion and thereby dilutes any prior "irregularities" of spacetime. As a result, the large-scale Universe becomes extremely homogeneous and isotropic. As shown in fig. 1.1, in simplest

models of inflation, the inflaton eventually reaches a minima of its potential around which it starts a rapid oscillation. This marks the end of the inflationary phase. During that oscillation, through its coupling to the SM fields, the inflaton can decay into SM radiation bath and the Universe gets reheated into a radiation dominated era.

Importantly, the inflaton ϕ also fluctuates quantum mechanically during this entire period. The quantum fluctuations generated during the inflationary period get stretched out to very large scales. Those fluctuations then source the inhomogeneities and anisotropies in the radiation-dominated reheated Universe. As the Universe keeps evolving, such fluctuations determine the anisotropies in CMB and eventually, via gravitational clustering form the LSS. We now give a very brief overview of inflationary dynamics, which will be treated in more detail in Chapter 2, to make some of the above statements more precise.

The general metric describing a 3+1 dimensional expanding, homogeneous and isotropic spacetime, characterized by coordinates $(t, \vec{x})$, can be written as

$$ds^2 = -dt^2 + a(t)^2 d\vec{x}^2 = a^2(\eta)(-d\eta^2 + d\vec{x}^2). \tag{1.1}$$

Here t and η are cosmic and conformal times respectively, related to each other by $d\eta = \frac{dt}{a(t)}$; and $a(t)$ is the scale factor that governs the spacetime expansion. The Hubble parameter $H(t)$,

$$H(t) = \frac{da(t)/dt}{a(t)}, \tag{1.2}$$

characterizes the rate at which the spacetime expands. The coupled classical dynamics of the inflaton field ϕ and the metric is governed by the equation of motion of the scalar field and the Friedmann equation which are respectively given by,

$$\ddot{\phi} + 3H\dot{\phi} + V^{''}(\phi) = \quad 0, \tag{1.3}$$

$$\frac{1}{2}\dot{\phi}^2 + V(\phi) = \quad 3H^2 M_{\rm pl}^2, \tag{1.4}$$

where an overdot denotes a derivative with respect to t. The Planck scale $M_{\rm pl}$ is determined by the Gravitational constant G_N via $M_{\rm pl}^2 \equiv 1/(8\pi G_N)$. During slow-roll inflation, $\dot{\phi}^2 \ll V(\phi)$, and eq. (1.4) shows that H approximately remains constant. Using eq. (1.2) we then see that the scale factor grows exponentially during inflation, i.e., $a(t) \sim e^{Ht}$. The conformal time η then goes as,

$$\eta \sim -\frac{1}{Ha}. \tag{1.5}$$

The end of inflation corresponds to an exponentially large value of the scale factor compared to its initial value and is reached when $|\eta_e| \ll |\eta|_{\rm CMB}$ where $\eta_{\rm CMB}$ is a time scale when a typical fluctuation mode, later observed via CMB, exit the horizon during inflation. To denote its smallness, we will take the time for the end of inflation, $\eta_e \approx 0$. As far as the classical evolution of the inflaton field is concerned, such a rapid expansion makes the Universe homogeneous and isotropic on largest of scales as mentioned earlier. However, its quantum evolution is more subtle and that gives rise to anisotripies and inhomogenities on smaller scales. We turn to this

next.

An enormous success of the inflationary paradigm is that it predicts some of the crucial qualitative properties of the observed density perturbations in CMB and LSS. To investigate this we need to consider the fluctiations of the inflaton field which can be written as,

$$\phi(t, \vec{x}) = \phi_0(t) + \xi(t, \vec{x}), \tag{1.6}$$

where $\phi_0(t)$ and $\xi(t, \vec{x})$ are the classical slowly rolling inflaton field and its quantum fluctuation respectively. In general, to study the evolution of $\xi(t, \vec{x})$ we need to consider the scalar fluctuations of the metric as well. However, for the purposes in this thesis where we will mostly be interested in calculating heavy-particle induced NG, such metric fluctuations can be ignored in the leading slow-roll approximation, as will be discussed in Chapter 2. Thus the leading dynamics of ξ can be analyzed as if it is a quantum field in the *unbackreacted* spacetime geometry given by eq. (1.1). Then the equation of motion of ξ, after Fourier transforming to 3-momentum space, is given by,

$$\partial_\eta^2 \xi - \frac{2}{\eta} \partial_\eta \xi + k^2 \xi = 0, \tag{1.7}$$

where we have neglected the potential of the inflaton field which is a valid approximation during slow-roll inflation. Here $\vec{k}$ is the "comoving" momentum, conjugate to $\vec{x}$ in eq. (1.1), and it remains constant in time as the spacetime expands. Its

magnitude is denoted by k. Eq. (1.7) can be solved as,

$$\xi(\eta, \vec{k}) \sim \frac{H}{k^{3/2}}(1 \pm ik\eta)e^{\mp ik\eta}. \tag{1.8}$$

Here, the overall normalization factor of $1/k^{3/2}$ has been fixed by noting that as $\eta \to -\infty$, eq. (1.7) can be reduced to an equation of motion of a harmonic oscillator by rewriting it in terms of the variable ξ/η. Thus the solution in eq. (1.8) should also have the usual $1/k^{1/2}$ normalization, as appropriate to a haromic oscillator mode function, in $\eta \to -\infty$ limit.

Importantly, from eq. (1.8), we see as a fluctuating $k-$mode evolves to a super-horizon scale characterized by $|k\eta| \ll 1$, it stops evolving in time and freezes to some constant non-zero value determined by its dynamics during inflation. When such fluctuating modes reenter our horizon during a much later era, they restart their evolution with the *same* conserved value and eventually seed the density perturbations. Although we do not have a complete observational picture of the early Universe between temperatures $\sim$ MeV and inflationary scales, which could be as high as 10^{13-14} GeV, this super-horizon conservation implies that any unknown dynamics at intermediate scales, especially during reheating, can not affect the evolution of large-scale primordial perturbations. This is the primary reason why we can still infer about primordial physics at inflationary scales from observations of CMB and LSS without having a detailed idea of physics at intermediate scales.

The basic idea behind cosmological particle production can also be obtained from eq. (1.7). By rewriting it in terms of the variable, $\varphi = \xi/(\eta H)$, we obtain the

equation of motion of a harmonic oscillator,

$$\varphi'' + \left(k^2 - \frac{2}{\eta^2}\right)\varphi = 0, \tag{1.9}$$

with a time-dependent frequency $\omega^2 = k^2 - \frac{2}{\eta^2}$. The existence of such a time-dependent frequency indicates a time-dependent Hamiltonian, and thus, the vacuum state of the theory at time η_1 is different from that at some other time η_2. Now suppose the Universe started from a vacuum state $|\Omega\rangle$ at very early times [1]. Focusing on the Heisenberg picture for a moment, at some later time η_{late} the Universe will still be in the same state $|\Omega\rangle$. However, due to the time-dependent Hamiltonian, the instantaneous vacuum state at η_{late} would be $|\Omega\rangle_{\text{late}} \neq |\Omega\rangle$. Since in this case ${}_{\text{late}}\langle\Omega|\Omega\rangle \neq 0$, the Universe would contain particles from the perspective of the vacuum at η_{late}. In other words, cosmological particle production due to a time-dependent background has taken place.

While our primary concern in this thesis will be analyzing non-Gaussianity mediated by heavy particles, it is worth quickly sketching how (almost) scale-invariant Gaussian primordial perturbations arise in minimal inflationary models. To do this we can first construct the power spectrum of ξ [2],

$$\langle\xi(\eta_e, \vec{k})\xi(\eta_e, -\vec{k})\rangle. \tag{1.10}$$

[1] The description of how to choose such a "Bunch-Davies" vacuum state is described in chapter 2.

[2] We will, for the moment, neglect the fact that ξ is not a gauge invariant quantity when the metric is treated fully dynamically. A gauge invariant observable characterizing NG will be constructed in Chapter 2.

Here we are evaluating the two point correlation function at some late time $\eta_e \approx 0$ towards the end of inflation, by when all the inflaton fluctuations have exited the horizon and become frozen in time. The spatial momenta of the two fluctuations are given by $\pm\vec{k}$ due to momentum conservation. Further details regarding how exactly such two point (and higher-point, in general) correlation functions are defined and computed will be reviewed in Chapter 2. Now using eq. (1.8), we see that the two-point function goes as,

$$\langle \xi(\eta_e, \vec{k}) \xi(\eta_e, -\vec{k}) \rangle|_{\eta_e \to 0} \sim \frac{H^2}{k^3}. \tag{1.11}$$

By Fourier transforming this momentum-space answer, one sees that the position space two point function is scale-invariant, upto almost constancy of H during inflation. A gauge invariant form of the power spectrum will be given in Chapter 2.

A simple way by which a statistical distribution of a given observable can be non-Gaussian (NG) is by developing a non-zero three-point correlation function which would have otherwise vanished if the distribution were Gaussian. Therefore, one way of characterizing NG is by computing three-point correlation functions of inflaton fluctuations, ξ:

$$\langle \xi(\eta_e, \vec{k}_1) \xi(\eta_e, \vec{k}_2) \xi(\eta_e, \vec{k}_3) \rangle. \tag{1.12}$$

Here the spatial momenta of the fluctuations are denoted by $\vec{k}_i$ for $i = 1, 2, 3$. In min-

imal inflationary models, the interactions of the inflaton field is very small, and hence any odd-point correlation function of ξ, in particular, $\langle \xi(\eta_e, \vec{k}_1)\xi(\eta_e, \vec{k}_2)\xi(\eta_e, \vec{k}_3)\rangle$ is small as well [16]. Furthermore, all even-point correlation functions are mostly determined in terms of the two-point function. Thus the minimal inflationary models predict an approximately Gaussian spectrum of primordial perturbations.

Having obtained some insight about the dynamics of primordial perturbations, let us now discuss the primary cosmological observable of interest that we will repeatedly use in this thesis, namely primordial non-Gaussianity. While four and higher-point correlation functions are also sensitive probes of non-Gaussianity, in this thesis, we will focus on the three-point function as a concrete example.

1.3 Primordial non-Gaussianity

Inflaton self-interactions, and more excitingly, interactions of the inflaton with other fields that could be present during inflation, can easily make the three-point function large so that it can be observable in CMB and LSS. This is especially important from a BSM point of view once we remember that the Hubble scale during inflation can be as big as 5×10^{13} GeV [8]. Thus by studying such three-point functions, and more generally NG, one can investigate particle physics operating at energy scales as much as 10 orders of magnitude larger than what can be done at the LHC for example. What makes this even more striking is the observation that if there were particles having masses $\sim H$ interacting with the inflaton, they can get produced during inflation and leave their *on-shell* mass and spin information in such

NG correlators [17, 18, 19, 20, 21]. It is this fact that the study of NG using CMB, LSS and 21-cm cosmology can let us do *spectroscopy* of ultra-high energy particle physics, which are otherwise completely inaccessible, that will be the recurring theme of this thesis. Since this process of extraction such on-shell particle properties using cosmology is similar in spirit to what is done at terrestrial colliders, such as the LHC, the above-mentioned paradigm has been dubbed as Cosmological Collider Physics [21].

Before giving an outline of the thesis, we pause to comment on two important observational aspects. Through out our discussion of NG, we will ignore the so-called "secondary" NG that the density perturbations develop as they grow under the effect of gravitational clustering, for a review see e.g. [22]. While such secondaries are extremely important from an observational point of view, in this thesis, we will assume that they can be modeled sufficiently well so that the primordial, inflationary contributions can be reliably extracted from the data and our conclusions can then be immediately applied. The second issue has to do with the precision by which NG can be measured. Such a precision, quite generally, improves as $\frac{1}{\sqrt{N}}$ as the number of independent measurements of the observable, N, is increased. Therefore, the best sensitivity to primordial NG will come from cosmic-variance limited 21-cm cosmology observations probing cosmic dark ages, spanning redshifts $z \sim 30 - 100$, since those can probe orders of magnitude more number of cosmological modes compared to CMB and LSS [23]. While for some of the conclusions obtained in this thesis, CMB and especially, LSS will be sufficient, for several others, 21-cm observatons will be of critical importance. We will give a rough estimate of the

sensitivity of such 21-cm observations in chapter 2.

1.4 Outline of the thesis

Having described the basic idea behind the inflationary paradigm and primordial NG from in a broad-brush manner, we will review it more rigorously in Chapter 2 which is based upon [24]. Following that, we extend the Cosmological Collider Physics program to investigate the observability of generic spontaneously broken Higgsed gauge theories for the first time in literature. By carefully imposing the constraints of gauge symmetry and its (partial) Higgsing, we identify that two different types of Higgs mechanisms can lead to observable NG signals. In the first category, the Higgs scale is constant before and after inflation, and one can observe NG effects of particles much heavier than those accsessible by laboratory experiments, as mentioned above. In the second category, which we dub as the "Heavy-lifting" scenario, the Higgs scale is determined by the curvature of spacetime and is time-dependent. Correspondingly we show how particles which are light in the current era, can nonetheless get heavy-lifted to inflationary energy scale and give non-trivial NG signals. Utilizing this feature, we show how NG can be used as a novel test of the severity of the Higgs Hierarchy Problem mentioned earlier.

We then move to Chapter 3, based upon [25], where we evaluate under what conditions GUTs can lead to observable NG signatures, demonstrating a unique *direct* probe of GUTs known in the literature. Since simplest GUTs predict a decay rate of the proton that is phenomenologically unacceceptable, we focus on higher-

dimensional theories of grand unification which can easily suppress such proton decay processes. We describe how the higher-dimensional geometry can be stabilized close to the onset of a "black-brane" horizon by doing a novel near-horizon stabilization analysis. In such a near-horizon configuration, the higher-dimensional GUT can give rise to NG signatures both from Kaluza-Klein modes of GUT gauge bosons and the graviton — a joint observation of which would not only give us strong hints of grand unification, but also of the presence of extra dimensions at high energy scales.

In many scenarios under the Cosmological Collider Physics program, the NG mediated by particles charged under some gauge group are often unobservably small. In Chapter 4, based upon [26], we show that a simple alternative to the standard inflationary paradigm involving a curvaton field can adress this issue, and NG signal from charged particles can be orders of magnitude bigger than in the standard scenario. As concrete examples, we calculate the leading loop-level NG contributions mediated by Higgs-like scalars and fermions, and show how this curvaton model brings an even broader of set BSM scenarios within the reach of the Cosmological Collider Physics program.

Hubble Units. In the rest of the thesis, the Hubble scale during inflation will be denoted by H. To reduce clutter, from now on we will set $H \equiv 1$ in most of the numbered equations, with a few exceptions where we explicitly write it for the sake of clarity. Factors of H can be restored via dimensional analysis. However, we will refer explicitly to H in the text throughout, again for ease of reading, and in the

unnumbered equations within the text.

Chapter 2: Heavy-Lifting of Gauge Theories By Cosmic Inflation

2.1 Introduction

Cosmic Inflation, originally invoked to help explain the homogeneity and flatness of the universe on large scales, provides an attractive framework for understanding inhomogeneities on smaller scales, such as the spectrum of temperature fluctuations in the CMB radiation. These fluctuations are consistent with an almost scale-invariant, adiabatic and Gaussian spectrum of primordial curvature perturbations $\mathcal{R}$ [8], a gauge-invariant variable characterizing the inflaton and metric fluctuations that will be defined below. The approximate scale invariance of these fluctuations can be naturally modeled as quantum oscillations of the inflaton field in a quasi-de Sitter (dS) spacetime. The adiabaticity property implies that among the fields driving inflation, there is a single "clock", the inflaton, which governs the duration of inflation and the subsequent reheating process. Finally, Gaussianity of the present data [27] reflects very weak couplings among inflationary and gravitational fields. While these features point to successes of the inflationary paradigm, few details of the fundamental physics at play during inflation have emerged. Observing small NG of the fluctuations could change this situation radically, giving critical insights not only into the inflationary dynamics itself but also into the particle physics

structure of that era.

Interactions of the inflaton with itself or other fields during or immediately after inflation can lead to a non-Gaussian spectrum of $\mathcal{R}$. However, NG can also be developed after fluctuation modes re-enter the horizon at the end of inflation. This can happen for various reasons, including, nonlinear growth of perturbations under gravity during structure formation (see [22, 28] for reviews in the context of CMB and LSS). Therefore it is crucial to understand and distinguish this latter type of NG which can "contaminate" the invaluable primordial NG. In this thesis we will assume that this separation can be achieved in future experiments involving LSS surveys [9] and 21-cm cosmology [10, 23], to reach close to a cosmic-variance-only limited precision. With this qualifier, a future measurement of NG can reveal important clues as to the underlying inflationary dynamics. For example, for the case single-field slow-roll inflation, there is a minimal amount of NG mediated by gravitational interactions [29, 30], while lying several orders of magnitude below the current limit on NG, can be achievable in the future.

There also exist a variety of models which predict a larger than minimal NG (see [31, 32] for reviews and references to original papers). A common feature among some of these models is the presence of additional fields beyond the inflaton itself. Such non-minimal structure can be motivated by the need to capture inflationary dynamics within a fully theoretically controlled and natural framework. If those additional fields are light with mass, $m \ll H$ (where H denotes the Hubble scale during inflation), they can oscillate and co-evolve along with the inflaton during inflation. These fields can generate significant NG after inflation, with a functional

form approximated by the "local" shape [33, 34, 35].

On the other hand, the additional fields can be heavy with masses $m \gtrsim H$. Such fields can be part of "quasi-single-field inflation" which was introduced in [17] and further developed in [18, 19, 20, 21, 36, 37, 38]. In the presence of these massive fields, the three-point correlation function of the curvature perturbation $\mathcal{R}$ has a distinctive *non-analytic* dependence on momenta,

$$\langle \mathcal{R}(\vec{k}_1)\mathcal{R}(\vec{k}_2)\mathcal{R}(\vec{k}_3)\rangle \propto \frac{1}{k_3^3}\frac{1}{k_1^3}\left(\frac{k_3}{k_1}\right)^{\Delta(m)} + \cdots, \text{ for } k_3 \ll k_1, \tag{2.1}$$

in the "squeezed" limit where one of 3-momenta becomes smaller than the other two. In the above,

$$\Delta(m) = \frac{3}{2} + i\sqrt{\frac{m^2}{H^2} - \frac{9}{4}}, \tag{2.2}$$

where m is the mass of the new particle. The non-analyticity reflects the fact that the massive particles are not merely virtual within these correlators, but rather are physically present "on-shell" due to cosmological particle production, driven by the inflationary background time-dependence. Such production is naturally suppressed for $m \gg H$, which is reflected by a "Boltzmann-like suppression" factor in the proportionality constant in (2.1). The only effect of $m \gg H$ particles is then virtual-mediation of interactions among the remaining light fields [39]. At the other extreme, for $m \ll H$ the distinctive non-analyticity is lost. Hence, we are led to a window of opportunity around H, where the non-analytic dependence of the three-point function is both non-trivial and observable, and can be used to do spectroscopy

of masses. Furthermore, if a massive particle has nontrivial spin [21, 40], there will be an angle-dependent prefactor in (2.1), which can enable us to determine the spin as well [41]. These observations point to a program of "Cosmological Collider Physics" [21] which can probe particle physics operating at very high scales as discussed in chapter 1. The sensitivity of the measurements is ultimately constrained by cosmic variance, very roughly in the ball park of

$$\frac{\langle \mathcal{R}\mathcal{R}\mathcal{R}\rangle}{\langle \mathcal{R}\mathcal{R}\rangle^{\frac{3}{2}}} \sim \frac{1}{\sqrt{N_{\text{21-cm}}}} \sim 10^{-8}, \tag{2.3}$$

where we have assumed the number of modes accessible by a cosmic variance limited 21-cm experiment is $N_{\text{21-cm}} \sim 10^{16}$ [23]. Achieving such a precision is very important for realizing the full potential of the program.

In this chapter, we couple gauge-Higgs theories with $m \sim H$ to inflationary dynamics and ask to what extent the associated states can be seen via the cosmological collider physics approach. The contributions of massive particle to the three point function $\langle \mathcal{R}(\vec{k}_1)\mathcal{R}(\vec{k}_2)\mathcal{R}(\vec{k}_3)\rangle$ can be represented via "in-in" diagrams in (quasi-)dS space such as in Fig. 2.1. From Fig. 2.1 (a), we see that since the inflaton has to

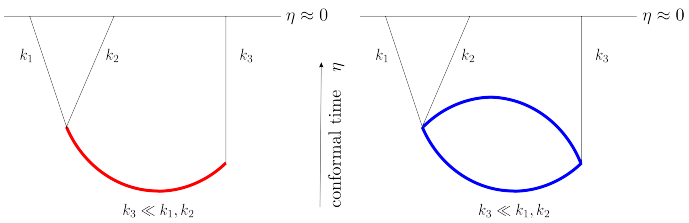

Figure 2.1: From left to right: (a) Tree level exchange of neutral massive scalar (in red) between inflatons (in black); (b) Loop level exchange of charged massive fields (in blue) between inflatons (in black). The external lines are taken to end at the end of inflation, conformal time, $\eta \approx 0$.

have the internal quantum numbers of the vacuum, [1] the same has to be true for the massive particles. The particles must therefore be gauge singlets. Keeping this fact in mind, let us analyze the two scenarios that can arise during inflation.

The gauge theory may be unbroken during inflation. Gauge singlet 1-particle states then can mediate NG via tree diagrams as shown in Fig. 2.1 (a). This is also the case that has been analyzed extensively in the literature. On the other hand, gauge charged states can contribute via loops, as shown in Fig. 2.1 (b), but are expected to be small. Alternatively, the gauge theory may be (partially) Higgsed during inflation. Then the massive particle in Fig. 2.1 (a) need only be a gauge singlet of a residual gauge symmetry, but may be charged under the full gauge group. This possibility, which has received less attention in the literature (however, see [43, 44] for a related scenario), will be our primary focus. There are two ways in which such a Higgsing can happen, as we discuss now.

First, such a breaking can be due to a fixed tachyonic mass term for the Higgs $\mathcal{H}$, $\mu_{\mathcal{H}}^2 \mathcal{H}^\dagger \mathcal{H}$ with $\mu_{\mathcal{H}} \sim H$. In this case, the gauge-Higgs theory remains Higgsed after inflation ends and its massive states can annihilate away as universe cools giving rise to standard cosmology. Grand unified theories are examples of gauge extensions of Standard Model (SM) containing very massive new particles and which are strongly motivated by existing lower energy experimental data. For example, non-supersymmetric unification is suggested by the near renormalization-group convergence of SM gauge couplings in the $10^{13} - 10^{14}$ GeV range, right in the

[1] In the context of Higgs inflation [42] however, inflaton is the physical charge neutral Higgs field.

high-scale inflation window [45] of opportunity for cosmological collider physics![2] This will be the subject of chapter 3. NG detection of some subset of these massive states could give invaluable clues to the structure and reality of our most ambitious theories. It is also possible that H-mass states revealed in NG are not connected to specific preconceived theories, but even this might provide us with valuable clues about the far UV.

Another very interesting and testable option is a tachyonic "mass" term of the form $\mathcal{L} \supset cR\mathcal{H}^\dagger\mathcal{H}$, where R is the Ricci scalar and $c > 0$ parametrizes the non-minimal coupling of Higgs to gravity. The effects of non-tachyonic terms for this form with $c < 0$ have been considered before (see e.g. [48, 49]). Note, spontaneous breaking triggered by $c > 0$ is completely negligible at low temperatures, say below 100 GeV. Whereas in the scenario above we needed the gauge-Higgs theory to fortuitously have states with $m \sim H$, here we naturally get the Higgs particle at H for $c \sim \mathcal{O}(1)$. Furthermore, if (gauge coupling $\times$ Higgs VEV) $\sim H$, we also get massive gauge bosons at H. In this way such a nonminimal coupling can lift up a gauge theory with a relatively low Higgs scale today, which we can access via collider or other probes, to the window of opportunity of cosmological collider physics during the inflationary era. We will call this the "heavy-lifting" mechanism. To make this idea concrete, we consider the example of heavy lifting the SM.

During the inflationary era the SM weak scale v can be lifted to be very high, but we do not know where precisely because of the unknown parameter c (even if

[2] Unification at such scales is disfavored in minimal unification schemes by proton decay constraints, but viable in non-minimal schemes such as that of Refs. [46, 47].

we knew H). However, this uncertainty drops out in mass ratios,

$$\begin{aligned}\frac{m_h}{m_Z} &= \frac{2\sqrt{2\lambda_h}}{\sqrt{g^2+g'^2}} \\ \frac{m_h}{m_W} &= \frac{2\sqrt{2\lambda_h}}{g} \\ \frac{m_h}{m_t} &= \frac{2\sqrt{\lambda_h}}{y_t}\end{aligned} \tag{2.4}$$

where, λ_h, g', g, y_t are Higgs quartic, $U(1)_Y$, $SU(2)_L$ and top Yukawa couplings of SM. While the top t and W boson can only appear in loops Fig. 2.1 (b), the physical Higgs h and the Z can appear in Fig. 2.1 (a) giving us one prediction in this case. However, an important subtlety of the couplings on the R.H.S. of the ratios above is that they are not those measured at the weak scale but rather are the results of running to $\sim H$. But it is well known that the SM effective potential develops an instability around $10^{10} - 10^{12}$GeV because of the Higgs quartic coupling running negative (see [50] and references therein for older works). Since the inflationary H can be higher, the Higgs field can sample values in its potential beyond the instability scale. Whether this is potentially dangerous for our universe has been considered before (see e.g. [48, 49, 50, 51, 52, 53, 54]). But it is possible that this instability is straightforwardly cured once dark matter (DM) is coupled to the SM. A simple example [55, 56, 57, 58] would be if future experiments determine that DM is a SM gauge singlet scalar S stabilized by a Z_2 symmetry, $S \to -S$. Then the most general renormalizable new couplings are given by the Higgs portal coupling and scalar self-interaction,

$$\frac{k}{2}S^2|\mathcal{H}|^2 + \frac{\lambda_S}{24}S^4. \tag{2.5}$$

Since the coupling k contributes positively to the Higgs quartic running, for appropriate choice of k (and less sensitively to λ_S) the Higgs quartic never becomes negative. This solves the vacuum instability problem of the SM and we can reliably trust our effective theory up to even high scale inflation energies.

Imagine a discovery of such a DM (S) is made in the coming years, along with a measurement of k and its mass m_S (and possibly a measurement of or at least a bound on, λ_S) . Also, imagine a measurement of H is obtained via detecting the primordial tensor power spectrum. Then we can use the Renormalization Group (RG) to run all the measured couplings to the high scale H. These would then allow us to compute the run-up couplings needed to make a cosmological verification of (2.4). Such a verification of this Next-to-Minimal SM (NMSM) would give strong evidence that no new physics intervenes between TeV and H. Since this NMSM clearly suffers from a hierarchy problem (worse than the SM), the precision NG measurements would therefore provide us with a test of "*un-naturalness*" in Nature, perhaps explained by the anthropic principle [59, 60]. Whether the naturalness principle is undercut by the anthropic principle or by other considerations is one of the most burning questions in fundamental physics.

Of course, the heavy-lifting mechanism may also apply to non-SM "dark" gauge-Higgs sectors, which we may uncover by lower energy experiments and observations in the coming years, or to gauge-Higgs extensions of the SM which may emerge from collider experiments. In this way, there may be more than one mass ratio of spin-0 and spin-1 particles that might appear in NG which we will be able to predict. As we will show, such new gauge structure may be more easily detectable in

NG than the (NM)SM, depending on details of its couplings. It is important to note that different gauge theory sectors in the current era, with perhaps very different Higgsing scales, can be heavy-lifted to the same rough scale H during inflation, with their contributions to NG being superposed.

The heavy-lifting mechanism may not be confined to unnatural gauge-Higgs theories. For example, if low energy supersymmetry (SUSY) plays a role in stabilizing the electro-weak hierarchy, a suitable structure of SUSY breaking may permit the heavy-lifting mechanism to work. Heavy-lifting can then provide us with a new test of naturalness! Possibly non-tachyonic squarks and sleptons in the current era were tachyonic during inflation, higgsing QCD or electro-magnetism back then. We leave a study of the requisite SUSY-breaking structure for future work. Cosmological collider physics studies incorporating SUSY but restricted to gauge singlet fields have appeared in [19, 61].

NG potentially provide us with the boon of an ultra-high energy "cosmological collider", but cosmic variance implies it operates at frustratingly low "luminosity"! We will see that this constrains how much we can hope to measure, even under the best experimental/observational circumstances. For example, a pair of spin-1 particles appearing in the NG will be more difficult to decipher than only one of them appearing, due to the more complicated functional form of the pair that must be captured in the limited squeezed regime under cosmic variance. And yet, we would ideally like to see a rich spectrum of particles at H. The key to visibility of new physics under these harsh conditions is then determined by the strength of couplings to the inflaton. This is the central technical consideration of this thesis, taking

into account the significant suppressions imposed by (spontaneously broken) gauge invariance. We study this within two effective field theory frameworks, one more conservative but less optimistic than the other. Single-field slow-roll inflation gives the most explicit known construction of inflationary dynamics, but we will see that minimal models under effective field theory control give relatively weak NG signals, although still potentially observable. We also consider the more agnostic approach in which the dynamics of inflation itself is parametrized as a given background process [62], but in which the interactions of the gauge-Higgs sector and inflaton fluctuations are explicitly described. This will allow for larger NG signals, capable in principle of allowing even multiple particles to be discerned.

This chapter is organized as follows. We start in Section 2.2 by reviewing the in-in formalism and its use in calculation of the relevant non-Gaussian observables. We also include a discussion of different gauges and conventions used for characterizing NG. Then in Section 2.3 we review the significance of the squeezed limit of cosmological correlators, both in the absence and presence of new fields beyond the inflaton. In particular, we review the derivation of (2.1). In Section 2.4 we discuss some general aspects of gauge-Higgs theory dynamics during inflation and elaborate upon the two alternatives for Higgs mechanism discussed above. We then specialize in Section 2.5 to slow-roll inflation where we study the couplings of Higgs-type and Z-type bosons to the inflaton in an effective field theory (EFT) framework. In section 2.6 we describe parallel considerations in the more agnostic EFT approach mentioned above. The two levels of effective descriptions are then used in Sections 2.7 and 2.8 (supplemented by technical Appendices A.1-A.4) to derive some of the

detailed forms of NG due to Higgs-type and Z-type exchanges respectively. We conclude in Section 2.9.

2.2 Preliminaries

2.2.1 The in-in Formalism for Cosmological Correlators

Primordial NG induced by inflaton fluctuations are calculated as "in-in" expectation values [63] of certain gauge-invariant (products of) operators at a fixed instant of time towards the end of inflation, denoted by t_f. The expectation needs a specification of the quantum state. The notion of "vacuum" is ill-defined because spacetime expansion gives a time-dependent Hamiltonian, $\mathsf{H}(t)$. However, for very short distance modes/physics at some very early time t_i, the expansion is negligible and we can consider the state to be the Minkowski vacuum, $|\Omega\rangle$. As such modes redshift to larger wavelengths at t_f, the state at t_f can then be taken to be given by $U(t_f, t_i)|\Omega\rangle$, where

$$U(t_f, t_i) = Te^{-i\int_{t_i}^{t_f} dt \mathsf{H}(t)}. \tag{2.6}$$

In order to capture arbitrarily large wavelengths at t_f in this manner, we formally take $t_i \to -\infty$. (For free fields, the state defined in this way at finite times, is the Bunch-Davies "vacuum".) Then the desired late-time expectation value of a gauge invariant operator Q is given in the Schroedinger picture by, $\langle\Omega|U(t_f, t_i = -\infty)^\dagger Q U(t_f, t_i = -\infty)|\Omega\rangle$.

Now the calculation of the expectation value becomes standard. First, we

go over to the interaction picture, and second we employ the standard trick of continuing the early evolution slightly into complex time to project the free vacuum $|0\rangle$ onto the interacting vacuum $|\Omega\rangle$. Thus we arrive at the in-in master formula,

$$\langle\Omega|U(t_f,t_i)^\dagger Q U(t_f,t_i)|\Omega\rangle \propto \langle 0|\bar{T}e^{+i\int_{-\infty(1+i\epsilon)}^{t_f} dt_2 \mathsf{H}_I^{\rm int}(t_2)} Q_I(t_f) T e^{-i\int_{-\infty(1-i\epsilon)}^{t_f} dt_1 \mathsf{H}_I^{\rm int}(t_1)}|0\rangle. \tag{2.7}$$

In the above, the subscript I denotes that the corresponding operator is to be evaluated in the interaction picture. Finally, $\mathsf{H}^{\rm int}(t)$ is the interaction part of the Hamiltonian of the fluctuations, i.e. $\mathsf{H} = \mathsf{H}_0 + \mathsf{H}^{\rm int}$ with H_0 being quadratic in fluctuations. We note that the anti-time ordered product also appears in (2.7). We have not written the proportionality constant in eq. (2.7) since that only characterizes the set of vacuum bubble diagrams which will not be relevant for our purpose in this thesis. The perturbative expansion of cosmological correlators of the above general type is facilitated as usual by expanding in products of Wick contractions, given by in-in propagators. This leads to a diagrammatic form, illustrated in Fig. 2.2.

2.2.2 Useful Gauges for General Coordinate Invariance

Metric and inflaton fluctuations are not gauge invariant under diffeomorphisms. Hence we now review two useful gauges and a gauge invariant quantity characterizing the scalar perturbations during inflation. Our discussion will be brief and for more details the reader is referred to [29, 64]. For simplicity, we will specialize here to single-field slow-roll inflation, but the considerations are more general.

The metric of dS space is given by,

$$ds^2 = -dt^2 + a^2(t)d\vec{x}^2, \tag{2.8}$$

with $a(t) = e^{Ht}$ being the scale factor in terms of Hubble scale H. To discuss the gauge choices, it is useful to decompose the spatial metric $h_{ij}dx^i dx^j$ in presence of inflationary backreaction as follows [64],

$$h_{ij} = a^2(t)\left((1+A)\delta_{ij} + \frac{\partial^2 B}{\partial x^i \partial x^j} + \partial_j C_i + \partial_i C_j + \gamma_{ij}\right), \tag{2.9}$$

where, A, B, C_i, γ_{ij} are two scalars, a divergenceless vector, and a transverse traceless tensor perturbation respectively. The inflaton field can also be decomposed into a classical part $\phi_0(t)$ and a quantum fluctuation $\xi(t, \vec{x})$,

$$\phi(t, \vec{x}) = \phi_0(t) + \xi(t, \vec{x}). \tag{2.10}$$

Using the transformation rules of the metric and scalar field, it can be shown that the quantity [65],

$$\mathcal{R} \equiv \frac{A}{2} - \frac{1}{\dot{\phi}_0}\xi, \tag{2.11}$$

is gauge invariant. This is the quantity that is conserved on superhorizon scales for single field inflation [33, 66, 67, 68, 69]. Although $\mathcal{R}$ seems to depend on more than one scalar fluctuation, there is only one physical scalar fluctuation which is captured by it. This is because among the five scalar fluctuations in the metric plus inflaton

system, two are non-dynamical constraints and two more can be gauged away by appropriate diffeomorphisms, leaving only one fluctuation. To make this manifest, we can do gauge transformations which set either A or ξ to zero in (2.11) to go to spatially flat and comoving gauge respectively. The first of these will be most useful for simplifying in-in calculations involving Hubble-scale massive particles external to the inflation dynamics, while the second one is useful for constraining the squeezed limit of the NG due to inflationary dynamics itself.

Spatially flat gauge [29] In this gauge the spatial metric (2.9) becomes

$$h_{ij} = a^2(t)\left(\delta_{ij} + \gamma_{ij}\right). \tag{2.12}$$

Gauge invariant answers can be obtained by writing ξ in terms of $\mathcal{R}$ using (2.11), which becomes in this gauge,

$$\mathcal{R} = -\frac{1}{\dot{\phi}_0}\xi. \tag{2.13}$$

Comoving gauge [29] In this gauge the spatial metric (2.9) looks like

$$h_{ij} = a^2(t)\left((1+A)\delta_{ij} + \gamma_{ij}\right), \tag{2.14}$$

with quantum inflaton field $\xi = 0$. This means the gauge invariant quantity $\mathcal{R}$ evaluated in the new gauge becomes,

$$\mathcal{R} = \frac{A}{2}, \tag{2.15}$$

which lets us rewrite the spatial metric (2.9) as

$$h_{ij} = a^2(t)\left((1+2\mathcal{R})\delta_{ij} + \gamma_{ij}\right), \tag{2.16}$$

with $\mathcal{R}$ being conserved after horizon exit (in single-field inflation).

2.2.3 Observables

Having discussed the gauge choices, we now move on to discussing the observables. The power spectrum for the density perturbations is given by,

$$P_k \equiv \langle \mathcal{R}(\vec{k})\mathcal{R}(-\vec{k})\rangle', \tag{2.17}$$

where the $'$ denotes the notation that momentum conserving delta functions are taken away i.e.

$$\langle \mathcal{R}(\vec{k}_1)\cdots\mathcal{R}(\vec{k}_n)\rangle = (2\pi)^3\delta^3(\vec{k}_1+\cdots+\vec{k}_n)\langle \mathcal{R}(\vec{k}_1)\cdots\mathcal{R}(\vec{k}_n)\rangle' \tag{2.18}$$

The power spectrum can be evaluated to be

$$P_k = \frac{1}{\dot{\phi}_0^2}\frac{1}{2k^3}, \tag{2.19}$$

where the R.H.S. is to be evaluated at the moment of horizon exit $k = aH$ for a given k-mode. Since different k-modes exit the horizon at different times and $\frac{H^4}{\dot{\phi}_0^2}$ has a slow time dependence, the combination k^3P_k is not exactly k-independent,

and we can write

$$k^3 P_k \propto \left(\frac{k}{k_*}\right)^{n_s-1} \tag{2.20}$$

where $1-n_s$ is the tilt of the power spectrum and k_* is a "pivot" scale. From Planck data [45] we get, $n_s \approx 0.96$ and $\frac{H^4}{\dot{\phi}_0^2} = 8.7 \times 10^{-8}$ at $k_* = 0.05$ Mpc^{-1}. In position space, the power spectrum takes the form,

$$\langle \mathcal{R}(\vec{x}_1)\mathcal{R}(\vec{x}_2)\rangle \sim \frac{1}{|x_1 - x_2|^{n_s-1}} \tag{2.21}$$

To calculate the bispectrum we will be evaluating $\langle \mathcal{R}(\vec{k}_1)\mathcal{R}(\vec{k}_3)\mathcal{R}(\vec{k}_3)\rangle$. By translational invariance the three momenta form a triangle, and by rotational invariance we are only interested in the shape and size of the triangle, not in the orientation of the triangle. Furthermore since we also have approximate scale invariance, we do not care about the overall size of the triangle, so effectively the momentum dependence of bispectrum is governed only by the ratios $\frac{k_3}{k_1}$ and $\frac{k_2}{k_1}$. We denote the bispectrum by the function $B(k_1, k_2, k_3)$,

$$B(k_1, k_2, k_3) = \langle \mathcal{R}(\vec{k}_1)\mathcal{R}(\vec{k}_3)\mathcal{R}(\vec{k}_3)\rangle'. \tag{2.22}$$

It is convenient to define a dimensionless version of this,

$$F(k_1, k_2, k_3) = \frac{B(k_1, k_2, k_3)}{P_{k_1} P_{k_3}}. \tag{2.23}$$

The crude estimate of cosmic variance (2.3) translates to $\delta F \sim 10^{-4} - 10^{-3}$. It is

often conventional in the literature to typify the size of NG by the value of F at the equilateral point,

$$f_{\rm NL} \equiv \frac{5}{18} F(k,k,k). \tag{2.24}$$

Since we are mostly interested here in the squeezed limit for future signals, $k_3 \ll k_1, k_2$, we will explicitly compute F in that limit, referring to $f_{\rm NL}$ only in the context of current NG limits (see subsection 2.6.1). In terms of the quantum inflaton field ξ, the function F can be rewritten as,

$$F(k_1,k_2,k_3) = -\dot{\phi}_0 \frac{\langle \xi(\vec{k}_1)\xi(\vec{k}_2)\xi(\vec{k}_3)\rangle'}{\langle \xi(\vec{k}_1)\xi(-\vec{k}_1)\rangle' \langle \xi(\vec{k}_3)\xi(-\vec{k}_3)\rangle'} |_{k_3 \ll k_1,k_2}, \tag{2.25}$$

and where the R.H.S. is evaluated at the point of horizon exit for each mode.

2.3 Squeezed Limit of Cosmological Correlators

2.3.1 NG from Single Field Inflation in the Squeezed Limit

In single field inflation, NG in the squeezed limit is proportional to the tilt of the inflaton power spectrum [29, 70, 71], i.e.

$$F^{\text{Single Field}}(k_1,k_2,k_3)|_{k_3 \ll k_1,k_2} = (1-n_s) + \mathcal{O}\left(\frac{k_3}{k_1}\right)^2. \tag{2.26}$$

Let us go to comoving gauge (2.16) to demonstrate this. We are interested in computing $\langle \mathcal{R}_h(\vec{k}_1)\mathcal{R}_h(\vec{k}_2)\mathcal{R}_s(\vec{k}_3)\rangle'$, where the subscript $h(s)$ means the associated momentum is hard(soft). We define position space coordinates $\vec{x}_i$ to be conjugate to

momentum $\vec{k}_i$. In the limit $k_3 \ll k_1, k_2$ we are interested in an "Operator Product Expansion (OPE)" regime, $|\vec{x}_1 - \vec{x}_2| \ll |\vec{x}_1 - \vec{x}_3|$. Consider just the leading tree-level

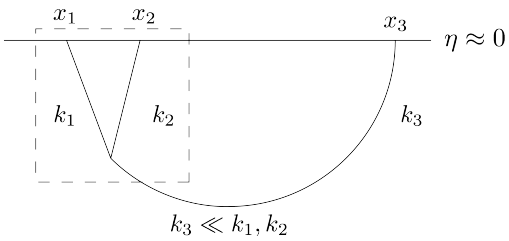

Figure 2.2: NG in single-field inflation

structure of the associated diagram in Fig. 2.2, and first focus on just the boxed subdiagram. We see that for this subdiagram the soft line is just a slowly-varying background field in which we are computing a hard 2-point correlator. Thus,

$$\langle \mathcal{R}_h(x_1)\mathcal{R}_h(x_2)\mathcal{R}_s(x_3)\rangle \approx \langle \langle \mathcal{R}_h(x_1)\mathcal{R}_h(x_2)\rangle_{\mathcal{R}_s(\frac{x_1+x_2}{2})}\mathcal{R}_s(x_3)\rangle. \tag{2.27}$$

The effect of the soft mode $\mathcal{R}_s$ is just to do the transform $\vec{x} \to (1+\mathcal{R}_s)\vec{x}$ of (2.16) within the leading 2-point function of (2.21):

$$\langle \mathcal{R}_h(x_1)\mathcal{R}_h(x_2)\rangle_{\mathcal{R}_s} \sim \frac{1}{(|x_1 - x_2|(1+\mathcal{R}_s))^{n_s-1}} \approx \frac{(1-n_s)}{|x_1-x_2|^{n_s-1}}\mathcal{R}_s\left(\frac{x_1+x_2}{2}\right). \tag{2.28}$$

To get the middle expression, we have taken $\mathcal{R}_s$ to be approximately constant over distances of order $|\vec{x}_1 - \vec{x}_2|$, a good approximation since $k_3 \to 0$. The last expression follows by expanding in (small) $\mathcal{R}_s$, evaluated at the midpoint $(\vec{x_1} + \vec{x_2})/2$. We have

also dropped a $\mathcal{R}_s$-independent piece since that goes away when we consider the three point function.

Thus the three point function becomes,

$$\langle \mathcal{R}_h(x_1)\mathcal{R}_h(x_2)\mathcal{R}_s(x_3)\rangle \approx \langle \langle \mathcal{R}_h(x_1)\mathcal{R}_h(x_2)\rangle_{\mathcal{R}_s(\frac{x_1+x_2}{2})}\mathcal{R}_s(x_3)\rangle$$
$$\approx (1-n_s)\frac{1}{(|x_1-x_2|)^{n_s-1}}\frac{1}{(|x_1-x_3|)^{n_s-1}}. \quad (2.29)$$

Fourier transforming to momentum space,

$$\langle \mathcal{R}_h(\vec{k}_1)\mathcal{R}_h(\vec{k}_2)\mathcal{R}_s(\vec{k}_3)\rangle' \sim (1-n_s)\frac{1}{k_1^{4-n_s}}\frac{1}{k_3^{4-n_s}}$$
$$\sim (1-n_s)\langle \mathcal{R}_h(\vec{k}_1)\mathcal{R}_h(-\vec{k}_1)\rangle'\langle \mathcal{R}_s(\vec{k}_3)\mathcal{R}_s(-\vec{k}_3)\rangle', \quad (2.30)$$

leading to (2.26). Subleading corrections proportional to $\left(\frac{k_3}{k_1}\right)$ are absent by rotational invariance, so the leading corrections are order $\left(\frac{k_3}{k_1}\right)^2$.

The importance of the above expression lies in the fact that in the squeezed limit any value of $F^{\text{Single Field}}$ bigger than $\mathcal{O}(1-n_s)$ will signal the presence of new physics beyond single-field inflationary dynamics. In particular, next we comment on what can happen to the squeezed limit if we have multiple light ($m \ll H$) fields ("multifield inflation") or $m \sim H$ fields ("quasi single field inflation" [18]) during inflation.

2.3.2 NG from Multifield Inflation in the Squeezed Limit

If we have light fields with $m \ll H$, other than the inflaton, then during inflation those fields can lead to larger NG in the squeezed limit than (2.26), see [72] and references therein. This can be understood again via similar in-in diagrammatics to Fig. 2.2 . In this case it is again true that we have to evaluate the hard two point function in the background of *some* soft mode, and correlate the result with a $\mathcal{R}$ soft mode. However, since $\mathcal{R}_s$ is no longer the only soft mode in the theory,

$$\langle \mathcal{R}_h(x_1)\mathcal{R}_h(x_2)\rangle_{\text{soft mode}} \neq \langle \mathcal{R}_h(x_1)\mathcal{R}_h(x_2)\rangle_{\mathcal{R}_s}. \tag{2.31}$$

Thus the derivation in the previous subsection does *not* go through. Consequently $F^{\text{Multi Field}}$ in the squeezed limit is no longer constrained to be order $(1-n_s)$, but rather it becomes model dependent.

2.3.3 NG from Hubble-scale Masses in the Squeezed Limit

The situation changes quite a lot if we have particles with $m \sim H$. Such particles can modify the bispectrum in a way that in the squeezed limit F contains a *non-analytic* part,

$$F^{\text{nonanalytic}} \propto f(\mu)\left(\frac{k_3}{k_1}\right)^{\frac{3}{2}+i\mu} + f(-\mu)\left(\frac{k_3}{k_1}\right)^{\frac{3}{2}-i\mu}, \tag{2.32}$$

where, $\mu = \sqrt{\frac{m^2}{H^2} - \frac{9}{4}}$ and $f(\mu)$ is a calculable function of the mass of the particle, which is of the order 1 when $\mu \sim 1$ but is "Boltzmann suppressed" $\sim e^{-\pi\mu}$ for large μ. We have a proportionality sign in (2.32) because there are model dependent prefactors which can take either large or small values, thus from (2.32) itself we can not get a complete estimate of NG. We will spell out the model dependent prefactors later.

The crucial aspect of (2.32) is that F now contains a *non-analytic* dependence on $\left(\frac{k_3}{k_1}\right)$ along with other analytic terms. Importantly this non-analytic behavior can *not* be captured by any single or multifield inflation models where all the masses are much smaller than H.

This dependence also encodes the information about the mass of the Hubble scale particle, via the exponent μ, [18, 19, 20, 21, 36, 37]. If the massive particle has a nonzero spin(s), then $F^{non-analytic}$ has an additional factor dependent on Legendre polynomials, $P_s(\cos\theta)$, where $\hat{k}_1 \cdot \hat{k}_3 = \cos\theta$. If we can measure this angular dependence precisely enough then we can get the information about spin as well [21, 40]. Furthermore, such angular dependence is absent in purely single-field and some of the multifield inflation models. This can in principle help us in distinguishing the "signal" of $m \sim H$ particles from the "background" of $m \ll H$ particles.

We see as we go to the region, $m \ll H$, the leading behavior reverts to being analytic $\approx \left(\frac{k_3}{k_1}\right)^{3/2-3/2}$, and indistinguishable from purely single-field or multi-field inflation. This means it is observationally challenging to reach the region $m \ll H$

and still distinguish and measure m accurately. Also, at the other extreme, for $m \gg H$ cosmological production is strongly Boltzmann suppressed, so observation will again be difficult. Therefore we are led to a window around H for doing spectroscopy of masses and spins.

Let us briefly explain the form of (2.32), first concentrating on just the soft k_3-dependence. In presence of new particles with $m \sim H$ there are additional contributions to the bispectrum beyond those in Fig. 2.2. At tree level we can have three diagrammatic forms, as shown in Fig. 2.3. These are called single, double and triple exchange diagram based on the number of massive propagators [40]. In the

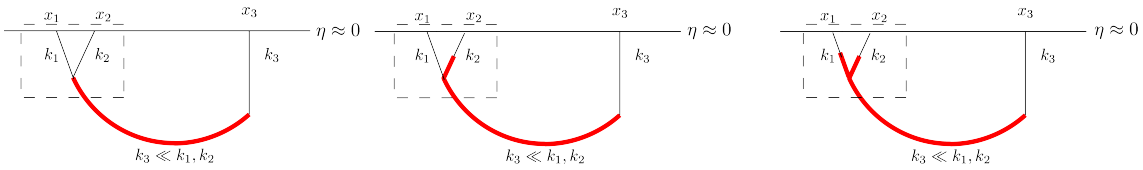

Figure 2.3: From left to right: (a) Single Exchange Diagram, (b) Double Exchange Diagram, (c) Triple Exchange Diagram. Note that all these diagrams rely on mixing between the inflaton fluctuation and massive scalar in the (implicit) non-trivial background of rolling $\phi_0(t)$.

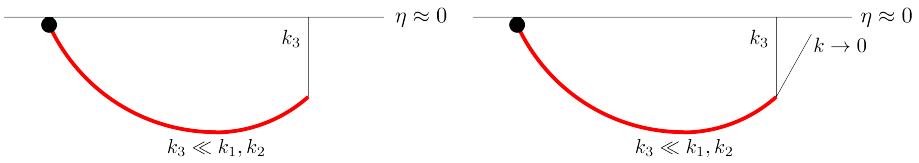

Figure 2.4: From left to right: (a) "OPE" approximation of three point function in squeezed limit as a two point function. The ϕ_0 background causing mixing is not explicitly shown, as in Fig. 2.3. (b) The same "OPE" approximation expressed an inflaton-h three point function with one inflaton leg set to zero momentum to now explicitly represent the background ϕ_0.

squeezed limit, we are once again interested in calculating $\langle \mathcal{R}_h(\vec{k}_1)\mathcal{R}_h(\vec{k}_2)\mathcal{R}_s(\vec{k}_3)\rangle'$ i.e. correlation of two hard modes with a soft mode. In position space, this again corresponds to an "OPE" limit, $|x_{12}| \ll |x_{13}|$, where the hard subdiagram is given

by an effective local vertex, depicted in Fig. 2.4 by the round black blob. The strength of this effective vertex is then given by the hard two-point function in the background of the massive but k_3-soft field, which is predominantly k_3-independent. Tracking only the k_3-dependence is then given by the two-point correlator shown in Fig. 2.4.

The leading k_3 dependence can be worked out by the scaling properties of the fields involved, which can be read off from their classical late time asymptotics. For a general scalar field,

$$\chi(\eta,\vec{x})|_{\eta\to 0} = (-\eta)^{\Delta_1}\mathcal{O}_1(\vec{x}) + (-\eta)^{\Delta_2}\mathcal{O}_2(\vec{x}), \tag{2.33}$$

where, $\Delta_{1,2} = \frac{3}{2} \pm i\sqrt{\frac{m^2}{H^2} - \frac{9}{4}}$. This means, $\mathcal{O}_{1(2)}(\vec{x})$ can be thought of as an operator with scale dimension $\Delta_{1(2)}$. So we will denote $\mathcal{O}_{1(2)} \equiv \mathcal{O}_{\Delta_{1(2)}}$.

As $\eta \to 0$, dS isometry generators in 4D acts as generators of the conformal group in 3D space. However, the leading effect of the inflationary background is to break this conformal invariance of late-time correlators, but only weakly for slow roll. Using the simple scaling symmetry subgroup of the 3D conformal invariance, we find [3] [4]

$$\langle \mathcal{O}_\Delta(\vec{x}_2)\mathcal{R}_s(\vec{x}_3)\rangle_{\rm inf} \propto |x_{23}|^{-\Delta}. \tag{2.34}$$

However, it is well known that 2-point correlators of differing scale dimension vanish

[3] There can be subleading slow-roll $\sim (1 - n_s)$ corrections to the exponent which are neglected here.

[4] Note that 4D dimensionful parameters, such as the Planck scale, do not break this 3D conformal or scale invariance.

if conformal invariance is exact, therefore the implicit proportionality "constant" is suppressed by slow-roll parameters here. Fourier transforming and writing $\Delta = \frac{3}{2} \pm i\mu$, we see F should have the factor $k_3^{\frac{3}{2}\pm i\mu}$. We can now put back the k_1 dependence, which again by the above scale invariance can only enter into the expression for F as shown in (2.32).

2.4 Gauge-Higgs Theory and Cosmological Collider Physics

2.4.1 The Central Plot and its Connections to the Literature

Having commented on NG and the squeezed limit in general, we focus on what kind of signature a gauge theory coupled to the inflaton will have on NG. In particular we study signatures of Higgs scalars and gauge bosons. Non-trivial spin of heavy particles in the context of slow-roll inflation was first considered in Ref. [21], primarily for even spin. In Ref. [40] both even and odd spin were considered. In both [21] and [40] no assumptions were made on the origins of the heavy masses. Here, we will impose the stringent constraints following from assuming that the heavy masses arise via the Higgs mechanism of weakly-coupled gauge field theory, in particular for spins 0 and 1. In particular, the relevant non-linear terms coupling the gauge-Higgs sector and the inflaton will be more suppressed by requiring gauge invariance than would be the case for massive fields unconnected to a Higgs mechanism.

For example, consider the interaction of a pair of massive spin-1 particles, Z_μ, with a pair of inflaton fields. Without considering a gauge theoretic origin for Z, a low dimension interaction respecting (approximate) inflaton shift symmetry has the

form,

$$\frac{1}{\Lambda^2}(\partial\phi)^2 Z^\mu Z_\mu, \tag{2.35}$$

where Λ is of order the cutoff of EFT. However, if Z_μ is a Higgsed gauge boson, the analogous interaction must arise from

$$\frac{1}{\Lambda^4}(\partial\phi)^2 |D\mathcal{H}|^2. \tag{2.36}$$

Crucially the interaction between Z_μ and inflaton has to happen in the presence of the Higgs field $\mathcal{H}$ since we are assuming inflaton to be a gauge singlet. Assuming the gauge theory is spontaneously broken, we see that the gauge theory interaction has a suppression of the order m_Z^2/Λ^2 compared to the non-gauge theoretic case.[5] This argument can be generalized to all the gauge boson interaction terms that we consider below. This also makes a general point that it can be harder to see NG due to gauge sector particles compared to non-gauge theoretic states. This is especially true for spin-1 particles as we saw above.

In [43, 44] the signature of gauge theory was considered, focusing on unbroken electroweak symmetry during the inflationary phase as well as the scenario of Higgs inflation (in which the inflaton is identified with the physical Higgs field). In a general gauge theory with unbroken gauge symmetry, the gauge bosons will be massless up to (small) loop corrections [73, 74]. Non-trivial spectroscopy must

[5]The non-gauge theoretic case can be viewed as the limit of the gauge case where $m_Z \sim \Lambda$. For example, a QCD ρ meson or a spin-one superstring excitation cannot be housed in point-particle EFT, except in the marginal sense where the effective cutoff is $\Lambda \sim m_Z$, where the constraints of gauge invariance disappear.

then proceed via gauge-charged matter, which can only appear in loops by charge conservation and the singlet nature of the inflaton. Such loops are difficult (but depending on specific models, may not be impossible [6]) to observe for several reasons. First, at one loop [21], $F^{\rm loop} \sim \tilde{f}(\mu)\left(\frac{k_3}{k_1}\right)^{3+2i\mu} + \tilde{g}(\mu)\left(\frac{k_3}{k_1}\right)^{3-2i\mu} + \cdots$, so the fall-off is faster compared to (2.32) as one goes to smaller k_3. Second, for heavier masses the Boltzmann suppression goes as $e^{-2\pi\mu}$ because there is now a pair of massive particles involved. Thirdly, we will obviously have the loop factor ($\sim \frac{1}{16\pi^2}$) suppression.

This gives us motivation to look for bigger tree level effects which will be present if gauge symmetry is broken spontaneously during inflation. In [43, 44] such a scenario was mentioned although the primary focus was on Higgs-inflation-like scenarios in which the Higgs VEV is very large compared to H and consequently the massive gauge bosons are too heavy to be seen via NG due to Boltzmann suppression. The situation is much better if one keeps the gauge theory and inflaton sectors distinct, with gauge symmetry spontaneously broken and Higgs VEV not too much larger than H. This is the case we focus on, and we will see that such scenarios can give rise to observable NG for both spin-0 and spin-1 particles.

Since the Hubble scale during inflation can be very high ($H \lesssim 5 \times 10^{13}$GeV), inflation and the study of NG provides an exciting arena to hunt for new particles. In this regard two distinct possibilities arise. We discuss them next.

[6] For example one can imagine working in an effective theory of inflation with its cutoff $\Lambda \gtrsim H$, however if we have a cutoff very close to Hubble then the gauge theory spectrum is no longer separated from the states coming from some UV completion of the field theory, and measurements of NG cannot be translated robustly into information about the gauge theory alone. Such a scenario, of course, is still interesting, but we do not focus on that in this chapter.

2.4.2 High Energy Physics at the Hubble Scale

We could imagine a scenario in which there exists some new spontaneously broken gauge theory at H. Then some of the gauge-charged matter and gauge-fields may become singlets under the residual unbroken gauge symmetry. Bosons of this type, spin-0 and spin-1, can therefore have Hubble scale masses, couple to the inflaton, and leave their signatures on NG at *tree-level*. For simplicity here, we focus on spontaneously broken $U(1)$ gauge theory with no residual gauge symmetry, but is straightforward to generalize to the nonabelian case. For example, we can imagine a scalar in the fundamental representation of $SU(N)$ breaking the symmetry to $SU(N-1)$. Then the gauge boson associated with the broken diagonal generator plays the role of the massive $U(1)$ gauge boson that we consider now.

Let us focus on the case of single-field slow-roll inflation. We write an effective theory with cutoff Λ. Since we are interested in effects of gauge theory on NG, we will write down higher derivative interaction terms between the gauge sector and inflaton. But we will not be explicit about higher derivative terms containing gauge sector fields alone or the inflaton alone, although we will ensure that such terms are within EFT control.

The lagrangian containing the inflaton ϕ (with an assumed shift symmetry), the Higgs ($\mathcal{H}$) and gauge bosons (not necessarily the SM Higgs and gauge bosons) has the form

$$\mathcal{L} = \frac{1}{2}M_{\rm pl}^2 R + \mathcal{L}_{\text{Gauge Theory}} - \frac{1}{2}(\partial\phi)^2 - V(\phi) + \mathcal{L}_{\rm int}^{\rm inf} + \mathcal{L}_{\rm int}^{\text{inf-gauge}}, \tag{2.37}$$

where $\mathcal{L}_{\text{Gauge Theory}}$ contains all the terms (including higher derivative terms) containing gauge theory fields alone. $V(\phi)$ is a generic slow roll potential. $\mathcal{L}_{\rm int}^{\rm inf}$ contains higher derivative terms containing inflaton alone. For our purpose the interesting interaction terms between gauge theory and the inflaton are contained in $\mathcal{L}_{\rm int}^{\text{inf-gauge}}$, which we write below assuming an UV cutoff $\sim \Lambda$ and a set of dimensionless EFT coefficients c_i,

$$\mathcal{L}_{\rm int}^{\text{inf-gauge}} = \frac{c_1}{\Lambda}\partial_\mu\phi(\mathcal{H}^\dagger D^\mu\mathcal{H}) + \frac{c_2}{\Lambda^2}(\partial\phi)^2\mathcal{H}^\dagger\mathcal{H} + \frac{c_3}{\Lambda^4}(\partial\phi)^2|D\mathcal{H}|^2 + \frac{c_4}{\Lambda^4}(\partial\phi)^2 Z_{\mu\nu}^2 + \frac{c_5}{\Lambda^5}(\partial\phi)^2\partial_\mu\phi(\mathcal{H}^\dagger D^\mu\mathcal{H}) + \cdots \tag{2.38}$$

In $\mathcal{L}_{\rm int}^{\rm inf}$, the first term gives a quadratic mixing between Higgs and Z^0. It also couples Higgs, Z and the inflaton. But it does not contain any quadratic mixing between the inflaton and Z; and also none between the inflaton and Higgs. But we do see, from Fig. 2.3, that we need one or more quadratic mixings between the inflaton and the massive particle of interest. Such quadratic mixing does arise from the second and the fifth term, which give quadratic mixing of the inflaton with Higgs and Z respectively. The third term gives, among other interactions, the interaction between an inflaton and a pair of Zs. We have not written operators coming from the

expansion in $\left(\frac{\mathcal{H}^\dagger\mathcal{H}}{\Lambda^2}\right)$ since these will be subdominant to the terms we have already considered.

To unpack (2.38) we can go to the unitary gauge for $U(1)$ gauge theory and write down some of the relevant terms,

$$\begin{aligned}\mathcal{L}_{\text{int}}^{\text{inf-gauge}} = \rho_{1,Z} Z^0 h + \rho_{1,h} h\dot{h} + \frac{\rho_{1,Z}}{2v} Z^0 h^2 + \frac{\rho_{1,Z}}{\dot{\phi}_0}\partial_\mu \xi Z^\mu h \\ + \alpha \mathcal{H}^\dagger\mathcal{H} - \rho_2 \dot{\xi} h + \frac{\rho_2 v}{4\dot{\phi}_0}(\partial\xi)^2 - \frac{\rho_2}{2v}\dot{\xi}h^2 + \frac{\rho_2}{2\dot{\phi}_0}(\partial\xi)^2 h \\ - \frac{c_3\dot{\phi}_0}{\Lambda^4}\dot{\xi}\left((\partial h)^2 + m^2 Z^\mu Z_\mu\right) \\ - \frac{2c_4\dot{\phi}_0}{\Lambda^4}\dot{\xi} Z_{\mu\nu}^2 \\ + \rho_{5,Z}\left(\dot{\xi} Z^0(1+\frac{2h}{v}) + \frac{\dot{\xi}\partial_\mu\xi Z^\mu}{\dot{\phi}_0} - \frac{(\partial\xi)^2 Z^0}{2\dot{\phi}_0}\right) \\ + \rho_{5,h}\left(\dot{\xi}\dot{h}(\frac{h}{v}+1) - \frac{\dot{\xi}\partial^\mu\xi\partial_\mu h}{\dot{\phi}_0} - \frac{(\partial\xi)^2\dot{h}}{2\dot{\phi}_0}\right), \quad (2.39)\end{aligned}$$

where we have expanded the Higgs field in unitary gauge $\mathcal{H} = \begin{pmatrix} 0 & \frac{(h+v)}{\sqrt{2}}\end{pmatrix}^T$ and the inflaton field $\phi = \phi_0 + \xi$. The inflationary background gives a correction to the Higgs quadratic term via the parameter $\alpha = -\frac{c_2\dot{\phi}_0^2}{\Lambda^2}$. We also have several quadratic mixing parameters, ρ_i,

$$\begin{aligned}\rho_{1,Z} = -\frac{\text{Im}(c_1)\dot{\phi}_0 m_Z}{\Lambda}; \quad \rho_{1,h} = -\frac{\text{Re}(c_1)\dot{\phi}_0}{2\Lambda}; \quad \rho_2 = \frac{2c_2\dot{\phi}_0 v}{\Lambda^2}; \\ \rho_{5,Z} = \frac{\text{Im}(c_5)\dot{\phi}_0^2 m_Z v}{\Lambda^5}; \quad \rho_{5,h} = \frac{\text{Re}(c_5)\dot{\phi}_0^2 v}{\Lambda^5}. \quad (2.40)\end{aligned}$$

2.4.3 Heavy-lifting of Gauge-Higgs Theory

Until now, we have been discussing theories with Higgs physics intrinsically of order H. Now although a future detection of $m \sim H$ particles via NG will be very interesting in its own right, given that H may well be orders of magnitude beyond the energies of foreseeable particle colliders, we would not have valuable complementary access to this physics in the lab. But as discussed in the introduction, the alternative is the "heavy-lifted" scenario, in which $m \sim H$ during inflation and again yields observable NG, and yet $m \ll H$ in the current post-inflationary era and therefore conceivably is accessible to collider and other "low-energy" probes.

Given a gauge theory at low energy, we can consider adding a non-minimal coupling of the Higgs to gravity, $cR\mathcal{H}^\dagger\mathcal{H}$ to the lagrangian (2.37), where we will consider c of order one. This gives a Higgs effective potential of the form,

$$V_{\text{eff}}(\mathcal{H}) = \lambda_h|\mathcal{H}|^4 - \mu_h^2|\mathcal{H}|^2 - cR\mathcal{H}^\dagger\mathcal{H}, \tag{2.41}$$

While the curvature is negligible in the current era, during inflation we have $R \approx 12H^2$, so that for $c > 0$, the symmetry breaking scale setting gauge-Higgs physical masses is naturally of order H. We can also see how this "heavy-lifting" mechanism appears in Einstein frame in which the inflaton and Higgs potential get modified to

$$(V(\phi) + V(\mathcal{H})) \to (V(\phi) + V(\mathcal{H}))/\Omega^4 \approx V(\phi)(1 - \frac{4c\mathcal{H}^\dagger\mathcal{H}}{M_{\text{pl}}^2}) + V(\mathcal{H}), \tag{2.42}$$

where $\Omega^2 = 1 + \frac{2c\mathcal{H}^\dagger\mathcal{H}}{M_{\rm pl}^2}$ is the Weyl scaling factor used to get to Einstein frame and we have kept the leading correction in $c\mathcal{H}^\dagger\mathcal{H}/M_{\rm pl}^2$[7]. For NG, the discussion in the previous subsection then carries over from this point.

As we elaborated in the introduction, one interesting fact about the heavy-lifting mechanism is that it is testable. This requires a knowledge of the couplings of the gauge theory sector in the current era, where they may be accessible at collider energies, and a measurement of H during inflation, as for example via the primordial tensor power spectrum. We can then use the renormalization group to run those couplings up to H, and thereby predict the mass ratios of spin-0 and spin-1 h and Z type particles (bosons charged under the full gauge symmetry which are singlets of the unbroken gauge symmetry) as they were in the inflationary epoch when they contributed to NG. Here the richer the set of h and Z type particles, and hence the larger the set of mass ratios, the less precision we would need to measure each ratio in NG in order to be convinced that we are seeing the *same* gauge theory in both regimes.

2.5 NG in Single Field Slow Roll Inflation

We saw in the previous section that the leading interaction between inflaton and gauge theory is captured by (2.38) and (2.39). These can be used to estimate

[7]There may in addition be direct Higgs-inflaton couplings even before the Weyl-rescaling to Einstein frame, in which case the Einstein frame couplings may be modified from that above. However, even this modification would have to share similar features, namely that during inflation the Higgs mass parameter is effectively raised to the H^2-scale and in the current post-inflationary era the Higgs mass parameter is much smaller in order to fit the current electroweak data. Therefore, we will not pursue this more general modified lagrangian, for simplicity

the magnitudes of NG induced by h and Z. However, the parameters appearing in those two lagrangians have to satisfy several consistency requirements. We first discuss such restrictions and then proceed with the estimation of NG. Our discussion in this section will be in the context of slow roll inflation.

2.5.1 Cutoff and Coupling Strengths of Effective Theory

We start with the restriction on Λ, which we saw in the previous section sets the most optimistic suppression scale for higher-dimensional interactions relevant to NG. We imagine that Λ roughly represents the mass scale of heavy particles that have been integrated out to give the effective non-renormalizable couplings we need between the gauge sector and inflaton. We can therefore think of them as Λ-mass "mediators" of the requisite effective interactions. But in general, if such mediators couple substantively to both the inflaton and to the gauge sector, they will also mediate inflaton (non-renormalizable) self-interactions, roughly powers of $\left(\frac{(\partial\phi)^2}{\Lambda^4}\right)$. In order for the effective expansion in these powers to be controlled, we should require Λ to exceed the inflationary kinetic energy [39],

$$\Lambda > \sqrt{\dot{\phi}_0}. \tag{2.43}$$

In our ensuing discussion of single-field inflation, we will take this bound to hold. We will assume an approximate inflaton shift symmetry during inflation, allowing the Λ^4 to be only as big as the slowly-rolling kinetic energy rather than a larger scale.

The potential energy of the inflaton field $V(\phi)$ gives rise to an even higher energy scale $V^{\frac{1}{4}}$, which is bigger than $\sqrt{\dot{\phi}_0}$. Approximate shift symmetry during inflation keeps this scale from spoiling the EFT expansion in higher-dimension operators, but after inflation this symmetry may be significantly broken and the higher scale can then affect dynamics significantly. In particular, EFT with $\Lambda < V^{\frac{1}{4}}$ can break down at reheating, signaling that the Λ-scale mediators can be reheated and subsequently decay. However, the NG produced and described by the controlled effective theory during inflation are already locked in on superhorizon scales and are insensitive to the subsequent post-inflationary breakdown of the EFT.

Furthermore, in theories involving large "vacuum" expectation values, non-renormalizable operators in the UV theory can become super-renormalizable (or marginal) in the IR, once some fields are set to their expectation values. There is then the danger of such effective super-renormalizable couplings becoming strong in the IR, and outside perturbative control, or becoming effective mass terms which are too large phenomenologically and have to be fine-tuned to be smaller. This general concern is realized in the present context, because of the large classical expectation given by $\dot{\phi}_0(t) \gg H^2$, as well as large $\langle \mathcal{H} \rangle > H$ within some of the interesting parameter space. We find that these issues are avoided for sufficiently small c_i in (2.38) with,

$$c_i \sim \mathcal{O}(H/\sqrt{\dot{\phi}_0}), \tag{2.44}$$

which we take to hold from now on. We go into more detail on such restrictions in the next subsection.

To concretely illustrate the above considerations, consider the following set up. We imagine a theory, with a cutoff $\Lambda' \gtrsim V^{\frac{1}{4}} > \sqrt{\dot{\phi}_0}$, in which the inflaton and Higgs do not interact directly. Thus a term like $\frac{1}{\Lambda'^2}(\partial\phi)^2\mathcal{H}^\dagger\mathcal{H}$ is absent in the lagrangian. However, we assume the presence of a "mediator" gauge-singlet particle σ with mass $m_\sigma \sim \sqrt{\dot{\phi}_0}$, which talks to both the inflaton and Higgs separately via the terms,

$$\frac{1}{\Lambda'}(\partial\phi)^2\sigma + \mu_\sigma\sigma\mathcal{H}^\dagger\mathcal{H}. \tag{2.45}$$

Then below m_σ, we can integrate σ out to write an effective coupling between the inflaton and Higgs,

$$\frac{\mu_\sigma}{\Lambda' m_\sigma^2}(\partial\phi)^2\mathcal{H}^\dagger\mathcal{H} \equiv \frac{c_2}{\Lambda^2}(\partial\phi)^2\mathcal{H}^\dagger\mathcal{H}. \tag{2.46}$$

Now in the previous paragraphs we have stated that the choice of $\Lambda \gtrsim \sqrt{\dot{\phi}_0}$ and $c_i \sim \mathcal{O}(H/\sqrt{\dot{\phi}_0})$ will lead to a controlled effective theory expansion. These parameters are reproduced naturally if we take, $\mu_\sigma \sim H; \Lambda' \sim V^{\frac{1}{4}} \sim \epsilon^{-1/4}\sqrt{\dot{\phi}_0}; m_\sigma \sim \sqrt{\dot{\phi}_0}$ in the theory containing the mediator. In the above we have take $\epsilon \lesssim 10^{-2}$ consistent with current bounds [45]. Note that we also induce the $(\partial\phi)^4$ operator, but with strength $\epsilon^{1/2}/\dot{\phi}_0^2$, so that the inflaton derivative expansion is controlled within the effective theory with σ integrated out.

This shows as a proof-of-principle how Λ can represent the mass scale of heavy particles which are integrated out in the inflation-era effective theory, consistent with the even higher mass scale $V^{1/4}$ driving the accelerated expansion. It is possible that reheating later accesses this higher mass scale and produces σ particles, but these rapidly decay and do not affect the NG signals derived in the effective theory with

σ integrated out.

2.5.2 Visibility of a Higgs Scalar

Let us start with (2.38) to discuss in detail the coupling between the inflaton and a Higgs scalar, h. As we briefly mentioned in the previous section, the first term of (2.38) does not give rise to any quadratic mixing between the inflaton and h. This can seen by going to the unitary gauge for Higgs and using the equation of motion for the inflaton. So we move on to the second term of (2.38),

$$\frac{c_2}{\Lambda^2}(\partial\phi)^2\mathcal{H}^\dagger\mathcal{H}. \tag{2.47}$$

To be more precise, we have separated the strength of the interaction into a dimensionless coupling c_2, and the physical cutoff Λ. One can think of c_2 as being typical of the dimensionless strength of couplings between the gauge-Higgs sector and the inflaton sector. Quantum loops are taken to be cutoff at Λ.

The coupling (2.47) gives rise to several terms,

$$\begin{aligned}\alpha\mathcal{H}^\dagger\mathcal{H} - \frac{\rho_2 v}{2}\dot{\xi} - \frac{\rho_2^2}{8\alpha}(\partial\xi)^2 - \rho_2\dot{\xi}h \\ + \frac{\alpha}{\dot{\phi}_0}\dot{\xi}h^2 + \frac{\rho_2}{2\dot{\phi}_0}(\partial\xi)^2 h \\ - \frac{\alpha}{2\dot{\phi}_0^2}(\partial\xi)^2 h^2,\end{aligned} \tag{2.48}$$

where,

$$\rho_2 = \frac{2c_2 v\dot{\phi}_0}{\Lambda^2}; \qquad \alpha = -\frac{c_2\dot{\phi}_0^2}{\Lambda^2}. \tag{2.49}$$

In (2.48) we have put in several terms that we dropped previously in (2.39) for brevity. Also looking at (2.39) we see that we have dropped terms involving ρ_5 which are subleading compared to terms involving ρ_2. Coming back to the first line of (2.48), we see that we have a quadratic mixing (denoted by ρ_2) between the inflaton and h. We also have a term contributing to classical Higgs potential given by the parameter α. Writing the scalar potential as

$$V(\mathcal{H}) = -\mu_h^2 \mathcal{H}^\dagger \mathcal{H} + \lambda_h (\mathcal{H}^\dagger, \mathcal{H})^4 \tag{2.50}$$

we see $\Delta\mu_h^2 = -\alpha$, so α should be thought of as a tuning parameter, which we ideally do not want to be much bigger than H^2 in order to avoid fine-tuning. Now we are in a position to summarize the different restrictions on the parameters.

Classical Restrictions We have several restrictions on the parameters ρ_2 and α,

- We have a tadpole for $\dot{\xi}$, but as long as we have $\rho_2 v \ll \dot{\phi}_0$ it does not give dangerously large kinetic energy into the effective theory.
- To have perturbative control, we should require $\rho_2 < H$.
- To not have large modification to inflaton kinetic term we should have $\frac{\rho_2^2}{4\alpha} \ll 1$.
- Also to have a controlled effective theory we should have $v \lesssim \Lambda$.

Quantum Corrections

- From the quartic interaction between Higgs and inflaton we have,

$$\Delta m_h^2 \sim \frac{1}{16\pi^2} c_2 \Lambda^2 < m_h^2. \tag{2.51}$$

- From the same quartic interaction we have,

$$\Delta \lambda_h \sim \frac{1}{16\pi^2} c_2^2 < \lambda_h. \tag{2.52}$$

The inequalities above just impose the constraint of quantum stability, or absence of loop-level fine tuning.

Estimates for NG A scalar particle can give rise to a nontrivial squeezed limit via three possible diagrams at tree level, as shown in Fig. 2.3. We can estimate the parametric strength of the associated NG quickly for each of the three diagrams using (2.48):

$$F_h^{\text{single}} \sim \rho_2^2; \qquad F_h^{\text{double}} \sim \rho_2^2 \alpha; \qquad F_h^{\text{triple}} \sim \rho_2^3 \lambda_h v \dot{\phi}_0 \sim \rho_2^2 \alpha, \tag{2.53}$$

where the right-hand sides are further modulated by functions of kinematic shape as sketched in (2.32), and detailed later in Section 2.7. We have used the subscript h to denote that we are estimating NG due to h. Importantly, when we do not have any classical tuning of the Higgs mass i.e. $\alpha \lesssim H^2$, all the diagrams give a similar contribution.

Specific Parameter Choice To have a feeling for all the above constraints and estimates we now focus on a benchmark parameter choice: $c_2 = \frac{H}{\sqrt{\dot{\phi}_0}}, \lambda_h = \frac{H^2}{2\dot{\phi}_0}, \Lambda = 3\sqrt{\dot{\phi}_0}$, that we use later in Section 2.7. Such a choice gives depending on m_h, $F \sim \mathcal{O}(0.1)$, which should be observable. One can also check with this choice that all the above constraints are satisfied with no fine-tuning of parameters.

2.5.3 Visibility of a Massive Gauge Boson

Let us start with lagrangian (2.38) again to get a coupling between the inflaton and a massive gauge boson Z. To organize the couplings, it is useful to look for the essential quadratic mixing between the inflaton and the timelike/longitudinal component of Z first.

Quadratic Mixing There is no such mixing when we consider terms up to dimension four. At dimension five, we get the term $\frac{c_1}{\Lambda}\partial_\mu\phi\mathcal{H}^\dagger D_\mu\mathcal{H}$ from (2.38). This term gives a coupling between h, the inflaton and Z. But after using the equation of motion for Z, we do not get the desired quadratic mixing. However, this term does give a mixing between h and Z^0, where the superscript 0 refers to the time component, not the charge of the Z (which is always taken to be neutral for our purposes, as discussed earlier),

$$\frac{c_1}{\Lambda}\partial_\mu\phi\mathcal{H}^\dagger D^\mu\mathcal{H} \supset \rho_{1,Z} h Z^0, \tag{2.54}$$

with, $\rho_{1,Z} = -\frac{\mathrm{Im}(c_1)\dot{\phi}_0 m_Z}{\Lambda}$. To look for quadratic mixing between the inflaton and Z we have to go to yet higher order terms. The leading operators come at dimension

nine due to shift symmetry of the inflaton couplings,

$$\frac{c_5}{\Lambda^5}(\partial\phi)^2\partial_\mu\phi\mathcal{H}^\dagger D^\mu\mathcal{H}. \tag{2.55}$$

This term gives a quadratic mixing both between h and Z^0 and also between the inflaton and Z^0. The former is subleading compared to what we already have from the dimension five operator. So focusing on the latter, we have

$$\rho_{5,Z}\dot{\xi}Z^0, \tag{2.56}$$

where, $\rho_{5,Z} = \frac{c_{5,I}\dot{\phi}_0^2 m_Z v}{\Lambda^5} \sim \rho_{1,Z}\frac{v\dot{\phi}_0}{\Lambda^4}$. In the last relation we have taken the EFT coefficients to be $\sim \frac{H}{\sqrt{\dot{\phi}_0}}$.

Cubic Interactions For brevity we will not write down all possible terms after expanding the lagrangian in unitary gauge. Rather we will focus on the terms that contribute to diagrams in Fig. 2.3. Focusing on cubic interactions between just the inflaton and Z we do not get any contribution from the dimension five term, $\frac{c_1}{\Lambda}\partial_\mu\phi\mathcal{H}^\dagger D_\mu\mathcal{H}$. The leading operators then comes in at dimension eight,

$$\frac{c_3}{\Lambda^4}(\partial\phi)^2|D\mathcal{H}|^2 \supset -\frac{c_3 m_Z^2\dot{\phi}_0}{\Lambda^4}\dot{\xi}Z_\mu^2 + \cdots, \tag{2.57}$$

and

$$\frac{c_4}{\Lambda^4}(\partial\phi)^2 Z_{\mu\nu}^2 \supset -\frac{2c_4\dot{\phi}_0}{\Lambda^4}\dot{\xi}Z_{\mu\nu}^2 + \cdots. \tag{2.58}$$

We also have another possible cubic interaction coming from the same dimension nine operator we considered above,

$$\frac{c_5}{\Lambda^5}(\partial\phi)^2\partial_\mu\phi\mathcal{H}^\dagger D_\mu\mathcal{H} \supset -\frac{\rho_{5,Z}}{2\dot{\phi}_0}(\partial\xi)^2 Z^0 + \frac{\rho_{5,Z}}{\dot{\phi}_0}\dot{\xi}\partial_\mu\xi Z^\mu + \cdots . \tag{2.59}$$

Lastly we also have another dimension nine operator,

$$\frac{c_6}{\Lambda^5}\partial_\mu\phi\mathcal{H}^\dagger D^\mu\mathcal{H}|D\mathcal{H}|^2 \supset \frac{\rho_{5,Z}m_Z^2}{4\dot{\phi}_0}Z^0 Z^\mu Z_\mu + \cdots , \tag{2.60}$$

where, in the last relation we have taken $c_6 \sim c_5$ just for simplicity.

To summarize we collect the essential terms in the Lagrangian,

$$\rho_{1,Z}hZ^0 + \rho_{5,Z}\dot{\xi}Z^0 - \frac{c_3 m_Z^2\dot{\phi}_0}{\Lambda^4}\dot{\xi}Z_\mu^2 - \frac{2c_4\dot{\phi}_0}{\Lambda^4}\dot{\xi}Z_{\mu\nu}^2 - \frac{\rho_{5,Z}}{2\dot{\phi}_0}(\partial\xi)^2 Z^0 + \frac{\rho_{5,Z}}{\dot{\phi}_0}\dot{\xi}\partial_\mu\xi Z^\mu + \frac{\rho_{5,Z}m_Z^2}{4\dot{\phi}_0}Z^0 Z^\mu Z_\mu + \cdots , \tag{2.61}$$

with, $\rho_{5,Z} = \frac{c_{5,I}\dot{\phi}_0^2 m_Z v}{\Lambda^5} \sim \rho_{1,Z}\frac{v\dot{\phi}_0}{\Lambda^4}$.

Estimates of NG Just like the case of scalars, we give the estimates for the three diagrams in Fig. 2.3 (assuming $c_i \sim \frac{H}{\sqrt{\dot{\phi}_0}}$):

$$F_Z^{\text{single}} \sim \left(\frac{\rho_{1,Z}v\dot{\phi}_0}{\Lambda^4}\right)^2 ; \;\; F_Z^{\text{double}} \sim F_Z^{\text{single}} \times \frac{\rho_{1,Z}\dot{\phi}_0}{\Lambda^3}; \;\; F_Z^{\text{triple}} \sim \left(F_Z^{\text{single}}\right)^{3/2} \times \rho_{1,Z}\frac{v\dot{\phi}_0}{\Lambda^4} \tag{2.62}$$

We note for perturbativity, $\rho_{1,Z} < H^2$. Since $\Lambda > \sqrt{\dot{\phi}_0}$ and $v < \Lambda$, the single exchange diagram is expected to dominate over the other two. But even the single

exchange diagram itself is too small to be observable. This is because it involves two suppressions, firstly due to the factor of $\rho_{1,Z}^2$. Secondly, there is a suppression, $\left(\frac{v\dot{\phi}_0 H}{\Lambda^4}\right)^2$ where $v, \sqrt{\dot{\phi}_0} < \Lambda$. Even assuming $\rho_{1,Z} \lesssim H^2$ and $v, \sqrt{\dot{\phi}_0} \lesssim \Lambda$ we have, $F_Z^{\rm single} \lesssim \frac{H^2}{\dot{\phi}_0} \lesssim 10^{-3}$, likely unobservably small. However, we will see in the next subsection that there is a loop-hole in this pessimistic conclusion.

2.5.4 Gauge Theory with a Heavy Higgs Scalar

In the above analysis we have seen that the couplings between just the inflaton and Z are too small to give any observable NG. However there can be bigger effects for the Z if the Higgs scalar h becomes somewhat heavier than the Hubble scale, so that we can integrate it out. As an example, the inflaton can mix with the Z via a virtual h exchange to have a quadratic mixing of the form, $\frac{\rho_{1,Z}\rho_2}{m_h^2}\dot{\xi}Z^0$. Similarly there can be a cubic interaction between the inflaton and Z of the form, $\frac{\rho_2 m_Z^2}{v m_h^2}\dot{\xi}Z_\mu^2$, and a similar term involving Z field strength, which we do not write down for brevity. To summarize, we have the following interactions below the mass of h,

$$\frac{\rho_{1,Z}\rho_2}{m_h^2}\dot{\xi}Z^0 + \frac{\rho_{1,Z}\rho_2}{m_h^2\dot{\phi}_0}\dot{\xi}\partial_\mu\xi Z^\mu + \frac{\rho_2 m_Z^2}{v m_h^2}\dot{\xi}Z_\mu^2 + \cdots . \tag{2.63}$$

Estimates of NG Taking $\rho_{1,Z}, \rho_2 \lesssim 1$ in Hubble units, we get the following estimates for NG,

$$F_Z^{\rm single} \lesssim \frac{1}{m_h^4}; \qquad F_Z^{\rm double} \lesssim \frac{\dot{\phi}_0}{v m_h^6}. \tag{2.64}$$

The triple exchange diagram, however, comes out to be smaller than the single exchange diagram. In this case it can be estimated as, $F_Z^{\text{triple}} \sim \frac{\dot{\phi}_0 H^4}{m_h^6} \times \frac{H^3}{v m_h^2}$.

Coming to the single and double exchange, as a benchmark choice of parameters which we use in Section 2.8, we take $m_h = 3H$; $v = \sqrt{\dot{\phi}_0}; \Lambda = 3\sqrt{\dot{\phi}_0}$; $\text{Im}c_1 = 6H/\sqrt{\dot{\phi}_0}$; and $c_2 = \frac{9}{2}H/\sqrt{\dot{\phi}_0}$. Then we have, $F_Z^{\text{single}} \sim \mathcal{O}(0.01)$ and $F_Z^{\text{double}} \sim \mathcal{O}(0.1)$ depending on m_h. This scenario can thus lead to a very weak but probably observable NG due to Z. The "price" we pay is that the Higgs scalar h which mediates the Z-inflaton interaction, with $m_h = 3H$, will itself be too Boltzmann suppressed to observe in NG. Of course this does not preclude having observable h-like NG from other lighter Higgs scalars in multi-scalar Higgs theories. For the above parameter choice there is no classical or quantum tuning.

In conclusion, we see that in single-field slow-roll inflation, we can get small but observable NG.

2.6 NG in the Effective Goldstone Description of Inflationary Dynamics

The suppression of NG in single-field slow-roll inflation is due to the fact that the effective cutoff Λ is constrained to be at least as large as the inflaton kinetic energy scale, $\sqrt{\dot{\phi}_0} \gg H$, in order to perturbatively control the derivative expansion of the inflaton. However, it is possible that the dynamics takes some other form than standard single-field slow-roll inflation, and the cutoff of effective field theory, Λ, may

then be lower, yielding stronger NG. We now turn to a more "agnostic" approach to the inflationary dynamics so as to explore this possibility. An elegant and powerful approach at this level is provided by the Effective Goldstone description [62]. It is based on the central requirement that the hot big bang has to emerge from the inflationary phase. In a relativistic theory this means that there must be a physical local "clock" field during inflation which dictates when inflation ends at each point in space. Such a clock field chooses a physical time coordinate during inflation and breaks the time diffeomorphism of dS spontaneously. The inflaton can then be thought of as the Goldstone boson associated with this spontaneous breaking. In this way, successful classical inflation is treated as a "black-box" input, providing a background process in which the gauge-Higgs dynamics coupled to quantum inflaton fluctuations play out.

We first review the construction of the EFT of this Goldstone field in the absence of the Gauge-Higgs sector. Then we extend this construction to couple the Goldstone field to a Gauge-Higgs sector and estimate the magnitude of NG due to h and Z particles.

2.6.1 Minimal Goldstone Inflationary Dynamics

2.6.1.1 Leading Terms in the Effective Theory and Power Spectrum

We start by writing in the effective lagrangian all the terms that are consistent with the unbroken 3D spatial diffeomorphisms on a fixed time slice. Such terms include 4D scalars and also any 3D diffeomorphism invariants made out of the

following variables:

$$t, g^{00}, g^{0\mu}V_\mu, K_{\mu\nu},$$

where, V_μ is any vector and $K_{\mu\nu}$ is the extrinsic curvature of the time slice. The above set of terms are allowed because they behave as scalars under spatial diffeomorphisms. This time slicing can be thought of as analogous to the unitary gauge of a spontaneously broken gauge theory in which the Goldstone boson is absent because it is "eaten up" by the gauge field i.e. the metric on the time slice. To restore the Goldstone boson, we do a transformation along the broken generator, which in the present context is a time translation,

$$t \to t + \pi(x), \tag{2.65}$$

and promote $\pi(x)$ to the quantum field denoting the Goldstone boson i.e the inflaton. Under such a time translation we record the transformation rules of the various terms mentioned above,

$$\begin{aligned} b(t) &\to b(t+\pi(x)) = b(t) + \dot{b(t)}\pi(x) + \cdots \\ g^{00} &\to \frac{\partial(t+\pi)}{\partial x^\mu}\frac{\partial(t+\pi)}{\partial x^\nu}g^{\mu\nu} \\ g^{0\mu}V_\mu &\to \frac{\partial(t+\pi)}{\partial x^\nu}g^{\nu\mu}V_\mu. \end{aligned} \tag{2.66}$$

The appearance of $\pi(x)$ in the specific combination $t+\pi(x)$ implies that we can restore 4D diffeomorphism by letting, $\pi(x) \to \pi(x) - \xi(t, \vec{x})$ under a time translation $t \to t + \xi(t, \vec{x})$ so that the combination $t + \pi(x)$ behaves as a scalar. In the above

we have not written the transformation of the extrinsic curvature terms, because as we will show below, we will be interested in a regime where one can ignore terms involving extrinsic curvature. Let us now use the above strategy for restoring 4D diffeomorphism invariance to get the effective lagrangian for $\pi(x)$.

We will expand around a background quasi-dS metric,

$$ds^2 = -dt^2 + e^{2H(t)}d\vec{x}^2. \tag{2.67}$$

The leading effective lagrangian for small fluctuations around this metric and up to two-derivative order (neglecting extrinsic curvature as noted above) is then given by

$$S = \int d^4x\sqrt{-g}\left(\frac{1}{2}M_{\rm pl}^2 R - b(t)(g^{00}+1) - \Lambda(t)\right). \tag{2.68}$$

The associated Einstein equations then look like

$$\begin{aligned} H^2 &= \frac{1}{3M_{\rm pl}^2}(\Lambda(t) + 2b(t)) \\ \dot{H} + H^2 &= \frac{1}{3M_{\rm pl}^2}(\Lambda(t) - b(t)). \end{aligned} \tag{2.69}$$

The above two equations fix the time-dependent couplings, $\Lambda(t)$ and $b(t)$, which when substituted back gives,

$$S = \int d^4x\sqrt{-g}\left(\frac{1}{2}M_{\rm pl}^2 R + M_{\rm pl}^2\dot{H}g^{00} - (3M_{\rm pl}^2H^2 + M_{\rm pl}^2\dot{H})\right). \tag{2.70}$$

We can restore the Goldstone field in the above action by doing the time

translation $t \to t + \pi$ under which,

$$g^{00} \to \frac{\partial(t+\pi)}{\partial x^\mu}\frac{\partial(t+\pi)}{\partial x^\nu} g^{\mu\nu} = (1+\dot{\pi})^2 g^{00} + 2(1+\dot{\pi})\partial_i \pi g^{0i} + (\partial_i \pi)(\partial_j \pi) g^{ij}. \quad (2.71)$$

The above transformation contains mixing of metric perturbations with the inflaton $\pi(x)$, but as we will justify soon, we can neglect such mixings. In that approximation, the transformation of $\delta g^{00} \equiv g^{00} + 1$ and $g^{0\mu} V_\mu$ simplifies,

$$\begin{aligned} \delta g^{00} &\to -2\dot{\pi} + (\partial\pi)^2 \\ g^{0\mu} V_\mu &\to -(1+\dot{\pi}) V_0 + a^{-2} \partial_i \pi V_i. \end{aligned} \quad (2.72)$$

Using this, and working to leading order in $\epsilon \ll 1$, the action (2.70) reduces to[8]

$$S = \int d^4x \sqrt{-g} \left(\frac{1}{2} M_{\rm pl}^2 R + M_{\rm pl}^2 \dot{H} (\partial\pi)^2 - 3 M_{\rm pl}^2 H^2 \right). \quad (2.73)$$

This yields a quadratic action for the Goldstone boson.

To canonically normalize the Goldstone boson, we can define the field $\pi_c(x)$,

$$\pi_c(x) = \sqrt{2} M_{\rm pl} (-\dot{H})^{\frac{1}{2}} \pi \equiv f_\pi^2 \pi, \quad (2.74)$$

where f_π itself is approximately constant in time as $\epsilon, \eta \ll 1$. This definition of f_π generalizes the "decay constant" of chiral lagrangians for Goldstone bosons of internal symmetries. In single-field inflation it is simply given by $f_\pi^4 = \dot{\phi}_0^2 = 2\epsilon H^2 M_{\rm pl}^2 =$

[8] The term linear in $\dot{\pi}$ cancels with a similar term coming from the expansion $H(t+\pi)$ after an integration by parts. We have also dropped a few subleading terms coming from the expansion $M_{\rm pl}^2 \dot{H}(t+\pi)$ and $M_{\rm pl}^2 H^2(t+\pi)$

$-2\dot{H}M_{\rm pl}^2$, but here we are not assuming single-field inflationary dynamics, and indeed our effective lagrangian makes no explicit reference to ϕ. The last term in the Goldstone action (2.73) act as the dominant energy density during inflation,

$$\rho = 3M_{\rm pl}^2 H^2, \tag{2.75}$$

which is the familiar relation.

Before calculating physical quantities we have to relate $\pi(x)$ to the gauge invariant quantity $\mathcal{R}$. This can be done by first noticing that in the absence of $\pi(x)$, i.e. in the unitary gauge, the spatial metric is the same as (2.16),

$$h_{ij} = a^2(t)\left((1+2\mathcal{R})\delta_{ij} + \gamma_{ij}\right). \tag{2.76}$$

To introduce $\pi(x)$ we again do the transformation $t \to t + \pi$. To relate π to $\mathcal{R}$ we demand that in presence of π the spatial metric should not contain any 3D-scalar metric fluctuations, so that it should be given by

$$h_{ij} = a^2(t)\left(\delta_{ij} + \gamma_{ij}\right). \tag{2.77}$$

This gives the leading order relation,

$$\mathcal{R} = -\pi. \tag{2.78}$$

Using (2.73), (2.74) and (2.78) we can calculate the inflaton power spectrum,

$$\langle \pi_c(\vec{k})\pi_c(-\vec{k})\rangle' = \frac{1}{2k^3} \qquad \Rightarrow \langle \mathcal{R}(\vec{k})\mathcal{R}(-\vec{k})\rangle' = \frac{1}{2f_\pi^4 k^3}, \tag{2.79}$$

which matches the single-field slow-roll calculation (2.19) [9], but now more agnostically with regard to the inflationary dynamics.

Before moving on to inflaton interaction terms, we pause to justify why we have ignored terms involving extrinsic curvature and mixing of the inflaton with metric perturbations. The transformation of $K_{\mu\nu}$ can be obtained by writing it down in terms of the induced metric $h_{\mu\nu}$ on the time slice, and the normal vector n^μ to the surface [75],

$$K_{\mu\nu} = \frac{1}{2}\big(n^\sigma \nabla_\sigma h_{\mu\nu} + h_{\mu\sigma}\nabla_\nu n^\sigma + h_{\sigma\nu}\nabla_\mu n^\sigma\big). \tag{2.80}$$

We note that being a type of curvature, $K_{\mu\nu}$ always has an extra derivative acting on the metric component. This means compared to terms like δg^{00}, scalars like $(\delta K_{\mu\nu})^2$ or $(\delta K^\mu_\mu)^2$ will have an extra $\frac{E^2}{\Lambda^2}$ suppression[10] where Λ is the cutoff of the effective theory presumed to suppress these higher-derivative terms. Since $E \sim H$ and we will be considering situations with $\Lambda \gtrsim 10H$, we can ignore contributions coming from extrinsic curvature.

We now turn to the mixing of the inflaton with metric fluctuations. From

[9] This is assuming that subsequent terms in the EFT do not contribute significantly to the quadratic lagrangian for the inflaton. If that is not the case, then the power spectrum depends on a combination of the scales f_π and c_s, the speed of propagation for the inflaton fluctuation

[10] K^μ_μ is suppressed only by $\frac{E}{\Lambda}$, however a term involving K^μ_μ can be reduced to a term containing g^{00}, and thus gives no new information [62]

the transformation of g^{00} we get a term of the form, $h^{00}\dot{\pi}$ along with $\dot{\pi}^2$. However from Einstein eqs. [29], $h^{00} \sim \sqrt{\epsilon}\frac{H}{M_{\rm pl}}$, which means the mixing term is suppressed compared to $\dot{\pi}^2$ by a factor of ϵ. Since we are interested in the regime, $E \sim H$ and $\epsilon \ll 1$, we can drop such mixing terms, which simplifies the transformation laws as advertised earlier,

$$\begin{aligned} \delta g^{00} &\to -2\dot{\pi} + (\partial\pi)^2 \\ g^{0\mu}V_\mu &\to +(1+\dot{\pi})V^0 + \partial_i\pi V^i. \end{aligned} \tag{2.81}$$

2.6.1.2 Higher Order Terms

Let us now move on to discuss higher order corrections to the quadratic-in-π lagrangian discussed above. Ignoring terms involving extrinsic curvature, we have terms of the form $M_n^4(\delta g^{00})^n$ where M_n's are some mass scales. In particular we have for $n = 2$,

$$M_2^4(\delta g^{00})^2 \supset 4M_2^4\dot{\pi}^2 + \cdots \tag{2.82}$$

This term modifies the kinetic term for the inflaton. However such modifications are small when $M_2^4 \lesssim f_\pi^4$ which we will take to be the case.[11] Then we can simplify the transformation of δg^{00} even further by noting that $(\partial\pi)^2 \sim \left(\frac{\partial\pi_c}{f_\pi^2}\right)^2 \sim \frac{H^4}{f_\pi^4} \ll \dot{\pi} \sim \frac{\dot{\pi}_c}{f_\pi^2} \sim \frac{H^2}{f_\pi^2}$, where we have used (2.74) and the fact that $\pi_c \sim H$. Thus we can write,

$$\delta g^{00} \to -\frac{2\dot{\pi}_c}{f_\pi^2}. \tag{2.83}$$

[11] It can happen that $M_2^4 \gg f_\pi^4$ in which limit the inflaton fluctuations propagate with a speed $c_s \ll 1$. While we will restrict to cases with $c_s \approx 1$, our analysis can be easily extended to include $c_s \ll 1$.

Since δg^{00} is dimensionless, a power counting rule in the EFT is not manifest. However this can be fixed by defining the dimension 2 operator δg_c^{00} which transforms as,

$$\delta g_c^{00} \equiv -\frac{1}{2} f_\pi^2 \delta g^{00} \to \dot{\pi}_c. \tag{2.84}$$

We will take a power-counting rule that higher-dimensional operators in terms of π_c are suppressed by powers of Λ, with order one coefficients. Let us illustrate this power counting rule by the example of the dimension six operator arising from $M_3^4(\delta g^{00})^3$. By our power counting rule we expect this term to go as

$$M_3^4(\delta g^{00})^3 \sim \frac{\bar{d}_1}{\Lambda^2}(\delta g_c^{00})^3 \to \frac{\bar{d}_1}{\Lambda^2}\dot{\pi}_c^3, \tag{2.85}$$

where $\bar{d}_1$ is an $\mathcal{O}(1)$ EFT coefficient. At higher orders we have an expansion like

$$\bar{d}_2 \frac{(\delta g_c^{00})^4}{\Lambda^4} + \bar{d}_3 \frac{(\delta g_c^{00})^5}{\Lambda^6} + \cdots . \tag{2.86}$$

Importantly, non-observation of NG in Planck data puts a bound on the cutoff Λ of the EFT. For example, the dimension-6 operator $\frac{\bar{d}_1}{\Lambda^2}\dot{\pi}_c^3$ that we discussed above induces an inflaton three-point function of the form,

$$F^{\dot{\pi}^3}(k_1, k_2, k_3) = -2\bar{d}_1 \frac{f_\pi^2}{\Lambda^2}\left(\frac{k_1^3 k_3^3}{k_1 k_2 k_3 (k_1+k_2+k_3)^3}\right), \tag{2.87}$$

from which we can calculate $f_{\rm NL}^{\dot{\pi}^3} = -\frac{5\bar{d}_1}{243}\frac{f_\pi^2}{\Lambda^2}$ (as defined in (2.24)). From the Planck bound [35] $f_{\rm NL}^{\rm equil} = -4 \pm 43$ we get the mild constraint $\Lambda > H$, where we have

assumed $\bar{d}_1 \sim 1$.[12]

2.6.2 Incorporating Gauge-Higgs Theory into the Goldstone Effective Description

We now couple the EFT to a gauge-Higgs theory and focus on inflaton-h and inflaton-Z couplings in turns, and discuss the estimates of NG.

2.6.2.1 Visibility of a Higgs Scalar

When we include the Gauge-Higgs theory in the EFT we encounter a new dimension-3 operator that we can write down on the fixed time slice,

$$\lambda_1 \mathcal{H}^\dagger D^0 \mathcal{H}. \tag{2.88}$$

After introducing $\pi(x)$ this gives rise to

$$\mathcal{H}^\dagger D^0 \mathcal{H} \to \mathcal{H}^\dagger D^0 \mathcal{H} + \frac{1}{f_\pi^2} \partial_\mu \pi_c \mathcal{H}^\dagger D^\mu \mathcal{H}. \tag{2.89}$$

The first term on the RHS gives, apart from some tadpoles which are safe in the sense discussed in subsection 2.5.2, a modification to the Higgs quadratic term h^2, a quadratic mixing between h and Z^0 and a cubic interaction between h and Z^0. The second term also gives a cubic interaction between inflaton, h and Z^0. However, it

[12] Of course the Planck analysis did not use exactly the shape of NG in (2.87). However, the equilateral template [76] they did use is "close" enough to (2.87), as measured by the standard "cosine" parameter [77].

does not couple inflaton to h alone, as can be seen by using the equation of motion for the inflaton.

Thus we consider next the marginal (in terms of the canonical inflaton field as in (2.84)) operator $\lambda_2 \delta g_c^{00} \mathcal{H}^\dagger \mathcal{H}$, which upon introducing $\pi(x)$ gives

$$\lambda_2 \delta g_c^{00} \mathcal{H}^\dagger \mathcal{H} \to \frac{1}{2} \lambda_2 \dot{\pi}_c (v^2 + 2hv + h^2). \tag{2.90}$$

For $v \sim H$ and $\lambda_2 < 1$, the inflaton tadpole above is safe again in the same sense as discussed in subsection 2.5.2.

At subsequent orders we have,

$$\begin{aligned}
&\frac{d_1}{\Lambda} \delta g_c^{00} \mathcal{H}^\dagger D^0 \mathcal{H} \to -\frac{\mathrm{Re}(d_1) v}{2\Lambda} \dot{\pi}_c \dot{h} - \frac{\mathrm{Re}(d_1)}{2\Lambda} \dot{\pi}_c h \dot{h} + \frac{\mathrm{Re}(d_1) v}{2\Lambda f_\pi^2} \dot{\pi}_c \partial_\mu \pi_c \partial^\mu h + \cdots , \\
&\frac{d_2}{\Lambda^2} (\delta g_c^{00})^2 \mathcal{H}^\dagger \mathcal{H} \to \frac{d_2 v^2}{2\Lambda^2} \dot{\pi}_c^2 + \frac{d_2 v}{\Lambda^2} \dot{\pi}_c^2 h + \cdots , \\
&\frac{d_3}{\Lambda^2} \delta g_c^{00} |D\mathcal{H}|^2 \to \frac{d_3}{2\Lambda^2} \dot{\pi}_c (\partial h)^2 + \cdots .
\end{aligned} \tag{2.91}$$

In the following, just for technical simplicity, we will use a set of benchmark values such that the inflaton-h quadratic mixing is predominantly given by λ_2 instead of $\mathrm{Re}(d_1)$. Then, the leading operators for Higgs-inflaton interactions have the form,

$$\lambda_2 v \dot{\pi}_c h + \frac{1}{2} \lambda_2 \dot{\pi}_c h^2 + \frac{d_2 v}{\Lambda^2} \dot{\pi}_c^2 h + \cdots . \tag{2.92}$$

Estimates of NG As before we can get quick estimates for NG given by the three diagrams shown in Fig. 2.3 (assuming $d_2 \sim 1$):

$$F_h^{\text{single}} \sim \frac{\lambda_2 v^2 f_\pi^2}{\Lambda^2}; \qquad F_h^{\text{double}} \sim \lambda_2^3 v^2 f_\pi^2; \qquad F_h^{\text{triple}} \sim \lambda_h v \lambda_2^3 v^3 f_\pi^2 \sim \lambda_2^3 v^2 f_\pi^2. \quad (2.93)$$

We see for a sample choice of parameters, $\lambda_2 \lesssim 1$, $\Lambda \lesssim 10H$ and $v \sim H$, we can easily achieve a promising $F_h \sim \mathcal{O}(1)$. Furthermore, with the above choices loop corrections are small.

2.6.2.2 Visibility of a Massive Gauge Boson

For Z we do not have any relevant or marginal pure inflaton-Z interaction. Inflaton-Z interactions coming from the term $\mathcal{H}^\dagger D^0 \mathcal{H}$ after restoring $\pi(x)$ vanish by equations of motion. So the leading inflaton-Z coupling is given by

$$\frac{d_1}{\Lambda}\delta g_c^{00}\mathcal{H}^\dagger D^0 \mathcal{H} \to -\frac{\text{Im}(d_1) m_Z v}{2\Lambda}\dot{\pi}_c Z^0 - \frac{\text{Im}(d_1) m_Z v}{2\Lambda f_\pi^2}\dot{\pi}_c \partial_\mu \pi_c Z^\mu \cdots, \quad (2.94)$$

which gives a quadratic mixing between inflaton and Z. At dimension 6 we have the operators,

$$\begin{aligned} \frac{d_3}{\Lambda^2}\delta g_c^{00}|D\mathcal{H}|^2 &\to \frac{d_3 m_Z^2}{2\Lambda^2}\dot{\pi}_c Z_\mu^2 + \cdots, \\ \frac{d_4}{\Lambda^2}\delta g_c^{00} Z_{\mu\nu}^2 &\to \frac{d_4}{\Lambda^2}\dot{\pi}_c Z_{\mu\nu}^2 + \cdots, \end{aligned} \quad (2.95)$$

where $Z_{\mu\nu}$ is the Z field strength.

We can summarize the inflaton-Z interaction as

$$-\frac{\mathrm{Im}(d_1)m_Z v}{2\Lambda}\dot{\pi}_c Z^0 - \frac{\mathrm{Im}(d_1)m_Z v}{2\Lambda f_\pi^2}\dot{\pi}_c \partial_\mu \pi_c Z^\mu + \frac{d_3 m_Z^2}{2\Lambda^2}\dot{\pi}_c Z_\mu^2 + \frac{d_4}{\Lambda^2}\dot{\pi}_c Z_{\mu\nu}^2 + \cdots . \quad (2.96)$$

Estimates of NG The estimates for the single and the double exchange diagram in Fig. 2.3 are

$$F_Z^{\text{single}} \sim \frac{v^2}{\Lambda^2}; \qquad F_Z^{\text{double}} \sim \frac{v^2 f_\pi^2}{\Lambda^4}. \quad (2.97)$$

We see for the choice $\Lambda \sim 10H$, $v \sim H$, the double exchange contribution dominates over the single exchange and can give $F_Z \sim \mathcal{O}(0.1)$. For $\Lambda \sim 5H$, $v \sim H$, $F_Z \sim \mathcal{O}(1)$. As with the case of single field slow roll, the triple exchange diagram comes out to be smaller than the single exchange diagram. It can be estimated as, $F_Z^{\text{triple}} \sim \frac{v^3}{\Lambda^3}\frac{f_\pi^2}{\Lambda^3}$.

To summarize, we have demonstrated a controlled EFT with $\Lambda \sim 5 - 10H$ can give rise to observable NG due to h and Z particles. Also, this scenario does not suffer from large destabilizing quantum corrections. In the context of slow roll inflation we saw that to see NG due to Z we had to consider a considerably heavier associated physical Higgs h, which is itself too Boltzmann-suppressed to see in NG. However in the context of the more general Goldstone description this is not necessary. That is, in the Goldstone description it is possible to see NG for both a Z and its associated h, while in single-field inflation the associated h would be too Boltzmann-suppressed to be visible. This therefore allows us to more thoroughly verify the heavy-lifting mechanism for a greater part of the gauge-Higgs spectrum.

2.7 Detailed Form of NG Mediated by h

In the previous sections we have given only crude estimates for NG due to h and Z. In this section, we derive the detailed expressions for $F(k_1, k_2, k_3)$ (2.23). We will consider the case of single-field slow-roll inflation as well as the more general effective Goldstone description of inflation.

We begin by first considering the general Goldstone description of inflation. Then, the Higgs-inflaton couplings from the previous section are (taking EFT coefficient $d_2 = 1$)

$$\lambda_2 v \dot{\pi}_c h + \frac{1}{2}\lambda_2 \dot{\pi}_c h^2 + \frac{v\dot{\pi}_c^2 h}{\Lambda^2}, \tag{2.98}$$

which gives rise to single, double and triple exchange diagrams as shown in Fig. 2.3. A similar single exchange diagram and an identical triple exchange diagram have been calculated in [21] and [18] respectively. Thus here we focus on calculating the double exchange diagram using the mixed propagator formalism developed in [78]. We also modify the existing calculation of the single exchange diagram for our particular case.

In the squeezed limit, $F(k_1, k_2, k_3)$ is only a function of $\frac{k_3}{k_1}$ and has the form

$$F = f(\mu)\left(\frac{k_3}{k_1}\right)^{\frac{3}{2}+i\mu} + f(\mu)^*\left(\frac{k_3}{k_1}\right)^{\frac{3}{2}-i\mu}. \tag{2.99}$$

Now we give the detailed expressions for $f(\mu)$ for different diagrams, leaving the details of the calculation for appendix A.2.

2.7.1 Single Exchange Diagram

As derived in appendix A.2 in (104),

$$F_h^{\text{single}} = -\frac{1}{8} \times \lambda_2 \left(\frac{v f_\pi}{\Lambda}\right)^2 \times$$
$$\Gamma\left(\frac{1}{2}+i\mu\right)^2 \Gamma(-2i\mu) \left(\frac{1}{2}+i\mu\right) \left(\frac{3}{2}+i\mu\right) (1+i\sinh(\pi\mu)) \left(\frac{k_3}{k_1}\right)^{\frac{3}{2}+i\mu} + (\mu \to -\mu). \tag{2.100}$$

The strength of the NG can be characterized by recasting the above equation as (2.99) and evaluating the quantity $\frac{5}{18}|f(\mu)|$ to conform with (2.24). We denote the resulting strength by $|f_h^{\text{single}}|$ and it is sampled in Table 2.1 for various masses for the benchmark values, $\lambda_2 = 0.2; \lambda_h = 0.5; \Lambda = 8H$.

mass	$\lvert f_h^{\text{single}} \rvert$
1.6 H	1.453
1.9 H	0.420
2.2 H	0.183

Table 2.1: NG mediated by h via single exchange diagram in effective Goldstone description.

Of course, for $m \gg H$, the NG become Boltzmann suppressed and unobservable.

We see that we can generically have $|f_h^{\text{single}}| \sim 0.1 - 1$, which can be accessible. Coming to the shape of NG, as we have mentioned before, $\frac{k_3}{k_1}$ dependence of F_h encodes the mass information of h, and to verify the heavy-lifting mechanism it is crucial to determine the mass with reasonable precision. In [11] such an analysis was done in the context of 21-cm cosmology. From their estimates, we see for

$|f_h^{\rm single}| > 0.1$ we should be able to determine the mass at 10 percent level or better.

We illustrate our results in Figs. 2.5 and 2.6.

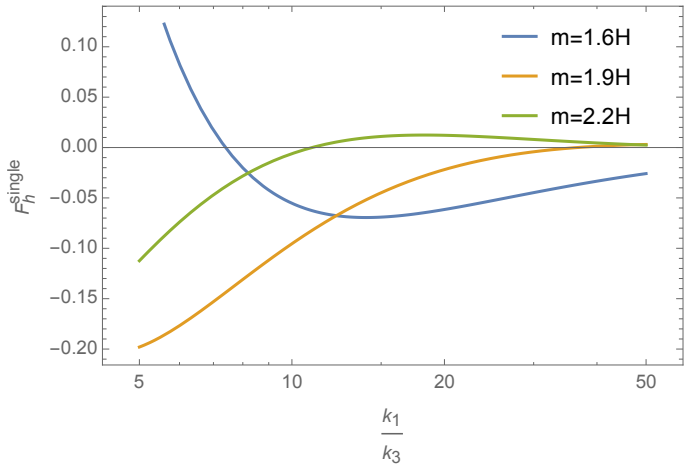

Figure 2.5: Dimensionless three-point function $F_h^{\rm single}$ (2.23) for different masses in Goldstone Effective description (104) with $\lambda_2 = 0.2; \lambda_h = 0.5; \Lambda = 8H$.

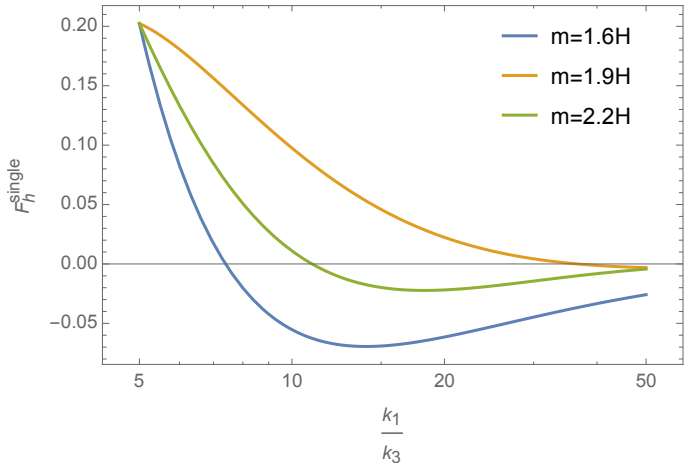

Figure 2.6: Shape sensitivity of $F_h^{\rm single}$ to m_h. We have chosen three plausible sets of parameters for which $F_h^{\rm single}$ agree at the fiducial ratio $\frac{k_1}{k_3} = 5$. This illustrates our ability to discriminate among different masses.

In the special case of single-field slow-roll inflation, the lagrangian reads from lagrangian (2.48),

$$-\rho_2 \dot{\xi} h + \frac{\alpha}{\dot{\phi}_0} \dot{\xi} h^2 + \frac{\rho_2}{2\dot{\phi}_0} (\partial \xi)^2 h \tag{2.101}$$

From the above by similar methods we find from (103),

$$F_h^{\text{single}} = -\frac{1}{4} \times \rho_2^2$$
$$\Gamma\left(\frac{1}{2}+i\mu\right)^2 \Gamma\left(-2i\mu\right)\left(\frac{3}{2}+i\mu\right)\left(\frac{5}{2}+i\mu\right)\left(1+i\sinh(\pi\mu)\right)\left(\frac{k_3}{k_1}\right)^{\frac{3}{2}+i\mu} + (\mu \to -\mu). \tag{2.102}$$

where, $\rho_2 = \frac{2c_2 v\dot{\phi}_0}{\Lambda^2}$. Now, we can again evaluate $|f_h^{\text{single}}|$ for some benchmark values, $c_2 = \frac{H}{\sqrt{\dot{\phi}_0}}, \lambda_h = \frac{H^2}{2\dot{\phi}_0}, \Lambda = 3\sqrt{\dot{\phi}_0}$ and the results are shown in Table 2.2.

mass	$\lvert f_h^{\text{single}}\rvert$
1.6 H	0.047
1.9 H	0.008
2.2 H	0.003

Table 2.2: NG mediated by h via single exchange diagram in single-field slow-roll inflation.

The above parameter choice implies classical Higgs mass tuning at the 25 percent level, and there are no large quantum corrections. For the function F_h^{single} we illustrate our results in Figs. 2.7 and 2.8.

2.7.2 Double Exchange Diagram

As derived in appendix A.2 in (117),

$$F_h^{\text{double}} = \lambda_2(\lambda_2 v f_\pi)^2 \frac{i\pi^2}{32}\left(A(\mu)s(\mu) - A^*(-\mu)s^*(-\mu)\right)\left(\frac{k_3}{k_1}\right)^{3/2}\left(\frac{k_3}{2k_1}\right)^{i\mu} + (\mu \to -\mu) \tag{2.103}$$

where, $A(\mu)$ and $s(\mu)$ are mass dependent coefficients:

$A(\mu) = -2\sqrt{2/\pi}\text{sech}(\pi\mu)\Gamma(-i\mu)\sin(\frac{\pi}{4} + \frac{i\pi\mu}{2})$; and $s(\mu)$ can be represented by the

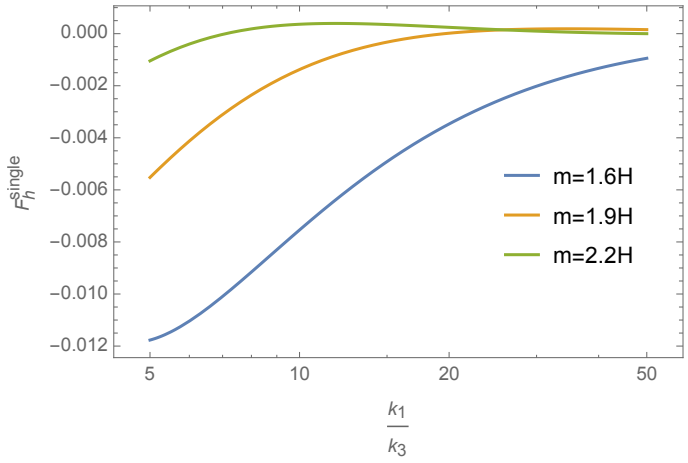

Figure 2.7: Dimensionless three-point function F_h^{single} (2.23) for different masses in Single-field Slow-roll description (103) with $c_2 = \frac{H}{\sqrt{\dot{\phi}_0}}, \lambda_h = \frac{H^2}{2\dot{\phi}_0}, \Lambda = 3\sqrt{\dot{\phi}_0}$.

integral, $s(\mu) = \int_0^\infty \frac{dx}{x^2} e^{-ix} J_+(x) x^{3/2+i\mu}$ where, $J_+(x)$ is a somewhat complicated function given in (109). We exemplify the strength of NG in Table 2.3 for the benchmark values, $\lambda_2 = 0.2; \lambda_h = 0.5$. We illustrate the momentum dependence of

mass	$\lvert f_h^{\text{double}} \rvert$
1.6 H	4.972
1.9 H	0.647
2.2 H	0.171

Table 2.3: NG mediated by h via double exchange diagram in effective Goldstone description.

F_h^{double} in Fig. 2.9 and 2.10. In the special case of single-field slow-roll inflation, using lagrangian (2.48), F_h^{double} takes an identical form to (117) except the coupling constants are now different (115),

$$F_h^{\text{double}} = \alpha \rho_2^2 \frac{i\pi^2}{16} \left(A(\mu) s(\mu) - A^*(-\mu) s^*(-\mu) \right) \left(\frac{k_3}{k_1} \right)^{3/2} \left(\frac{k_3}{2k_1} \right)^{i\mu} + (\mu \to -\mu) \tag{2.104}$$

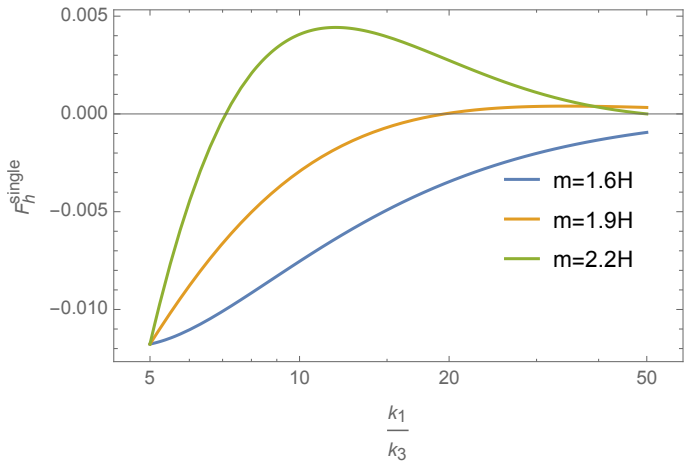

Figure 2.8: Shape sensitivity of F_h^{single} to m_h. We have chosen three plausible sets of parameters for which F_h^{single} agree at the fiducial ratio $\frac{k_1}{k_3} = 5$. This illustrates our ability to discriminate among different masses.

The strength of the NG then, for the same set of benchmark values, $c_2 = \frac{H}{\sqrt{\dot{\phi}_0}}$, $\lambda_h = \frac{H^2}{2\dot{\phi}_0}$, $\Lambda = 3\sqrt{\dot{\phi}_0}$, is shown in Table 2.4. The shape dependence is identical to Figs.

mass	$\lvert f_h^{\text{double}} \rvert$
1.6 H	0.117
1.9 H	0.015
2.2 H	0.003

Table 2.4: NG mediated by h via double exchange diagram in single-field slow-roll inflation.

2.9 and 2.10, so not shown explicitly.

2.7.3 Triple Exchange Diagram

The triple exchange diagram has been calculated in [78], but we include it here for completeness and comparison to the other diagrams. As derived in appendix A.2

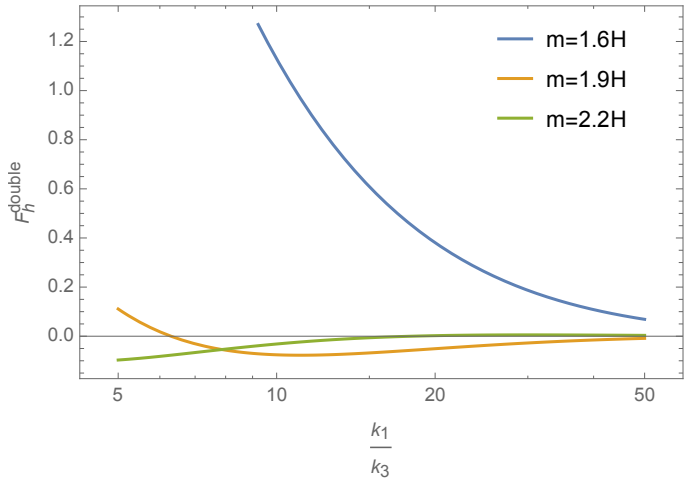

Figure 2.9: Dimensionless three-point function F_h^{double} (2.23) for different masses in Goldstone Effective description (117) with $\lambda_2 = 0.2; \lambda_h = 0.5$.

in (121),

$$F_h^{\text{triple}} = \frac{i\pi^3 \lambda_2^3 v^3 f_\pi^2 \lambda_h v}{128 \times 2^{i\mu}} \left(A(\mu)t(\mu) - A^*(-\mu)t^*(-\mu)\right) \left(\frac{k_3}{k_1}\right)^{\frac{3}{2}+i\mu} + (\mu \to -\mu), \tag{2.105}$$

where $A(\mu)$ is the same coefficient as introduced above and $t(\mu) = \int_0^\infty \frac{dx}{x^4} J_+(x)^2 x^{\frac{3}{2}+i\mu}$.

We exemplify the strength of NG below for the benchmark values, $\lambda_2 = 0.2$ and $\lambda_h = 0.5$ in Table 2.5. We illustrate the momentum dependence of F_h^{triple} in Fig.

mass	$\lvert f_h^{\text{triple}} \rvert$
1.6 H	10.1
1.9 H	0.772
2.2 H	0.148

Table 2.5: NG mediated by h via triple exchange diagram in effective Goldstone description.

2.11 and 2.12. In the special case of single-field slow-roll inflation, using lagrangian (2.48), F_h^{triple} takes an identical form except the coupling constants are now different

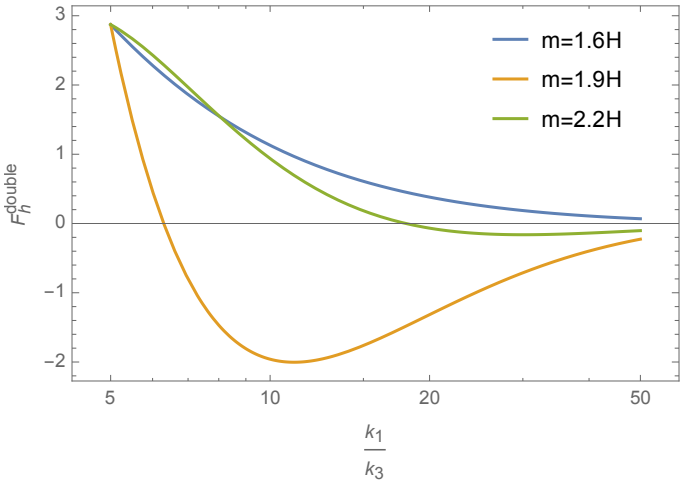

Figure 2.10: Shape sensitivity of F_h^{double} to m_h. We have chosen three plausible sets of parameters for which F_h^{double} agree at the fiducial ratio $\frac{k_1}{k_3} = 5$. This illustrates our ability to discriminate among different masses.

(120),

$$F_h^{\text{triple}} = \frac{\pi^3 \rho_2^3 \dot{\phi}_0 \lambda_h v}{128}(+i)\left(A(\mu)t(\mu) - A^*(-\mu)t^*(-\mu)\right)\left(\frac{k_3}{k_1}\right)^{\frac{3}{2}}\left(\frac{k_3}{2k_1}\right)^{i\mu} + (\mu \to -\mu) \tag{2.106}$$

The strength of the NG then, for the same set of benchmark values, $c_2 = \frac{H}{\sqrt{\dot{\phi}_0}}, \lambda_h = \frac{H^2}{2\dot{\phi}_0}, \Lambda = 3\sqrt{\dot{\phi}_0}$, is shown in Table 2.6. The shape dependence is identical to Figs.

mass	$\lvert f_h^{\text{triple}} \rvert$
1.6 H	0.239
1.9 H	0.018
2.2 H	0.003

Table 2.6: NG mediated by h via triple exchange diagram in single-field slow-roll inflation.

2.11 and 2.12, so not shown explicitly.

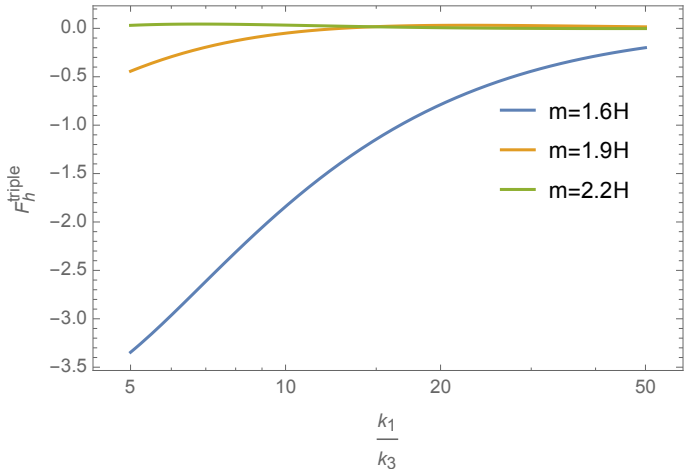

Figure 2.11: Dimensionless three-point function F_h^{triple} (2.23) for different masses in Goldstone Effective description (121) with $\lambda_2 = 0.2; \lambda_h = 0.5$.

2.8 Detailed Form of NG Mediated by Z

To discuss the form of F for NG mediated by Z, we again first focus on the Goldstone effective description as before, and specialize to the single-field slow-roll description following that. Since the triple exchange diagram is too small to make any observable contribution we will restrict ourselves to single and double exchange diagrams.

The Goldstone effective lagrangian needed for this case is given by (2.96) which we rewrite,

$$-\frac{\text{Im}(d_1)m_Z v}{2\Lambda}\dot{\pi}_c Z^0 - \frac{\text{Im}(d_1)m_Z v}{2\Lambda f_\pi^2}\dot{\pi}_c \partial_\mu \pi_c Z^\mu + \frac{d_3 m_Z^2}{2\Lambda^2}\dot{\pi}_c Z_\mu^2 + \frac{d_4}{\Lambda^2}\dot{\pi}_c Z_{\mu\nu}^2 + \cdots \quad (2.107)$$

In this case in the squeezed limit, $F(k_1, k_2, k_3)$ is a function of $\frac{k_3}{k_1}$ and also the angle

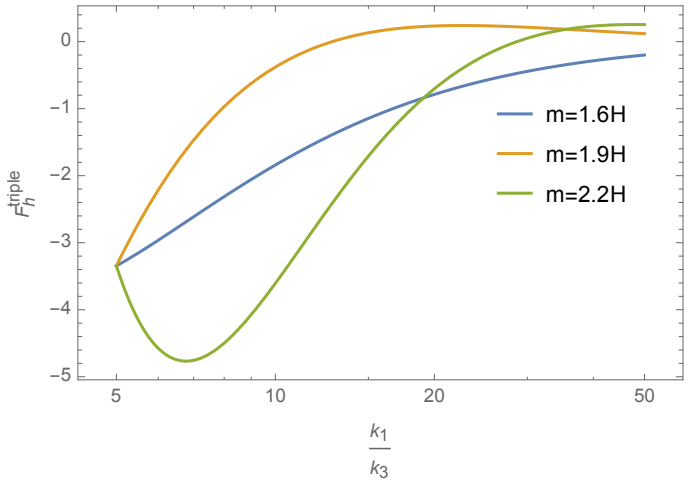

Figure 2.12: Shape sensitivity of F_h^{triple} to m_h. We have chosen three plausible sets of parameters for which F_h^{triple} agree at the fiducial ratio $\frac{k_1}{k_3} = 5$. This illustrates our ability to discriminate among different masses.

between $\hat{k}_3$ and $\hat{k}_1$,

$$F = \left(f(\mu) \left(\frac{k_3}{k_1}\right)^{\frac{5}{2}+i\mu} + f(\mu)^* \left(\frac{k_3}{k_1}\right)^{\frac{5}{2}-i\mu} \right) \sin^2\theta \tag{2.108}$$

where, $\theta = \hat{k}_3 \cdot \hat{k}_1$. We also see that F falls faster with $\frac{k_3}{k_1}$. The angle dependence, in principle, gives an important handle to determine the spin-1 nature of Z. Recently in [41] it was analyzed to what extent future galaxy surveys can constrain mass and spin. A forecast using 21-cm cosmology would also be important and possibly more constraining.

Now we give the expressions for $f(\mu)$ for the single exchange diagram, leaving the details for the appendix A.4. The computation of double exchange diagram will not be performed in this thesis, however using the mixed propagator formalism [78] it can be done. Here, we will only give some reasonable estimates.

2.8.1 Single Exchange Diagram

As derived in Appendix A.4 in (A.4),

$$F_Z^{\text{single}} = \left(\frac{v}{2\Lambda}\right)^2 \frac{1}{16\pi} \sin^2\theta \Gamma(\frac{3}{2}+i\mu)\Gamma(\frac{3}{2}-i\mu)\cosh(\pi\mu)\times$$
$$\left((7-5i\mu+16\mu^2+4i\mu^3)\Gamma(\frac{3}{2}+i\mu)^2\Gamma(-2-2i\mu)(1-i\sinh(\pi\mu))\left(\frac{k_3}{k_1}\right)^{\frac{5}{2}+i\mu} + (\mu\to-\mu)\right), \tag{2.109}$$

where, $\theta = \hat{k}_3 \cdot \hat{k}_1$. We illustrate the strength of NG, for the parameter choices, $v = 3H; \Lambda = 8H$ in Table 2.7. We see the strengths are quite weak, hence 21-cm

mass	$\lvert f_Z^{\text{single}}\rvert$
0.4 H	0.003
0.8 H	0.001

Table 2.7: NG mediated by Z via single exchange diagram in effective Goldstone description.

cosmology is critical if we are to see NG due to the single exchange diagram. Note that even an imprecise measurement should be readily distinguishable from scalar-mediated NG and NG purely due to the inflationary dynamics (analytic in $\frac{k_3}{k_1}$), due to the non-trivial angular dependence.

We now discuss single-field slow-roll inflation. The relevant lagrangian for a non-negligible Z-mediated signal arises when the associated Higgs scalar h is heavy enough that its on-shell propagation is Boltzmann suppressed, but can be integrated out to yield new Z vertices, as in (2.63). It has an identical structure to the Goldstone lagrangian (2.107) above, as shown in A.4. Hence F can be obtained

just by the replacement,

$$\frac{vm_Z}{2\Lambda} \to \frac{\rho_{1,Z}\rho_2}{m_h^2}. \tag{2.110}$$

We see for $\rho_{1,Z} = 1, \rho_2 = 1, m_h = 3H$ we have roughly the same strength of NG as the effective Goldstone theory. However, we get parametrically bigger NG in both effective theories from the double exchange diagram in Fig. 2.3, which we now discuss.

2.8.2 Double Exchange Diagram

As we mentioned above, in this thesis we will give only an estimate of the double exchange diagram. As we have explained in Sec. 2.3, in the squeezed limit diagrams factorize into contributions from hard and soft processes. This means in Fig. 2.3 (b), the Z propagator having hard momenta k_2 is expected to be a function of $\mathcal{O}(1)$ (in Hubble units). In that approximation the diagram then has the same topology as the single exchange diagram. However, as can be seen from the lagrangian (2.107), the parametric strength of the diagram goes like

$$\left(\frac{v}{2\Lambda}\right)^2 \times \frac{f_\pi^2}{\Lambda^2}, \tag{2.111}$$

which has the enhancement by $\frac{f_\pi^2}{\Lambda^2}$. Thus, while we saw that the single-exchange contribution was at best marginally detectable in the future, the double-exchange contribution should be much more promising in magnitude for $\Lambda \sim 5 - 10H$, $v \sim 2 - 3H$, with $f_Z \sim 0.1 - 1$. We leave a precise calculation of this for later work, to

hopefully confirm this expectation.

Moving to the case of single-field slow-roll inflation, from (2.63) arising from integrating out the associated heavy h, we see that the double-exchange diagram is parametrically enhanced over single-exchange by a factor of $\frac{H\dot{\phi}_0}{vm_h^2}$, so that $f_Z \sim 0.01$ for $v \sim \sqrt{\dot{\phi}_0}; m_h \sim 3H$. This should yield a weak but detectable signal.

2.9 Concluding Remarks and Future Directions

Cosmological Collider Physics builds on the distinctive non-analytic momentum dependence of primordial NG mediated by particles with masses $m \sim H$, in contrast to the analytic dependence of NG due purely to the inflationary dynamics, driven by fields with $m \ll H$. In this chapter, we focused on the question of whether gauge-theories with such ultra-high $\sim H$ mass scales could be detected by this means, since such theories are obviously very highly motivated. If the gauge symmetry is unbroken during inflation, gauge-charged states can only affect primordial NG via very small loop-level effects, difficult to observe. However, we showed that when the gauge-symmetry is (partially) Higgsed, the Higgs-type spin-0 and Z-type spin-1 bosons can contribute at *tree level* to potentially observable NG. The simplest effective vertices one can write connecting the gauge-Higgs states to the inflaton so as to mediate NG are non-renormalizable, suppressed at least by powers of the cutoff of the inflationary EFT, Λ, representing the threshold of even heavier physics that has been integrated out. The largest NG will then come by considering the lowest consistent Λ. We studied these NG within two effective descriptions

of the inflationary dynamics: a) generic slow-roll inflation models, and b) the effective Goldstone description of inflaton quantum fluctuations. In slow-roll, the minimal cutoff Λ is given by the scale of kinetic energy of the rolling inflaton field, $\sqrt{\dot{\phi}_0} \sim 60H$. The effective Goldstone description is more agnostic about inflationary dynamics, treating this as a given classical background process, in which case Λ can be as low as a few H. Of course, the detailed strengths of NG, F, that we get in the two cases are model-parameter dependent, but we can briefly summarize the results in Sections 2.7 and 2.8 in Table 2.8. The dimensionless bispectrum F

F	Goldstone EFT with $\Lambda \sim 5H$	Goldstone EFT with $\Lambda \sim 10H$	Slow-roll Models with $\Lambda \sim 60H$
h	$1-10$	$0.1-1$	$0.01-0.1$
Z	$0.1-1$	$0.01-0.1$	$0.001-0.01$

Table 2.8: Summary of strength of NG mediated by h and Z.

(see (2.22),(2.23)) given above is the maximum value taken in the squeezed regime. Based on the above table, several remarks are in order. While the above choices for EFT cutoffs lead to an observable strength of NG, we cannot make the cutoffs much bigger, since the NG falls rapidly as a function of squeezing and the observable precision is limited by cosmic variance, $\delta F \sim 10^{-4} - 10^{-3}$, (2.3). The scale of Higgsing, v, is also relevant to our theoretical control. Higgsing obviously relaxes the tight constraints of gauge invariance, allowing tree-level NG. But there are non-trivial constraints of the gauge structure following from having to expand observables in powers of v/Λ. In the UV limit $v \sim \Lambda$, the constraints of gauge-invariance disappear altogether. To stay in theoretic control, we have chosen $\frac{v}{\Lambda} \lesssim \frac{1}{3}$ in our studies.

We have used effective non-renormalizable vertices for this chapter, but it

is obviously of great interest and importance to seek a more UV-complete level of theoretical description to have greater confidence in the opportunity to detect gauge theory states in NG. We see that the strength of NG is bigger when it is mediated by h's compared to mediation by Z's. Furthermore, if cosmological collider physics turns out to be in a purely gauge-theoretic domain, then we would not see any states with spin > 1, and their associated angular dependences. Spin > 2 mediated NG would signal a breakdown of point-particle field theories, perhaps signaling the onset of string theoretic structure. On the other hand, observing spins $0, 1$ only, with stronger spin-0 signals, would give strong evidence for the structure studied above. While the (NM)SM gives only one h and one Z, extensions of it (for example, even just some colored scalars) or whole new gauge sectors are capable of giving multiple h/Z-type states to observe.

We have argued that a strong possibility for $m_{\text{gauge}-\text{theory}} \sim H$ is that they arise via a "heavy-lifting" mechanism from much lower-scale gauge theories in the current era. If these gauge theories are already seen at lower-scale terrestrial experiments, then the renormalization group allows us to predict expected mass ratios in NG. In principle, such corroboration would provide spectacular evidence for the large range of validity of such gauge theories, and the absence of intervening (coupled) states. However, we cannot hope to get a very precise measurement of such mass ratios, given cosmic variance. But if we are ever in the position to predict even a few such ratios, modestly precise measurements in NG would still be compelling. Alternatively, of course, we may discover wholly unexpected gauge-structure within the NG, at least dimly seen.

There are multiple future directions which remain to pursue. There is obviously the need for an explicit calculation of the double-exchange diagram involving Z-type particles which would provide a check for our estimates. Cosmological correlations derived from inflationary expansion are famously nearly spatially scale-invariant. But in large regimes of slow-roll inflation or in the Goldstone description, the correlators are actually nearly spatially *conformally* invariant, that is they are close to the isometries of dS spacetime. In this chapter, we have assumed this regime of inflationary dynamics. But it is possible to relax this assumption of approximate conformal invariance, and just keep approximate scale invariance, for example allowing a small speed of inflaton fluctuations, $c_s \ll 1$, which can give rise to larger NG [62, 79, 80], even allowing us to probe loop effects of charged states. This remains to be explored. There is also the generic question of how efficiently we can use NG templates to look for simultaneous presence of spin-0 and spin-1 particles, with a "background" of inflationary NG as well as late-time effects. Recent preliminary studies in these directions appear in [11, 41] which suggest that some of the stronger signals we describe above would be visible with reasonable precision.

We can view the heavy-lifting mechanism as leveraging un-naturalness, by noting that the low-dimension Higgs mass term of elementary Higgs fields is very "unstable" to curvature-related corrections. In that sense, confirming heavy-lifting of an unnatural gauge-Higgs theory, such as the (NM)SM, would be a strong sign that naturalness is massively violated in Nature. Of course, the validity of naturalness is one of the burning debates and concerns within fundamental physics. But it is also possible that terrestrial experiments show us a natural theory, such as a

supersymmetric gauge theory. One can then consider the possibility of heavy-lifting of such a natural theory. Depending on the nature of supersymmetry-breaking it is possible that the lifted gauge theory exhibits a different pattern of supersymmetry soft breaking and associated Higgsing than the unlifted theory in the current era. We leave an investigation of supersymmetric gauge-Higgs theory for the future.

We have seen that invaluable information on the gauge-theoretic structure of the laws of nature can be imprinted on cosmological NG, but we have also seen that these signals are extremely weak given cosmic variance. To have any chance of seeing and deciphering such exciting physics will require pushing experimental precision and understanding of systematic uncertainties to the their limits. Heavy-lifting indeed!

Chapter 3: Seeing Higher-Dimensional Grand Unification in Primordial Non-Gaussianities

3.1 Introduction

It is an intriguing experimental fact that the $SU(3) \times SU(2) \times U(1)$ gauge couplings, when extrapolated using the minimal Standard Model (SM) Renormalization Group Evolution (RGE), become approximately equal to each other at an energy scale $M_U \sim 10^{14}$ GeV as seen from Fig. 3.1. This can be thought of as

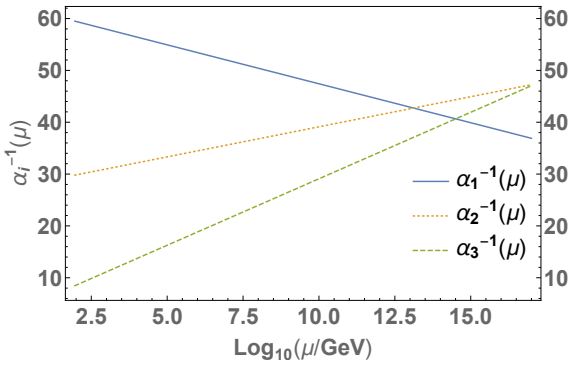

Figure 3.1: SM Renormalization Group Evolution (RGE) of gauge couplings g_i at 1-loop written in terms of $\alpha_i \equiv g_i^2/4\pi$. The label "i = 1,2,3" denotes the $U(1)$, $SU(2)$ and $SU(3)$ SM subgroups respectively with the normalization that $g_1 = \sqrt{5/3}g'$ where g' is the SM hypercharge coupling.

a strong circumstantial evidence for the attractive possibility that the SM gauge theory becomes part of a Grand Unified Theory (GUT) at that scale, as alluded to in chapter 1, characterized by a simple gauge group and a single gauge coupling.

Some imperfection in the meeting of couplings at M_U, such as is seen in Fig. 3.1, is to be expected from beyond-SM thresholds, either $\gtrsim$ TeV as in the weak scale supersymmetric (SUSY) paradigm, or from splittings $\sim M_U$. In this chapter, we consider the minimal scenario where only the non-supersymmetric SM exists in the infrared, with only M_U-scale threshold corrections from beyond the SM (BSM).

However, indirect constraints on such theories exist [81]. In the simplest GUT gauge theories such as $SU(5)$ and $SO(10)$, unified matter multiplets contain both quarks and leptons, leading to the prediction of proton decay mediated by GUT bosons. Non-observation of proton decay then puts a lower bound, $M_U \gtrsim 10^{15}$ GeV, apparently ruling out minimal SM unification. While it is possible to build purely 4D models (for e.g. see the review [82] and references therein) that evade these stringent bounds, these are somewhat intricate. On the other hand, the extra dimensional framework of orbifold GUTs (see [83, 84, 85]) offers a very simple and plausible mechanism to suppress proton decay and still achieve unification. (Also see [46, 47] for orbifold GUT inspired 4D realizations.) In their simplest incarnations, orbifold GUTs are theories where a unified gauge theory lives in a (4+1)D spacetime with the extra dimension being an interval. Boundary conditions (BC's) on the bulk gauge fields then must be specified at the two ends of the interval and it is these conditions that determine which gauge fields will have zero modes and thus be present in the low energy theory. Since BC's need not respect the complete GUT gauge invariance, a breaking GUT $\to SU(3)\times SU(2)\times U(1)$ can be achieved simply through a suitable choice of BC's. See Fig. 3.2. The unification will only be manifest when we reach energy scales $\sim M_U \sim M_{KK}$, the mass of the lightest Kaluza-Klein (KK) excitations,

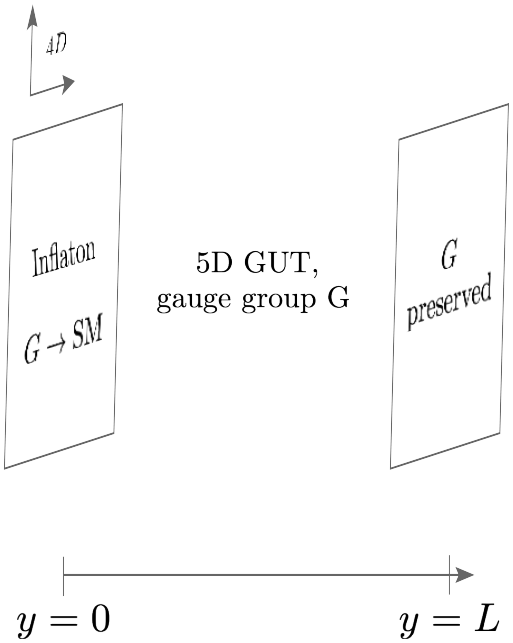

Figure 3.2: 5D spacetime having two boundaries at $y = 0$ and $y = L$. (a) Dirichlet Boundary Conditions (BC's) on the gauge bosons of GUT/SM achieves the breaking $G \to$ SM on the left boundary, also housing the inflaton $\phi(x)$. Neumann BC's on all gauge bosons preserve G on the right boundary.

that is at energies high enough to directly detect the extra dimension. The proton decay bounds can be avoided by having separate GUT multiplets for SM quarks and leptons so that conserved baryon and lepton numbers can be consistently assigned to these multiplets [86]. Again, suitable boundary conditions on these 5D fermion multiplets can be imposed such that only the SM fermions have chiral zero modes and appear in the low energy effective theory.

Without new TeV scale particles such as in SUSY or a robust proton decay signal, it seems impossible to directly test the orbifold GUT hypothesis at foreseeable colliders or other terrestrial experiments given that the non-SM states reside at $\sim M_U \sim M_{KK} \sim 10^{14}$ GeV. However, the primordial universe presents us with a unique opportunity in this regard. The Hubble scale H during an era of cosmic

inflation in the early universe could be as large as 5×10^{13} GeV [8], and hence GUT scale states having masses $M_U \sim H$ can be cosmologically produced during that era due to the time-dependence of the inflationary background. Furthermore, provided there is a suitable coupling, these states can decay into inflatons. As mentioned in chapter 1, this can, in turn, give a very distinctive non-Gaussian contribution to the spectrum of primordial curvature fluctuations $\mathcal{R}$ [18, 19, 20, 21, 24, 36, 37, 38, 40, 87, 88, 89, 90, 91], that we can probe via CMB [92, 93], LSS [41, 94, 95, 96, 97, 98, 99, 100], and 21-cm cosmology [11]. An interesting application of this idea related to the Higgs Hierarchy Problem was discussed in chapter 2. For other ideas see e.g. [43, 44, 74, 101, 102, 103, 104, 105, 106]. Chapter 2 and Refs. [43, 44, 74, 104] discussed visibility (in the sense we describe now) of (B)SM Higgs, (B)SM gauge bosons and (B)SM fermions via primordial non-Gaussianity (NG).

For the sake of completeness, let us again briefly review the structure of these non-Gaussian contributions, at the cost of being slightly repeatative. Massive fields with H-scale masses, if present during inflation with appreciable coupling to the inflaton, lead to a *non-analytic* momentum dependence of the three-point function (i.e. the bispectrum) of $\mathcal{R}$ [18, 19, 20, 21, 36, 37],

$$\langle \mathcal{R}(\vec{k}_1)\mathcal{R}(\vec{k}_2)\mathcal{R}(\vec{k}_3)\rangle \propto \mathcal{F}_s(\theta)\frac{1}{k_3^3}\frac{1}{k_1^3}\left(\frac{k_3}{k_1}\right)^{\Delta_s(m)} + \cdots, \text{ for } k_3 \ll k_1, \tag{3.1}$$

in the "squeezed" limit where one momentum is much smaller than the other two. Importantly, in eq. (3.1), the exponent $\Delta_s(m)$ and the pre-factor $\mathcal{F}_s(\theta)$, with $\theta = \vec{k}_3 \cdot \vec{k}_1$, depend on the mass ($m$) and spin ($s$) of the massive particle. For example,

for a spin-1 particle $\mathcal{F}_1(\theta) = \cos(\theta)$ and $\Delta_1(m) = \frac{5}{2} + i\sqrt{\frac{m^2}{H^2} - \frac{1}{4}}$ [40]. Thus a precise measurement of the bispectrum and its momentum dependence in the squeezed limit can capture the precious mass and spin information of the massive field. The contribution of such massive fields to the bispectrum can be represented by "in-in" diagrams, where the initial state is given approximately by the interacting Bunch-Davies de Sitter "vacuum" and the final time is essentially the end of inflation. In particular we show in Fig. 3.3 the three tree level contributions to the bispectrum which will be called single, double and triple exchange diagrams depending on the number of massive propagators.

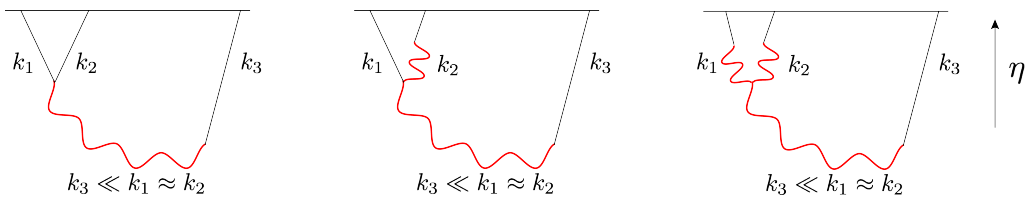

Figure 3.3: Tree level contributions to bispectrum due to massive particle exchange. From left to right: (a) single exchange diagram, (b) double exchange diagram, (c) triple exchange diagram. All the three diagrams depend on the mixing between the massive particle (in red) and the inflaton fluctuation (in black) in the (implicit) non-trivial background of slowly rolling $\phi_0(t)$. η is (conformal) time, ending at the end of inflation.

The non-analytic momentum dependence in eq. (3.1) signifies the fact that the massive particle is produced *on-shell* during inflation and its effects can not be integrated out [21]. For $m \gg H$, the non-analytic contribution to the bispectrum will be very small since cosmological, on-shell productions of such heavy particles will be "Boltzmann suppressed". This suppression is captured by the proportionality factor in eq. (3.1), which we will write out explicitly in Secs. 3.6 and 3.7. But when $m \ll H$ the non-analyticity in the three point function becomes insignificant as can

be seen from the expression of $\Delta_1(m)$ above. Hence only the regime $m \sim H$ yields both a non-trivial and observable bispectrum carrying signatures of new physics.

Thus, the above considerations show that if during inflation H is comparable to the GUT scale, then by studying primordial NG we may be able to do mass-spin spectroscopy of GUT states! A robust feature of orbifold GUTs is that at the unification scale $\sim M_{KK}$ spacetime is necessarily higher-dimensional, and therefore there must be KK graviton excitations at this scale in addition to GUT/KK gauge states. This has two important, related consequences in the scenario we are focusing on with $H \sim M_{KK}$. First, the KK graviton will also have a mass $\sim H$ and a *model independent* coupling to the inflaton, guaranteed by 5D diffeomorphism invariance. Therefore, in a set-up with orbifold GUTs, we expect to see not only the NG signatures of the GUT/KK gauge states but also striking spin-2 signatures due to KK gravitons. The second consequence is that, to describe inflationary dynamics completely, which involves energies $\sim H \sim M_{KK}$, we have to take into account the higher-dimensional geometry and cannot just focus on a 4D effective theory where all the KK modes are integrated out.

The 5D geometry brings in a subtlety. To illustrate that, first consider a set-up where the inflaton is localized on one boundary of a *semi-infinite* extra dimension. The inflationary vacuum energy backreacts significantly on the 5D geometry and an event horizon will be formed at some finite distance, characterized by H, away from the inflationary boundary [107, 108, 109, 110]. See Fig. 3.4. Although such a horizon forms quite generally, it has a particularly nice holographic interpretation via the AdS_5/CFT_4 correspondence [16] when there is a negative 5D Cosmological

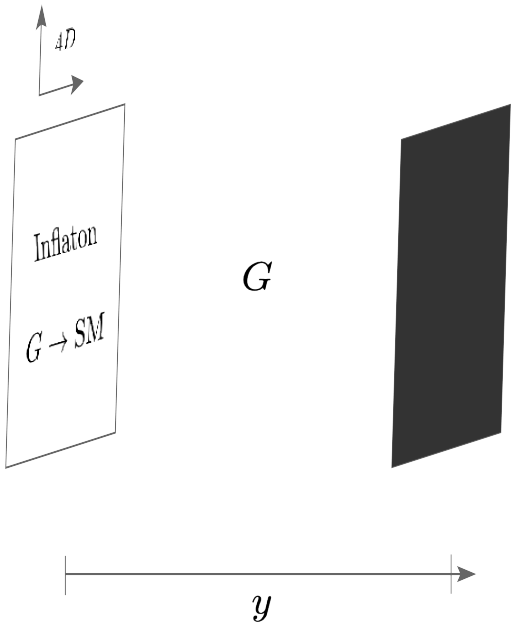

Figure 3.4: Same set-up as in Fig. 3.2 except the right boundary is absent and a "black brane" horizon has formed due to the backreaction of the inflationary vacuum energy on the left boundary.

Constant (CC) in the bulk. The 5D spacetime is given by a detuned RS2 [111] set-up [110, 112, 113], dual to a purely 4D inflationary dynamics coupled to CFT_4 self-interacting radiation. The temperature of the horizon, as we will show later, is equal to $\frac{H}{2\pi}$ which can be interpreted by the hot "AdS/CFT" correspondence (see e.g. [114]) as the temperature of the dual 4D CFT. The CFT in this case is being heated due to the Gibbons-Hawking temperature [115] of dS_4. In this case, where the extra dimension is only cut off by a horizon, the KK spectra form a *continuum* of states above a $\mathcal{O}(H)$ gap, dual to the states of the hot CFT plasma. On the other hand, we would like to do spectroscopy of a *discrete* set of KK states, in a detuned RS1 set-up [116], so we must ensure that the right boundary, in Fig. 3.2, is stabilized to appear before the horizon is reached. The 4D dual statement is that the (deformed) CFT confines in the IR, but in order to do so the Gibbons-Hawking

temperature must not exceed the deconfinement temperature. If this temperature is exceeded, the (deformed) CFT is deconfined, dual to the horizon in 5D appearing before the second boundary. We will find that there is a "window of opportunity" for doing discrete spectroscopy using NG, constrained by the need for the de Sitter temperature $H/(2\pi)$ to be below the deconfinement temperature, but not so low that cosmological production of the confined states (dual to discrete KK modes) is Boltzmann suppressed. Studying this window will be a central part of our work. It is complicated by the fact that in this regime there is a significant backreaction on the Goldberger-Wise extra-dimensional stabilization mechanism [117] for the second boundary due to the H-scale inflation. We perform a novel near-horizon analysis in which this backreaction is systematically controllable. The final strength of NG signals will also depend on the backreaction away from the near-horizon regime, but only up to $\mathcal{O}(1)$ uncertainties, which do not affect their basic observability. We hope to address these uncertainties in later work.

While the case of non-zero 5D CC offers a simple dual 4D interpretation, as above, we will mostly focus on the case of vanishing 5D CC for technical simplicity. However, the qualitative behavior is very similar to that with a CC, and the latter continues to provide good intuition for our results. Although our focus in this chapter will be on the orbifold GUTs scenario, our results related to KK gravitons and stabilization of the extra dimension are quite general and will apply whenever the size of the extra dimension is $\mathcal{O}(H^{-1})$.

This chapter is organized as follows. In Sec. 3.2 we detail the specific orbifold set-up that we will be considering in this chapter and recall some aspects of the gauge

coupling unification in orbifold GUTs. In particular, we will see that with boundary localized, non-GUT-symmetric 4D gauge kinetic terms one can easily fit the observed values of gauge couplings. In Sec. 3.3 we will briefly review the NG signals mediated by heavy particles. Sec. 3.4 focuses on various extra dimensional features of the inflationary spacetime, as alluded to above, and ends with an estimation of the strength of NG mediated by KK gravitons. Sec. 3.5 describes the inflationary couplings of the KK gauge bosons of the GUT, listing all the higher dimensional operators relevant for NG. We discuss the prospects of visibility when the GUT group is either $SU(5)$ or $SO(10)$. Secs. 3.6 and 3.7 give the explicit form of NG mediated by KK gravitons and KK gauge bosons respectively and calculate the strengths of NG. We conclude in Sec. 3.8. Two technical appendices supplement the discussion in the main text of the chapter. In Appendix B.1 we derive the KK decomposition of the KK graviton-radion system, both reproducing some of the existing results from the literature and establishing some new results that are used in Sec. 3.4. In Appendix B.2 we derive the bispectrum mediated by KK gravitons via a direct computation using the "in-in" formalism. This, as it should, reproduces the form of [21] obtained via exploiting conformal symmetries of the late time slice. Furthermore, our calculation also determines the overall normalization of the in-in correlator.

3.2 Orbifold GUTs and Gauge Coupling Unification

3.2.1 Orbifold GUTs

We consider the simplest orbifold GUT structure with a 5D bulk, and with a simple GUT gauge group such as $SO(10)$ or $SU(5)$. The 5D gauge theory is necessarily a non-renormalizable effective field theory (EFT). The extra dimension is physically an interval, although we will realize this as an $S^1/(Z_2 \times Z_2')$ quotient of a circle in order to precisely specify boundary conditions. While the 5D bulk preserves the GUT gauge symmetry, it is broken on one of the boundaries of the extra-dimensional interval (effectively Higgsed at the 5D EFT cutoff) down to just the SM gauge group. We can think of this as effectively being given by imposing Dirichlet boundary conditions (BC's) on the broken gauge fields and Neumann BC's on the unbroken (SM) gauge fields on the GUT-breaking boundary, and all-Neumann BC's on the other GUT-symmetric boundary. Lastly, we will take the SM fermions and the SM Higgs to be present in the bulk as well.

Before discussing gauge coupling unification in such a set-up, we give the explicit extra dimensional profiles of the KK modes of the bulk gauge bosons given our choice of BC's. In this section we will assume a simple fixed 5D spacetime product geometry consisting of 4D Minkowski spacetime and the extra-dimensional interval. We will account for 5D curvature in later sections, but this will not change the central structure of unification and its low-energy implications. For finding the free-field profiles we can ignore the self-interactions of the bulk non-Abelian gauge

field.

Then the equation of motion (EOM) for each gauge field component is identical to the Maxwell equations for a bulk $U(1)$ gauge field. These are given by (suppressing the adjoint index on the gauge field),

$$\partial_M F^{MN} = 0. \tag{3.2}$$

By a suitable gauge transformation we can go to the gauge where $A_5(x, y) = A_5(x)$ with y being the coordinate along the extra dimension. Furthermore, with our choice of BC's above, $A_5(x) = 0$. Hence the Maxwell equations for A_ν are given by,

$$\partial^\nu F_{\nu\mu} + \partial_y^2 A_\mu = 0. \tag{3.3}$$

Via a KK decomposition,

$$A_\mu = \sum_l A_{l,\mu}(x)\vartheta_l(y), \tag{3.4}$$

the 5D EOM (3.3) can be separated into a 4D EOM for a massive spin-1 particle and an equation governing the extra dimensional profile,

$$\partial^\nu F_{l,\nu\mu} = m_l^2 A_{l,\mu}, \tag{3.5}$$

$$\partial_y^2 \vartheta_l + m_l^2 \vartheta_l = 0. \tag{3.6}$$

Here m_l is the mass of the l-th KK mode. Using eq. (3.6) we can derive the profile

of SM and broken gauge fields (part of GUT/SM coset) for the above choice of BC's,

$$\vartheta_l^{\rm SM}(y) = \cos(l\pi y/L), \tag{3.7}$$

$$\vartheta_l^{\rm GUT/SM}(y) = \sin((l+1/2)\pi y/L), \tag{3.8}$$

with l being a non-negative integer. We have placed the boundaries at $y = 0$ and $y = L$. Taking $l = 0$ we see that only the SM gauge bosons have a zero mode, $m = 0$, whereas the lightest of GUT/SM bosons have a mass of $m = \frac{\pi}{2L}$ and hence no zero mode. This choice of BC's has broken the GUT down to the SM at the compactification scale, as expected.

3.2.2 Gauge Coupling Unification

The action for the gauge sector is given by,

$$S \supset \int d^4x \int_0^L dy \sqrt{-G} \left(\frac{1}{g_5^2} F_{MN} F^{MN} + \delta(y) \sum_i \kappa_i F_{i,\mu\nu} F_i^{\mu\nu} \right), \tag{3.9}$$

where M, N and μ, ν run over the 5D and 4D indices respectively. The first term describes the field strength for the bulk GUT gauge theory. For generality, we have also included boundary localized, *non*-GUT-symmetric 4D gauge kinetic terms, where the label "$i = 1, 2, 3$" denotes the $U(1)$, $SU(2)$ and $SU(3)$ SM subgroups. We can now relate the gauge couplings $g_{4,i}$ [1] in the 4D low energy effective theory with the 5D gauge coupling g_5. To this end, we note that the zero modes of the gauge

[1] Here we are making a small change in notation compared to Fig. 3.1 by making the replacement $g_i \to g_{4,i}$ for $i = 1, 2, 3$.

bosons have a flat profile, as seen from eq. (3.7) for $l = 0$, in the extra dimension. Then using the Lagrangian (3.9) and doing an integration over the extra dimension we get the relation between the SM gauge couplings at the compactification scale (see e.g. [85]),

$$\alpha_i^{-1}\left(\frac{1}{L}\right) \equiv \frac{4\pi}{g_{4,i}^2} = \frac{4\pi L}{g_5^2} + 4\pi\kappa_i. \tag{3.10}$$

Below the unification scale $m_{KK} \sim 1/L$, the couplings $g_{4,i}$ evolve as per the usual SM RGE which at 1-loop reads as,

$$\alpha_i^{-1}(\mu) = \frac{4\pi L}{g_5^2} + \frac{b_i}{2\pi}\log\left(\frac{m_{KK}}{\mu}\right) + 4\pi\kappa_i. \tag{3.11}$$

In the above $b_i = (\frac{41}{10}, -\frac{19}{6}, -7)$ are the three 1-loop SM beta functions with the notation that $g_{4,1} = \sqrt{5/3}g'$ where g' is the SM hypercharge coupling. This has precisely the one-loop form of a traditional 4D GUT, if we translate $\alpha_{GUT} = g_5^2/4\pi L, M_{GUT} = m_{KK}$ and the κ_i are interpreted as GUT threshold corrections. We see that for sufficiently large L and sufficiently long running, the first two terms on the right dominate, with the "threshold corrections" κ_i giving a subleading contribution. This structure then predicts that plotting $1/\alpha_i(\mu)$ vs. $\log\mu$ will give three lines almost meeting at a point, as indeed the data suggests in Fig. 3.1.[2] As a benchmark choice taking, $\kappa_1 = \frac{40}{16\pi^2}, \kappa_2 = \frac{60}{16\pi^2}$ and $\kappa_3 = \frac{1}{16\pi^2}$ we can describe the observed gauge couplings at the weak scale and achieve unification in the sense described above with,

[2]The minimal radiatively stable size of the κ_i is $\sim \frac{1}{16\pi^2}$. But it is perfectly natural for the the κ_i to take larger values, required to interpret Fig. 3.1 in the orbifold GUT scenario as we do here.

$$\alpha_G^{-1} = 39, \qquad m_{KK} = 5 \times 10^{13}\text{GeV}. \tag{3.12}$$

The lower unification scale of non-supersymmetric GUTs $\sim 10^{14}$ GeV raises the danger of an unacceptably large proton decay rate mediated by GUT states. In orbifold GUTs this is straightforwardly avoided by the mechanism of "split multiplets" whereby SM quarks and leptons are housed within different GUT multiplets, so that baryon and lepton number can be separately assigned, and unwanted fermionic zero-modes in these multiplets are removed by Dirichlet BC's on the GUT-breaking boundary [86].

3.3 Non-gaussianity and Massive Particles

In this section we briefly review NG signals arising from massive particles during inflation. For a more thorough explanation of how cosmological correlation functions are defined and the formalism used to calculate them, the reader is referred to chapter 2, along with the literature [32, 63]. Inflaton self-interactions or presence of other light fields with masses $\ll H$, can contribute to primordial NG. However, a very distinctive non-Gaussian feature of primordial fluctuations can emerge, if massive fields with $m \sim H$ are produced during inflation with sufficiently strong coupling to the inflaton, in the "squeezed" limit when one of the inflaton momenta becomes much smaller than the others (say, $k_3 \ll k_1 \sim k_2$). Depending on the mass (m) and spin (s) of such a particle, the bispectrum mediated by it will have a

non-analytic momentum dependent part of the form [18, 19, 20, 21, 36, 37, 40],

$$F_{s=0}^{\text{nonanalytic}} \propto f_0(\mu_0)\left(\frac{k_3}{k_1}\right)^{\frac{3}{2}+i\mu_0} + f_0(-\mu_0)\left(\frac{k_3}{k_1}\right)^{\frac{3}{2}-i\mu_0}, \tag{3.13}$$

$$F_{s=1}^{\text{nonanalytic}} \propto \sin^2\theta \times \left(f_1(\mu_1)\left(\frac{k_3}{k_1}\right)^{\frac{5}{2}+i\mu_1} + f_1(-\mu_1)\left(\frac{k_3}{k_1}\right)^{\frac{5}{2}-i\mu_1}\right), \tag{3.14}$$

$$F_{s=2}^{\text{nonanalytic}} \propto \left(\cos^2\theta - \tfrac{1}{3}\right) \times \left(f_2(\mu_2)\left(\frac{k_3}{k_1}\right)^{\frac{3}{2}+i\mu_2} + f_2(-\mu_2)\left(\frac{k_3}{k_1}\right)^{\frac{3}{2}-i\mu_2}\right). \tag{3.15}$$

In the above, $\mu_0 = \mu_2 = \sqrt{\frac{m^2}{H^2} - \frac{9}{4}}$ and $\mu_1 = \sqrt{\frac{m^2}{H^2} - \frac{1}{4}}$ are given in terms of the mass m of the massive particle. The spin dependence is encoded in the prefactors with $\theta = \hat{k}_1 \cdot \hat{k}_3$. The non-analytic dependence on momenta also follows from simple considerations as reviewed in chapter 2. The functions $f_s(\mu_s)$ can be calculated given the coupling between inflaton and the massive particle. For the detailed form of $f_s(\mu_s)$ see e.g. [18, 19, 20, 21, 24, 36, 37, 40, 78] for spin-0; [24] for spin-1; eq. (169) of the present thesis and [21, 40, 91] for spin-2. While the Hubble spacetime expansion can readily produce particles with masses of order H or smaller, for larger masses there is a "Boltzmann suppressed" production amplitude, generically $f_s(\mu_s) \sim e^{-\pi\mu_s} \sim e^{-\pi m/H}$ for $m \gg H$. While extra dimensions certainly give rise to higher spin particles such as our KK gravitons, with a lower bound on their masses to avoid horizon formation, there is an even more robust bound on higher spin masses in 4D dS spacetime regardless of their origin. For spin-2 this is given by the Higuchi bound, [118]. We will show that horizon non-formation is a stronger condition in the extra dimensional scenario so that the Higuchi bound is automatically satisfied.

Importantly, the non-analytic momentum dependence shown above cannot be "faked" by inflaton self-interactions since the NG contribution of the latter have

only an analytic momentum dependence in the squeezed limit—making the non-analyticity a "smoking gun" signal of new particles during inflation [21].

3.4 Inflation and the Fifth Dimension

3.4.1 General Set-up

We consider a 5D spacetime in which the extra dimension is an interval and localize a 4D inflaton on one of the boundaries at an end of the interval. Technically, we will realize this interval as an $S^1/(Z_2 \times Z_2')$ orbifold in order to determine BC's. Set-ups with boundary localized inflaton have been considered in the literature, see e.g. [109, 110, 112, 113, 119, 120, 121, 122]. We will see that for sufficiently large H the non-inflaton boundary can become shrouded by a black brane horizon, effectively leaving a set-up with a single boundary. To most simply explore this, we will also consider the limiting case of semi-infinite extra dimension.

The 5D action has the basic structure,

$$\begin{aligned} S = &\int d^4x \int_0^L dy \sqrt{-G}(2M_5^3 R_5 - \Lambda_5) - \int d^4x \int_0^L dy \sqrt{-G}\delta(y) V_0 \\ &+ \int d^4x \int_0^L dy \sqrt{-G} \left(-\delta(y-L)V_L + \left(-\frac{1}{2} G^{MN} \partial_M \Sigma \partial_N \Sigma - V(\Sigma) \right) \right), \end{aligned} \tag{3.16}$$

where the bulk metric is denoted by G_{MN} and $G = \det(G_{MN})$. R_5 is the 5D Ricci scalar. Here we have placed the boundaries at $y = 0$ and $y = L$ where y is the coordinate along the extra dimension. There are boundary-localized potentials

V_0, V_L at $y = 0$ and $y = L$ respectively. M_5 is the 5D Planck scale whereas Λ_5 is the 5D cosmological constant. We take the inflaton field to live at $y = 0$, but begin by neglecting its rolling, so that its potential is a approximately constant $V_0 \sim M_4^2 H^2$, where M_4 is the final effective 4D Planck scale. We will however consider V_L to be an exactly constant "brane tension". We also have a bulk 5D Goldberger-Wise (GW) scalar Σ [117] with a potential $V(\Sigma)$ that stabilizes the extra dimension. The case with a single boundary will be realized by taking $L \to \infty$ limit.

Requiring a dS_4 foliation (in the limit of no-rolling of the inflaton) and a static extra dimension we are lead to the ansatz,

$$ds^2 = -n(y)^2 dt^2 + n(y)^2 a(t)^2 d\vec{x}^2 + dy^2, \tag{3.17}$$

where $a(t) = e^{Ht}$ is the scale factor, and $n(y)$ is the warp factor. In the presence of dS_4 isometry, only the 00 and 55 Einstein equations are independent,

$$H^2 - n(y)n''(y) - n'(y)^2 = \frac{1}{4M_5^3}\frac{n(y)^2}{3}\left(\frac{1}{2}\Sigma'(y)^2 + V(\Sigma) + \Lambda_5\right), \tag{3.18}$$

$$n'(y)^2 - H^2 = \frac{1}{4M_5^3}\frac{n^2(y)}{6}\left(\frac{1}{2}\Sigma'(y)^2 - V(\Sigma) - \Lambda_5\right). \tag{3.19}$$

Here and in the rest of the chapter the $'$ will always denote a derivative with respect to the explicitly mentioned argument of the function. For example, $n'(y)$ and $n'(z)$ will denote $\frac{dn(y)}{dy}$ and $\frac{dn(z)}{dz}$ respectively. The Einstein equations above have to be

supplemented with BC's [3],

$$\lim_{\epsilon\to 0}\left[\frac{n'(y)}{n(y)}\right]_{-\epsilon}^{+\epsilon} = -\frac{V_0}{12M_5^3}, \tag{3.20}$$

$$\lim_{\epsilon\to 0}\left[\frac{n'(y)}{n(y)}\right]_{L-\epsilon}^{L+\epsilon} = -\frac{V_L}{12M_5^3}. \tag{3.21}$$

3.4.1.1 Gravitational Fluctuations

The inflationary dS_4 foliation necessarily "warps" the extra dimension, even when there is no bulk energy-momentum tensor. Thus the KK spectrum is also expected to be different from the non-inflationary 4D Lorentz-invariant case, with Mink_4 foliation. General gravitational fluctuations around the metric (3.17), contains the graviton $h_{\mu\nu}(x,y)$ and, in presence of the second boundary, the radion $\Pi(x,y)$. We will show in Appendix B.1 that the linearized equation of motion for the spin-2 graviton and spin-0 radion decouple for a general warp factor $n(y)$. Thus postponing the discussion of radion to a later subsection, we focus only on the 4D graviton and its KK modes for now. These fluctuations can be parametrized at the linearized level as,

$$ds^2 = -n(y)^2dt^2 + n(y)^2a(t)^2d\vec{x}^2 + dy^2 + h_{\mu\nu}(x,y)dx^\mu dx^\nu, \tag{3.22}$$

[3] We are considering the extra dimension to be a $S^1/(Z_2\times Z_2')$ orbifold which gives rise to the BC's mentioned here.

where μ, ν denote 4D indices $t, \vec{x}$. In the above we have chosen $h_{5\mu} = 0$ by a suitable gauge transformation, and $h_{\mu\nu}$ satisfies transverse and traceless conditions,

$$\nabla_\mu h^{\mu\nu} = 0; \qquad h^\mu{}_\mu = 0. \tag{3.23}$$

The equation of motion for the graviton can be obtained as [123, 124, 125] (for a derivation see Appendix B.1)

$$\Box_{dS} h_{\mu\nu}(x,y) + \left(n^2(y)\partial_y^2 - 2n'(y)^2 - 2n(y)n''(y) - 2H^2\right) h_{\mu\nu}(x,y) = 0, \tag{3.24}$$

where $\Box_{dS} = g^{\mu\nu}\nabla_\mu\nabla_\nu$ is the laplacian operator for dS_4 with $g_{\mu\nu}$ is the metric for dS_4 i.e. $ds^2_{\text{4D}} = g^{\mu\nu}dx_\mu dx_\nu = -dt^2 + a^2(t)d\vec{x}^2$. To make the KK decomposition manifest we can redefine $h_{\mu\nu} = n^2\tilde{h}_{\mu\nu}$ to get

$$\Box_{dS}\tilde{h}_{\mu\nu}(x,y) + n^2(y)\partial_y^2\tilde{h}_{\mu\nu}(x,y) + 4n(y)n'(y)\partial_y\tilde{h}_{\mu\nu}(x,y) - 2H^2\tilde{h}_{\mu\nu}(x,y) = 0. \tag{3.25}$$

Expanding $\tilde{h}_{\mu\nu}$ into KK modes $\tilde{h}_{l,\mu\nu}(x)$ with profile $\chi_l(y)$

$$\tilde{h}_{\mu\nu}(x,y) = \sum_l \tilde{h}_{l,\mu\nu}(x)\chi_l(y), \tag{3.26}$$

we get

$$\Box_{dS}\tilde{h}_{l,\mu\nu}(x) = (m^2 + 2H^2)\tilde{h}_{l,\mu\nu}(x) \tag{3.27}$$

$$n^2(y)\chi_l''(y) + 4n(y)n'(y)\chi_l'(y) + m^2\chi_l(y) = 0. \tag{3.28}$$

These describe $\tilde{h}_{l,\mu\nu}$ as spin-2 particles with mass m in dS_4. The form taken by the bulk profile is most clear in the analog 1D "quantum mechanics" coordinate system, where eq. (3.28) has the same form as Schroedinger equation with some potential determined by the warp factor $n(y)$ [111]. To achieve this, we can do a variable change $n(y)\frac{d}{dy} = \frac{d}{dz}$ and a field redefinition

$$\chi_l(z) = n^{-\frac{3}{2}}(z)\psi_l(z) \tag{3.29}$$

to get,

$$-\frac{1}{2}\frac{d^2}{dz^2}\psi_l(z) + \left(\frac{3}{8}\left(\frac{n'(z)}{n(z)}\right)^2 + \frac{3}{4}\frac{n''(z)}{n(z)}\right)\psi_l(z) = \frac{m^2}{2}\psi_l(z). \tag{3.30}$$

We note that the effect of the bulk scalar Σ comes only through the dependence on the warp factor $n(y)$ given via eqs. (3.18) and (3.19). This is because the spin-0 fluctuations of Σ cannot mix with spin-2 $h_{\mu\nu}$ at the linearized level. The zero mode profile for $m = 0$ in eq. (3.30) can be obtained for a general warp factor $n(z)$ with $\psi_0(z) \propto n^{\frac{3}{2}}(z)$.

3.4.2 Semi-Infinite Extra Dimension

We now specialize to the case in which there is only one boundary at $y = 0$, housing the inflaton. In this case, the radion is no longer in the spectrum. We therefore drop the stabilizing GW fields, and for simplicity consider vanishing 5D bulk cosmological constant. Then the warp factor $n(y)$ satisfying eqs. (3.18), (3.19) and KK graviton profile obeying eq. (3.30) simplifies significantly as we now

demonstrate.

3.4.2.1 Background Solution and the Horizon

The solution to eq. (3.18) and eq. (3.19) along with BC eq. (3.20) and normalization $n(y=0)=1$ is then given by

$$n = 1 - Hy, \tag{3.31}$$

with $V_0 = 24M_5^3 H > 0$. We see that the presence of the inflationary vacuum energy, characterized by $H \neq 0$, has "warped" the extra dimension giving rise to a horizon at $y = H^{-1}$ [109, 110].

Horizon Temperature. The temperature of the horizon can be found by studying the near horizon geometry. A variable change $\mathcal{Y} = H^{-1} - y$ shows that the line element transverse to the boundary becomes identical to a Rindler metric,

$$ds^2 = -H^2\mathcal{Y}^2 dt^2 + d\mathcal{Y}^2. \tag{3.32}$$

The temperature of this Rindler horizon can be found by the standard method of going to Euclidean time and demanding regularity of the metric at the horizon,

$$T_{\text{horizon}} = \frac{H}{2\pi}. \tag{3.33}$$

This is same as the Gibbons-Hawking temperature of dS_4 space [115]. At first, this coincidence of these temperatures is not clear.

We gain insight by considering the case with negative 5D cosmological constant $\Lambda_5 = -24M_5^3k^2$ in the bulk, which corresponds to the RS2 set-up [111], but with de-tuned boundary tension giving rise to dS_4 foliation rather than Mink_4 foliation. The bulk equations (3.18) and (3.19) can again be solved [110, 112, 113],

$$n(y) = \cosh(ky) - \frac{\sqrt{H^2 + k^2}}{k} \sinh(ky). \tag{3.34}$$

With this warp factor, we again see the presence of a horizon with an identical near horizon geometry as before and horizon temperature $T_{\text{horizon}} = \frac{H}{2\pi}$. This can be interpreted as the temperature of the 4D CFT dual to RS2, as follows from the "hot" AdS/CFT correspondence. The CFT in this case is being heated by the dS_4 Gibbons-Hawking temperature due to 4D inflation. For aspects of such "hot" AdS/CFT correspondence, see [114] and references therein.

3.4.2.2 KK Graviton Wavefunction

For now, let us return to the technically simpler case with vanishing Λ_5 (at the loss of holographic insight). Using the explicit form of the warp factor eq. (3.31) in eq. (3.30) we obtain

$$\frac{d^2}{dz^2}\psi_l(z) + (m^2 - \frac{9}{4}H^2 + \frac{V_0}{8M_5^3}\delta(z))\psi_l(z) = 0, \tag{3.35}$$

where the coordinate z is defined by $e^{-zH} = 1 - Hy$ [4]. Thus the horizon has been pushed to $z = \infty$, whereas the $y = 0$ boundary resides at $z = 0$.

Remarkably, there is a $m = 0$ normalizable and localized graviton mode,

$$\psi_0(z) \propto e^{-\frac{3}{2}Hz}, \tag{3.36}$$

corresponding to a finite 4D effective Planck scale, M_4, as we will detail later. This is similar to the RS2 graviton localization giving an effective 4D gravity despite the infinite extra dimension, but here the localization relies on 4D inflation, $H \neq 0$. Intuitively, the horizon provides a second boundary cutting off the infinite extra dimension. We also see that for $m \neq 0$ there is a mass gap of $3H/2$ and a continuum of modes for $m > 3H/2$. These modes are non-normalizable and their profile in the extra dimension is sinusoidal. This mass gap aligns nicely with the fact that a massive spin-2 particle in dS_4 has to obey the Higuchi bound [118] $m^2 \geq 2H^2$, which can be derived just by unitarity of the 4D theory. (In inflationary scenarios where the dS_4 isometries are significantly broken, the Higuchi bound can be evaded and it is consistent to have spin-2 particles with $m^2 < 2H^2$ [126].) It should be mentioned that for $\Lambda_5 < 0$, some of these features persist and have been pointed out in the literature, for e.g. [123, 124, 125].

In this chapter we will be interested in inflaton NG mediated by massive particles (with or without spin) having a *discrete* spectrum. Hence to discretize the continuum modes with $m > \frac{3H}{2}$ above, we need to reintroduce a second boundary

[4] The delta function $\delta(z)$ originates because of the R^1/Z_2 quotient of an infinite extra dimension to obtain a semi-infinite extra dimension in the present case.

before the horizon is reached at $y = H^{-1}$. We turn to this next.

3.4.3 Introduction of the Second Boundary

When the second boundary is introduced, the KK graviton wave function $\psi_l(z)$ has to obey two BC's so that the KK continuum above becomes discretized. Furthermore the radion is a physical degree of freedom and we have to stabilize it.

3.4.3.1 Radion Mass and Stabilization

We first set $\Lambda_5 = 0$ and ask what happens in the absence of a GW field. Using the metric solution, subject to dS_4 ansatz, given in eq. (3.31), and the jump equations (3.20) and (3.21) the radius of the extra dimension is determined

$$L = \frac{V_L + V_0}{V_L H}, \tag{3.37}$$

even in the absence a GW field. Note that we need to have $V_L < 0$ for there to be no horizon formed between the two boundaries. However, this dS_4-symmetric configuration is unstable as we discuss now.

We can parametrize the linearized radion fluctuation as [127]

$$ds^2 = -n(y)^2(1 - 2\Pi(x,y))dt^2 + n(y)^2a(t)^2(1 - 2\Pi(x,y))d\vec{x}^2 + (1 + 2\Xi(x,y))dy^2. \tag{3.38}$$

Although we have two seemingly independent functions, $\Pi(x,y)$ and $\Xi(x,y)$ to denote the radion, the perturbed $0i$ Einstein equations force $\Xi(x,y) = 2\Pi(x,y)$ [127].

Then the perturbed 55 Einstein equation, along with the background solution, gives the linearized radion equation of motion (for a derivation see Appendix B.1),

$$\Box_{dS}\Pi + 4H^2\Pi = 0. \tag{3.39}$$

We see that the radion has a tachyonic mass $m_r^2 = -4H^2$, signalling instability [128].

For the case of $\Lambda_5 < 0$, it is still true that $m_r^2 = -4H^2$ [129, 130, 131]. Although this can again be deduced by considering the perturbed Einstein equations, we can get the same result from a "simple" holographic insight. To this end we calculate the radius of the extra dimension via a similar procedure as above. Using eq. (3.34) and eqs. (3.20), (3.21) we get,

$$\tanh(kL) = \frac{V_0 + V_L}{24M_5^3 k + \frac{V_0 V_L}{24M_5^3 k}}. \tag{3.40}$$

To have a solution to the above equation we need $V_L < -24M_5^3 k$. Now let us write down an effective potential for the canonically normalized radion field Π_c (which is proportional to Π) on this dS_4 symmetric background. As the Goldstone boson of spontaneous conformal symmetry breaking of the CFT dual to the bulk dynamics, the only possible conformally invariant form of the radion potential is,

$$V_r(\Pi_c) = H^2\Pi_c^2 + \lambda\Pi_c^4. \tag{3.41}$$

A conformal coupling of the radion to the 4D Ricci scalar, $\mathcal{L} \supset -\frac{1}{12}R\Pi_c^2 + \cdots$ fixes the mass term above with $R = 12H^2$ for dS_4. A quartic coupling λ is also expected

to be present whenever the tension on the second boundary V_L is not equal to the tuned RS1 value of $-24M_5^3k$, with sgn(λ) being fixed by sgn($V_L + 24M_5^3k$) (see e.g. [132]). Since we needed $V_L < -24M_5^3k$ in the present case, we have $\lambda < 0$. If we now expand around the correct minima of Π_c, we get back the identical tachyonic mass $m_r^2 = -4H^2$ as before.

The tachyonic radion necessitates the presence of some stabilization mechanism. Since the tachyonic instability is $\sim -\mathcal{O}(H^2)$ and we are interested in having $m_{KK} \sim H$ for observability of NG, the stabilization will necessarily have an $\mathcal{O}(1)$ backreaction on the geometry. However, this makes the analysis technically more difficult since we have to solve coupled field equations for the GW field and the metric. Fortunately, as we discuss below, this analysis simplifies in a near-horizon approximation and yields important qualitative insights.

3.4.3.2 Near-horizon Analysis of Stabilization

We begin by noting that the observability of KK gravitons of the compactified (2-boundary) scenario is tightly constrained by purely 4D considerations: Boltzmann suppression $\sim e^{-\pi\mu}$ for large m and the Higuchi lower bound $m > \sqrt{2}H$ (following from unitarity). The former can be seen by an explicit calculation of the bispectrum due to KK graviton exchange which we carry out in Appendix B.2 and detail further in Section 3.6. In Fig. 3.5 we plot the function $f_2(\mu)$ (defined in eq. (3.90)) which characterizes the strength of NG due to KK graviton exchange and from there it is evident that significant Boltzmann suppression kicks in soon as m

gets bigger than $\frac{3H}{2}$ [5]. Hence to have an observable NG mediated by KK gravitons, we need to have their masses within a narrow window about $\frac{3H}{2}$.

Fortunately, we saw above that in the absence of a second boundary, there is a horizon at a finite proper distance $y = H^{-1}$ and a continuum of KK graviton modes starting precisely at $\frac{3H}{2}$. In the presence of a second boundary this continuum spectrum must turn into a discrete one. However if the warp factor $n(y)$ on the second boundary is $\ll 1$, i.e. if the second boundary is placed just in front of a "would-be" horizon, we expect to get back a finely discretized spectrum of KK gravitons starting around $m = 3H/2$, thereby avoiding significant Boltzmann suppression. To show this we first write the linearized warp factor near the second boundary as,

$$n(\varepsilon) \approx H\varepsilon, \tag{3.42}$$

where ε is the coordinate along the extra dimension and the horizon is reached as $\varepsilon \to 0$ [6]. Again with the coordinate transformation $-n\frac{d}{d\varepsilon} = \frac{d}{dz}$ we can write the equation of motion for the wave function in the analog 1D "quantum mechanics" coordinate system, as in eq. (3.30),

$$-\psi_l''(z) + (\frac{9H^2}{4} - m^2)\psi_l(z) = 0. \tag{3.43}$$

This form is identical to what we had in the absence of the second boundary, eq.

[5] The apparent divergence of $|f_2(\mu)|$ as $\mu \to 0$ is actually absent in the full bispectrum, since in the limit of $\mu \to 0$ only the real part of $f_2(\mu)$ contributes which remains finite.

[6] ε can be related to y once we know the warpfactor along the entire extra dimension, but in this chapter we will be solving for the warp factor only near the second boundary.

(3.35), without the delta function source [7]. However, unlike that case, now the z coordinate does not extend to ∞, but rather to some finite, but large (in units of $1/H$) value. Since $n(\varepsilon) \approx e^{-zH}$, by making the warp factor on the second boundary smaller, we can make the size of the "box" bigger in the analog quantum mechanics problem, and thereby decreasing the spacing between the KK modes.

Having motivated the need for a near-horizon boundary, we now have to ask whether such a configuration can actually be stabilized. To this end, we reintroduce a GW field Σ with a bulk mass m_Σ. Then its extra dimensional profile follows the bulk equation of motion with dS_4 ansatz,

$$\Sigma''(y) + 4n'(y)/n(y)\Sigma'(y) = m_\Sigma^2 \Sigma(y). \tag{3.44}$$

We have to solve the coupled set of equations (3.18), (3.19) and (3.44) to obtain a consistent background solution, which is difficult to do in general. But in the near-horizon limit we are interested in we can solve the coupled set of equations perturbatively in $H\varepsilon$. We take the ansatz for the warp factor and the profile to be

$$n(\varepsilon) = a_1 H\varepsilon + a_2 H^2\varepsilon^2/2 + a_3 H^3\varepsilon^3/3 + \cdots \tag{3.45}$$

$$\Sigma(\varepsilon) = b_0 + b_1 H\varepsilon + b_2 H^2\varepsilon^2/2 + b_3 H^3\varepsilon^3/3 + \cdots . \tag{3.46}$$

We will focus on the regime $H^{-1} \gg \varepsilon > \varepsilon_c$ with ε_c being the location of the second

[7] Note that by a slight abuse of notation we used the same variable z in both eqs. (3.35) and (3.43) whereas they match only very near the horizon

boundary. The solution to eqs. (3.18),(3.19) and (3.44) is given by,

$$n(\varepsilon) = H\varepsilon - \frac{1}{72}v^2 m_\Sigma^2 H\varepsilon^3 + \cdots \tag{3.47}$$

$$\Sigma(\varepsilon) = \sqrt{4M_5^3}\left(v + \frac{1}{10}vm_\Sigma^2\varepsilon^2 + \cdots\right), \tag{3.48}$$

where v is some constant fixed by the BC's on the GW field. Note when the stabilizer is absent i.e. $v = 0$, we get back the near horizon behavior given in (3.31) with $\varepsilon = H^{-1} - y$.

Now let us analyze the radion equation of motion. For this we have to consider the fluctuation $\sigma(x, y)$ of the background GW field $\Sigma(y)$, since the former can mix with the radion. We can go through the perturbed Einstein equations once again to get the equation of motion for the radion (144),

$$\frac{1}{n^2}\Box_{dS}\Pi = -\Pi'' - 2n'\Pi'/n + 4((\frac{n'}{n})^2 - \frac{n''}{n})\Pi + 2\frac{\Sigma''}{\Sigma'}(\Pi' + 2n'\Pi/n) - 6H^2\Pi/n^2. \tag{3.49}$$

In the above, we have used the bulk equation,

$$\Pi' + 2\frac{n'}{n}\Pi = \frac{1}{12M_5^3}\sigma\Sigma', \tag{3.50}$$

to eliminate σ dependence in eq. (3.49). We have also used $'$ to denote $\frac{\partial}{\partial y}$. We can now plug in the background solutions given by eqs. (3.47) and (3.48) in eq. (3.49) to find,

$$\Pi(x, \varepsilon) \propto (H\varepsilon)^{\frac{1}{2}\pm\nu} + \cdots \tag{3.51}$$

with $\nu = \sqrt{\frac{9}{4} - \frac{m_r^2}{H^2}}$. In the absence of the GW field we had to have $m_r^2 = -4H^2$ to satisfy the radion equation of motion (3.39). Now, with the stabilizer such a constraint has disappeared since eq. (3.51) is a near-horizon solution for arbitrary m_r, and with a suitable choice of BC's we can make $m_r^2 > 0$. Thus by studying the near horizon geometry, we have shown how to stabilize the radion in presence of a GW field.

We see that we can stabilize the second boundary arbitrarily close to the would-be horizon, and that this results in a finely-spaced spin-2 KK spectrum beginning arbitrarily close to $m = 3H/2$. This demonstrates that the KK modes need not suffer large Boltzmann suppressions in their NG contributions.

Before proceeding further, let us make a comment about the KK spectrum during and after inflation which we denote by $M_{KK}^{\rm inf}$ and $M_{KK}^{\rm today}$ respectively. We should note that the observed values of the SM gauge couplings suggest, within the orbifold GUT paradigm, an extra dimension with size $M_{KK}^{\rm today} \sim 10^{14}$ GeV *today*. On the other hand, an inflationary Hubble scale $H_{\rm inf} \sim 5 \times 10^{13}$ GeV is allowed by data and motivated by high-scale inflation models. Thus we see that it is entirely possible to have $M_{KK}^{\rm today} \sim H_{\rm inf}$. But this alone does not guarantee that we will see interesting and observable NG signals due to KK states, since for that we actually need $M_{KK}^{\rm inf} \sim H_{\rm inf}$. Here is where the stabilizing GW scalar plays a crucial role by determining the size of the extra dimension, in the low curvature regime given by

$$M_{KK}^{\rm today} \underset{H_{\rm today} \approx 0}{\sim} m_\Sigma \ln(v_1/v_2), \tag{3.52}$$

where the $v_{1,2}$ are the VEVs of the GW scalar on the two boundaries. Since we are considering $M_{KK}^{\text{today}} \sim 10^{14}$ GeV *today*, this implies $m_\Sigma \sim 10^{14}\text{GeV} \sim H_{\text{inf}}$. With $m_\Sigma \sim H_{\text{inf}}$, our near-horizon analysis then shows that there is no obstruction in stabilizing the non-inflaton boundary near the would-be horizon, guaranteeing $M_{KK}^{\text{inf}} \approx 3H_{\text{inf}}/2$. We can contrast this with what would have happened if either $M_{KK}^{\text{today}} \gg H_{\text{inf}}$ or $M_{KK}^{\text{today}} \ll H_{\text{inf}}$. In the former case, we would have $m_\Sigma \gg H_{\text{inf}}$, and Hubble expansion would generically[8] be subdominant in the stabilization dynamics from the time of inflation all the way until today, so that $M_{KK}^{\text{inf}} \approx M_{KK}^{\text{today}} \gg H_{\text{inf}}$, and seeing the GUT states would be highly Boltzmann suppressed. In the latter case, we would have $m_\Sigma \ll H_{\text{inf}}$, and the σ mixing terms in eq. (3.50) would be negligible, so we would approximately have the unstabilized result that the radion would be tachyonic if the boundary is near the horizon. Thus, the rough coincidence $M_{KK}^{\text{today}} \sim H_{\text{inf}}$ plays a critical role in allowing us to see the GUT states in NG.

3.4.4 Inflationary Couplings

3.4.4.1 Wavefunction of KK Graviton on Inflationary Boundary

To determine the coupling of the KK graviton to the inflaton, localized at the $y = 0$ boundary, we will need the wavefunction of the KK graviton at $y = 0$. However, we have argued above that to stabilize the radion, the backreaction of the GW field on the metric will typically be $\mathcal{O}(1)$, so that this will also affect the

[8] We can see this in eqs. (3.47) and (3.48), where the near-horizon expansion for large $m_\Sigma \gg H$ clearly requires parametrically small ϵ_c, which in turn requires ϵ_c-level tuning of parameters to stabilize. Generically there is no such tuning and hence no near-horizon stabilization for $m_\Sigma \gg H$.

KK graviton wavefunction at the $\mathcal{O}(1)$ level. In order to precisely calculate this we would have to extend our near-horizon analysis of the last subsection to the entire extra-dimensional interval. It would be interesting to find some analytic means of doing this (non-perturbative in H) , but as yet we do not have such an analysis. The superpotential approach taken in [133] may be useful in this regard. Here, we will simply estimate the KK graviton wavefunctions by ignoring the backreaction completely, but assign an $\mathcal{O}(1)$ uncertainty to this estimate.

We therefore proceed by beginning with the metric for the single boundary set-up, eq. (3.31), but taking the extra dimension to simply be cut off by the location of the second boundary at say y_c before reaching the horizon. This neglects the backreaction of the requisite stabilization of the second boundary, as discussed above. In terms of the coordinate z defined by $n\frac{d}{dy} = \frac{d}{dz}$, we have $n(z) = e^{-zH}$ with the extra dimension ranging from $z = 0$ to $z_c = -\frac{1}{H}\ln(1 - Hy_c)$. Furthermore in this coordinate system the profile of KK modes, obeying eq. (3.35), is sinusoidal. The orthonormality condition is given by

$$2M_5^3 \int_0^{z_c} dz \psi_l^*(z)\psi_m(z) = \frac{M_4^2}{2}\delta_{lm}, \tag{3.53}$$

where the numerical factor is chosen to ensure that the 4D action is given by $\frac{M_4^2}{2}\int d^4x R_4$ with R_4 and M_4 being the 4D Ricci scalar and the 4D Planck scale respectively. As will be explained below M_4 differs from the standard Planck scale $M_{\rm pl} = 2.4 \times 10^{18}$ GeV by some $\mathcal{O}(1)$ amount due to inflationary dynamics. However in the end, this difference will not be important for us because the final strength of

KK graviton NG (3.90) will be dependent on M_4 only via the tensor-to-scalar ratio r. Thus only the observational upper bound on r [8], rather than an actual knowledge of M_4, will be important. Thus in the z coordinate system, the wavefunction behaves as if it is in a flat extra dimension and after normalization, it will carry the usual "$\frac{1}{\sqrt{\text{Volume}}}$ dilution factor" (see e.g. [134]). On the boundary containing the inflaton, the wavefunction is given by,

$$\psi_l(z=0) \sim \frac{1}{\sqrt{Hz_c}} \sim \frac{1}{\sqrt{-\ln(n(y_c))}} \tag{3.54}$$

with z_c being the "volume" of the extra dimension. In the above, we have used the relation $z_c = -\frac{1}{H}\ln(1-Hy_c) = -\frac{1}{H}\ln(n(y_c))$. As we show in the following, the strength of the coupling between the inflaton and the KK graviton is proportional to $\psi_l(z=0)$ and eq. (3.54) shows that such a coupling is only logarithmically suppressed when we place the second boundary very near a would-be horizon. Crucially, this will allow us to get an observable NG signal mediated by KK gravitons, without paying a large wavefunction suppression in the coupling strength. This *logarithmic* suppression, however, seems unavoidable in our set up. This is because, although decreasing the size of the extra dimension will increase the overlap between the inflaton and the KK graviton—hence increasing the coupling—it is also expected to make the KK gravitons heavier and thereby we will incur *exponential* Boltzmann suppression in NG signals. Let us now write down the explicit inflaton-KK graviton coupling using which we estimate the strength of NG mediated by KK gravitons in the subsequent discussion.

3.4.4.2 Coupling of KK Graviton to the Inflaton

At the linear order, the graviton fluctuations couple to the energy-momentum tensor of the inflaton in the standard way, namely,

$$S_{\rm int} = \int d^4x \frac{\delta S_{inf}}{\delta g_{\mu\nu}} h_{\mu\nu} = -\frac{1}{2}\int d^4x \sqrt{-g} T^{\mu\nu}_{inf} h_{\mu\nu} \tag{3.55}$$

where we have used the definition of the energy momentum tensor $T^{\mu\nu}_{inf} = -\frac{2}{\sqrt{-g}}\frac{\delta S_{inf}}{\delta g_{\mu\nu}}$. Since we are using the convention that the warp factor $n(y=0)=1$ on the inflationary boundary, using the expansion (3.26) and eq. (3.29) we can simplify eq. (3.55) as,

$$-\frac{1}{2}\sum_{l=0}^{\infty}\int d^4x \sqrt{-g} T^{\mu\nu}_{inf} \tilde{h}_{l,\mu\nu}\psi_l(0). \tag{3.56}$$

Upon canonically normalizing [9] the massless 4D graviton and the KK modes, from the above we get,

$$-\frac{1}{M_4}\int d^4x \sqrt{-g} T^{\mu\nu}_{inf}(\tilde{h}_{0,\mu\nu} + \tilde{h}_{1,\mu\nu}\psi_1(0) + \cdots) \tag{3.57}$$

We have set $\psi_0(0)=1$ without loss of generality and focused only on the first (i.e. the lightest) KK mode for concreteness. Finally using the fact that we are in the gauge $h^{\mu}{}_{\mu}=0$ we get the coupling between the inflaton and the KK graviton,

$$-\frac{1}{M_4}\int d^4x \sqrt{-g} \partial^\mu\phi\partial^\nu\phi(\tilde{h}_{1,\mu\nu}\psi_1(0) + \cdots). \tag{3.58}$$

[9] We will continue to denote the canonically normalized KK gravitons by the same variable $\tilde{h}_{l,\mu\nu}$ to simplify the notation.

3.4.4.3 Estimate of NG Mediated by KK Graviton

Let us now give a quick estimate of the NG mediated by KK graviton using the coupling in eq. (3.58). We can expand the inflaton in terms of the background ϕ_0 and the fluctuation ξ to get,

$$-\frac{\psi_1(0)}{M_4}\tilde{h}_1^{\mu\nu}\partial_\mu\phi\partial_\nu\phi = -\frac{\psi_1(0)}{M_4}\tilde{h}_1^{\mu\nu}\left(\partial_\mu\phi_0\partial_\nu\phi_0 + 2\partial_\mu\phi_0\partial_\nu\xi + \partial_\mu\xi\partial_\nu\xi\right) \tag{3.59}$$

The first term gives a small tadpole, which can be shifted via a field redefinition without affecting the relevant couplings significantly, whereas the second term after using $\nabla_\mu h^{\mu\nu} = 0$ gives,

$$-\frac{2\psi_1(0)}{M_4}H\dot{\phi}_0\xi\tilde{h}_1^{00}. \tag{3.60}$$

Hence the relevant couplings are given by,

$$-\frac{2\psi_1(0)}{M_4}H\dot{\phi}_0\xi\tilde{h}_1^{00} - \frac{\psi_1(0)}{M_4}\tilde{h}_1^{\mu\nu}\partial_\mu\xi\partial_\nu\xi. \tag{3.61}$$

From the above we can get a quick estimate of the parametric strength of NG defined in eq. (4.6),

$$F \sim \frac{\psi_1(0)}{M_4}\times\frac{\psi_1(0)\dot{\phi}_0}{M_4}\times\frac{\dot{\phi}_0}{H^2} \sim \frac{\dot{\phi}_0^2}{M_4^2H^2}\times\psi_1(0)^2, \tag{3.62}$$

while a detailed form containing the momentum dependence as in eq. (3.15) will be given in Sec. 3.6.

The quantity $\frac{\dot{\phi}_0^2}{M_4^2H^2}$ differs by an $\mathcal{O}(1)$ factor from its standard value of 2ϵ in a purely 4D set-up [121] where $\epsilon \equiv -\frac{\dot{H}}{H^2}$. To understand why, note that ordinarily

after compactification, the 4D EFT is generally an expansion in $E/m_{KK} < 1$. In cosmology a characteristic energy scale is $E \sim H$, and in the present context we seek m_{KK} comparable to H for KK visibility in NG. Therefore we should expect $\mathcal{O}(1)$ corrections relative to the leading 4D predictions. To see this explicitly we can consider the inflaton EOM with the potential V_0 (which we previously approximated as a constant) on the inflationary boundary,

$$\ddot{\phi}_0 + 3H\dot{\phi}_0 + \frac{dV_0}{d\phi} = 0. \tag{3.63}$$

The Friedman equation, following from eq. (3.20) (with the warp factor $n(y) = 1 - Hy$) reads as,

$$\frac{1}{2}\dot{\phi}_0^2 + V_0 = 24M_5^3 H. \tag{3.64}$$

Using the relation (3.67) between M_5, M_4 and H, $M_4^2 = 4M_5^3 L\left(1 - HL + \frac{H^2L^2}{3}\right)$, and using the usual definition of $\epsilon = -\frac{\dot{H}}{H^2}$, one sees that $\frac{\dot{\phi}_0^2}{M_4^2H^2} \neq 2\epsilon$.

It will be useful to write the quantity $\frac{\dot{\phi}_0^2}{M_4^2H^2}$ in terms of the tensor to scalar ratio, r, in order to estimate the strength of the KK graviton mediated NG signals in Sec. 3.6. In our set-up, the scalar power spectrum will be unaffected, to the leading order in slow-roll parameters, by the presence of the extra dimension since the inflaton fluctuations are localized on the boundary [120, 121]. Hence r is given by,

$$r \equiv \frac{P_{T,k}}{P_{S,k}} = 8\frac{\dot{\phi}_0^2}{H^2M_4^2}. \tag{3.65}$$

In the above, we have used the tensor power spectrum, $P_{T,k} = \frac{H^2}{M_4^2}\frac{4}{k^3}$, and the scalar

power spectrum $P_{S,k} = \frac{H^4}{\dot{\phi}_0^2}\frac{1}{2k^3}$.

Now we come back to the estimate of F in eq. (3.62). As argued earlier, the wavefunction suppression above is quite mild and hence the KK graviton mediated NG is expected to be of the order of $f_{\rm NL} \sim r < 10^{-1}$. While inaccessible by future large-scale structure surveys [9], such a level of NG should be potentially observable by 21-cm experiments probing the dark ages [11] if we have a high scale inflation scenario with $H \lesssim 10^{13}$ GeV. We conclude this section by checking whether such a large value of H is consistent within our set-up.

Cutoff of 5D Gravity. To have quantum gravity corrections under control, we should have $V_0 < M_5^4$. To check that, first we recall the graviton zero mode profile given in eq. (3.36),

$$\psi_0 = e^{-\frac{3H}{2}z}, \tag{3.66}$$

and use the normalization condition in eq. (3.53) to get,

$$M_4^2 = 4M_5^3 L\left(1 - HL + \frac{H^2L^2}{3}\right) \tag{3.67}$$

In the above we have assumed the warp factor is given by $n(y) = 1 - Hy$ ignoring the backreaction of the stabilizer field. Taking $L \approx 1/H$ we get,

$$\frac{V_0}{M_5^4} = 24(4/3)^{1/3} \times (H/M_4)^{2/3} \ll 1. \tag{3.68}$$

3.5 Gauge Theory States

Whereas observing a KK graviton resonance via NG would be striking, it would be even more so if we see the accompanying signatures of massive gauge bosons. The latter can arise naturally in our set up as the KK modes of the bulk unified gauge fields. The observability of NG mediated by such KK gauge bosons will depend both on their masses and coupling to the inflaton. Interestingly, we will see below that the set-up with a near-horizon second boundary, chosen above to give us $m_{\rm KK}^{\rm graviton} \sim \mathcal{O}(H)$, also yields $m_{\rm KK}^{\rm gauge} \sim \mathcal{O}(H)$. Thus in such a set-up, the cosmological production of KK gauge bosons will not be significantly Boltzmann suppressed and the observability of KK gauge boson mediated NG will depend solely on their coupling strength to the inflaton. We start by analysing the mass spectrum of the KK gauge bosons.

3.5.1 KK Analysis of 5D Gauge Theory

Let us focus on the case of a bulk $U(1)$ gauge theory which is sufficient for finding free-field profiles of the self-interacting bulk non-Abelian gauge theory. The 5D action is given by,

$$S_{U(1)} = \int \sqrt{-G} G^{MN} G^{PQ} F_{MP} F_{NQ}, \tag{3.69}$$

where

$$ds^2 = G_{MN} dx^M dx^N = n(y)^2 g_{\mu\nu} dx^\mu dx^\nu + dy^2. \tag{3.70}$$

G_{MN} corresponds to the 5D metric governing the line element (3.17) while $g_{\mu\nu}$ denotes the metric of dS_4 in flat Poincare coordinates. M, N and μ, ν run over the 5D and 4D indices respectively.

By a suitable gauge transformation and orbifold BC's, A_y can be eliminated from the physical spectrum. The equation of motion for the gauge boson is then given by,

$$\nabla^\nu F_{\nu\mu}(x,y) + \partial_y(n^2 \partial_y A_\mu(x,y)) = 0, \tag{3.71}$$

where ∇ denotes the covariant derivative w.r.t dS_4. Via a KK decomposition,

$$A_\mu(x,y) = \sum_l A_{l,\mu}(x)\vartheta_l(y), \tag{3.72}$$

the equation of motion (3.71) can be rewritten as,

$$\nabla^\nu F_{l,\nu\mu}(x) = m_l^2 A_{l,\mu}(x), \tag{3.73}$$

$$\partial_y(n^2 \partial_y \vartheta_l(y)) + m_l^2 \vartheta_l(y) = 0. \tag{3.74}$$

Eq. (3.73) describes the usual 4D equation of motion for a massive/massless gauge field in dS_4, whereas eq. (3.74) governs the profile of the KK gauge boson in the extra dimension. With our earlier variable change, $n(y)\frac{d}{dy} = \frac{d}{dz}$, and a field redefinition

$$\vartheta_l(y) = n^{-1/2}(y)\tilde{\vartheta}_l(y), \tag{3.75}$$

we can rewrite the eq. (3.74) as,

$$\tilde{\vartheta}_l''(z) + \left(\frac{1}{4} \left(\frac{n'(z)}{n(z)} \right)^2 - \frac{1}{2} \frac{n''(z)}{n(z)} + m_l^2 \right) \tilde{\vartheta}_l(z) = 0. \tag{3.76}$$

The zero mode profile can be obtained for a general warp factor $n(z)$ and is given by $\tilde{\vartheta}_0(z) \propto n^{1/2}(z)$.

Mass Spectrum. To analyze the KK gauge boson mass spectrum we can proceed in a manner similar to the case of the KK graviton. For a moment let us go to the case where the second boundary is absent, so that the extra dimension ends in the horizon $z = \infty$. Then the warp factor (3.31) is given by $n(z) = e^{-zH}$ and correspondingly eq. (3.76) reduces to,

$$\tilde{\vartheta}_l''(z) + \left(m_l^2 - \frac{H^2}{4} \right) \tilde{\vartheta}_l(z) = 0. \tag{3.77}$$

First, note that for $m_l = 0$ we will have a zero mode whose profile is given by,

$$\tilde{\vartheta}_0(z) \propto e^{-\frac{Hz}{2}}. \tag{3.78}$$

Furthermore, we will have a continuum of KK gauge bosons above $m_l > \frac{H}{2}$. This particular lower bound is significant because if we now place the second boundary very near, but before we reach the horizon, the KK modes will get discretized and the lightest of the KK modes will have masses $\approx \frac{H}{2}$. These lightest KK modes can mediate observable NG without significant Boltzmann suppression.

Wavefunction of KK Gauge Boson on Inflationary Boundary. The coupling of the KK gauge boson to the inflaton, localized at the $y = 0$ boundary, is determined by the wavefunction of the KK gauge boson at $y = 0$. To find the wavefunction, in principle, we have to solve eq. (3.76) after the backreaction of the stabilizing GW field has been taken into account. However, using the same reasoning as in the previous section, we will simply estimate the KK gauge boson wavefunction by ignoring the effects of backreaction completely and assigning an $\mathcal{O}(1)$ uncertainty in our estimate. Under this approximation the KK gauge boson profile, obeying eq. (3.77) between the two boundaries at $z = 0$ and $z = z_c = -\frac{1}{H}\ln(n(y_c))$, behaves as if it is in a flat extra dimension. Hence the profiles will be sinusoidal and when normalized they will carry the usual "$\frac{1}{\sqrt{\text{volume}}}$ dilution factor". Thus on the boundary containing the inflaton, the KK gauge boson wavefunction is given by,

$$\tilde{\vartheta}_l'(z=0) \sim \frac{1}{\sqrt{H z_c}} \sim \frac{1}{\sqrt{-\ln(n(y_c))}}. \tag{3.79}$$

As for KK gravitons, the fact that this wavefunction suppression is only logarithmic, will allow us to get an observable NG.

3.5.2 Contribution of KK Gauge Boson to NG

Cutoff of 5D Gauge Theory. To explain the observed smallness of the slow roll parameter $\eta \sim 10^{-2}$, in the following, we will impose an (approximate) shift symmetry on the inflaton. This implies that the inflaton-gauge boson couplings will necessarily involve higher dimension operators suppressed by some field theory cutoff scale Λ_{inf}.

For consistency of the derivative expansion in $\frac{(\partial\phi)^2}{\Lambda_{\rm inf}^4}$, we require $\Lambda_{\rm inf} > \sqrt{\dot{\phi}_0} \sim 60H$ [39]. Furthermore the 5D gauge theory, being non-renormalizable, will be valid only below a certain energy scale $\Lambda_{\rm gauge}$. A naive dimensional analysis shows that such a scale is given by,

$$\Lambda_{\rm gauge} \sim \frac{1}{N}\frac{16\pi^2}{g_5^2}, \tag{3.80}$$

where N is the number of colors if the gauge group is of SU type. Note the gauge zero mode profile (3.78) is flat in the y coordinate system defined in eq. (3.17). Hence the 5D gauge coupling g_5 will be related to the 4D gauge coupling g_4 via eq. (3.10) (using $L \sim H^{-1}$),

$$\frac{1}{Hg_5^2} \sim \frac{1}{g_4^2}. \tag{3.81}$$

In the above, we have used the fact that in the near-horizon set-up we are working in, the size of the extra dimension is $\sim \frac{1}{H}$. Taking $m_{\rm KK} \sim H$ we get,

$$\frac{m_{\rm KK}}{\Lambda_{\rm gauge}} \sim \frac{g_4^2 N}{16\pi^2}. \tag{3.82}$$

As an example, with $N \sim 5$ and the gauge coupling at the unification scale, $\frac{g_4^2}{4\pi} \sim \frac{1}{40}$, (see Fig. 3.1) we get,

$$\Lambda_{\rm gauge} \sim 100H. \tag{3.83}$$

Since $\Lambda_{\rm gauge} \gtrsim \sqrt{\dot{\phi}_0} \sim 60H$ we can simply take $\Lambda_{\rm inf} \sim \Lambda_{\rm gauge} \sim 100H$ to have the derivative expansion in $\frac{(\partial\phi)^2}{\Lambda_{\rm inf}^4}$ under control. From now on we will use Λ to denote this common cut-off scale. Alternatively, we can switch to the effective theory of

inflation [62] in which the scale $\dot{\phi}_0$ does not appear, in which case a lower Λ, and consequently larger NG, is allowed. We will not pursue this direction further in this chapter.

For the choice $H \sim 5 \times 10^{13}$ GeV, motivated by the observed (approximate) unification of the gauge couplings (Fig. 3.1), we have $V_{\rm inf}^{1/4} \sim 10^{16}{\rm GeV} \gtrsim \Lambda_{\rm gauge} \sim 5 \times 10^{15}{\rm GeV}$. This suggests that the 5D gauge theory may need to be UV completed a little below the inflationary vacuum energy scale. This does not conflict with obtaining effective inflaton-gauge interactions suppressed only by Λ if these are mediated by massive states, as explored in chapter 2.

The interaction between the inflaton and KK gauge boson is constrained by the fact that we take the inflaton to be a singlet under the bulk gauge group. As a consequence, if we restrict ourselves to tree level "in-in" diagrams (for the sake of observability), the KK gauge boson must also be singlet under the broken gauge group to mediate a non-zero NG. To illustrate this restriction, we now discuss two well motivated scenarios where the unified gauge groups in the bulk are respectively $SO(10)$ and $SU(5)$.

3.5.2.1 $SO(10)$ GUT in the Bulk

In this case, with Neumann inflationary-BC's for the the SM subgroup gauge fields and Dirichlet inflationary-BC's for the remaining $SO(10)$/SM gauge fields, as well as Neumann BC's on all $SO(10)$ gauge bosons on the near-horizon boundary (preserving the entire $SO(10)$ symmetry there), we end up with only SM gauge

field zero-modes after KK reduction. We need only respect the preserved SM gauge invariance in coupling on the inflationary boundary. Under the SM gauge symmetry one of the broken generators is a singlet, corresponding to $B-L$ symmetry. The associated gauge field, which we simply denote by A_μ, can therefore be coupled to the SM-singlet inflaton, unconstrained except for spacetime symmetries. While A_μ has no zero-mode, its KK excitations can thereby mediate NG.

Inflationary Couplings of the B-L Gauge Boson. Our choice of Dirichlet BC on the inflationary boundary and the absence of restrictions imposed by gauge invariance give the following lowest dimension operators that give the *leading* contributions to NG,

$$\mathcal{L}_{\text{inf-gauge}} \supset \frac{c_1}{\Lambda^3}(\partial_y A_\nu)(\partial_y A_\mu)\nabla^\mu\nabla^\nu\phi + \frac{c_2}{\Lambda^4}(\nabla\phi)^2(\partial_y A_\mu)^2 + \frac{c_3}{\Lambda^4}(\nabla_\mu\phi\partial_y A^\mu)^2 + \\ + \frac{c_4}{\Lambda^4}(\nabla\phi)^2\nabla_\mu\phi\partial_y A^\mu + \frac{c_5}{\Lambda^4}\partial_y A^\mu\nabla_\mu\phi\partial_y A_\nu\partial_y A^\nu + \cdots \quad (3.84)$$

In the above c_i's are some coefficients of $\mathcal{O}(1)$. We have omitted a term of the type $\rho_1\nabla_\mu\phi\partial_y A_\mu$, since its effects are negligible for $\rho_1 \lesssim 1$, which is natural.

To obtain the couplings required for estimating the bispectrum, we expand the inflaton field, $\phi = \phi_0(t) + \xi(t,\vec{x})$ as before. It can be seen that $\mathcal{L}_{\text{inf-gauge}}$ contains a gauge boson tadpole coming from the term with coefficient c_4. Such a tadpole can be removed by a field redefinition, without significantly affecting the relevant couplings for the parameter choice we will be focusing on. $\mathcal{L}_{\text{inf-gauge}}$ also contains several terms of the form A_0^2 and A_μ^2. Such mass corrections also will not give a large

effect within the same parameter choice. Keeping up to cubic order in fluctuations, $\mathcal{L}_{\text{inf-gauge}}$ is then given by

$$\frac{c_1}{\Lambda^3}\left(A'^\mu A'^\nu(\partial_\mu\partial_\nu\xi-\Gamma^\alpha_{\mu\nu}\partial_\alpha\xi)\right)+\frac{2c_2}{\Lambda^4}\dot{\phi}_0\dot{\xi}A'^2_\mu+\frac{2c_3}{\Lambda^4}\dot{\phi}_0A'^0\partial_\mu\xi A'^\mu \\ +\frac{2c_4}{\Lambda^4}\dot{\phi}_0\dot{\xi}\partial_\mu\xi A'^\mu+\frac{c_4}{\Lambda^4}\dot{\phi}_0A'^0(\partial_\mu\xi)^2+\frac{2c_4}{\Lambda^4}\dot{\phi}_0^2\dot{\xi}A'^0 \\ +\frac{c_5}{\Lambda^4}\dot{\phi}_0A'^0A'^2_\nu. \quad (3.85)$$

In the above the $' \equiv \frac{\partial}{\partial y}$.

Estimates of NG. Eq. (3.85) contains interactions that can give rise to single, double and triple exchange diagrams for NG based on the number of gauge boson propagators, see Fig. 3.3. Let us estimate each of these in turn,

$$F^{\text{single}}\sim c_4^2\times\frac{\dot{\phi}_0^4}{\Lambda^8}\times\vartheta_1'(0)^2, \quad (3.86)$$

$$F^{\text{double}}\sim(c_2\text{ or }c_3)\times c_4^2\times\frac{\dot{\phi}_0^4}{\Lambda^8}\times\frac{\dot{\phi}_0^2}{\Lambda^4}\times\vartheta_1'(0)^4, \quad (3.87)$$

$$F^{\text{triple}}\sim c_5\times c_4^3\times\frac{\dot{\phi}_0^6}{\Lambda^{12}}\times\frac{\dot{\phi}_0^2}{\Lambda^4}\times\vartheta_1'(0)^6. \quad (3.88)$$

In the above we have kept the $\mathcal{O}(1)$ coefficients c_i's to be explicit about the particular couplings contributing to each of the diagrams. The fact that F^{single} is sensitive to a very high power of the cut-off scale Λ, namely $\sim\Lambda^{-8}$ implies that NG will be significantly suppressed (and, possibly unobservable) if $\Lambda\gg\sqrt{\dot{\phi}_0}$. However, we saw above that the 5D gauge theory breaks down at a scale $\Lambda_{\text{gauge}}\gtrsim\sqrt{\dot{\phi}_0}$, hence taking $\Lambda\sim\Lambda_{\text{gauge}}$ we can have $F^{\text{single}}\lesssim 1$. For the same scenario, F^{double} and F^{triple} are

somewhat smaller than $F^{\rm single}$ because of the extra suppressions due to $\vartheta_1'(0) \lesssim 1$ and $\frac{\dot{\phi}_0^2}{\Lambda^4} \lesssim 1$, but they can still be observable for favorable values of Λ and $\vartheta_1'(0)$. In Section 3.7 we will give the detailed form of NG mediated by the single exchange diagram using the results from the previous chapter 2.

3.5.2.2 $SU(5)$ GUT in the Bulk

In this case, with Neumann inflationary-BC's for the the SM subgroup gauge fields and Dirichlet inflationary-BC's for the X, Y gauge fields, as well as Neumann near-horizon BC's on all $SU(5)$ gauge bosons (preserving the entire $SU(5)$ symmetry there), we again end up with only SM gauge field zero-modes after KK reduction.

Two scenarios can arise now: (a) the SM gauge group remains unbroken at energies $\sim H$, and (b) through the presence of a non-minimal Higgs-curvature coupling $\mathcal{L} \supset cR_4\mathcal{H}^\dagger\mathcal{H},\ c > 0$ the electroweak symmetry gets spontaneously broken at inflationary scales $\sim H$. After inflation ends, the curvature effect of such a non-minimal coupling decreases rapidly and electroweak symmetry gets restored until the SM temperature falls below ~ 100 GeV. This is the scenario of "heavy-lifting" as described in chapter 2. For case (a) there are massive gauge singlets (under the unbroken SM gauge group), namely the KK excitations of hypercharge gauge boson, $B_{l,\mu}$. However because $U(1)_Y$ is *un*broken, the quadratic mixing between the inflaton and $B_{l,\mu}$—necessary for a non-zero bispectrum—will be highly suppressed. Hence the resulting bispectrum is expected to be unobservably small. But this does not mean that a bulk $SU(5)$ GUT will not have any NG signature, since for case (b),

there will be a massive Z boson. This will have $\mathcal{O}(H)$ mass for $\mathcal{O}(1)$ non-minimal coupling (i.e. $c \sim 1$) and can couple to the inflaton with appreciable strength to mediate observable NG. This type of scenario has been discussed at length in the previous chapter 2 and hence, we will not pursue it here further.

3.6 Detailed Form of NG Mediated by Spin-2

In the following we focus on the single exchange diagram, given in Fig. 3.3, for KK graviton mediated NG. Since the inflaton-KK graviton couplings are $\sim M_4$ suppressed, the double and triple exchange diagrams will be more suppressed compared to the single exchange diagram. The couplings relevant for computing this diagram can be obtained from eq. (3.61) [10],

$$-\frac{2\psi(0)}{M_4}H\dot{\phi}_0\xi h^{00} - \frac{\psi(0)}{M_4}h^{\mu\nu}\partial_\mu\xi\partial_\nu\xi, \tag{3.89}$$

and the resulting NG is given by eq. (169), (using eq. (3.65) to write $\frac{\dot{\phi}_0^2}{M_4^2H^2} = \frac{r}{8}$)

$$\begin{aligned}\frac{5}{18}F^{\text{single}}_{\text{KK Graviton}} &= \frac{5}{18}\psi(0)^2\frac{r}{8}\times(\cos^2\theta-\frac{1}{3})\frac{\sqrt{\pi}}{8(1+4\mu_2^2)^2\cosh(\pi\mu_2)}\times \\ &\left(A(\mu_2)(1+i\sinh\pi\mu_2)\left(\frac{k_3}{k_1}\right)^{3/2+i\mu_2}+(\mu_2\to-\mu_2)\right) \\ &\equiv\left(\cos^2\theta-\frac{1}{3}\right)\times\left(f_2(\mu_2)\left(\frac{k_3}{k_1}\right)^{\frac{3}{2}+i\mu_2}+f_2(-\mu_2)\left(\frac{k_3}{k_1}\right)^{\frac{3}{2}-i\mu_2}\right),\end{aligned} \tag{3.90}$$

[10] We will drop the subscript in $\psi_1(0)$ for brevity.

with

$$A(\mu) = (-27 + 120i\mu + 152\mu^2 - 32i\mu^3 + 16\mu^4)\Gamma(5/2 + i\mu)\Gamma(-i\mu)2^{-2i\mu}, \quad (3.91)$$

and $\mu_2 = \sqrt{\frac{m^2}{H^2} - \frac{9}{4}}$. The factor of $\frac{5}{18}$ is present to conform with the definition of $f_{\rm NL}$ parameter in eq. (2.24). We plot $|f_2(\mu_2)|$ in Fig. 3.5 to illustrate the strength of NG signal mediated by KK gravitons. Using the discussion following eq. (3.36), we

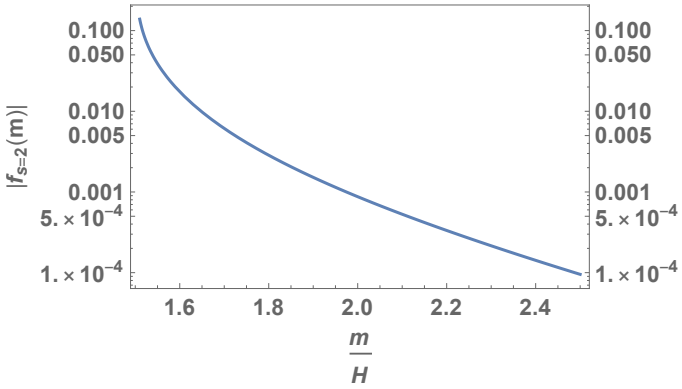

Figure 3.5: Strength of NG mediated by spin-2 KK graviton for tensor-to-scalar ratio $r = 0.1$ and KK wavefunction on inflationary boundary $\psi(0) = 1$. Such strengths for the range of masses shown are observable within cosmic variance (see Section 3.3)

see that as the non-inflaton boundary approaches the would-be horizon the effective mass parameter $\mu_2 \to 0$ [11]. We will encounter an identical feature for the case of gauge bosons in the following.

3.7 Detailed Form of NG Mediated by Spin-1

In the following we focus on the single exchange diagram for KK gauge boson mediated NG. The double and triple exchange diagrams are expected to be some-

[11] This feature persists even when there is a bulk cosmological constant, see e.g. [123, 124, 125].

what suppressed compared to the single exchange diagram, as we estimated in eqs. (3.86)-(3.88). For the single exchange diagram, the relevant couplings that give an angular dependence that is characteristic of a spin-1 exchange, can be obtained from eq. (3.85),

$$+\frac{\rho}{\dot{\phi}_0}\dot{\xi}\partial_i\xi A'^i+\rho\dot{\xi}A'^0, \tag{3.92}$$

where $\rho=\frac{2c_4}{\Lambda^4}\dot{\phi}_0^2$ gives the inflaton-KK gauge boson mixing. The resulting strength of NG has been calculated in [24] and is given by,

$$\begin{aligned}\frac{5}{18}F^{\text{single}}_{\text{KK Gauge Boson}}&=\frac{5}{18}\left(\frac{\rho}{m}\right)^2\frac{1}{16\pi}\sin^2\theta\Gamma(\frac{3}{2}+i\mu_1)\Gamma(\frac{3}{2}-i\mu_1)\cosh(\pi\mu_1)\vartheta'(0)^2\times\\&(7-5i\mu_1+16\mu_1^2+4i\mu_1^3)\Gamma(\frac{3}{2}+i\mu_1)^2\Gamma(-2-2i\mu_1)(1-i\sinh(\pi\mu_1))\left(\frac{k_3}{k_1}\right)^{\frac{5}{2}+i\mu_1}\\&+(\mu_1\to-\mu_1)\\&\equiv\sin^2\theta\times\left(f_1(\mu_1)\left(\frac{k_3}{k_1}\right)^{\frac{5}{2}+i\mu_1}+f_1(-\mu_1)\left(\frac{k_3}{k_1}\right)^{\frac{5}{2}-i\mu_1}\right),\end{aligned} \tag{3.93}$$

where $\mu_1=\sqrt{\frac{m^2}{H^2}-\frac{1}{4}}$ and $\vartheta'(0)$ is the derivative of the wavefunction of the KK gauge boson on the inflationary boundary. As in the case of KK gravitons, we plot $|f_1(\mu_1)|$ in Fig. 3.6 to illustrate the strength of NG signal mediated by KK gauge bosons. Using the discussion following eq. (3.78), we see that as the non-inflaton boundary approaches the would-be horizon the effective mass parameter $\mu_1\to 0$, similarly to the case of KK gravitons above. Furthermore, it can be seen using eq. (3.76) (which is valid for a general warp factor $n(z)$), that the above feature persists even if there is a negative bulk cosmological constant. In fact, for such a case of $\approx AdS_5$ geometry in the bulk, the non-inflaton boundary being very close to the

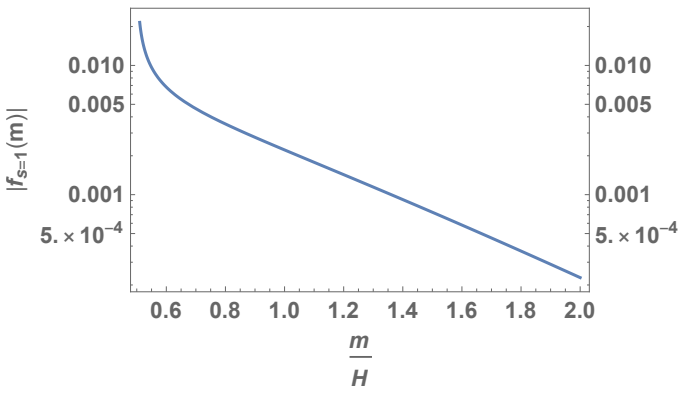

Figure 3.6: Strength of NG mediated by spin-1 KK gauge bosons for inflaton-KK mixing $\rho = 0.3$ and derivative of KK wavefunction on the inflationary boundary $\vartheta'(0) = 1$. Such strengths for the range of masses shown are observable within cosmic variance (see Section 3.3)

horizon is holographically dual to a strongly-interacting and confining matter sector, which due to the inflationary Gibbons-Hawking temperature is heated to be close to its confinement-deconfinement phase transition. We expect that there is some deep (holographic) significance to $\mu_{1,2} \to 0$ at this transition, but we have not found it beyond just direct 5D computation. A simpler and deeper understanding would also allow us to predict if $\mu \to 0$ applies to more general spins in more general models. We hope to come back to this issue in future work.

3.8 Conclusion and Future Directions

The observation that the SM gauge couplings become approximately equal to each other at $M_U \sim 10^{14}$ GeV hints at the exciting possibility of grand unification around that scale. Although such a scale is too high to directly probe using terrestrial colliders, an inflationary era in the primordial universe offers a unique opportunity in that regard. Since the inflationary Hubble scale H can be as big as

M_U, inflationary spacetime can produce such M_U-scale GUT states *on-shell* which can then decay into inflatons and give distinct, non-analytic NG contributions to the spectrum of primordial curvature perturbations, from which one can extract the masses and spins of such GUT states.

Motivated by their simplicity and the ease of suppressing proton decay, we have focused on orbifold GUTs and studied the strength of such NG signals mediated by KK GUT gauge bosons and KK gravitons. An optimal scenario is identified where the extra dimension is stabilized, via a Goldberger Wise scalar, close to the onset of a bulk event horizon such that there is a discrete KK spectrum but with small enough splittings that their production does not suffer significant Boltzmann suppression. In such a scenario, we have found that *both* the KK gravitons and KK gauge bosons can mediate potentially observable NG allowing for a unique and direct probe of orbifold GUTs. A (near) future discovery of primordial gravity waves from inflation—implying $H \sim M_U$—combined with a discovery of both spin-1 and spin-2 mediated NG signals, and an absence of higher spin signals (hinting at the absence of composite or stringy effects during inflation) would make a strong observational case for an orbifold GUT structure during inflation.

There remain various interesting directions for future work. From Figs. 3.5 and 3.6 we see that the strengths of NG—characterized by the $f_{\rm NL}$ parameter—mediated by KK gravitons and KK gauge bosons are typically $f_{\rm NL} < 0.1$. Although such a level of NG can be potentially observable using futuristic 21-cm cosmology experiments, they will be difficult to detect via upcoming Large Scale-Structure surveys which will mostly probe $f_{\rm NL} \sim \mathcal{O}(1)$ (See [9] for a summary). Hence it is

important to look for variations in our set-up in which stronger NG can be obtained. Let us briefly mention two separate possibilities in which one can get potentially larger NG mediated by KK gravitons and KK gauge bosons respectively.

We saw in Sec. 3.4 that the inflationary couplings of the KK gravitons are model independent and suppressed by the 4D Planck scale, M_4. Hence to get a larger KK graviton mediated NG, we have to increase the strength of this gravitational coupling. Fortunately, Randall Sundrum models [111, 116] already provide an example where the 4D Planck scale gets warped down, in the presence of a bulk 5D cosmological constant, as one moves towards the infrared (IR) boundary. Thus with the inflaton localized on the IR boundary or in the bulk one can expect to have stronger coupling between the inflaton and the KK graviton. However, one has to be careful as to whether the large inflationary vacuum energy stored on the IR boundary can backreact significantly on the geometry and take into account the effect of that on the KK graviton mode functions.

Interactions between the KK gauge bosons and the inflaton involve higher dimension operators suppressed by the cutoff scale Λ. This is due to the shift symmetry of the inflaton and the Dirchlet boundary conditions on the non-SM gauge fields on the inflationary boundary in Fig. 3.2. Since we described the inflationary dynamics in the paradigm of single-field slow-roll inflation we had to impose the constraint $\Lambda > \sqrt{\dot{\phi}_0} \sim 60H$. However it is possible that the single-field slow-roll paradigm is not an appropriate description of inflationary dynamics and in particular some unknown new physics comes in at energies $\Lambda_{\rm EFT} \ll \sqrt{\dot{\phi}_0}$. To capture the effects of such new physics, we can write an effective field theory (EFT), valid $\lesssim H$, for the

inflaton which is a Goldstone of the time translation breaking [62]. Within such an EFT one can parametrize the inflaton interactions systematically in an expansion in $\frac{H}{\Lambda_{\rm EFT}}$. With $\Lambda_{\rm EFT} \ll \sqrt{\dot{\phi}_0}$ one can then obtain larger KK gauge boson mediated NG signals.

We have seen that a complete description of a stabilization mechanism of the extradimensional set-up with two boundaries involves solving the coupled Einstein equations for the stabilizer field and the metric simultaneously. In general, this is difficult to do analytically. In this chapter, we have done a near-horizon analysis of stabilization by which we can systematically solve the coupled equations perturbatively, and the warp factor $n(y)$ very near the second boundary is determined that way. This allows us to compute NG but with $\mathcal{O}(1)$ uncertainties. It would therefore be very useful to find an analytic way of solving the coupled equations in the entire extra dimension. The superpotential approach taken in [133] can help in this regard. In that case, we could calculate the precise inflationary couplings of the KK modes by determining their profile in the entire extra dimension and thereby obtain a more precise calculation of the NG they mediate.

Chapter 4: Cosmological Collider Physics and the Curvaton

4.1 Introduction

In the earlier chapters 2 and 3, we discussed that $f_{\rm NL} \sim 10^{-4}$ can be taken to be the ultimate limiting strength of NG for observability. We also saw that given this lower bound, with some rare exceptions [18], many of the prime targets of the cosmological collider program such as, massive gauge bosons [24, 25, 43, 44, 74], charged scalars and fermions [24, 43, 44, 74, 104, 135, 136], Kaluza-Klein modes of the graviton [25] give rise to small, and sometimes even unobservable, strength of NG in the standard inflationary paradigm where the dynamics of inflation is *explicitly* described in terms of scalar fields. The primary goal of the present chapter is to describe a simple, alternative paradigm, in which the above mentioned NGs are naturally orders of magnitude larger, and the associated targets can naturally be brought into the scope of the cosmological collider program. Let us first understand what suppresses such NG contributions in the standard paradigm.

The inflaton (ϕ) is a light field (with mass $\ll H$) during inflation. To ensure that it remains light in the presence of potentially large radiative corrections due to heavy states, one normally imposes a shift symmetry $\phi \to \phi + c$, with c being a constant, which is broken only weakly by its potential. Under the restriction

of such a shift symmetry, the dominant coupling of ϕ to a generic operator $\mathcal{O}$ is schematically described within an effective field theory (EFT) framework as,

$$\frac{1}{\Lambda_\phi^{2n+\dim(\mathcal{O})-4}}(\partial\phi)^n\mathcal{O}, \tag{4.1}$$

where $\dim(\mathcal{O})$ is the scaling dimension of the operator $\mathcal{O}$, and Λ_ϕ is a scale by which the EFT description must break down. Strengths of such non-renormalizable couplings are thus characterized by inverse powers of Λ_ϕ, and a smaller value of Λ_ϕ implies a larger coupling, leading to a larger strength of NG. So from an observational perspective, it is important to ask how small Λ_ϕ can be while our description still remains in theoretical control. Several possible choices of Λ_ϕ exist, with varying levels of conservatism and assumptions about the ultra-violet (UV) physics. A schematic representation of the relevant scales is shown in fig. 4.1.

Due to quantum gravity effects any EFT description is expected to break down at $M_{\rm pl}$ and thus $\Lambda_\phi \sim M_{\rm pl}$ can be a reasonable choice, assuming no new physics comes in between H and $M_{\rm pl}$. With such a high value of Λ_ϕ, the strength of NG is small, but can be observable in a few cases [18, 21, 25]. Stronger NG can be obtained by taking $\Lambda_\phi \gtrsim V_{\rm inf}^{\frac{1}{4}}$ where $V_{\rm inf} \sim H^2 M_{\rm pl}^2$ is the potential energy density that drives the inflationary expansion. Such a choice of Λ_ϕ is still conservative because $V_{\rm inf}^{\frac{1}{4}}$ is the highest energy scale available during and after inflation. For example the reheat temperature, T_R, during the reheating stage at the end of inflation can be maximally $\sim V_{\rm inf}^{\frac{1}{4}}$. Thus an EFT with $\Lambda_\phi \gtrsim V_{\rm inf}^{\frac{1}{4}}$ is capable of describing the universe

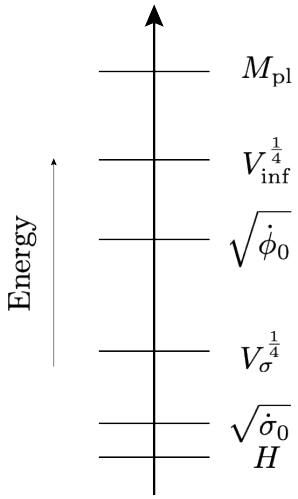

Figure 4.1: Various energy scales discussed in this chapter. H and $M_{\rm pl}$ are respectively, the inflationary Hubble scale and the Planck scale. $V_{\rm inf}^{1/4}$ and $\sqrt{\dot{\phi}_0}$ are respectively the potential and kinetic energy scales of the inflaton field. Similarly, $V_\sigma^{1/4}$ and $\sqrt{\dot{\sigma}_0}$ are respectively the potential and kinetic energy scales of the curvaton field. A sample set of values of the above scales can be obtained using the benchmark parameter point given in eq. (4.31).

both during and after inflation. Keeping this in mind, in this chapter we will take

$$\Lambda_\phi \gtrsim V_{\rm inf}^{\frac{1}{4}} > 250H, \tag{4.2}$$

where we have used the Planck constraint [8] $H/M_{\rm pl} < 2.7 \times 10^{-5}$ on tensor-to-scalar ratio. We will show later that the above restriction (4.2) implies that the NG mediated by heavy particles in several scenarios of interest are quite small or even unobservable.

We note that if one only demands theoretical control of the series of higher dimensional terms in the EFT which involve an expansion in $\frac{(\partial\phi)^2}{\Lambda_\phi^4}$, a weaker restriction of $\Lambda_\phi \gtrsim \sqrt{\dot{\phi}_0} \sim 60H$ can be obtained [39], where $\phi_0(t)$ denotes the homogeneous part of the inflaton field and we have used the fact that the scalar power spectrum

implies $\frac{H^4}{\dot{\phi}_0^2} \approx 10^{-7}$ [8]. However, such low Λ_ϕ does not explicitly capture the scalar field source of inflation, $V_{\rm inf}$. We will not pursue this less conservative Λ_ϕ here.

Even more agnostically, as discussed in chapter 4, the Goldstone effective theory of inflation [62], which describes only the cosmological *fluctuations* during inflation, but not the dynamics driving inflation, can avoid even the restriction $\Lambda_\phi \gtrsim \sqrt{\dot{\phi}_0}$. To ensure control over the description of just the fluctuations which probe energy scales $\sim H$, one need only have the EFT cut off $\Lambda_{\rm fluctuations} \gtrsim H$. One can then have stronger couplings between the inflationary fluctuations and H-mass particles, leading to significantly larger NG than what is obtained by demanding (4.2).

This Goldstone description is completely agnostic about whether such low values of $\Lambda_{\rm fluctuations}$ are consistent with higher scales such as $\sqrt{\dot{\phi}_0}$ and $V_{\rm inf}^{1/4}$ since the latter scales, which control the homogeneous background, do not even appear in the Goldstone dynamics of inflationary fluctuations. The Goldstone description simply assumes that a suitable homogeneous inflationary background is given. There do exist subtle mechanisms beyond the Goldstone description (e.g. [79, 137]) which achieve compatibility between the two sets of scales. In this chapter we explore a very simple alternative where such a compatibility is readily obtained. This is achieved by having an explicit separation of the field degrees of freedom responsible for the inflationary background and for seeding the density fluctuations. We assume that along with the inflaton field, there exists a second light field σ, the "curvaton" [138, 139, 140], whose role is to predominantly give rise to primordial fluctuations (today), whereas the role of the inflaton is reduced to just sourcing the background

expansion (with subdominant fluctuations). Then it is completely consistent to have separate EFT cutoff scales for σ and ϕ, which automatically implies separate cutoffs for inflationary fluctuations and the homogeneous background. This can then naturally, but in a controlled way, lead to large NG if the EFT scale characterizing nonrenormalizable σ interactions is parametrically smaller than the EFT cutoff of ϕ dynamics.

Concretely, one can have ϕ and σ belong to two different sectors which are sequestered from each other (say, via having different locations in an extra dimension) with each having their own EFT cutoffs, Λ_ϕ and Λ_σ respectively. Since σ does not have to drive the background expansion, its energy density V_σ can be $\ll V_{\rm inf}$. Then an argument similar to the one leading to (4.2), will only imply

$$\Lambda_\sigma \gtrsim V_\sigma^{\frac{1}{4}}, \tag{4.3}$$

while still allowing $\Lambda_\sigma \ll V_{\rm inf}^{\frac{1}{4}} < \Lambda_\phi$. Such a scenario with $\Lambda_\sigma \ll \Lambda_\phi$ can arise in several ways. One possibility is that the scale Λ_σ could represent the masses of new mediator fields which couple to σ and H-mass particles, but not to ϕ. An example along this line will be studied in sec. 4.5. Another possibility is that Λ_σ could represent a compositeness/confinement scale for the $\sigma-$sector and/or heavy fields interacting with it. Via the AdS/CFT duality, this latter scenario is dual to an extra-dimensional set-up where ϕ and σ are localized on two distinct "branes" and the extra-dimensional warping (redshifts) between the two branes explains why $\Lambda_\sigma \ll \Lambda_\phi$.

Since the two sectors are decoupled (up to gravitational effects) and can undergo separate reheating, $\Lambda_\sigma \ll V_{\rm inf}^{\frac{1}{4}}$ does not lead to a break down of the EFT description for σ at the end of inflation. If the $H-$mass particles now couple to σ, such couplings need only be suppressed by Λ_σ, instead of Λ_ϕ, and thus one can then have orders of magnitude bigger NG of primordial density fluctuations. Compared to the Goldstone EFT of inflation framework, this scenario can successfully describe inflationary and post-inflationary dynamics as will be discussed in sec. 4.3, giving us an example of a controlled field theoretic scenario having potentially larger NG than the standard paradigm.

This chapter is organized as follows. In sec. 4.2, we will set up the notation and discuss some essential aspects of the cosmological collider physics program. We will review the curvaton scenario and note the current set of observational constraints on it in sec. 4.3. The detailed analysis of the EFT couplings of the heavy particles will then be carried out, both in the standard inflationary scenario, sec. 4.4, and in the curvaton scenario, sec. 4.5. Three types of NG contribution of heavy particles—tree-level effects of spontaneously broken charged scalars (Higgs bosons), and loop-level effects of unbroken charged scalars and charged Dirac fermions will be considered. We will discuss an issue of *classical* tuning that arises in the inflationary paradigm and see that if we forego such tuning, the loop-mediated NG are unobservably small. While enhanced NG signals can be obtained with tuning, we will show that such tunings and enhancements are limited. The curvaton scenario will, on the other hand, have no such tunings but still gives rise to orders of magnitude larger NG compared to the standard inflationary scenario. In appendices C.1 and C.2 we will

calculate the NG contributions explicitly to confirm those statements. We conclude in sec. 4.6. Throughout this chapter we work in the $(-,+,+,+)$ sign convention for the spacetime metric.

As this work was being completed, ref. [141] appeared which discusses how Higgs fluctuations, different from inflaton fluctuations, can source primordial density perturbations through reheating via Higgs-modulated inflaton decay. The curvaton scenario we present here allows a larger enhancement of NG signals compared to ref. [141] and also makes the robust prediction of the strength of a "local" type of NG, $f_{\rm NL}^{\rm loc} = -5/4$, absent in ref. [141]. Nevertheless, there are some structural similarities between the present chapter and ref. [141].

4.2 Observables and cosmological collider physics

For the sake of completeness, we once again review some of the key aspects of cosmological correlation functions, at the cost of being slightly repeatative. For more details the reader is referred to secs. 2.2 and 2.3 of chapter 2. We denote the gauge invariant curvature perturbation of uniform density hypersurfaces, which will be defined below, by ζ [1], and use the primed notation to denote its momentum space correlation functions,

$$\langle \zeta(\vec{k}_1)\cdots\zeta(\vec{k}_n)\rangle = (2\pi)^3\delta^3(\vec{k}_1+\cdots+\vec{k}_n)\langle\zeta(\vec{k}_1)\cdots\zeta(\vec{k}_n)\rangle'. \tag{4.4}$$

[1] On superhorizon scales and in the presence of adiabatic perturbations, ζ coincides with the $\mathcal{R}$ variable used in chapters 2 and 3.

The power spectrum is denoted by,

$$P_k = \langle \zeta(\vec{k})\zeta(-\vec{k})\rangle'. \tag{4.5}$$

The dimensionless three point function parametrizing the strength of NG is defined as,

$$F\left(k_1, k_2, k_3\right) = \frac{\langle \zeta(\vec{k}_1)\zeta(\vec{k}_2)\zeta(\vec{k}_3)\rangle'}{P_{k_1}P_{k_3}}. \tag{4.6}$$

The function F defined above is in general momentum dependent and thus it is conventional in the literature to define an "amplitude" of NG in the equilateral limit $k_1 = k_2 = k_3$,

$$f_{\rm NL} = \frac{5}{18}F(k,k,k). \tag{4.7}$$

Using the above definition of $f_{\rm NL}$ one has a very rough estimate of the precision by which $f_{\rm NL}$ can be measured in an only-cosmic-variance limited 21-cm experiment. Such a precision is controlled only by the number of modes $N_{\text{21-cm}}$ and is given by,

$$\sigma_{f_{\rm NL}} \sim \frac{\langle\zeta^3\rangle}{\langle\zeta^2\rangle^2} \sim \frac{1}{\sqrt{N_{\text{21-cm}}}}\frac{1}{\zeta}. \tag{4.8}$$

Thus using the estimate $N_{\text{21-cm}} \sim 10^{16}$ [23], one has very roughly $\sigma_{f_{\rm NL}} \sim 10^{-4} - 10^{-3}$.

We will be interested in the so-called "squeezed limit" of F in eq. (4.6) for which $k_3 \ll k_1 \approx k_2$. In that case, F becomes a function of only $\frac{k_3}{k_1}$. In particular, heavy fields with $M \sim H$, can mediate non-analytic momentum dependence of F

of the type,

$$F_{\text{non-analytic}} \overset{k_3 \ll k_1}{=} f_s(M) \left(\frac{k_3}{k_1}\right)^{\Delta_s(M)} P_s(\cos\theta) + c.c. \tag{4.9}$$

where $\theta = \hat{k}_1 \cdot \hat{k}_3$. The functions $\Delta_s(M), f_s(M), P_s(\cos\theta)$ depend on the mass M and spin s of the heavy particle and can be calculated given its coupling to the inflaton. The prospect of extracting the mass and spin of the such heavy fields via measuring $\Delta_s(M)$ and P_s, forms the basis of cosmological collider physics. In the following, we will quantify the strength of NG by the absolute value $|f_s(M)|$.

While the time dependent inflationary spacetime readily produces particles with masses $\sim \mathcal{O}(H)$, production of heavier particles are "Boltzmann suppressed" with $f_s(M) \sim e^{-\pi M/H}$ for $M \gg H$. Furthermore, for $M \ll H$, F becomes analytically dependent on k_3 so that the distinctive non-analytic, on-shell information characterizing heavy-particle mediation is no longer apparent. For example, for a scalar particle, $\Delta_0(M) = 3/2 \pm i\sqrt{M^2/H^2 - 9/4} \to 0$ or 3 for $M \ll H$. Thus the cosmological collider program operates most efficiently in a window of heavy masses around $\sim H$ to give us on-shell mass and spin information.

4.3 Curvaton paradigm

4.3.1 Cosmological history

We will now briefly review the cosmological history in the curvaton paradigm and emphasize some of the important differences between it and the standard infla-

tionary paradigm. For more details on the curvaton paradigm, the reader is referred to the original papers [138, 139, 140].

We will model the curvaton field, σ, as a pseudo Nambu-Goldstone boson (pNGB) whose shift symmetry is broken (softly) by a mass term $m \ll H$,

$$V_\sigma = \frac{1}{2} m^2 \sigma^2. \tag{4.10}$$

Any significant interaction term involving the curvaton and another field will need to respect a shift symmetry $\sigma \to \sigma + c$ with c being some constant. Furthermore, for simplicity, we will assume that ϕ and σ belong to two separate sectors sequestered from each other (say, by different locations in an extra-dimensional geometry) and ignore any interaction between them. Thus our model is specified by the lagrangian,

$$\mathcal{L} = -\frac{1}{2}(\partial\phi)^2 - V_{\rm inf}(\phi) + \mathcal{L}^{\rm int}_\phi(\partial_\mu\phi, \{\chi\}) - \frac{1}{2}(\partial\sigma)^2 - \frac{1}{2}m^2\sigma^2 + \mathcal{L}^{\rm int}_\sigma(\partial_\mu\sigma, \{\chi\}), \tag{4.11}$$

where $V_{\rm inf}(\phi)$ is the inflaton potential and $\mathcal{L}^{\rm int}_{\phi(\sigma)}$ captures the shift-symmetric interactions of the inflaton (curvaton) with a collection of the other heavy fields $\{\chi\}$ that we will specify in sec. 4.5. During inflation, the potential energy is dominated by $V_{\rm inf}(\phi) \gg \frac{1}{2}m^2\sigma^2$ so that ϕ drives the inflationary expansion and σ acts as a spectator field.

To describe the fluctuations, we will split both the inflaton and the curvaton fields into homogeneous and fluctuating components: $\phi(t, \vec{x}) = \phi_0(t) + \delta\phi(t, \vec{x})$ and

$\sigma(t,\vec{x}) = \sigma_0(t)+\delta\sigma(t,\vec{x})$. The equations of motion (EOM) for ϕ and σ are decoupled (neglecting gravitational backreaction) and in particular, the homogeneous EOMs are given by [2],

$$\ddot{\phi}_0 + 3H\dot{\phi}_0 + V'_{\rm inf}(\phi_0) = 0, \tag{4.12}$$

$$\ddot{\sigma}_0 + 3H\dot{\sigma}_0 + m^2\sigma_0 = 0. \tag{4.13}$$

Assuming that the kinetic energy of the inflaton is much bigger than that of the curvaton, we get the standard relation,

$$\epsilon \equiv -\frac{\dot{H}}{H^2} \approx \frac{\dot{\phi}_0^2}{2H^2M_{\rm pl}^2}. \tag{4.14}$$

Since $m^2 \ll H^2$ and $\epsilon \ll 1$, the curvaton rolls very slowly along its potential, satisfying

$$\dot{\sigma}_0 \approx -\frac{m^2}{3H}\sigma_0. \tag{4.15}$$

Curvature fluctuations can be characterized by the gauge invariant quantity ζ defined by,

$$\zeta = -\psi - H\frac{\delta\rho}{\dot{\rho}_0}. \tag{4.16}$$

In the above, ψ is a spatial metric fluctuation appearing as,

$$ds^2 = ((1-2\psi)\delta_{ij} + \cdots)a^2(t)dx^i dx^j + \cdots, \tag{4.17}$$

[2] We will treat $\mathcal{L}^{\rm int}_{\phi(\sigma)}$ in a perturbative manner so that they do not affect the free EOMs at the leading order.

and we have split the density $\rho(t,\vec{x}) = \rho_0(t) + \delta\rho(t,\vec{x})$ into a homogeneous and a fluctuation part. For brevity, we have not explicitly written the other scalar, vector and tensor fluctuations. Since the inflaton dominates the energy density during inflation, the curvature perturbation when the relevant momentum modes exit the horizon, $\zeta_{\rm exit}$, is sourced only by $\delta\phi$ to a good approximation and thus, in a gauge in which $\psi = 0$,

$$\zeta_{\rm exit} \approx -H\frac{\delta\phi}{\dot{\phi}_0}. \tag{4.18}$$

One of the important features of the curvaton paradigm is that the fluctuations of the inflaton are subdominant to those of the curvaton, and in particular $\ll 10^{-5}$, the characteristic size of the observed primordial fluctuations. For example, for the benchmark set of parameters given in eq. (4.31), $\zeta_{\rm exit} \sim \frac{H^2}{2\pi\dot{\phi}_0} \sim 10^{-6}$. However, significant curvature perturbations can get generated after the end of inflation since there is a second light field σ during inflation and thus ζ need not necessarily be conserved on superhorizon scales [3]. Let us now see how this happens.

We assume that at the end of inflation, the inflaton reheats into a radiation bath largely decoupled from σ. In the meantime, σ keeps rolling very slowly along its potential until the Hubble scale $\lesssim m$, following which σ starts oscillating around its minimum and dilutes like matter. At such a point the content of the universe comprises of radiation coming from the inflaton decay, having energy density $\rho_{\rm rad}$, and matter due to the curvaton energy density ρ_σ. Thus using eq. (4.16) and using the gauge $\psi = 0$ the curvature perturbation after inflaton reheating can be written

[3] This is to be contrasted with single-field inflation where quite generally ζ remains conserved on superhorizon scales [66, 67].

as,

$$\zeta = \frac{1}{3}\frac{\delta\rho_\sigma}{\rho_\sigma} f_\sigma + \frac{1}{4}\frac{\delta\rho_{\rm rad}}{\rho_{\rm rad}}(1 - f_\sigma), \tag{4.19}$$

where $f_\sigma = \frac{3\rho_\sigma}{3\rho_\sigma + 4\rho_{\rm rad}}$ is related to the energy density in the curvaton field compared to the radiation energy density $\rho_{\rm rad}$. $\frac{\delta\rho_\sigma}{\rho_\sigma}$ and $\frac{\delta\rho_{\rm rad}}{\rho_{\rm rad}}$ are respectively fluctuations corresponding to the curvaton and the radiation (in the $\psi = 0$ gauge), and they are conserved on super-horizon scales since the two fluids do not interact with each other, other than via gravity which is weak on these scales. Since the radiation bath originates from the inflaton decay, we will have $\frac{1}{4}\frac{\delta\rho_{\rm rad}}{\rho_{\rm rad}} = \zeta_{\rm exit}$ which however is far subdominant in the curvaton scenario. Now, importantly since radiation dilutes faster than matter, assuming there is sufficient time between the start of curvaton oscillation and its decay, we will reach a stage at which $f_\sigma \approx 1$ when we can write,

$$\zeta \approx \frac{1}{3}\frac{\delta\rho_\sigma}{\rho_\sigma}, \tag{4.20}$$

which remains conserved on superhorizon scales subsequently. We assume all the relevant fluids during the later stage of evolution i.e. the SM photon, neutrinos, baryons and dark matter all originate from the decay of the curvaton. This way we do not generate any isocurvature fluctuations at a later stage. The differential evolution between $\sigma-$matter and radiation has converted the initial isocurvature fluctuations in the curvaton field into adiabatic ones.

We will now relate $\frac{\delta\rho_\sigma}{\rho_\sigma}$ to the quantum fluctuations of the curvaton field which will later help us to write expressions for NG of primordial density perturbations.

Since the curvature perturbation is negligible at the end of inflation and we are assuming a mass-only potential for the curvaton, both σ_0 and $\delta\sigma(t,\vec{x})$ dilutes in an identical way so as to give [139, 142],

$$\frac{\delta\rho_\sigma}{\rho_\sigma} = 2\frac{\delta\sigma}{\sigma_0} = 2\frac{\delta\sigma}{\sigma_0}|_* \tag{4.21}$$

where $*$ denotes the fact that fluctuations are evaluated at the epoch of horizon exit. This then finally gives,

$$\zeta_{\rm final} \approx \zeta_\sigma = \frac{2}{3}\frac{\delta\sigma}{\sigma_0}|_*, \tag{4.22}$$

which relates the final curvature perturbation in terms of the quantum fluctuations of the curvaton field. It is in this limit that the adiabatic curvaton fluctuations can be identified as the Goldstone mode for spontaneous time translation breaking in the Goldstone effective theory of inflation [62], the inflaton fluctuations having become completely subdominant. Unless otherwise mentioned, in the following, we will omit the subscript in $\zeta_{\rm final}$ and simply use ζ to denote the primordial density perturbations which act as "initial" conditions for the modes that subsequently re-enter the horizon after inflation. We are now in a position to note the present observational constraints on this paradigm.

4.3.2 Observational constraints

Scalar power spectrum. Due to the fact that σ is a light spectator field during inflation, its fluctuations $\delta\sigma$ acquire an approximately scale invariant spectrum.

Thus the scalar power spectrum is given by,

$$\langle\zeta(\vec{k})\zeta(-\vec{k})\rangle' = \frac{4}{9\sigma_0^2}\langle\delta\sigma(\vec{k})\delta\sigma(-\vec{k})\rangle' = \frac{4}{9}\frac{H^2}{2\sigma_0^2 k^3}, \tag{4.23}$$

where the r.h.s. is evaluated at the time of horizon exit $k = aH$ for a given $k-$mode. The amplitude of scalar power spectrum from Planck data [27] then implies,

$$\frac{H}{\sigma_0} \approx 4.4 \times 10^{-4}. \tag{4.24}$$

Tilt of the scalar power spectrum. Defining $\Delta_\zeta = \frac{k^3}{2\pi^2}\langle\zeta(\vec{k})\zeta(-\vec{k})\rangle' = \frac{1}{9}\frac{H^2}{\pi^2\sigma_0^2}$, the tilt can be derived as,

$$\frac{d\ln\Delta_\zeta}{d\ln k} = -2\epsilon + \frac{2}{3}\eta_\sigma. \tag{4.25}$$

where $\eta_\sigma = \frac{m^2}{H^2}$ is fixed by the mass of the curvaton and $\epsilon \equiv -\frac{\dot{H}}{H^2} \approx \frac{\dot{\phi}_0^2}{2H^2M_{\rm pl}^2}$ is still determined by the homogeneous inflaton field. Planck data [8] requires,

$$-2\epsilon + \frac{2}{3}\eta_\sigma \approx -0.04. \tag{4.26}$$

Tensor-to-Scalar ratio. The ratio of the power spectrum of tensor fluctuations to that of the scalar fluctuations, denoted by r, is given by,

$$r = \frac{\frac{8H^2}{M_{\rm pl}^2}}{\frac{4H^2}{9\sigma_0^2}} = \frac{18\sigma_0^2}{M_{\rm pl}^2}. \tag{4.27}$$

The upper bound $r < 0.06$ from Planck data [8] requires

$$\sigma_0 < 0.06 M_{\rm pl}. \tag{4.28}$$

Non-Gaussianity. A very stringent constraint on the curvaton paradigm comes from the upper bound on the "local" type of NG, defined as $\zeta = \zeta_g + \frac{3}{5} f_{\rm NL}^{\rm loc} \zeta_g^2$, where ζ_g is a purely Gaussian field. Here the NG arises due to the fact that square of a Gaussian fluctuation is non-Gaussian. In the scenario when the curvaton dominates the energy density of the universe during before its decay, one can derive [143, 144, 145],

$$\zeta = \frac{2}{3}\frac{\delta\sigma}{\sigma} - \frac{1}{3}\left(\frac{\delta\sigma}{\sigma}\right)^2. \tag{4.29}$$

This has precisely the same form as the local type of NG defined above since $\delta\sigma$ is a Gaussian field, and in particular we have [4],

$$f_{\rm NL}^{\rm loc} = -\frac{5}{4}. \tag{4.30}$$

It should be noted that the above value of $f_{\rm NL}^{\rm loc}$ is parametrically larger than the slow-roll parameter suppressed $f_{\rm NL}^{\rm loc}$ in single-field inflationary models, as dictated by single-field consistency relations [29, 70] in the squeezed limit. Thereby in this curvaton scenario, even in the absence of heavy fields that will be considered below, a large $f_{\rm NL}^{\rm loc}$ is a tell-tale sign of beyond single-field inflationary dynamics. The above value of $f_{\rm NL}^{\rm loc}$ in eq. (4.30) also serves as a crucial difference between the

[4] Note that compared to [143] our definition of $f_{\rm NL}$ differs by an overall sign.

curvaton paradigm and Goldstone description of single-field inflation since $f_{\rm NL}^{\rm loc}$ is parametrically suppressed in the latter.

The above constraints can easily be satisfied. For example, one can choose a benchmark set of values:

$$\sigma_0 = 5 \times 10^{-3} M_{\rm pl}; \quad H = 2.2 \times 10^{-6} M_{\rm pl}; \quad \epsilon = 0.02; \quad \eta_\sigma = 10^{-3}, \tag{4.31}$$

to get $r = 4.5 \times 10^{-4}$. Although the robust prediction of $f_{\rm NL}^{\rm loc}$ in eq. (4.30) lies below the Planck upper bound on NG, quite excitingly, such a strength of NG will soon be tested by upcoming LSS observations [9].

While it is true that the signal in the squeezed limit is dominated by the curvaton itself, the distinctive signaures of the heavy fields are imprinted in characteristic non-analytic "oscillations" in the squeezed limit as explained in eq. (4.9). Multifield inflationary models having additional particles with masses $\ll H$ can not give such non-analytic momentum dependence. The observability of such oscillatory signals have been investigated in the literature in the context of single-field inflation, for example, in Refs. [11, 41, 97]. We expect that with some adaptations the above studies continue to be applicable in our case, but a detailed investigation lies beyond the scope of the present chapter.

The fact that in the curvaton paradigm the background inflationary expansion and the (eventual) primordial density perturbations are sourced by two different fields, opens up an interesting possibility. In particular, during inflation both the kinetic and the potential energy stored in σ can be much smaller than the kinetic

and the potential energy stored in ϕ, as can be checked by using the benchmark point in eq. (4.31). As will be explained below, this feature can allow significantly stronger coupling of some new degrees of freedom to σ than to ϕ in light of non-renormalizability and shift symmetry of the couplings. We will illustrate this by considering the coupling of a charged scalar, with and without Higgsing, to both ϕ and σ, and the case of a Dirac fermion to both ϕ and σ.

4.4 Charged heavy particles in the standard inflationary paradigm

Since ϕ is a light field, we can model it as a pNGB in the low energy EFT, just like the curvaton, and impose a shift symmetry $\phi \to \phi + c$ which is broken only by its potential. This implies that the interaction of the inflaton will be characterized predominantly by a derivative expansion in $\frac{(\partial\phi)^2}{\Lambda_\phi^4}$ where Λ_ϕ is the EFT cutoff in the inflationary sector. As discussed in the introduction, theoretical control of such an expansion implies,

$$\Lambda_\phi > \sqrt{\dot{\phi}_0} \sim 60H. \tag{4.32}$$

A stronger restriction on Λ_ϕ can be placed if we demand that the EFT explicitly describes the scalar/gravity dynamics of inflation and reheating. All known descriptions of this refer to an inflaton potential as the source of inflationary expansion. Thus the control of such an EFT requires (4.2),

$$\Lambda_\phi > V_{\rm inf}^{\frac{1}{4}} > 250H. \tag{4.33}$$

In the following we will keep only the restriction in eq. (4.2) in mind while considering the strengths of NG.

The leading coupling of the inflaton to a scalar field χ, charged under some gauge/global symmetry group, is given by a dimension-6 operator

$$\mathcal{L} \supset \frac{1}{\Lambda_\phi^2}(\partial\phi)^2\chi^\dagger\chi. \tag{4.34}$$

This term will also contribute to the mass of χ since, $\frac{1}{\Lambda_\phi^2}(\partial\phi)^2\chi^\dagger\chi \supset -\alpha\chi^\dagger\chi$ where $\alpha = \frac{\dot{\phi}_0^2}{\Lambda_\phi^2}$ is approximately constant in slow-roll inflation. In the presence of a "bare" mass m_χ and a quartic coupling λ_χ, the lagrangian for χ then reads as,

$$\mathcal{L} \supset -|\partial\chi|^2 - (m_\chi^2 + \alpha)\chi^\dagger\chi - \lambda_\chi(\chi^\dagger\chi)^2, \tag{4.35}$$

where the effective mass for χ is given by,

$$m_{\chi,\text{eff}}^2 = m_\chi^2 + \alpha. \tag{4.36}$$

Two scenarios arise depending on the sign of $m_{\chi,\text{eff}}^2$.

4.4.1 Higgs exchange in the broken phase

We first discuss the case when $m_{\chi,\text{eff}}^2 < 0$, leading to a Higgsing of the symmetry. Due to spontaneous symmetry breaking, one can now have inflationary couplings which are linear in the heavy field. Consequently, one can have tree level

processes that can mediate NG and since such processes do not have the usual $\sim \frac{1}{16\pi^2}$ loop suppression, the associated NG are more readily observable. We consider a $U(1)$ symmetry group for simplicity. Given the coupling in eq. (4.34), one can expand $\chi = (0, \frac{1}{\sqrt{2}}(v+\tilde{\chi}))$ in the unitary gauge, to read off the vertices necessary for tree level NG. In the above, v and $\tilde{\chi}$ are respectively the VEV and fluctuations of the Higgs field.

The details have been discussed in chapter 2 and the summary is that one can have three types of diagrams giving rise to NG as shown in fig. 4.2.

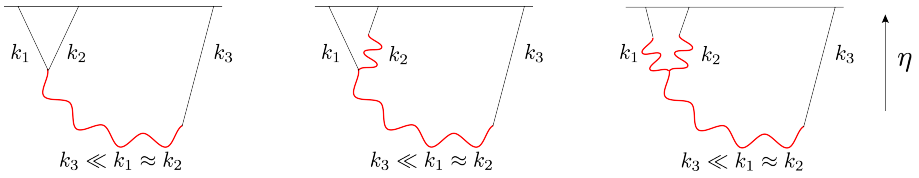

Figure 4.2: Massive Higgs mediated (in red) tree level "in-in" contributions to the inflaton (in black) three point function. Depending on the number of massive scalar propagators, these diagrams are labelled from left to right: (a) single exchange diagram, (b) double exchange diagram, (c) triple exchange diagram. η denotes conformal time which ends at the end of inflation.

The rough strengths of NG, in terms of f defined eq. (4.9), corresponding to each of the diagrams are given in chapter 2,

$$|f_{\chi,\,\text{single, tree}}| \sim \frac{\rho_1^2}{H^2}; \qquad |f_{\chi,\,\text{double, tree}}| \sim \frac{\rho_1^2\alpha}{H^4}; \qquad |f_{\chi,\,\text{triple, tree}}| \sim \frac{\rho_1^2\alpha}{H^4}, \tag{4.37}$$

where $\rho_1 = \frac{2\alpha v}{\dot{\phi}_0}$ denotes the quadratic mixing between ϕ and $\tilde{\chi}$.

For observable strengths of NG, we need the masses of the heavy particles $\sim H$, otherwise the cosmological production of the massive particle will be severely Boltzmann suppressed. Eq. (4.36) then implies that in the absence of any *classical*

tuning between m_χ^2 and α we need to have both $\alpha \sim m_\chi^2 \sim H^2$, in which case all three diagrams will give similar strength of NG, $|f_{\chi,\text{ natural, tree}}| \sim \rho_1^2/H^2$. Since a quadratic mixing between ϕ and $\tilde{\chi}$ also gives rise to a correction to the scalar power spectrum $k^3 P_k \sim \frac{H^4}{\dot{\phi}_0^2}(1+\mathcal{O}(\rho_1^2/H^2))$, we will require $\rho_1^2/H^2 \lesssim 0.1$ for perturbativity of such corrections. Then we see that NG contributions are given by,

$$|f_{\chi,\text{ natural, tree}}| \lesssim 0.1. \tag{4.38}$$

The natural choice of $\alpha \sim H^2$ implies $\Lambda > V_{\text{inf}}^{\frac{1}{4}} > \sqrt{\dot{\phi}_0}$, also ensuring a controlled EFT description.

From eq. (4.37) it is clear that by choosing a larger value of α and consequently fine tuning it against m_χ^2 to obtain $m_{\chi,\text{eff}}^2 \sim H^2$, a larger strength of NG can be obtained. However, one can not do this tuning to more than a percent level since the (slow) time evolution of $\alpha = \frac{\dot{\phi}_0^2}{\Lambda^2}$ will generically push $m_{\chi,\text{eff}}^2$ away from its tuned value $\sim H^2$ in a few Hubble times.

4.4.2 Charged scalar exchange in the symmetric phase

Here we assume $m_{\chi,\text{eff}}^2 > 0$ so that there is no spontaneous symmetry breaking and χ mediated NG appear only via loop diagrams. The coupling to the inflaton is described by the same operator as above, namely $\frac{1}{\Lambda_\phi^2}(\partial\phi)^2\chi^\dagger\chi$. With the symmetry being unbroken the relevant couplings between the inflaton and χ are given by,

$$\mathcal{L}_{\phi-\chi} \supset \frac{1}{\Lambda_\phi^2}(\partial\phi)^2\chi^\dagger\chi = \left(-\alpha - \frac{2\alpha}{\dot{\phi}_0}\dot{\delta\phi} + \frac{\alpha}{\dot{\phi}_0^2}(\partial(\delta\phi))^2\right)\chi^\dagger\chi, \tag{4.39}$$

with an effective χ mass given by eq. (4.36) and $\alpha = \frac{\dot{\phi}_0^2}{\Lambda_\phi^2}$.

Based on the couplings given in eq. (4.39), there are two loop diagrams that can contribute to a three point function which we list in fig. 4.3. The associated

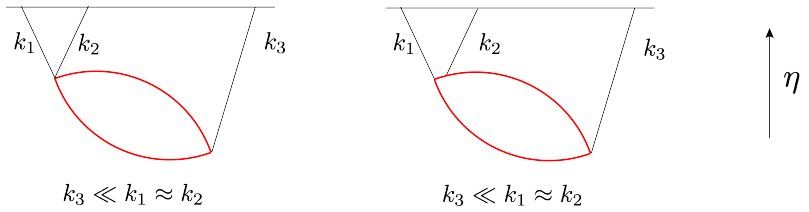

Figure 4.3: Massive charged particle mediated (in red) loop level "in-in" contributions to the inflaton (in black) three point function. Depending on the number of massive charged particle propagators, these diagrams are labelled from left to right: (a) double exchange diagram, (b) triple exchange diagram. η denotes conformal time which ends at the end of inflation.

NG can be estimated, in terms of f defined eq. (4.9), as

$$|f_{\chi,\text{ double, loop}}| \sim \frac{1}{16\pi^2}\frac{\alpha^2}{\dot{\phi}_0^2}; \qquad |f_{\chi,\text{ triple, loop}}| \sim \frac{1}{16\pi^2}\frac{\alpha^3}{H^2\dot{\phi}_0^2}. \tag{4.40}$$

The above discussion of the "classical" tuning also applies here and in the natural case i.e. when $\alpha \sim H^2$, eq. (4.40) gives,

$$|f_{\chi,\text{ natural, loop}}| \sim \frac{1}{16\pi^2}\frac{H^4}{\dot{\phi}_0^2} \sim 10^{-9}, \tag{4.41}$$

where we have used the fact that $\frac{H^4}{\dot{\phi}_0^2} \sim 10^{-7}$. Such a strength of NG is unobservably small. Note already with $\alpha \sim H^2$, $m^2_{\chi,\text{eff}}$ receives $\mathcal{O}(1)$ "contamination" from the inflationary background and a measurement of $m^2_{\chi,\text{eff}}$ via NG would not have given us the underlying value of the "pure" mass m^2_χ. For $\alpha \ll H^2$, such a contamination is small but the strength of NG becomes even smaller.

4.4.3 Charged Dirac fermion

We consider a charged Dirac fermion coupled to the inflaton via a dimension-7 operator $\frac{1}{\Lambda_\phi^3}(\partial\phi)^2\bar{\Psi}\Psi$. A dimension-5 operator of type $\frac{1}{\Lambda_\phi}\partial_\mu\phi\bar{\Psi}\gamma^\mu\Psi$ can be eliminated by integration by parts and current conservation if the Ψ couplings respect a $U(1)$ symmetry.

There could exist another dimension-5 operator involving the axial current, $\frac{\partial_\mu\phi\bar{\Psi}\gamma^\mu\gamma^5\Psi}{\Lambda_\phi}$ if it is not forbidden by parity. Such a coupling is special since it gives rise to an effective "chemical potential" $\lambda = \dot{\phi}_0/\Lambda_\phi$ for the fermion Ψ once the inflaton is set to its background value [104, 135, 136]. It can help production of Ψ even when the fermion mass, m_Ψ is somewhat heavier than H without paying significant Boltzmann suppression. However, if we impose the restriction in (4.2) i.e. $\lambda \lesssim 15H$, and demand theoretical control of the calculation of NG in the squeezed limit, which forces $\frac{k_3}{k_1} < \frac{H}{\lambda}$ [136], we find $F \lesssim$ few $\times 10^{-4}$ for the function defined in eq. (4.6). We will see in the next section that the curvaton scenario will allow a larger strength of NG with just the analog of the dimension-7 operator defined above. Furthermore, in the regime where there is a substantial NG signal due to λ, the inflationary background also significantly contaminates the "pure" fermion mass m_Ψ, so that the non-analytic signatures are predominantly sensitive to λ, not m_Ψ. Because of these reasons we will not consider the dimension-5 operator $\frac{\partial_\mu\phi\bar{\Psi}\gamma^\mu\gamma^5\Psi}{\Lambda_\phi}$ further.

In the coupling $\frac{1}{\Lambda_\phi^3}(\partial\phi)^2\bar{\Psi}\Psi$, the VEV of the inflaton will give a contribution to the fermion mass as for charged scalars, and we can write the relevant couplings

as,

$$\mathcal{L} \supset \frac{1}{\Lambda_\phi^3}(\partial\phi)^2\bar{\Psi}\Psi = \left(-\beta - \frac{2\beta}{\dot{\phi}_0}\dot{\delta\phi} + \frac{\beta}{\dot{\phi}_0^2}(\partial(\delta\phi))^2\right)\bar{\Psi}\Psi, \tag{4.42}$$

where $\beta = \frac{\dot{\phi}_0^2}{\Lambda_\phi^3}$. Thus the effective fermion mass becomes,

$$m_{\Psi,\text{eff}} = m_\Psi + \beta. \tag{4.43}$$

Naturalness requires $\beta \sim H$. Furthermore, even if we choose to tune, the requirement of $\Lambda_\phi > \sqrt{\dot{\phi}_0}$ already implies,

$$\beta < \sqrt{\dot{\phi}_0}. \tag{4.44}$$

Focusing on the natural case we can estimate the strength of NG for a fermion-mediated loop process given in fig. 4.3, where the internal lines now represent Ψ, in terms of f defined eq. (4.9),

$$|f_{\Psi,\text{ double, loop}}| \sim \frac{1}{16\pi^2}\frac{\beta^2 H^2}{\dot{\phi}_0^2}; \qquad |f_{\Psi,\text{ triple, loop}}| \sim \frac{1}{16\pi^2}\frac{\beta^3 H}{\dot{\phi}_0^2}. \tag{4.45}$$

We see in the natural case i.e. $\beta \sim H$ such NG are again unobservably small with

$$|f_{\Psi,\text{ natural, loop}}| \sim 10^{-9}. \tag{4.46}$$

As in the case of the charged scalar, if we demand the "contamination" to $m_{\Psi,\text{eff}}$ from the inflationary background to be small, the NG becomes even smaller.

Having discussed the case with inflationary couplings, let us see how things change when the heavy charged scalar and fermion fields are coupled to a curvaton instead of the inflaton as the dominant source of fluctuations.

4.5 Charged heavy particles in the curvaton paradigm

In the inflationary scenario, it is the same field ϕ that drives the inflationary expansion and also sources the observed primordial fluctuations. That is why the very high scales such as $\dot{\phi}_0^{1/2}$ and $V_{\rm inf}^{1/4}$ inversely bound the strength of EFT couplings, making the associated NG small. However, in the curvaton scenario, σ sources the observed fluctuations and ϕ drives the inflationary expansion. In particular, assuming ϕ and σ belong to two different sectors, sequestered from each other, the scales $\dot{\phi}_0^{1/2}$ and $V_{\rm inf}^{1/4}$ need not even be relevant for the couplings between σ and heavy fields. The only relation that is relevant for control of the curvaton EFT is, eq. (4.3),

$$\Lambda_\sigma > V_\sigma^{\frac{1}{4}}, \tag{4.47}$$

where V_σ is the energy density in the curvaton. To see how big V_σ can be we write,

$$V_\sigma = \frac{1}{2} m^2 \sigma_0^2 \approx 2.5 \times 10^6 \times \eta_\sigma H^4, \tag{4.48}$$

where we have used eq. (4.24) and $\eta_\sigma = \frac{m^2}{H^2}$. We then see that for the benchmark choice of $\eta_\sigma \sim 10^{-3}$ discussed in sec. 4.3 allows us to have using eq. (4.2),

$$\Lambda_\phi \gtrsim 250H \gg \Lambda_\sigma \gtrsim V_\sigma^{1/4} \sim 10H \tag{4.49}$$

This relation $\Lambda_\phi \gg \Lambda_\sigma \gtrsim V_\sigma^{1/4}$ plays a central role in giving significantly larger NG in the curvaton paradigm while also ensuring theoretical control of the set-up. Compared to the standard inflationary paradigm, in the curvaton scenario there are no *classical* tunings so long as we make sure $\dot{\sigma}_0 \lesssim H^2 < \Lambda_\sigma^2$. As an example, the contribution of the curvaton to the mass term of the charged scalar field χ, $\frac{(\partial\sigma)^2}{\Lambda_\sigma^2}\chi^\dagger\chi \supset -\frac{\dot{\sigma}_0^2}{\Lambda_\sigma^2}\chi^\dagger\chi$ remains small for the above choices of $\dot{\sigma}_0$ and Λ_σ and correspondingly there is no "contamination" to the "pure" scalar mass m_χ.

Constraints from curvaton self-interaction mediated NG. Given the derivative expansion, we can also write a term $\frac{1}{\Lambda_\sigma^4}(\partial\sigma)^4$. This will contribute to both bispectrum and trispectrum. For bispectrum, the relevant couplings are,

$$\frac{1}{\Lambda_\sigma^4}(\partial\sigma)^4 = 4\frac{\dot{\sigma}_0}{\Lambda_\sigma^4}\dot{\delta\sigma}^3 - 4\frac{\dot{\sigma}_0}{\Lambda_\sigma^4}\frac{1}{a(t)^2}\dot{\delta\sigma}(\partial_i\delta\sigma)^2 + \cdots . \tag{4.50}$$

From such a coupling we can do a naive estimate of curvaton self-interaction mediated NG, in terms of f defined eq. (4.9),

$$|f_{\text{curvaton, self-int.}}| \sim \frac{\dot{\sigma}_0\sigma_0 H}{\Lambda_\sigma^4}. \tag{4.51}$$

Thus with $\dot{\sigma}_0 \sim H^2, \Lambda_\sigma \sim 4H$, a choice which will be justified below, and using eq. (4.24) we get, $f_{\text{curvaton, self- int.}} \sim 10$. This is below the current upper bound on orthogonal and equilateral type of NG which is the kind of NG induced by the above self-interaction. Doing a more careful calculation shows that $f_{\text{curvaton self int.}}$ is actually smaller than the above crude estimate, so that a choice of $\Lambda_\sigma \gtrsim 4H$ is more than sufficient to avoid current constraints. With such a choice of Λ_σ, the trispectrum is also smaller than the current bound [27].

Cut-off of the effective theory and field range of the curvaton. With the above choice of $\eta_\sigma \sim 10^{-3}$, the requirement $\Lambda_\sigma > V_\sigma^{\frac{1}{4}}$ reduces to $\Lambda_\sigma \gtrsim 10H$. However, even with $\Lambda_\sigma \sim 10H$, we do still need $\sigma_0 \gg \Lambda_\sigma$ to satisfy eq. (4.24). Thus one can ask whether it is problematic to have curvaton field range much bigger than the EFT cut-off, although both the derivative expansion remains under full control and $\Lambda_\sigma > V_\sigma^{\frac{1}{4}}$. This is analogous to the problem of super-Planckian inflaton field range in high scale inflation models, given by the Lyth bound. Thus, one can borrow the mechanisms that are used to create large effective field ranges, such as axion monodromy or multi-axion alignment. These mechanisms illustrate that having field ranges larger than the EFT cutoff can naturally emerge from controlled UV completions. In particular, following the bi-Axion mechanism [146, 147, 148, 149, 150, 151], one can imagine having two axionic curvatons with potential,

$$V_{\text{curv}} = V_1 \left(1 - \cos\left(\frac{N\sigma_1}{f_1} + \frac{\sigma_2}{f_2}\right)\right) + V_2 \left(1 - \cos\left(\frac{\sigma_1}{f_1}\right)\right). \tag{4.52}$$

With $V_1 \sim V_2$, $f_1 \sim f_2$ and $N \gg 1$, there is a heavier curvaton which gets stabilized at $\frac{N\sigma_1}{f_1} + \frac{\sigma_2}{f_2} \approx 0$ so that the effective light curvaton potential is given by,

$$V_{\text{eff}} = V_2 \left(1 - \cos\left(\frac{\sigma_2}{N f_2}\right)\right). \tag{4.53}$$

We see that the light curvaton σ_2 has an effective field space $\sim N f_2$ that is parametrically bigger than the fundamental field space f_2 and we can consistently have $N f_2 \gg \Lambda_\sigma \gtrsim f_2$ for a sufficiently large N. This UV completion then serves as a proof-of-principle that it is consistent to have field ranges that are significantly bigger than the EFT cutoff scales. The light curvaton σ_2 can still interact with heavy fields of interest with suppressions given by $\Lambda_\sigma \sim f_2$ rather than $N f_2$, so that we can have stronger couplings leading to significant NG. Expanding eq. (4.53) around its minima gives rise to the approximately mass-only potential for the curvaton considered in eq. (4.10) with $\sigma_2 = \sigma$ and $m^2 = \frac{V_2}{N^2 f_2^2}$.

Mediators and stronger EFT couplings. The curvaton will couple to heavy particles via higher dimensional operators and hence the NG will be proportional to multiple powers of $\frac{1}{\Lambda_\sigma}$, instead of multiple powers of $\frac{1}{\Lambda_\phi}$ as in the inflationary scenario. As we have discussed above, the strength of NG in the curvaton scenario can therefore be much stronger since $\Lambda_\sigma \ll \Lambda_\phi$ is consistent with EFT control. However, the restriction of $\Lambda_\sigma > 10H$ still corresponds to somewhat suppressed NG. We will now show that in the presence of heavier "mediator" particles, the effective scale of Λ_σ can be brought down from $\sim 10H$ and we can obtain even stronger NG.

For example, one can have the following coupling between the curvaton, the mediator Σ and the scalar χ:

$$\frac{1}{\Lambda_\sigma}(\partial\sigma)^2\Sigma + \mu_\Sigma \Sigma\chi^\dagger\chi. \tag{4.54}$$

Upon integrating out the mediator Σ, we can get an effective dimension-6 operator,

$$\frac{\mu_\Sigma}{M_\Sigma^2\Lambda_\sigma}(\partial\sigma)^2\chi^\dagger\chi, \tag{4.55}$$

which implies an effective cutoff,

$$\Lambda_{\sigma,\text{eff}}^2 = \frac{M_\Sigma^2\Lambda_\sigma}{\mu_\Sigma}. \tag{4.56}$$

As an example, for $M_\Sigma = 3H, \mu_\Sigma = 6H$ and $\Lambda_\sigma = 10H$, one gets $\Lambda_{\sigma,\text{eff}} \approx 4H < \Lambda_\sigma$. A similar procedure can be repeated for fermionic couplings by starting with,

$$\frac{1}{\Lambda_\sigma}(\partial\sigma)^2\Sigma + y\Sigma\bar{\Psi}\Psi \tag{4.57}$$

to get (for $y = 1$),

$$\Lambda_{\sigma,\text{eff}}^3 = M_\Sigma^2\Lambda_\sigma. \tag{4.58}$$

This effective cutoff is again smaller than Λ_σ for the same choice of M_Σ and Λ_σ.

To summarize, demanding theoretical control of the curvaton derivative expansion and $\Lambda_\sigma > V_\sigma^{\frac{1}{4}}$ in the presence of somewhat heavy mediators, gives us $\Lambda_{\sigma,\text{eff}} \gtrsim 4H$. In the following, we will give parametric estimates of NG in terms of $\Lambda_{\sigma,\text{eff}}$ but for

numerical results we will take $\Lambda_{\sigma,\text{eff}} = 4H$. For brevity, in the rest of the chapter we will denote $\Lambda_{\sigma,\text{eff}}$ by just Λ_σ.

4.5.1 Higgs exchange in the broken phase

The coupling of the curvaton with the charged scalar is given by the dimension-6 operator,

$$\mathcal{L}_{\phi-\chi} \supset \frac{1}{\Lambda_\sigma^2}(\partial\sigma)^2\chi^\dagger\chi. \tag{4.59}$$

Expanding around the correct vacuum, $\chi = (0, \frac{1}{\sqrt{2}}(\tilde{\chi}+v))$ as in sec. 4.4, we can get the relevant terms coupling $\tilde{\chi}$ to σ,

$$\mathcal{L}_{\sigma-\chi} \supset \frac{1}{\Lambda_\sigma^2}(\partial\sigma)^2\chi^\dagger\chi - \lambda_\chi(\chi^\dagger\chi)^2 \supset \left(-\frac{2\dot{\sigma}_0 v}{\Lambda_\sigma^2}\dot{\delta\sigma}\tilde{\chi} - \frac{\dot{\sigma}_0}{\Lambda_\sigma^2}\dot{\delta\sigma}\tilde{\chi}^2 + \frac{v}{\Lambda_\sigma^2}(\partial\delta\sigma)^2\tilde{\chi} - \lambda_\chi v\tilde{\chi}^3\right) + \cdots . \tag{4.60}$$

The above couplings give NG mediated by diagrams given in fig. 4.2 where the external legs represent fluctuations of the curvaton instead of the inflaton. The leading contribution comes from the single exchange diagram for which one can roughly estimate the NG, in terms of f defined eq. (4.9) as

$$|f_{\chi,\,\text{tree}}| \sim 3\times 10^3 \times \frac{\rho_2^2}{\dot{\sigma}_0}, \tag{4.61}$$

where we have denoted the quadratic mixing as $\rho_2 = \frac{2\dot{\sigma}_0 v}{\Lambda_\sigma^2}$. Since $\dot{\sigma}_0 \sim H^2$, compared to the result in the inflationary paradigm given in eq. (4.37), we can have orders

of magnitude larger NG in the curvaton scenario, and importantly, *without* any classical tuning.

While the above is a rough estimate, the necessary ingredients for a precise calculation of the single exchange diagram in fig. 4.2, can be found in [21] using which we get,

$$
\begin{aligned}
F_{\chi,\text{tree}}\left(m_\chi, \frac{k_3}{k_1}\right) &= \frac{\langle\zeta(\vec{k}_1)\zeta(\vec{k}_2)\zeta(\vec{k}_3)\rangle'}{\langle\zeta(\vec{k}_1)\zeta(-\vec{k}_1)\rangle'\langle\zeta(\vec{k}_3)\zeta(-\vec{k}_3)\rangle'} \\
&= -\frac{3\sigma_0\rho_2^2}{8\dot{\sigma}_0 H}\Gamma(\frac{1}{2}+i\mu)^2\Gamma(-2i\mu)(\frac{3}{2}+i\mu)(\frac{5}{2}+i\mu)(1+i\sinh(\pi\mu))\left(\frac{k_3}{k_1}\right)^{\frac{3}{2}+i\mu} \\
&+ \mu \to -\mu \\
&\equiv |f_{\chi,\text{tree}}(\mu)|\left(e^{i\delta_1(\mu)}\left(\frac{k_3}{k_1}\right)^{\frac{3}{2}+i\mu} + \mu \to -\mu\right),
\end{aligned}
\tag{4.62}
$$

where $\mu = \sqrt{m_\chi^2/H^2 - 9/4}$. In fig. 4.4 we plot the function $|f_{\chi,\text{tree}}|$ which gives the strength of NG as a function of the scalar mass, m_χ.

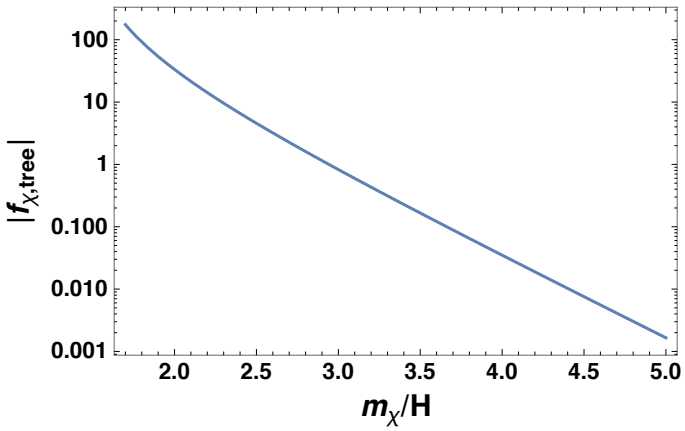

Figure 4.4: The strength of NG for tree level Higgs exchange as a function of Higgs mass m_χ for $\rho_2 = 0.3H$ and $\dot{\sigma}_0 = -H^2$. The function $|f_{\chi,\text{tree}}(\mu)|$ is defined in eq. (4.62).

4.5.2 Charged scalar exchange in the symmetric phase

The leading coupling is again given by a similar dimension-6 operator,

$$\mathcal{L} \supset \frac{1}{\Lambda_\sigma^2}(\partial\sigma)^2\chi^\dagger\chi. \tag{4.63}$$

In the absence of symmetry breaking, the relevant curvaton-χ interaction terms are given by,

$$\left(-\frac{2\dot{\sigma}_0}{\Lambda_\sigma^2}\dot{\delta\sigma} + \frac{1}{\Lambda_\sigma^2}(\partial(\delta\sigma))^2\right)\chi^\dagger\chi. \tag{4.64}$$

Using eq. (4.64) we can estimate the strengths of NG. The relevant diagrams are still given by fig. 4.3 except the external legs now represent curvaton fluctuations instead of inflaton fluctuations. The leading NG is given by the double exchange diagram in fig. 4.3 whose parametric strength, in terms of f defined eq. (4.9), is given by,

$$|f_{\chi,\text{loop}}| \sim \frac{1}{16\pi^2}\frac{\dot{\sigma}_0 H^2}{\Lambda_\sigma^4} \times \frac{\sigma_0}{H}. \tag{4.65}$$

Since $\Lambda_\sigma \ll \sqrt{\dot{\phi}_0}$, compared to the result in the inflationary paradigm given in eq. (4.41), we can have orders of magnitude bigger NG in the curvaton scenario, and again, *without* any classical tuning.

The dimensionless three point function, defined in eq. (4.6), due to the double exchange diagram in fig. 4.3 will be calculated in appendix C.1. The result is given

by eq. (180),

$$
\begin{aligned}
F_{\chi,\text{loop}}\left(m_\chi, \frac{k_3}{k_1}\right) &= \frac{\langle\zeta(\vec{k}_1)\zeta(\vec{k}_2)\zeta(\vec{k}_3)\rangle'}{\langle\zeta(\vec{k}_1)\zeta(-\vec{k}_1)\rangle'\langle\zeta(\vec{k}_3)\zeta(-\vec{k}_3)\rangle'} \\
&= -\frac{3\sigma_0}{2}\frac{2\dot{\sigma}_0 H}{\Lambda_\sigma^4}\left(\frac{\frac{1}{16\pi^5}\Gamma(-i\mu)^2\Gamma(3/2+i\mu)^2}{\frac{1}{4\pi^{5/2}}\Gamma(-3/2-2i\mu)\Gamma(3+2i\mu)}\mathcal{F}\left(3+2i\mu, \frac{k_3}{k_1}\right) + \mu \to -\mu\right) \\
&\equiv |f_{\chi,\text{loop}}(\mu)|\left(e^{i\delta_2(\mu)}\left(\frac{k_3}{k_1}\right)^{3+2i\mu} + \mu \to -\mu\right),
\end{aligned} \tag{4.66}
$$

where $\mathcal{F}$ is defined in eq. (174) and $\mu = \sqrt{m_\chi^2/H^2 - 9/4}$. In fig. 4.5 we plot the function $|f_{\chi,\text{loop}}(\mu)|$ as a function of the scalar mass, m_χ.

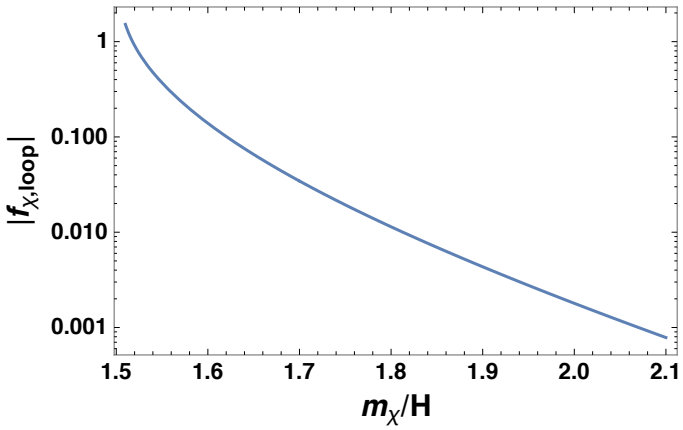

Figure 4.5: The strength of NG for loop level scalar exchange as a function of scalar mass m_χ for $\Lambda_\sigma = 4H$ and $\dot{\sigma}_0 = -H^2$. The function $|f_{\chi,\text{loop}}(\mu)|$ is defined in eq. (4.66).

4.5.3 Charged Dirac fermion

We again consider a charged Dirac fermion, and its coupling to the curvaton is given by a similar dimension-7 operator,

$$
\frac{1}{\Lambda_\sigma^3}(\partial\sigma)^2\bar{\Psi}\Psi. \tag{4.67}
$$

As before, there can be a dimension-5 axial coupling $\frac{\partial_\mu \sigma \bar{\Psi}\gamma^\mu\gamma^5\Psi}{\Lambda_\sigma}$ between σ and Ψ if it is not forbidden by parity. However, such a coupling does not give rise to a significant chemical potential as in the inflationary scenario, and correspondingly there is no substantial enhancement of NG signals. We leave a detailed study of this coupling for future work, focusing only on the dimension-7 operator in the present chapter.

Through a reasoning identical to the case of scalars, one can check that the mass correction to the fermion due to the curvaton coupling is negligible with similar choice of parameters as above. The relevant curvaton-fermion interaction terms are given by,

$$\left(-\frac{2\dot{\sigma}_0}{\Lambda_\sigma^3}\dot{\delta\sigma} + \frac{1}{\Lambda_\sigma^3}(\partial(\delta\sigma))^2\right)\bar{\Psi}\Psi. \tag{4.68}$$

Using eq. (4.68) we can estimate the strengths of NG for which the relevant diagrams are still given by fig. 4.3, except the external legs now represent curvaton fluctuations instead of inflaton fluctuations. The leading NG is given by the double exchange diagram in fig. 4.3 whose parametric strength, in terms of f defined eq. (4.9), is given by,

$$f_{\Psi,\text{loop}} \sim \frac{1}{16\pi^2}\frac{\dot{\sigma}_0 H^4}{\Lambda_\sigma^6} \times \frac{\sigma_0}{H}|_*. \tag{4.69}$$

Since $\Lambda_\sigma \ll \sqrt{\dot{\phi}_0}$, compared to the result in the inflationary paradigm given in eq. (4.45), once again we can have orders of magnitude bigger NG in the curvaton scenario *without* any classical tuning.

The dimensionless three point function, defined in eq. (4.6), due to the double exchange diagram in fig. 4.3 will be calculated in appendix C.2. The result is given

by eq. (185),

$$
\begin{aligned}
F_{\Psi,\text{loop}}\left(m_\Psi, \frac{k_3}{k_1}\right) &= \frac{\langle\zeta(\vec{k}_1)\zeta(\vec{k}_2)\zeta(\vec{k}_3)\rangle'}{\langle\zeta(\vec{k}_1)\zeta(-\vec{k}_1)\rangle'\langle\zeta(\vec{k}_3)\zeta(-\vec{k}_3)\rangle'} \\
&= -\frac{3\sigma_0}{2}\frac{2\dot{\sigma}_0 H^3}{\Lambda_\sigma^6}\left(\frac{-\frac{3}{\pi^5}\frac{\Gamma(1/2-i\tilde{\mu})^2\Gamma(2+i\tilde{\mu})^2}{(1+2i\tilde{\mu})}}{\frac{1}{4\pi^{5/2}}\Gamma(-5/2-2i\tilde{\mu})\Gamma(4+2i\tilde{\mu})}\mathcal{F}\left(4+2i\tilde{\mu}, \frac{k_3}{k_1}\right) + \tilde{\mu}\to-\tilde{\mu}\right) \\
&\equiv |f_{\Psi,\text{loop}}(\tilde{\mu})|\left(e^{i\delta_3(\tilde{\mu})}\left(\frac{k_3}{k_1}\right)^{4+2i\tilde{\mu}} + \tilde{\mu}\to-\tilde{\mu}\right), \qquad (4.70)
\end{aligned}
$$

where $\mathcal{F}$ is defined in eq. (174) and $\tilde{\mu} = m_\Psi/H$. In fig. 4.6 we plot the function $|f_{\Psi,\text{loop}}|$ as a function of fermion mass, m_Ψ.

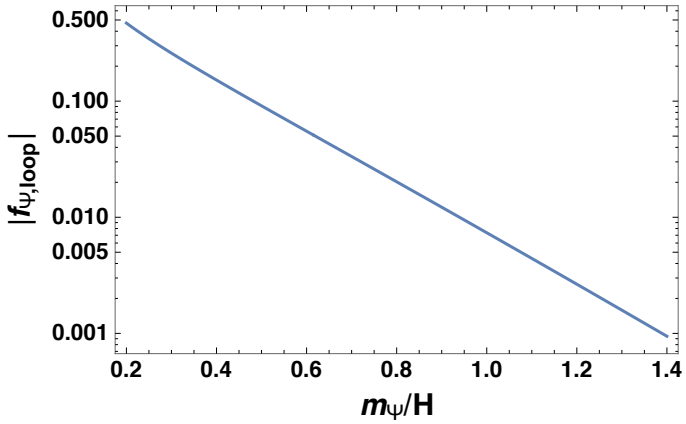

Figure 4.6: The strength of NG for loop level charged fermion exchange as a function of fermion mass m_Ψ for $\Lambda_\sigma = 4H$ and $\dot{\sigma}_0 = -H^2$. The function $|f_{\Psi,\text{loop}}(\tilde{\mu})|$ is defined in eq. (4.70).

4.6 Conclusions and future directions

In the standard inflationary scenario, the inflaton-heavy particle couplings are suppressed by (at least) inverse powers of an EFT cutoff scale Λ_ϕ, which has to satisfy $\Lambda_\phi \gtrsim V_{\text{inf}}^{\frac{1}{4}} > 250H$ if we demand that the EFT explicitly describes the scalar field source of inflation V_{inf}. Such a high value of Λ_ϕ leads to small or even unobserv-

able strengths of NG in various otherwise well-motivated scenarios of cosmological collider physics.

We have studied a non-standard inflationary paradigm in which the space-time expansion and the predominant production of primordial fluctuations are due to two *different* fields. In particular, we have focused on the curvaton scenario, where the above two roles are played by the inflaton and the curvaton respectively. Heavy particles can then couple to the curvaton suppressed only by inverse powers of $\Lambda_\sigma \gtrsim V_\sigma^{\frac{1}{4}}$, where V_σ is the energy density contained in the curvaton field which can be as low as $\sim (10H)^4$ for the benchmark parameter choice considered in this chapter. With the choice $V_\sigma^{\frac{1}{4}} \lesssim \Lambda_\sigma \ll \Lambda_\phi$, the heavy particles can couple to the primordial fluctuations much more strongly and lead to orders of magnitude larger NG while still ensuring controlled EFT description of the inflationary and reheating dynamics. To illustrate this fact, we have considered NG mediated by charged scalars, both in the Higgs phase and in the unbroken phase, as well as charged Dirac fermions. In particular, we have shown that even loop-level NG effects are observable!

Several future directions remain open. We have considered a scenario in which the curvaton and the inflaton belong to two decoupled sectors (up to gravitational effects), which can naturally be achieved, for example, by having an extra dimension in which the two fields are localized on two different branes. Since the presence of Kaluza-Klein (KK) gravitons is a robust feature of such an extra-dimensional set-up, it would be interesting to see whether appreciable KK-graviton mediated NG can be generated using our scenario. In particular, this may be applicable to the strongly motivated case of orbifold unification [83, 84, 85] along the lines of chapter

3.

We have restricted our attention to bispectra of primordial scalar fluctuations which required us to use a non-zero value of $\dot{\sigma}_0$ in the "in-in" diagrams. Demanding $\dot{\sigma}_0 \sim H^2$ then implied $V_\sigma \sim (10H)^4$ via eqs. (4.48), (4.15) and (4.24). Considering trispectra (four-point correlation functions) on the other hand, such insertions of $\dot{\sigma}_0$ are not essential, and consequently one can have even smaller values of V_σ. This will then allow smaller Λ_σ and larger NG. It would also be very interesting to analyze all the "heavy-lifted" SM signals [24, 43, 44, 74] considered in chapter 2, especially the signal due to the loops of massive W bosons, in the curvaton scenario that was presented in this chapter.

A.1 Scalar Fields in dS Space

The metric for the Poincare patch of dS spacetime in Hubble units can be written as

$$ds^2 = \frac{-d\eta^2 + d\vec{x}^2}{\eta^2}. \tag{71}$$

A.1.1 Massive Fields

We want to get the mode functions for a quantum field in dS. This can be obtained by first solving the classical equation of motion and then by canonically quantizing the theory. Let us start by writing the equation of motion,

$$\partial_\mu(\sqrt{-g}g^{\mu\nu}\partial_\nu\phi) = \sqrt{-g}m^2\phi \tag{72}$$

$$\Rightarrow \partial_\eta^2\phi - \frac{2}{\eta}\partial_\eta\phi - \partial_i^2\phi + \frac{m^2}{\eta^2}\phi = 0. \tag{73}$$

This can be solved in terms of Hankel (or equivalently, Bessel) functions. After Fourier transforming to $\vec{k}$-space, we can write a general classical solution as,

$$\phi(\eta, \vec{k}) = c_1(-\eta)^{\frac{3}{2}}H_{i\mu}^{(1)}(-k\eta) + c_2(-\eta)^{\frac{3}{2}}H_{i\mu}^{(2)}(-k\eta), \tag{74}$$

where, $\mu = \sqrt{\frac{m^2}{H^2} - \frac{9}{4}}$.

As usual, to canonically quantize the theory, we elevate the coefficients c_1, c_2 to linear combinations of creation and destruction operators, $a_{\vec{k}}^\dagger, a_{\vec{k}}$, on the Bunch-

Davies vacuum. The quantum field thereby has the form,

$$\phi(\eta, \vec{k}) = f_k(\eta) a^\dagger_{\vec{k}} + \bar{f}_k(\eta) a_{-\vec{k}}, \tag{75}$$

where the mode functions, $f_k(\eta)$ and $\bar{f}_k(\eta)$ (or equivalently, the linear combinations referred to above), are determined as follows. We first find the conjugate momentum $\pi = \frac{\partial \mathcal{L}}{\partial_\eta \phi}$ and demand, $[\pi(\eta, \vec{x}), \phi(\eta, \vec{y})] = i\delta^3(\vec{x} - \vec{y})$ and $[a_{\vec{k}}, a^\dagger_{\vec{k}'}] = (2\pi)^3 \delta^3(\vec{k} - \vec{k}')$. This gives the Wronskian condition on the mode functions at $\eta \to -\infty$,

$$\bar{f}_k(\eta) f'_k(\eta) - \bar{f}'_k(\eta) f_k(\eta) = i\eta^2. \tag{76}$$

To impose the Bunch Davies vacuum we demand $f_k(\eta) \propto e^{ik\eta}$, and using the Wronskian condition (76) we can also fix the normalization of $f_k(\eta)$ up to a phase. In summary, we demand

$$\lim_{\eta \to -\infty} f_k(\eta) = (-\eta) \sqrt{\frac{1}{2k}} e^{ik\eta}. \tag{77}$$

This can be satisfied by choosing

$$f_k(\eta) = (+ie^{-i\pi/4}) \frac{\sqrt{\pi}}{2} e^{\pi\mu/2} (-\eta)^{\frac{3}{2}} H^{(2)}_{i\mu}(-k\eta), \tag{78}$$

and

$$\bar{f}_k(\eta) = (-ie^{i\pi/4}) \frac{\sqrt{\pi}}{2} e^{-\pi\mu/2} (-\eta)^{\frac{3}{2}} H^{(1)}_{i\mu}(-k\eta). \tag{79}$$

Here, we have introduced some phase factors which are just conventions, which drop out when we calculate propagators.

We note that in (2.7) we have both time and anti-time ordered expressions appearing. Since a propagator involves two mode functions, we can have a total of four types of propagators depending on the mode functions coming from either the time or anti-time ordered part. We denote time(anti-time) ordering by a $+(-)$ sign. As an example, a propagator $G_{+-}(k,\eta,\eta')$ means the mode function with argument $\eta(\eta')$ is coming from time(anti-time) ordering. Similarly, $G_{++}(k,\eta,\eta')$ means both the mode functions are coming from time ordering. Thus we can write

$$\begin{aligned}
G_{++}(k,\eta,\eta') &= \bar{f}_k(\eta')f_k(\eta)\theta(\eta'-\eta) + \bar{f}_k(\eta)f_k(\eta')\theta(\eta-\eta') \\
G_{+-}(k,\eta,\eta') &= \bar{f}_k(\eta')f_k(\eta) \\
G_{-+}(k,\eta,\eta') &= \bar{f}_k(\eta)f_k(\eta') \\
G_{--}(k,\eta,\eta') &= \bar{f}_k(\eta')f_k(\eta)\theta(\eta-\eta') + \bar{f}_k(\eta)f_k(\eta')\theta(\eta'-\eta).
\end{aligned} \tag{80}$$

Among these four, G_{+-}, G_{++} are conjugates of G_{-+}, G_{--} respectively, and so we only have two independent propagators.

A.1.2 Inflaton Mode Functions

Mode functions for massless fields, in particular the inflaton, follow by using $\mu = 3i/2$ in (78) and (79), which gives

$$\begin{aligned} f_k(\eta) &= \frac{(1-ik\eta)e^{ik\eta}}{\sqrt{2k^3}} \\ \bar{f}_k(\eta) &= \frac{(1+ik\eta)e^{-ik\eta}}{\sqrt{2k^3}}. \end{aligned} \tag{81}$$

A.1.3 Some Useful Relations for Diagrammatic Calculations

For later use we also note a few relations involving Hankel and hypergeometric functions that arise upon evaluating the Feynman diagrams for the NG correlators of interest. We can write the following integral involving Hankel functions in terms of a hypergeometric function (valid for real μ and $\nu \equiv i\mu < \frac{1}{2}$),

$$\begin{aligned} &e^{\pi\mu/2}\int_0^\infty dx x^n e^{-ipx} H^{(2)}_{i\mu}(x) = \\ &\frac{(-i/2)^n}{\sqrt{\pi}\Gamma(n+3/2)}\Gamma(n+1+i\mu)\Gamma(n+1-i\mu)\,{}_2F_1\left(n+1+i\mu, n+1-i\mu, n+\frac{3}{2}, \frac{(1-p)}{2}\right) \end{aligned} \tag{82}$$

$$\begin{aligned} &e^{-\pi\mu/2}\int_0^\infty dx x^n e^{+ipx} H^{(1)}_{i\mu}(x) = \\ &\frac{(+i/2)^n}{\sqrt{\pi}\Gamma(n+3/2)}\Gamma(n+1-i\mu)\Gamma(n+1+i\mu)\,{}_2F_1\left(n+1-i\mu, n+1+i\mu, n+\frac{3}{2}, \frac{(1-p)}{2}\right) \end{aligned} \tag{83}$$

It is useful later to approximate these expressions for large p by using limiting forms of Hankel and hypergeometric functions,

$$e^{\pi\mu/2}H^{(2)}_{i\mu}(z) = \frac{i}{\pi}\left(\Gamma(i\mu)(z/2)^{-i\mu}e^{\pi\mu/2} + \Gamma(-i\mu)(z/2)^{+i\mu}e^{-\pi\mu/2}\right) \tag{84}$$

$$e^{-\pi\mu/2}H^{(1)}_{i\mu}(z) = -\frac{i}{\pi}\left(\Gamma(-i\mu)(z/2)^{+i\mu}e^{\pi\mu/2} + \Gamma(+i\mu)(z/2)^{-i\mu}e^{-\pi\mu/2}\right). \tag{85}$$

We also need large negative argument expansion of hypergeometric function,

$${}_2F_1(a,b,c;z) = \frac{\Gamma(b-a)\Gamma(c)}{\Gamma(b)\Gamma(c-a)}(-z)^{-a} + \frac{\Gamma(c)\Gamma(a-b)}{\Gamma(a)\Gamma(c-b)}(-z)^{-b}. \tag{86}$$

A.2 NG due to h Exchange

A.2.1 Calculation of Single Exchange Diagram

We will use the in-in formula (2.7) to calculate NG due to the single exchange diagram which is depicted in Fig. 2.3 (a). We begin by reviewing this calculation in the context of single-field slow-roll inflation, as originally performed in [21]. The relevant terms in the lagrangian (2.48) for such a diagram are

$$\mathcal{L} \supset -\rho_2\dot{\xi}h + \frac{\rho_2}{2\dot{\phi}_0}(\partial\xi)^2 h + \cdots. \tag{87}$$

Note in (2.7) we have both time and anti-time ordering. Thus each vertex can contribute either from time or anti-time ordering. So an in-in diagram with n vertices gives rise to 2^n subdiagrams. These subdiagrams differ in the type of propagators used for the massive particle and inflatons. For example if both the vertices are coming from time ordering, we should use G_{++} for the massive propagator as defined in (80). We call the subdiagram containing G_{++} to be I_{++}. Thus for the single exchange diagram we have four subdiagrams which we denote by $I_{++}, I_{+-}, I_{-+}, I_{--}$ depending on which kind of massive propagator has been used. However, to compute the entire three point function due to single exchange diagram, we have to consider only two subdiagrams, since the other two are related by complex conjugation. For example, we will calculate only I_{--} and I_{+-} which are related to I_{++} and I_{-+} respectively by complex conjugation. We sum all four contributions to get the final answer. To clarify the above comments, we write the expressions for four subdiagrams schematically,

$$I_{\pm\pm} \propto (\pm i)(\pm i) \int \frac{d\eta}{\eta^4} \int \frac{d\eta'}{\eta'^4} g_{\pm}(k_3;\eta') \tilde{g}_{\pm}(k_1,k_2;\eta) G_{\pm\pm}(k_3;\eta,\eta'). \tag{88}$$

The prefactors $\mp i$ arise depending on whether we use $e^{-i\int H dt}$ for time ordering or $e^{+i\int H dt}$ for anti-time ordering. $g_{\pm}, \tilde{g}_{\pm}$ are inflaton bulk-boundary propagators (which we define below); and $G_{\pm\pm}$ are bulk-bulk propagators (80) for h.

A.2.1.1 Calculation of I_{+-}

Let us start with I_{+-} diagram. This diagram factorizes into a product of two integrals with one coming from time ordering and another from anti time ordering.

Anti-time Ordered Contribution We first calculate inflaton contribution using inflaton mode function (81),

$$g_-(k;\eta) \equiv \langle \dot{\xi}(\eta,\vec{k})\xi(\eta_0 \to 0,-\vec{k})\rangle = -\frac{\eta^2 k^2}{2k^3} e^{-ik\eta}, \tag{89}$$

to write the anti time ordered contribution as

$$\text{Anti-time Ordered Contribution} = (+i)\int_{-\infty}^{0} \frac{d\eta'}{\eta'^4}\left(-\frac{\eta'^2 k_3^2}{2k_3^3} e^{-ik_3\eta'}\right)\bar{f}_{k_3}(\eta'). \tag{90}$$

Using the mode functions (79) and relation (83) we get

$$\text{Anti-time Ordered Contribution} = -\frac{1}{2\sqrt{2}}\frac{1}{k_3^{\frac{3}{2}}}\Gamma\left(\frac{1}{2}+i\mu\right)\Gamma\left(\frac{1}{2}-i\mu\right). \tag{91}$$

Time Ordered Contribution Let us first calculate the inflaton contribution again. Now we have to do a little more work since based on (87) we see that we have to find the contraction which can be schematically written as $\langle\xi\xi|(\partial\xi)^2\rangle$. Writing $\tilde{g}_+(k_1,k_2,\eta)$ as,

$$\tilde{g}_+(k_1,k_2,\eta) \equiv \langle \xi(\eta_0,\vec{k}_1)\xi(\eta_0,\vec{k}_2)(\partial_\mu\xi(\eta,-\vec{k}_1)\partial^\mu\xi(\eta,-\vec{k}_2))\rangle, \tag{92}$$

we get, using inflaton mode function (81),

$$\tilde{g}_+(k_1,k_2,\eta) = -\left(-\frac{1}{2k_1^3}\right)\left(-\frac{1}{2k_2^3}\right)e^{ik_{12}\eta}k_1^2k_2^2\eta^4 + \eta^2(-ik_{1i})(-ik_{2i})\frac{(1-ik_1\eta)(1-ik_2\eta)}{2k_1^3 2k_2^3}e^{ik_{12}\eta}, \quad (93)$$

where we have defined, $k_{12} = k_1 + k_2$. We can simplify this by removing some η-dependent factors by writing the above as an operator $\mathcal{D}$ acting on $e^{ik_{12}\eta}$, where

$$\mathcal{D} \equiv k_1^2k_2^2\partial_{k_{12}}^2 + (-\vec{k}_1\cdot\vec{k}_2)(1 - k_{12}\partial_{k_{12}} + k_1k_2\partial_{k_{12}}^2). \quad (94)$$

Then,

$$\tilde{g}_+(k_1,k_2,\eta) = \frac{\eta^2}{4k_1^3k_2^3}\mathcal{D}e^{ik_{12}\eta}. \quad (95)$$

Thus the time ordered contribution looks like

$$\text{Time Ordered Contribution} = (-i)\frac{1}{4k_1^3k_2^3}\mathcal{D}\int_{-\infty}^{0}\frac{d\eta}{\eta^2}e^{ik_{12}\eta}f_{k_3}(\eta). \quad (96)$$

The integral can be evaluated using (82) and (78) to get a hypergeometric function. Since we will be interested in squeezed limit, $k_3 \ll k_1, k_2$, we can expand the answer using (165). We then get

$$\text{Time Ordered Contribution} = \frac{1}{4\sqrt{2}k_1^3k_2^3\sqrt{k_3}}\mathcal{D}\left(\frac{\Gamma(-2i\mu)\Gamma(1/2+i\mu)}{\Gamma(1/2-i\mu)}\left(\frac{p}{2}\right)^{-1/2-i\mu} + (\mu\to-\mu)\right). \quad (97)$$

The action of $\mathcal{D}$ simplifies in the squeezed limit,

$$\mathcal{D}k_{12}^{\alpha} = \frac{1}{8}(\alpha-1)(\alpha-2)k_{12}^{2+\alpha}, \tag{98}$$

using which,

$$\begin{aligned}\text{Time Ordered Contribution} &= \frac{1}{4\sqrt{2}k_1^3k_2^3\sqrt{k_3}} \\ &\times \frac{1}{8}(3/2+i\mu)(5/2+i\mu) \times \frac{\Gamma(-2i\mu)\Gamma(1/2+i\mu)}{\Gamma(1/2-i\mu)}k_{12}^2\left(\frac{k_{12}}{2k_3}\right)^{-1/2-i\mu} + (\mu\to-\mu).\end{aligned} \tag{99}$$

Now we are ready to put together both the contributions:

$$I_{+-} = \frac{\rho_2^2}{\dot{\phi}_0}\frac{1}{64k_1^2k_2^2k_3^2}\Gamma(1/2+i\mu)^2\Gamma(-2i\mu)(3/2+i\mu)(5/2+i\mu)\left(\frac{k_1}{k_3}\right)^{-1/2-i\mu} + (\mu\to-\mu). \tag{100}$$

A.2.1.2 Calculation of I_{--}

I_{--} diagram is in general complicated since it does not factorize into η and η' integrals. But we can still calculate the the nonanalytic terms in k_3 in the squeezed limit. This is because in the squeezed limit, η' integral contributes when $-\eta' \sim \mathcal{O}(\frac{1}{k_3})$, whereas the contribution of η integral is dominant when $-\eta \sim \mathcal{O}(\frac{1}{k_{12}})$. Thus when $k_3 \ll k_{12}$, one of the step functions in G_{--} (80) drops out and the integral approximately factorizes. The η' integral then is identical to what we had for I_{+-};

whereas the only change for η integral is that $k_{12} \to -k_{12}$. Thus we have

$$I_{--} + I_{+-}$$
$$= \frac{\rho_2^2}{\dot{\phi}_0} \frac{1}{64 k_1^2 k_2^2 k_3^2} \Gamma\left(\frac{1}{2} + i\mu\right)^2 \Gamma(-2i\mu) \left(\frac{3}{2} + i\mu\right) \left(\frac{5}{2} + i\mu\right) \left(\frac{k_1}{k_3}\right)^{-\frac{1}{2} - i\mu} (1 - e^{i\pi(-\frac{1}{2} - i\mu)})$$
$$+ (\mu \to -\mu). \quad (101)$$

A.2.1.3 Three-Point Function

The full three point function can be written as a sum of $I_{++}, I_{+-}, I_{-+}, I_{--}$. This gives

$$\langle \xi(\vec{k}_1) \xi(\vec{k}_2) \xi(\vec{k}_3) \rangle = \frac{\rho_2^2}{\dot{\phi}_0} \frac{1}{16 k_1^2 k_2^2 k_3^2} \times$$
$$\Gamma\left(\frac{1}{2} + i\mu\right)^2 \Gamma(-2i\mu) \left(\frac{3}{2} + i\mu\right) \left(\frac{5}{2} + i\mu\right) (1 + i \sinh(\pi\mu)) \left(\frac{k_3}{k_1}\right)^{\frac{1}{2} + i\mu} + (\mu \to -\mu). \quad (102)$$

This gives F as a function of $\left(\frac{k_3}{k_1}\right)$ as defined in (2.23) to be

$$F_h^{\text{single}} = -\frac{1}{4} \times \rho_2^2 \times$$
$$\Gamma\left(\frac{1}{2} + i\mu\right)^2 \Gamma(-2i\mu) \left(\frac{3}{2} + i\mu\right) \left(\frac{5}{2} + i\mu\right) (1 + i \sinh(\pi\mu)) \left(\frac{k_3}{k_1}\right)^{\frac{3}{2} + i\mu} + (\mu \to -\mu). \quad (103)$$

where, $\rho_2 = \frac{2 c_2 v \dot{\phi}_0}{\Lambda^2}$; $\qquad \alpha = -\frac{c_2 \dot{\phi}_0^2}{\Lambda^2}$.

For the case of the Goldstone effective description of inflation, with $\Lambda \ll f_\pi$,

the relevant terms in the lagrangian are given by (2.92). The calculation of $F_h^{\rm single}$ follows identical steps as above with the difference that the operator $\mathcal{D} = k_1^2 k_2^2 \partial_{k_{12}}^2$. This results into, the replacement $\left(\frac{3}{2}+i\mu\right)\left(\frac{5}{2}+i\mu\right) \to \frac{1}{2}\left(\frac{1}{2}+i\mu\right)\left(\frac{3}{2}+i\mu\right)$. Hence the final answer reads (taking $d_2 = 1$),

$$F_h^{\rm single} = -\frac{1}{8} \times \lambda_2 \left(\frac{v f_\pi}{\Lambda}\right)^2 \times$$
$$\Gamma\left(\frac{1}{2}+i\mu\right)^2 \Gamma\left(-2i\mu\right) \left(\frac{1}{2}+i\mu\right)\left(\frac{3}{2}+i\mu\right)\left(1+i\sinh(\pi\mu)\right)\left(\frac{k_3}{k_1}\right)^{\frac{3}{2}+i\mu} + (\mu \to -\mu). \tag{104}$$

A.2.2 Calculation of Double Exchange Diagram

We see from the Fig. 2.3 (a) that there is a quadratic mixing between inflaton and Higgs field h. For numerical simplification one can define a mixed propagator which captures this mixing [78]. Using this mixed propagator, we then calculate double exchange diagram numerically. We first focus on single field slow roll inflation.

A.2.2.1 Mixed Propagators

A mixed propagator is characterized by the 3−momentum (say k) flowing through the line and bulk time coordinate η. We have to sum over all time instants η' where the mixing occurs. The bulk time coordinate η can be part of either time or anti-time ordering. Let us first consider the case where η comes from time ordering, and denote that mixed propagator by, $D_+(\eta, k)$. Then we have two possibilities, (a)

η' comes also from time ordering, in which case the we can write the contribution of the mixing part of the entire diagram as,

$$\mathcal{I}_+ = -\int_{-\infty}^{0} \frac{d\eta'}{\eta'^4} g_+(k,\eta') \left(\theta(\eta-\eta')\bar{f}(\eta)f(\eta') + \theta(\eta'-\eta)\bar{f}(\eta')f(\eta)\right), \tag{105}$$

and, (b) η' comes from anti-time ordering, for which we get,

$$\mathcal{I}_- = +\int_{-\infty}^{0} \frac{d\eta'}{\eta'^4} g_-(k,\eta')\bar{f}(\eta')f(\eta). \tag{106}$$

The overall signs are due to again $e^{\pm i\int dtH}$ and we have omitted a factor of $+i$ for simplicity which we will restore in the final expression for the mixed propagator. We can then rewrite $\mathcal{I}_+$ as

$$\mathcal{I}_+ = -(\mathcal{I}_-)^* + \bar{f}(\eta)\int_{\eta}^{0} \frac{d\eta'}{\eta'^4} g_+(k,\eta')f(\eta') - f(\eta)\int_{\eta}^{0} \frac{d\eta'}{\eta'^4} g_+(k,\eta')\bar{f}(\eta'). \tag{107}$$

So the whole contribution of the mixed propagator when η comes from time ordering is

$$\begin{aligned} &D_+(\eta,k) = (-i\rho_2)(\mathcal{I}_+ + \mathcal{I}_-) \\ &= (+i)(-\rho_2)\left(2i\mathrm{Im}(\mathcal{I}_-) + \bar{f}(\eta)\int_{\eta}^{0} \frac{d\eta'}{\eta'^4} g_+(k,\eta')f(\eta') - f(\eta)\int_{\eta}^{0} \frac{d\eta'}{\eta'^4} g_+(k,\eta')\bar{f}(\eta')\right). \end{aligned} \tag{108}$$

We have restored the factor of $+i$ and also put the mixing vertex $-\rho_2$ from (2.48).

Using the mode functions for inflatons (81) and massive scalars (78) and (79),

and also the relations, (83),(82), we can evaluate the mixed propagator analytically. For convenience, we define the function $J_+(-\eta k) = \frac{8k^3}{\pi\rho}\mathcal{D}_+(\eta, k)$:

$$\begin{aligned} J_+(x) = x^{\frac{3}{2}} \Big[& \sqrt{2\pi}\mathrm{sech}(\pi\mu)e^{\pi\mu/2}\left(H^{(2)}_{i\mu}(x)e^{i\pi/4} + H^{(1)}_{-i\mu}(x)e^{-i\pi/4}\right) \\ & -2\sqrt{x}H^{(1)}_{i\mu}(x)\left(\mathrm{csch}(\pi\mu)\mathsf{F}(\mu,x) + (1-\coth(\pi\mu))\mathsf{F}(-\mu,x)\right) \\ & -2\sqrt{x}H^{(2)}_{i\mu}(x)\left(\mathrm{csch}(\pi\mu)\mathsf{F}(\mu,x) - (1+\coth(\pi\mu))\mathsf{F}(-\mu,x)\right)\Big], \end{aligned} \quad (109)$$

where $x = -k\eta$, and $\mathsf{F}(\mu, x)$ is given in terms of hypergeometric function ${}_2F_2$,

$$\mathsf{F}(\mu,x) = \frac{1}{\Gamma(1-i\mu)}\frac{1}{2\mu+i}\left(\frac{x}{2}\right)^{-i\mu}{}_2F_2\left(\frac{1}{2}-i\mu, \frac{1}{2}-i\mu; \frac{3}{2}-i\mu, 1-2i\mu; -2ix\right). \quad (110)$$

We will be using the small argument limit of $J_+(x)$,

$$J_+(x) = A(\mu)x^{\frac{3}{2}}(x/2)^{i\mu} + A(-\mu)x^{\frac{3}{2}}(x/2)^{-i\mu}, \quad (111)$$

where $A(\mu) = -2\sqrt{2/\pi}\mathrm{sech}(\pi\mu)\Gamma(-i\mu)\sin(\frac{\pi}{4} + \frac{i\pi\mu}{2})$.

A.2.2.2 Three-Point Function

After we incorporate appropriate internal lines into mixed propagators, the double exchange diagram effectively contains a single vertex. Thus we only have two diagrams to calculate, with one of them being the conjugate of the other. Let us start with the time ordered contribution. Since the lagrangian (2.48) contains a

term of the form $\frac{\alpha}{\dot{\phi}_0}\dot{\xi}h^2$ then we get

$$+i\frac{\alpha}{\dot{\phi}_0}\int\frac{d\eta}{\eta^4}\left(-\frac{k_1^2\eta^2}{2k_1^3}\right)e^{ik_1\eta}D_+(\eta,k_2)D_+(\eta,k_3). \tag{112}$$

Once again we will be interested in the limit $k_3 \ll k_1$, so using the small argument expansion of J_+,

$$\begin{aligned}+\,i\frac{\alpha}{\dot{\phi}_0}\left(-\frac{1}{2k_1}\right)\int\frac{d\eta}{\eta^2}e^{ik_1\eta}\mathcal{D}_+(\eta,k_1)\mathcal{D}_+(\eta,k_3)\\ =-\frac{i}{2}\frac{\alpha}{\dot{\phi}_0}\frac{\pi^2\rho_2^2}{64k_1^3k_3^3}\left(A(\mu)s(\mu)\left(\frac{k_3}{k_1}\right)^{3/2}\left(\frac{k_3}{2k_1}\right)^{i\mu}+(\mu\to-\mu)\right),\end{aligned} \tag{113}$$

where we have defined $s(\mu)=\int_0^\infty\frac{dx}{x^2}e^{-ix}J_+(x)x^{3/2+i\mu}$. The full three point function then becomes, after adding the anti-time ordered contribution,

$$\frac{\pi^2\rho_2^2}{64k_1^3k_3^3}(-\frac{i}{2}\frac{\alpha}{\dot{\phi}_0})\left(A(\mu)s(\mu)-A^*(-\mu)s^*(-\mu)\right)\left(\frac{k_3}{k_1}\right)^{3/2}\left(\frac{k_3}{2k_1}\right)^{i\mu}+(\mu\to-\mu). \tag{114}$$

This gives F as a function of $\left(\frac{k_3}{k_1}\right)$ after summing over permutation $k_1\leftrightarrow k_2$,

$$F_h^{\text{double}}=\alpha\rho_2^2\frac{i\pi^2}{16}\left(A(\mu)s(\mu)-A^*(-\mu)s^*(-\mu)\right)\left(\frac{k_3}{k_1}\right)^{3/2}\left(\frac{k_3}{2k_1}\right)^{i\mu}+(\mu\to-\mu). \tag{115}$$

For $m<\frac{3H}{2}$ we get an appropriately modified version of the above expression. In terms of the function, $\bar{s}(\nu)=\int_0^\infty\frac{dx}{x^2}e^{-ix}I_+(x)x^{3/2-\nu}$ we have,

$$F_h^{\text{double}}=-\alpha\rho_2^2\frac{\pi^2}{8}B(\nu)\text{Im}(\bar{s}(\nu))\left(\frac{k_3}{k_1}\right)^{\frac{3}{2}-\nu}, \tag{116}$$

where $B(\nu) \equiv -2^{\nu+1}\Gamma(\nu)\sqrt{2/\pi}\sec(\pi\nu)\sin(\pi/4 - \pi\nu/2)$. In deriving the above we have not kept a contribution of the form $\left(\frac{k_3}{k_1}\right)^{3/2+\nu}$.

For the Goldstone description we see from (2.92) that the functional form for F_h^{double} is identical to above. For the overall coefficient we change, $\rho_2^2\alpha \to \frac{1}{2}\lambda_2(\lambda_2 v)^2 f_\pi^2$, and hence,

$$F_h^{\text{double}} = \lambda_2(\lambda_2 v f_\pi)^2 \frac{i\pi^2}{32}\left(A(\mu)s(\mu) - A^*(-\mu)s^*(-\mu)\right)\left(\frac{k_3}{k_1}\right)^{3/2}\left(\frac{k_3}{2k_1}\right)^{i\mu} + (\mu \to -\mu). \tag{117}$$

A.2.3 Calculation of Triple Exchange Diagram

Using the mixed propagator, the triple exchange diagram can also be calculated in an identical manner [78]. Using the cubic Higgs vertex, $\frac{\lambda_h v}{2}h^3$ we can write the time ordered diagram as,

$$(-i)\frac{\lambda_h v}{2}\int \frac{d\eta}{\eta^4} D_+(\eta, k_1)D_+(\eta, k_2)D_+(\eta, k_3). \tag{118}$$

Again in the limit $k_3 \gg k_1$ we can use the small argument expansion of $J_+(x)$,

$$\begin{aligned}(-i)\frac{\lambda_h v}{2}\int \frac{d\eta}{\eta^4} D_+(\eta, k_1)D_+(\eta, k_2)D_+(\eta, k_3) \\ = (-i)\frac{\lambda_h v}{2} \times \frac{\pi^3\rho_2^3}{8^3 k_1^3 k_3^3}\left(A(\mu)t(\mu)\left(\frac{k_3}{k_1}\right)^{\frac{3}{2}}\left(\frac{k_3}{2k_1}\right)^{i\mu} + (\mu \to -\mu)\right),\end{aligned} \tag{119}$$

where $A(\mu) = -2\sqrt{2/\pi}\text{sech}(\pi\mu)\Gamma(-i\mu)\sin(\frac{\pi}{4} + \frac{i\pi\mu}{2})$ and $t(\mu) = \int_0^\infty \frac{dx}{x^4} J_+(x)^2 x^{\frac{3}{2}+i\mu}$. After adding the anti-time ordered contribution and permutation $k_1 \leftrightarrow k_2$ we get

$$F_h^{\text{triple}} = \frac{\pi^3 \rho_2^3 \dot{\phi}_0 \lambda_h v}{128}(+i)\left(A(\mu)t(\mu) - A^*(-\mu)t^*(-\mu)\right)\left(\frac{k_3}{k_1}\right)^{\frac{3}{2}}\left(\frac{k_3}{2k_1}\right)^{i\mu} + (\mu \to -\mu). \tag{120}$$

For the Goldstone description we see from (2.92) that the functional form for F_h^{triple} is identical to above. For the overall coefficient we change, $\rho_2^3 \to (\lambda_2 v)^3$, and hence,

$$F_h^{\text{triple}} = \frac{\pi^3 \lambda_2^3 v^3 f_\pi^2 \lambda_h v}{128}(+i)\left(A(\mu)t(\mu) - A^*(-\mu)t^*(-\mu)\right)\left(\frac{k_3}{k_1}\right)^{\frac{3}{2}}\left(\frac{k_3}{2k_1}\right)^{i\mu} + (\mu \to -\mu). \tag{121}$$

A.3 Massive Vector Fields in dS Space

Here we will derive mode functions for massive spin-1 fields [40], which will be useful in the next appendix in computing NG mediated by Z-type particles.

A.3.1 Mode Functions in Momentum Space

We start with the lagrangian,

$$\int d^4x\sqrt{-g}\left(-\frac{1}{4}F_{\mu\nu}^2 - \frac{1}{2}m^2 Z_\mu^2\right), \tag{122}$$

where $F_{\mu\nu} = \nabla_\mu Z_\nu - \nabla_\nu Z_\mu$. Variation of the action yields the equation of motion,

$$\nabla_\mu F^{\mu\nu} = m^2 Z^\nu. \tag{123}$$

Taking the divergence of both sides and also using the fact that $\nabla_\mu \nabla_\nu F^{\mu\nu} \propto R_{\mu\nu} F^{\mu\nu} = 0$, we get

$$\nabla_\mu Z^\mu = 0. \tag{124}$$

Mode functions for Z^μ are then obtained by solving (123) and (124). The NG correlators involve mixing the inflaton with the Z, which is constrained by the spatial rotation and translation invariance. Therefore only the longitudinal Z polarization, which is a spatial scalar, can appear since the inflaton is obviously scalar. We are interested in the mode functions for this degree of freedom. It is shared between the timelike component Z_η and the longitudinal spatial component $Z_{\rm long} = \vec{Z} \cdot \hat{k}$ with $\hat{k}$ being a unit vector pointing in the direction of propagation.

Fourier transforming from $(\eta, \vec{x})$ to $(\eta, \vec{k})$ coordinates, the constraint equation reads,

$$\eta^2 \partial_\eta Z_\eta - 2\eta Z_\eta = i\eta^2 k Z_{\rm long}. \tag{125}$$

From (123) and (125) we get the equation of motion for the component Z_η,

$$\partial_\eta^2 Z_\eta - \frac{2}{\eta}\partial_\eta Z_\eta - \partial_i^2 Z_\eta + \frac{(m^2+2)}{\eta^2} Z_\eta = 0. \tag{126}$$

This is almost identical to the equation of motion for the scalar (73). The solutions are again given in terms of Hankel functions, but with $\mu^2 = m^2 + 2 - \frac{9}{4} = m^2 - \frac{1}{4}$. After we obtain the mode function for Z_η, that for $Z_{\rm long}$ is simply obtained from the constraint equation (125). In parallel with the case of scalars, the quantum field is obtained by elevating the free superposition coefficients in the general classical

solution to linear combinations of creation and destruction operators on the Bunch-Davies vacuum,

$$\begin{aligned} Z_\eta(\eta,\vec{k}) &= h_{k,0}(\eta)b^\dagger_{\vec{k}} + \bar{h}_{k,0}(\eta)b_{-\vec{k}}, \\ Z_{\rm long}(\eta,\vec{k}) &= h_{k,l}(\eta)b^\dagger_{\vec{k}} + \bar{h}_{k,l}(\eta)b_{-\vec{k}}, \end{aligned} \tag{127}$$

where the mode functions are

$$\bar{h}_{k,0}(\eta) = Ne^{-\frac{\pi\mu}{2}}(-\eta)^{\frac{3}{2}}H^{(1)}_{i\mu}(-k\eta) \tag{128}$$

$$\bar{h}_{k,l}(\eta) = Ne^{-\frac{\pi\mu}{2}}\left(+\frac{i}{2k}\right)(-\eta)^{\frac{1}{2}}\left(-H^{(1)}_{i\mu}(-k\eta) + k\eta H^{(1)}_{i\mu+1}(-k\eta) - k\eta H^{(1)}_{i\mu-1}(-k\eta)\right), \tag{129}$$

with $N = e^{\frac{i\pi}{4}}\frac{\sqrt{\pi}}{2}\frac{k}{m}$. In the above b and $b^\dagger$ are annihilation and creation operators for the longitudinal degree of freedom for spin-1.

A.4 NG due to Z Exchange

For single-field slow-roll inflation, the lagrangian involving the inflaton and spin-1 Z relevant for single-exchange (diagram (a) in Fig. 2.3) is given by (2.63) to be

$$\mathcal{L} = \rho\eta\dot{\xi}Z_\eta + \frac{\rho}{\dot{\phi}_0}\eta^2\dot{\xi}\partial_i\xi Z_i, \tag{130}$$

where $\rho = \frac{\rho_{1,Z}\rho_2}{m_h^2}$. As discussed earlier, we defer the computation of the double-exchange contribution to future work, although we have estimated its strength and it seems readily detectable in future measurements. We have also shown earlier that

the triple-exchange contribution is suppressed and can be neglected.

We now parallel the steps taken in the calculation of NG for the case of single-exchange of a scalar h. We start with I_{-+} diagram. In this case the time ordered and anti-time ordered contribution factorize, and we can evaluate them separately.

Time Ordered Contribution

$$(+i\rho)\int_{-\infty}^{0}\frac{d\eta'}{\eta'^4}\eta'\left(-\frac{k_3^2\eta'^2}{2k_3^3}\right)e^{ik_3\eta'}h_{k,0}(\eta)=\rho\frac{1}{4\sqrt{2}}\frac{1}{m_Z k_3^{\frac{3}{2}}}\Gamma\left(\frac{3}{2}+i\mu\right)\Gamma\left(\frac{3}{2}-i\mu\right). \tag{131}$$

Anti-time Ordered Contribution Defining $p=\frac{k_1}{k_3}$,

$$(-i\frac{\rho}{\dot{\phi}_0})\int_{-\infty}^{0}\frac{d\eta}{\eta^4}\eta^2\left(\frac{-k_2^2\eta^2}{2k_2^3}\right)e^{-ik_2\eta}\left(\frac{-ik_{1i}}{2k_1^3}\right)e^{-ik_1\eta}(1+ik_1\eta)\hat{k}_{3i}\bar{h}_{k,l}(\eta) \tag{132}$$

$$=\frac{i\rho}{\dot{\phi}_0}\frac{1}{16k_2k_1^2k_3^{\frac{3}{2}}}\frac{\sqrt{\pi}}{m_Z}e^{\frac{i\pi}{4}}(\hat{k}_1\cdot\hat{k}_3)\times \tag{133}$$

$$\left(-f_1(\frac{1}{2},2p)+ipf_1(\frac{3}{2},2p)+f_2(\frac{3}{2},2p)-ipf_2(\frac{5}{2},2p)-f_3(\frac{3}{2},2p)+ipf_3(\frac{5}{2},2p)\right), \tag{134}$$

where different integrals involving Hankel functions have been evaluated using (83),

$$\begin{aligned}
f_1(n,p) &= \frac{(+i/2)^n}{\Gamma(n+3/2)}\frac{1}{\sqrt{\pi}}\Gamma(n+1-i\mu)\Gamma(n+1+i\mu) \\
&\quad \times {}_2F_1(n+1+i\mu, n+1-i\mu, n+3/2, (1-p)/2) \\
f_2(n,p) &= (+i)\frac{(+i/2)^n}{\Gamma(n+3/2)}\frac{1}{\sqrt{\pi}}\Gamma(n+2-i\mu)\Gamma(n+i\mu) \\
&\quad \times {}_2F_1(n+i\mu, n+2-i\mu, n+3/2, (1-p)/2) \\
f_3(n,p) &= (-i)\frac{(+i/2)^n}{\Gamma(n+3/2)}\frac{1}{\sqrt{\pi}}\Gamma(n+2+i\mu)\Gamma(n-i\mu) \\
&\quad \times {}_2F_1(n+2+i\mu, n-i\mu, n+3/2, (1-p)/2)
\end{aligned} \tag{135}$$

We multiply the above two contributions and also sum over I_{++}, I_{--}, I_{+-} diagrams. Finally we sum over permutations $\vec{k}_1 \leftrightarrow \vec{k}_2$ to get,

$$\begin{aligned}
F_Z^{\text{single}} &= \frac{\rho^2}{16\pi m_Z^2}\sin^2\theta\Gamma(\frac{3}{2}+i\mu)\Gamma(\frac{3}{2}-i\mu)\cosh(\pi\mu)\times \\
&(7-5i\mu+16\mu^2+4i\mu^3)\Gamma(\frac{3}{2}+i\mu)^2\Gamma(-2-2i\mu)(1-i\sinh(\pi\mu))\left(\frac{k_3}{k_1}\right)^{\frac{5}{2}+i\mu} \\
&\quad +(\mu\to-\mu),
\end{aligned} \tag{136}$$

where $\theta = \hat{k}_1\cdot\hat{k}_3$ and we have used large negative argument expansion of hypergeometric function.

For the Goldstone description, we see from (2.96) that the functional form of F_Z^{single} is identical to the above. The overall coefficient is changed to $\rho \to \frac{vm_Z}{2\Lambda}$(taking

$\mathrm{Im}(d_1) = 1$). Hence we get

$$F_Z^{\text{single}} = \left(\frac{v}{2\Lambda}\right)^2 \frac{1}{16\pi} \sin^2\theta \Gamma(\frac{3}{2} + i\mu)\Gamma(\frac{3}{2} - i\mu)\cosh(\pi\mu)\times$$
$$(7 - 5i\mu + 16\mu^2 + 4i\mu^3)\Gamma(\frac{3}{2} + i\mu)^2\Gamma(-2 - 2i\mu)(1 - i\sinh(\pi\mu))\left(\frac{k_3}{k_1}\right)^{\frac{5}{2}+i\mu}$$
$$+(\mu \to -\mu). \tag{137}$$

B.1 KK Reduction of the Graviton-Radion System

The linearized gravitational fluctuations to the background metric (3.17) can be characterized by,

$$ds^2 = -n(y)^2(1-2\Pi(x,y))dt^2 + n(y)^2a(t)^2(1-2\Pi(x,y))d\vec{x}^2 + (1+4\Pi(x,y))dy^2 + h_{\mu\nu}(x,y)dx^\mu dx^\nu, \quad (138)$$

where $h_{\mu\nu}$ and $\Pi(x,y)$ denote the graviton and the radion fluctuations respectivey. We have chosen a gauge such that $\nabla_\mu h^{\mu\nu} = 0 = h^\mu{}_\mu$. In the following we derive the linearized equation of motion for the graviton and the radion from the perturbed Einstein equations,

$$\delta R_{MN} = \frac{1}{4M_5^3}\delta\tilde{T}_{MN}, \quad (139)$$

where $\tilde{T}_{MN} = T_{MN} - \frac{1}{3}g_{MN}T^A{}_A$ with T_{MN} being the bulk stress-energy tensor. Our approach will be similar to [127] and we generalize their results appropriately to the case of a dS_4 foliation with $H \neq 0$.

For a generic metric fluctuation δG_{MN}, we can get the linearized perturbed Ricci tensor [118],

$$\delta R_{MN} = \frac{1}{2}\left(\nabla_A\nabla_M\delta G^A{}_N + \nabla_A\nabla_N\delta G^A{}_M\right) - \frac{1}{2}\nabla_A\nabla^A\delta G_{MN} - \frac{1}{2}\left(\nabla_N\nabla_M\delta G^A{}_A\right). \quad (140)$$

To show that the graviton and the radion equation of motion decouple at the lin-

earized level, we split δR_{MN} into,

$$\delta R_{MN} = \delta R^h_{MN} + \delta R^\Pi_{MN}, \tag{141}$$

where $\delta R^{h(\Pi)}_{MN}$ is linear in $h_{\mu\nu}(\Pi)$. Then using eq. (140) and the identity,

$$[\nabla_A, \nabla_M]\delta G^A{}_N = \bar{R}_{BM}\delta G^B{}_N - \bar{R}^B{}_{NAM}\delta G^A{}_B, \tag{142}$$

we can derive,

$$\delta R^h_{\mu 5} = 0; \qquad \delta R^h_{55} = 0. \tag{143}$$

This implies the 55 and 5μ Einstein equations can only contribute to the radion eq. of motion which we now derive. To do this first we evaluate,

$$\delta R^F_{\mu 5} = 3\partial_\mu \Pi' + 6\frac{n'}{n}\partial_\mu \Pi,$$
$$\delta R^F_{55} = -\frac{2}{n^2}\Box_{dS}\Pi + 4\Pi'' + 16\frac{n'}{n}\Pi',$$

where $\Box_{dS}$ d'Alembertian for dS_4. In the above and the rest of this Appendix, $' \equiv \frac{\partial}{\partial y}$. We will also need the perturbed stress energy tensors,

$$\delta\tilde{T}_{5\mu} = \partial_\mu \sigma \Sigma',$$
$$\delta\tilde{T}_{55} = 2\Sigma'\sigma' + \frac{2}{3}\frac{dV(\Sigma)}{d\Sigma}\sigma + \frac{8}{3}V(\Sigma)\Pi.$$

The GW field is expanded as $\Sigma(y)+\sigma(x,y)$ where σ is the fluctuation of the background GW field Σ. Then the 55 Einstein equation gives the radion eq. of motion,

$$\frac{1}{n^2}\Box_{dS}\Pi = -\Pi'' - 2n'\Pi'/n + 4((\frac{n'}{n})^2 - \frac{n''}{n})\Pi + 2\frac{\Sigma''}{\Sigma'}(\Pi' + 2n'\Pi/n) - 6H^2\Pi/n^2, \tag{144}$$

while the 5μ Einstein equations give (after doing an integration to get rid of ∂_μ),

$$3\Pi' + 6\frac{n'}{n}\Pi = \sigma\Sigma'. \tag{145}$$

We can consider the special case of an unstabilized extra dimension where the GW field is absent. In that case eq. (145) simplifies to give $3\Pi' + 6\frac{n'}{n}\Pi = 0$, so that (144) becomes,

$$\frac{1}{n^2}\Box_{dS}\Pi = 2((\frac{n'}{n})^2 - \frac{n''}{n})\Pi - 6H^2\Pi/n^2 \qquad \text{(No Stabilization)}. \tag{146}$$

Then using the background eqs. (3.18) and (3.19) we get,

$$\Box_{dS}\Pi = -4H^2\Pi \qquad \text{(No Stabilization)}, \tag{147}$$

which shows that the radion gets a tachyonic mass of $-4H^2$ in absence of a stabilizing GW field.

Now let us study the $\mu\nu$ equations. We expect these to give the graviton eq. of motion, but first we have to show that the radion decouples from these equations.

This can be done using the expressions,

$$\delta R^{\Pi}_{\mu\nu} = g_{\mu\nu}\Box_{dS}\Pi - g_{\mu\nu}n^2(-24\Pi(n'/n)^2 - 6\Pi(n'/n)' - 10\Pi' n'/n - \Pi''), \quad (148)$$

$$\delta\tilde{T}^{\Pi}_{\mu\nu} = -\frac{4}{3}V\Pi n^2 g_{\mu\nu} + \frac{2}{3}\frac{dV}{d\Sigma}\sigma n^2 g_{\mu\nu}, \quad (149)$$

where $g_{\mu\nu}$ is the metric for background dS_4 spacetime (without the $n(y)^2$ warp factor). Using the eqs. (148), (149) and (144) we can derive that $\delta R^{\Pi}_{\mu\nu} = \frac{1}{4M_5^3}\delta\tilde{T}^{\Pi}_{\mu\nu}$. Hence the $\mu\nu$ eqs. imply $\delta R^{h}_{\mu\nu} = \frac{1}{4M_5^3}\delta\tilde{T}^{h}_{\mu\nu}$, from which we will get the graviton eq. of motion. Thus we have decoupled the graviton-radion system. $\delta R^{h}_{\mu\nu}$ can be evaluated to be,

$$\delta R^{h}_{\mu\nu} = -\frac{1}{2n^2}\Box_{dS}h_{\mu\nu} - \frac{1}{2}h''_{\mu\nu} - 2(n'/n)^2 h_{\mu\nu} + 4\frac{H^2}{n^2}h_{\mu\nu}. \quad (150)$$

Using $\delta\tilde{T}^{h}_{\mu\nu} = \frac{2V}{3}h_{\mu\nu}$ we finally arrive at the graviton eq. of motion,

$$\frac{1}{n^2(y)}\Box_{dS}h_{\mu\nu} + h''_{\mu\nu} - 2(n'(y)/n(y)^2 h_{\mu\nu} - 2n''(y)/n(y)h_{\mu\nu} - 2H^2/n^2(y)h_{\mu\nu} = 0. \quad (151)$$

B.2 NG Mediated by the KK Graviton

To calculate KK graviton mediated NG, we will need the mode functions of a massive spin-2 field in dS_4 [40] which we now derive.

B.2.1 Mode Functions for Helicity-0 component of a Massive Spin-2 Field in dS_4

Helicity Decomposition. The NG contribution that we are interested in involves quadratic mixing between the inflaton and the KK graviton. Since the inflaton is a scalar, only the scalar degree of freedom (DOF), or the helicity 0 component of a massive spin-2 particle in 4D, can be relevant. This DOF will come from metric fluctuation $h_{\eta\eta}$ and helicity 0 components of $h_{i\eta}$ and h_{ij}. To isolate the helicity 0 component from the 3-vector $h_{i\eta}$ we can write it as a gradient of a scalar and a divergenceless vector, in momentum space,

$$h_{i\eta}(\eta,\vec{k}) = \hat{k}_i h_V(\eta,\vec{k}) + \cdots \,, \tag{152}$$

where we have omitted the divergenceless vector for brevity. To isolate the same from h_{ij} we first note that to implement $h^{\mu}{}_{\mu} = 0$ we can write, $h_{ij}(\eta,\vec{k}) = h_{ij}^{\rm traceless} + \frac{1}{3}h_{\eta\eta}\delta_{ij}$, and then write the traceless part as,

$$h_{ij}^{\rm traceless}(\eta,\vec{k}) = \epsilon_{ij}(\vec{k}) h_{\rm T}(\eta,\vec{k}) + \cdots \,, \tag{153}$$

where $\epsilon_{ij}(\vec{k}) = \frac{3}{2}(\hat{k}_i\hat{k}_j - \frac{1}{3}\delta_{ij})$ and $\cdots$ contain the helicity ±1 and ±2 fluctuations which we have not kept for brevity. In the above $\hat{k}_i$'s are unit vectors.

Mode Functions. We now focus on deriving the mode functions for $h_{\eta\eta}$ and h_T which will be required for computing KK graviton mediated NG that will have a

characteristic spin-2 angular dependence. First, from the eq. of motion $\Box_{dS} h_{\eta\eta} = (m^2 + 2H^2) h_{\eta\eta}$ we get,

$$\partial_\eta^2 h_{\eta\eta} + \frac{2}{\eta}\partial_\eta h_{\eta\eta} - \frac{4}{\eta}\partial_i h_{i\eta} - \frac{2}{\eta^2} h_{ii} + \frac{m^2/H^2 - 6}{\eta^2} h_{\eta\eta} - \partial_i^2 h_{\eta\eta} = 0. \tag{154}$$

To convert the above into an eq. of motion involving only $h_{\eta\eta}$, we apply the constraints $h^\mu{}_\mu = 0$ and

$$\nabla^\mu h_{\mu\eta} = \partial_\eta h_{\eta\eta} - \frac{1}{\eta} h_{\eta\eta} - \partial_i h_{i\eta} - \frac{1}{\eta} h_{ii} = 0, \tag{155}$$

to get,

$$\partial_\eta^2 h_{\eta\eta} - \frac{2}{\eta}\partial_\eta h_{\eta\eta} + \frac{m^2}{H^2\eta^2} h_{\eta\eta} - \partial_i^2 h_{\eta\eta} = 0. \tag{156}$$

Using the constraint,

$$\nabla^\mu h_{\mu i} = \partial_\eta h_{\eta i} - \frac{2}{\eta} h_{i\eta} - \partial_j h_{ij} = 0, \tag{157}$$

we can obtain an *algebraic* equation for h_{ij},

$$\partial_\eta^2 h_{\eta\eta} - \frac{4}{\eta}\partial_\eta h_{\eta\eta} + \frac{6}{\eta^2} h_{\eta\eta} = \partial_i \partial_j h_{ij}. \tag{158}$$

Note the above equation is sufficient to determine the helicity-0 component of h_{ij}, i.e. h_T. Hence to summarize, by solving eqs. (156) and (158) we will get the desired mode functions. To canonically quantize the spin-2 field we can follow the standard

procedure as in the case of scalars. We write the fields $h_{\eta\eta}$ and h_T in terms of linear combinations of the creation and destruction operators,

$$h_{\eta\eta}(\eta,\vec{k}) = h_{k,0}(\eta)a^{\dagger}_{\vec{k}} + \bar{h}_{k,0}(\eta)a_{-\vec{k}}, \tag{159}$$

$$h_T(\eta,\vec{k}) = h_{k,T}(\eta)a^{\dagger}_{\vec{k}} + \bar{h}_{k,T}(\eta)a_{-\vec{k}}, \tag{160}$$

where $h_{k,0}(\eta), \bar{h}_{k,0}(\eta)$ and $h_{k,T}(\eta), \bar{h}_{k,T}(\eta)$ are solutions of eqs. (156) and (158) respectively. In particular,

$$\bar{h}_{k,0}(\eta) = e^{i\pi/4}e^{-\pi\mu/2}\mathcal{N}(-k\eta)^{\frac{3}{2}}H^{(1)}_{i\mu}(-k\eta), \tag{161}$$

and,

$$\bar{h}_{k,T}(\eta) = \frac{1}{12}e^{i\pi/4}e^{-\pi\mu/2}\mathcal{N}(-k\eta)^{-\frac{1}{2}}$$
$$\times\Big(-6(2-i\mu)k\eta H^{(1)}_{i\mu-1}(-k\eta) + 6(2+i\mu)k\eta H^{(1)}_{i\mu+1}(-k\eta) - (9-8k^2\eta^2)H^{(1)}_{i\mu}(-k\eta)\Big),$$

where $\mathcal{N} = \sqrt{\frac{\pi}{6}}\frac{\sqrt{k}}{H}\frac{H}{m\sqrt{m^2/H^2-2}}$ is a normalization factor which can be derived by demanding the orthonormality of the mode functions [40], and $\mu = \sqrt{m^2/H^2 - 9/4}$.

B.2.2 Calculation of Single Exchange Diagram

In this subsection we will be interested in computing the NG mediated by a single KK graviton exchange as in Fig. 3.3 using the master formula (2.7) for computing an in-in expectation values. Our discussion here will be very brief and

for a more detailed explanation of the set-up and the notation, we refer the reader to our previous work [24]. We will also momentarily work in $H = 1$ units and restore H in the final expression for NG in eq. (169).

The lagrangian relevant for the single exchange diagram can be obtained from eq. (3.61),

$$\mathcal{L} = -\frac{2\psi_1(0)}{M_4}\eta^2\dot{\phi}_0\xi h_{\eta\eta} - \frac{\psi_1(0)}{M_4}\eta^4\partial_i\xi\partial_j\xi\epsilon_{ij}h_T + \cdots . \tag{162}$$

In the cubic term above we have kept only the spatial metric fluctuation h_{ij}, since that gives an angular dependence that is characteristic of a spin-2 exchange, and used its helicity-0 piece. The three point function corresponding to this single exchange diagram will consist of 4 diagrams, I_{ab}, where $a, b = \pm$. The indices a and b correspond respectively to the mixing and cubic vertex in Fig. 3.3 (a). For example, $a = +(-)$ when the mixing vertex, comes from anti-time ordered (time ordered) part of the interaction Hamiltonian in eq. (2.7).

We will first evaluate I_{-+} for which the time-ordered and anti-time ordered components factorize. We will do this in the squeezed limit where $k_1 \approx k_2 \gg k_3$ and denote the angle between $\vec{k}_1$ and $\vec{k}_3$ by θ.

Time ordered contribution.

$$\begin{aligned}(-i) \times \frac{2\psi_1(0)\dot{\phi}_0}{M_4} \times \int_{-\infty}^{0} \frac{d\eta'}{\eta'^4}\eta'^2 \times h_{k_3,0}(\eta) \times \frac{(1 - ik_3\eta')}{2k_3^3}e^{ik_3\eta'} \\ = (-i)\frac{2\psi_1(0)\dot{\phi}_0}{M_4}\frac{m^2}{H^2} \times \frac{\mathcal{N}\sqrt{\pi}}{2\sqrt{2}k_3^2\cosh(\pi\mu)}.\end{aligned} \tag{163}$$

Anti-time ordered contribution.

$$(+i)\times\frac{\psi_1(0)}{M_4}\times\int_{-\infty}^{0}\frac{d\eta}{\eta^4}\eta^4\times\epsilon_{ij}\bar{h}_{k_3,T}(\eta)\times(-ik_{1i})(-ik_{2j})\frac{(1+ik_1\eta)}{2k_1^3}\frac{(1+ik_2\eta)}{2k_2^3}e^{-ik_{12}\eta}$$
$$=(+i)\times\frac{\psi_1(0)}{M_4}\times\frac{\mathcal{N}}{32k_1^4k_3}(\cos^2\theta-1/3)e^{i\pi/4}e^{-\pi\mu/2}\times$$
$$\int_0^\infty\frac{dx}{\sqrt{x}}\left[6x\left((2-i\mu)H^{(1)}_{i\mu-1}-(2+i\mu)H^{(1)}_{i\mu+1}\right)-(9-8x^2)H_{i\mu}\right](1-2ipx-p^2x^2)e^{2ipx}$$
$$=(+i)\times\frac{\psi_1(0)}{M_4}\times\frac{\mathcal{N}}{32k_1^4k_3}(\cos^2\theta-1/3)e^{i\pi/4}\times(T_1+T_2+T_3),$$

where

$$\begin{aligned}
T_1&=8\mathcal{F}(\frac{3}{2},2p,\mu)-9\mathcal{F}(-\frac{1}{2},2p,\mu)+\\
&\quad+6(2-i\mu)\mathcal{F}(\frac{1}{2},2p,\mu+i)(i)+6i(2+i\mu)\mathcal{F}(\frac{1}{2},2p,\mu-i),\\
T_2&=-2ip\left(8\mathcal{F}(\frac{5}{2},2p,\mu)-9\mathcal{F}(\frac{1}{2},2p,\mu)\right)+\\
&\quad(-2ip)\left(+6(2-i\mu)\mathcal{F}(\frac{3}{2},2p,\mu+i)(i)+6i(2+i\mu)\mathcal{F}(\frac{3}{2},2p,\mu-i)\right),\\
T_3&=-p^2\left(8\mathcal{F}(\frac{7}{2},2p,\mu)-9\mathcal{F}(\frac{3}{2},2p,\mu)\right)+\\
&\quad(-p^2)\left(+6(2-i\mu)\mathcal{F}(\frac{5}{2},2p,\mu+i)(i)+6i(2+i\mu)\mathcal{F}(\frac{5}{2},2p,\mu-i)\right),
\end{aligned}\tag{164}$$

and,

$$\mathcal{F}(n,p,\mu)\equiv e^{-\pi\mu/2}\int_0^\infty dx x^n e^{ipx}H^{(1)}_{i\mu}(x)$$
$$=\frac{(+i/2)^n}{\sqrt{\pi}\Gamma(n+3/2)}\Gamma(n+1-i\mu)\Gamma(n+1+i\mu){}_2F_1(n+1-i\mu,n+1+i\mu,n+3/2,\frac{1-p}{2}).$$

Using the asymptotic form of the hypergeometric function ${}_2F_1$ for large negative argument,

$$ {}_2F_1(a,b,c;z) = \frac{\Gamma(b-a)\Gamma(c)}{\Gamma(b)\Gamma(c-a)}(-z)^{-a} + \frac{\Gamma(c)\Gamma(a-b)}{\Gamma(a)\Gamma(c-b)}(-z)^{-b}, \tag{165} $$

we can simplify the anti-time ordered contribution to get,

$$ \text{Anti-time ordered contribution} = (+i) \times \frac{\psi_1(0)}{M_4}\frac{3}{128\sqrt{2}\pi}\frac{\mathcal{N}}{k_1^4 k_3}\frac{(\cos^2\theta - 1/3)}{(1+4\mu^2)} \times \left(A(\mu)\left(\frac{k_3}{k_1}\right)^{1/2+i\mu} + A(-\mu)\left(\frac{k_3}{k_1}\right)^{1/2-i\mu}\right), $$

where

$$ A(\mu) = (-27 + 120i\mu + 152\mu^2 - 32i\mu^3 + 16\mu^4)\Gamma(5/2+i\mu)\Gamma(-i\mu)2^{-2i\mu}. \tag{166} $$

Multiplying the time and anti-time ordered contributions we get,

$$ I_{-+} \;=\; \frac{\psi_1(0)^2\dot{\phi}_0}{M_4^2}\frac{\sqrt{\pi}(\cos^2\theta - \frac{1}{3})}{128 k_1^4 k_3^2 (1+4\mu^2)^2\cosh(\pi\mu)}\left(A(\mu)\left(\frac{k_3}{k_1}\right)^{1/2+i\mu} + (\mu \to -\mu)\right). \tag{167} $$

Next we have to take into account I_{+-}, I_{++} and I_{--}. However, I_{+-} and I_{--} are just complex conjugates of I_{-+} and I_{++} respectively, hence we need only I_{++}. Computing I_{++} analytically is difficult in general, however, in the squeezed limit $k_3 \ll k_1$ we can get the non-analytic terms in I_{--} by just making the variable change $k_1 \to -k_1$

and changing the overall sign, i.e. for non-analytic pieces [21],

$$I_{++}(k_1, k_3) = -I_{-+}(-k_1, k_3). \tag{168}$$

Using the above relation to sum over all diagrams and momenta gives finally (after reintroducing H),

$$F_{KK}^{\text{single}} = \frac{\psi_1(0)^2\dot{\phi}_0^2}{M_4^2H^2} \times (\cos^2\theta - \frac{1}{3})\frac{\sqrt{\pi}}{8(1+4\mu^2)^2\cosh(\pi\mu)}\times \left(A(\mu)(1+i\sinh\pi\mu)\left(\frac{k_3}{k_1}\right)^{3/2+i\mu} + (\mu\to-\mu)\right). \tag{169}$$

This can equivalently put into another form,

$$F_{KK}^{\text{single}} = \frac{4\psi_1(0)^2\dot{\phi}_0^2}{M_4^2H^2} \times (\cos^2\theta - \frac{1}{3})\frac{\sqrt{\pi}}{(1+4\mu^2)\cosh(\pi\mu)}\times \frac{\frac{9}{2}+i\mu}{-\frac{1}{2}-i\mu}\frac{\Gamma(5/2+i\mu)\Gamma(5/2-i\mu)\Gamma(-i\mu)}{\Gamma(1/2-i\mu)}(1+i\sinh\pi\mu)\left(\frac{k_3}{4k_1}\right)^{3/2+i\mu} + (\mu\to-\mu), \tag{170}$$

which agrees with the results of [21, 91] obtained via exploiting conformal symmetries of the late time slice.

C.1 Charged scalar loop

The three point function induced by an interaction of the type $g(\partial\phi)^2\mathcal{O}$, where $\mathcal{O}$ could be either an elementary or a composite operator, was calculated in [21]. This was done by evaluating the coefficients c_Δ and the scaling dimensions Δ which appear in the late-time limit (i.e. $\eta, \eta' \to 0$) of the position space two point correlation function:

$$\langle \mathcal{O}(\eta, \vec{x})\mathcal{O}(\eta', \vec{x}')\rangle = \sum_\Delta c_\Delta \left(\frac{\eta\eta'}{|\vec{x}-\vec{x}'|}\right)^\Delta . \tag{171}$$

Given c_Δ's for the set of Δ's, the three point function can be written as [21],

$$\langle \delta\phi(\vec{k}_1)\delta\phi(\vec{k}_2)\delta\phi(\vec{k}_3)\rangle' = -\frac{g^2\dot{\phi}_0}{2}\frac{1}{k_1^3 k_3^3}\sum_\Delta \frac{c_\Delta}{c_{\rm free}(\Delta)}\mathcal{F}\left(\Delta, \frac{k_3}{k_1}\right), \tag{172}$$

where

$$c_{\rm free}(\Delta) = \frac{1}{4\pi^{5/2}}\Gamma(3/2-\Delta)\Gamma(\Delta), \tag{173}$$

and

$$\mathcal{F}\left(\Delta, \frac{k_3}{k_1}\right) = \frac{4^{-\Delta+3/2}\pi^{3/2}}{4\cos(\pi(\Delta-3/2))^2}\frac{(1+\sin(\pi(\Delta-3/2)))\Delta(\Delta+1)\Gamma(3/2-\Delta)}{\Gamma(2-\Delta)}\left(\frac{k_3}{k_1}\right)^\Delta . \tag{174}$$

In this and the following appendix, we will work in the units where $H = 1$.

Now we are ready to give the three point function induced by a Higgs loop.

To get the associated c_Δ's we first write,

$$\langle \chi^\dagger \chi(\eta, \vec{x}) \cdot \chi^\dagger \chi(\eta', \vec{x}') \rangle = \langle \chi_1(\eta, \vec{x}) \chi_1(\eta', \vec{x}') \rangle^2, \tag{175}$$

where we have written $\chi = \frac{1}{\sqrt{2}}(\chi_1 + i\chi_2)$ and used the fact that $\langle \chi_1(\eta, \vec{x}) \chi_1(\eta', \vec{x}') \rangle = \langle \chi_2(\eta, \vec{x}) \chi_2(\eta', \vec{x}') \rangle$. Using the fact that the non-analytic pieces of the two point function are given by,

$$\langle \chi_1(\eta, \vec{x}) \chi_1(\eta', \vec{x}') \rangle^2|_{\eta,\eta' \to 0} = \frac{1}{16\pi^5} \left(\frac{\eta\eta'}{|\vec{x} - \vec{x}'|^2} \right)^{3+2i\mu} \Gamma(-i\mu)^2 \Gamma(3/2 + i\mu)^2 + \mu \to -\mu, \tag{176}$$

where $\mu = \sqrt{m_\chi^2 - 9/4}$, we see that the composite operator $\chi^\dagger \chi$ gives rise to scaling dimensions $\Delta = 3 \pm 2i\mu, 3$. More generally, in the squeezed limit, a loop diagram can be decomposed into a set of effective "tree" diagrams, each involving a dS mass eigenstate corresponding to such a scaling dimension Δ [21]. This is schematically shown in fig. 7. Thus from eqs. (171), (173) and (176), we will have,

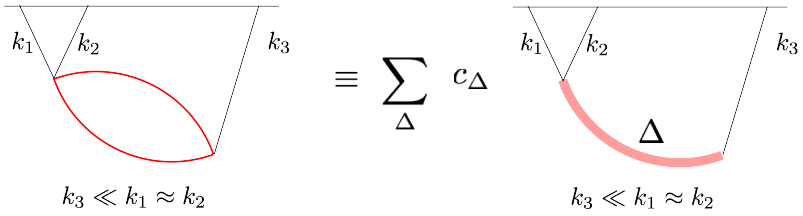

Figure 7: Reduction of a loop diagram into a linear combination of tree diagrams in the squeezed limit.

$$c_{3+2i\mu} = \frac{1}{16\pi^5} \Gamma(-i\mu)^2 \Gamma(3/2 + i\mu)^2, \tag{177}$$

$$c_{\text{free}}(3 + 2i\mu) = \frac{1}{4\pi^{5/2}} \Gamma(-3/2 - 2i\mu) \Gamma(3 + 2i\mu), \tag{178}$$

which can be used to get the inflaton three point function in eq. (172). We can quickly generalize this to the case of curvaton fluctuations by using eq. (4.64) to get,

$$\begin{aligned}
&\langle\delta\sigma(\vec{k}_1)\delta\sigma(\vec{k}_2)\delta\sigma(\vec{k}_3)\rangle' \\
&= -\frac{\dot{\sigma}_0}{2\Lambda_\sigma^4}\frac{1}{k_1^3k_3^3}\left(\frac{\frac{1}{16\pi^5}\Gamma(-i\mu)^2\Gamma(3/2+i\mu)^2}{\frac{1}{4\pi^{5/2}}\Gamma(-3/2-2i\mu)\Gamma(3+2i\mu)}\mathcal{F}\left(3+2i\mu,\frac{k_3}{k_1}\right)+\mu\to-\mu\right).
\end{aligned} \tag{179}$$

Using the above and eq. (4.22), we derive the dimensionless three point function of the curvature perturbation,

$$\begin{aligned}
F_{\chi,\text{loop}}\left(m_\chi,\frac{k_3}{k_1}\right) &= \frac{\langle\zeta(\vec{k}_1)\zeta(\vec{k}_2)\zeta(\vec{k}_3)\rangle'}{\langle\zeta(\vec{k}_1)\zeta(-\vec{k}_1)\rangle'\langle\zeta(\vec{k}_3)\zeta(-\vec{k}_3)\rangle'} \\
&= -\frac{3\sigma_0}{2}\frac{2\dot{\sigma}_0}{\Lambda_\sigma^4}\left(\frac{\frac{1}{16\pi^5}\Gamma(-i\mu)^2\Gamma(3/2+i\mu)^2}{\frac{1}{4\pi^{5/2}}\Gamma(-3/2-2i\mu)\Gamma(3+2i\mu)}\mathcal{F}\left(3+2i\mu,\frac{k_3}{k_1}\right)+\mu\to-\mu\right) \\
&\equiv |f_{\chi,\text{loop}}(\mu)|\left(e^{i\delta_2(\mu)}\left(\frac{k_3}{k_1}\right)^{3+2i\mu}+\mu\to-\mu\right).
\end{aligned} \tag{180}$$

C.2 Fermion loop

To calculate the NG induced by the coupling given in eq. (4.68), we need the late time two point function of the type $\langle\bar{\Psi}\Psi(\eta,\vec{x})\cdot\bar{\Psi}\Psi(\eta',\vec{x}')\rangle$. This can be calculated by squaring and taking a trace of the spinor two point function

$\langle\Psi(\eta,\vec{x})\bar{\Psi}(\eta',\vec{x}')\rangle$ derived in [152]. The result is,

$$\begin{aligned}&\langle\bar{\Psi}\Psi(\eta,\vec{x})\bar{\Psi}\Psi(\eta',\vec{x}')\rangle|_{\eta,\eta'\to 0}\\&=-\frac{3}{\pi^5}\left(\frac{\eta\eta'}{|\vec{x}-\vec{x}'|^2}\right)^{4+2i\mu}\frac{\Gamma(1/2-i\tilde{\mu})^2\Gamma(2+i\tilde{\mu})^2}{(1+2i\tilde{\mu})}+\tilde{\mu}\to-\tilde{\mu},\end{aligned}\tag{181}$$

where $\tilde{\mu}=m_\Psi$. This matches with the answer obtained in [141]. We thus get using eqs. (171) and (173),

$$c_{4+2i\tilde{\mu}}=-\frac{3}{\pi^5}\frac{\Gamma(1/2-i\tilde{\mu})^2\Gamma(2+i\tilde{\mu})^2}{(1+2i\tilde{\mu})},\tag{182}$$

$$c_{\rm free}(4+2i\tilde{\mu})=\frac{1}{4\pi^{5/2}}\Gamma(-5/2-2i\tilde{\mu})\Gamma(4+2i\tilde{\mu}).\tag{183}$$

Using eq. (4.68) we can get the three point function of the curvaton fluctuations,

$$\begin{aligned}&\langle\delta\sigma(\vec{k}_1)\delta\sigma(\vec{k}_2)\delta\sigma(\vec{k}_3)\rangle'\\&=-\frac{\dot{\sigma}_0}{2\Lambda_\sigma^6}\frac{1}{k_1^3k_3^3}\left(\frac{-\frac{3}{\pi^5}\frac{\Gamma(1/2-i\tilde{\mu})^2\Gamma(2+i\tilde{\mu})^2}{(1+2i\tilde{\mu})}}{\frac{1}{4\pi^{5/2}}\Gamma(-5/2-2i\tilde{\mu})\Gamma(4+2i\tilde{\mu})}\mathcal{F}\left(4+2i\tilde{\mu},\frac{k_3}{k_1}\right)+\tilde{\mu}\to-\tilde{\mu}\right).\end{aligned}\tag{184}$$

Using the above and eq. (4.22), the dimensionless bispectrum is given by,

$$\begin{aligned}&F_{\Psi,\rm loop}\left(m_\Psi,\frac{k_3}{k_1}\right)=\frac{\langle\zeta(\vec{k}_1)\zeta(\vec{k}_2)\zeta(\vec{k}_3)\rangle'}{\langle\zeta(\vec{k}_1)\zeta(-\vec{k}_1)\rangle'\langle\zeta(\vec{k}_3)\zeta(-\vec{k}_3)\rangle'}\\&=-\frac{3\sigma_0}{2}\frac{2\dot{\sigma}_0}{\Lambda_\sigma^6}\left(\frac{-\frac{3}{\pi^5}\frac{\Gamma(1/2-i\tilde{\mu})^2\Gamma(2+i\tilde{\mu})^2}{(1+2i\tilde{\mu})}}{\frac{1}{4\pi^{5/2}}\Gamma(-5/2-2i\tilde{\mu})\Gamma(4+2i\tilde{\mu})}\mathcal{F}\left(4+2i\tilde{\mu},\frac{k_3}{k_1}\right)+\tilde{\mu}\to-\tilde{\mu}\right)\\&\equiv|f_{\Psi,\rm loop}(\tilde{\mu})|\left(e^{i\delta_3(\tilde{\mu})}\left(\frac{k_3}{k_1}\right)^{4+2i\tilde{\mu}}+\tilde{\mu}\to-\tilde{\mu}\right).\end{aligned}\tag{185}$$

Bibliography

[1] Mary K. Gaillard, Paul D. Grannis, and Frank J. Sciulli. The Standard model of particle physics. *Rev. Mod. Phys.*, 71:S96–S111, 1999. doi:10.1103/RevModPhys.71.S96.

[2] N. Aghanim et al. Planck 2018 results. VI. Cosmological parameters. 7 2018.

[3] Y. Fukuda et al. Evidence for oscillation of atmospheric neutrinos. *Phys. Rev. Lett.*, 81:1562–1567, 1998. doi:10.1103/PhysRevLett.81.1562.

[4] Georges Aad et al. Observation of a new particle in the search for the Standard Model Higgs boson with the ATLAS detector at the LHC. *Phys. Lett. B*, 716: 1–29, 2012. doi:10.1016/j.physletb.2012.08.020.

[5] Serguei Chatrchyan et al. Observation of a New Boson at a Mass of 125 GeV with the CMS Experiment at the LHC. *Phys. Lett. B*, 716:30–61, 2012. doi:10.1016/j.physletb.2012.08.021.

[6] M. Tanabashi et al. Review of Particle Physics. *Phys. Rev.*, D98(3):030001, 2018. doi:10.1103/PhysRevD.98.030001.

[7] Apollinari G., Béjar Alonso I., Brüning O., Fessia P., Lamont M., Rossi L., and Tavian L. *High-Luminosity Large Hadron Collider (HL-LHC): Technical Design Report V. 0.1*. CERN Yellow Reports: Monographs. CERN, Geneva, 2017. doi:10.23731/CYRM-2017-004. URL `https://cds.cern.ch/record/2284929`.

[8] Y. Akrami et al. Planck 2018 results. X. Constraints on inflation. 2018.

[9] Marcelo Alvarez et al. Testing Inflation with Large Scale Structure: Connecting Hopes with Reality. 2014.

[10] Julian B. Muñoz, Yacine Ali-Haïmoud, and Marc Kamionkowski. Primordial non-gaussianity from the bispectrum of 21-cm fluctuations in the dark ages. *Phys. Rev. D*, 92(8):083508, 2015. doi:10.1103/PhysRevD.92.083508.

[11] P. Daniel Meerburg, Moritz Munchmeyer, Julian B. Muñoz, and Xingang Chen. Prospects for Cosmological Collider Physics. *JCAP*, 1703(03):050, 2017. doi:10.1088/1475-7516/2017/03/050.

[12] Alan H. Guth. The Inflationary Universe: A Possible Solution to the Horizon and Flatness Problems. *Adv. Ser. Astrophys. Cosmol.*, 3:139–148, 1987. doi:10.1103/PhysRevD.23.347.

[13] Andrei D. Linde. A New Inflationary Universe Scenario: A Possible Solution of the Horizon, Flatness, Homogeneity, Isotropy and Primordial Monopole Problems. *Adv. Ser. Astrophys. Cosmol.*, 3:149–153, 1987. doi:10.1016/0370-2693(82)91219-9.

[14] Andreas Albrecht and Paul J. Steinhardt. Cosmology for Grand Unified Theories with Radiatively Induced Symmetry Breaking. *Adv. Ser. Astrophys. Cosmol.*, 3:158–161, 1987. doi:10.1103/PhysRevLett.48.1220.

[15] Daniel Baumann. Inflation. In *Physics of the large and the small, TASI 09, proceedings of the Theoretical Advanced Study Institute in Elementary Particle Physics, Boulder, Colorado, USA, 1-26 June 2009*, pages 523–686, 2011. doi:10.1142/9789814327183_0010.

[16] Juan Martin Maldacena. The Large N limit of superconformal field theories and supergravity. *Int. J. Theor. Phys.*, 38:1113–1133, 1999. doi:10.1023/A:1026654312961, 10.4310/ATMP.1998.v2.n2.a1. [Adv. Theor. Math. Phys.2,231(1998)].

[17] Xingang Chen and Yi Wang. Large non-Gaussianities with Intermediate Shapes from Quasi-Single Field Inflation. *Phys. Rev. D*, 81:063511, 2010. doi:10.1103/PhysRevD.81.063511.

[18] Xingang Chen and Yi Wang. Quasi-Single Field Inflation and Non-Gaussianities. *JCAP*, 1004:027, 2010. doi:10.1088/1475-7516/2010/04/027.

[19] Daniel Baumann and Daniel Green. Signatures of Supersymmetry from the Early Universe. *Phys. Rev.*, D85:103520, 2012. doi:10.1103/PhysRevD.85.103520.

[20] Toshifumi Noumi, Masahide Yamaguchi, and Daisuke Yokoyama. Effective field theory approach to quasi-single field inflation and effects of heavy fields. *JHEP*, 06:051, 2013. doi:10.1007/JHEP06(2013)051.

[21] Nima Arkani-Hamed and Juan Maldacena. Cosmological Collider Physics. 2015.

[22] N. Bartolo, S. Matarrese, and A. Riotto. Non-Gaussianity and the Cosmic Microwave Background Anisotropies. *Adv. Astron.*, 2010:157079, 2010. doi:10.1155/2010/157079.

[23] Abraham Loeb and Matias Zaldarriaga. Measuring the small - scale power spectrum of cosmic density fluctuations through 21 cm tomography prior to the epoch of structure formation. *Phys. Rev. Lett.*, 92:211301, 2004. doi:10.1103/PhysRevLett.92.211301.

[24] Soubhik Kumar and Raman Sundrum. Heavy-Lifting of Gauge Theories By Cosmic Inflation. *JHEP*, 05:011, 2018. doi:10.1007/JHEP05(2018)011.

[25] Soubhik Kumar and Raman Sundrum. Seeing Higher-Dimensional Grand Unification In Primordial Non-Gaussianities. *JHEP*, 04:120, 2019. doi:10.1007/JHEP04(2019)120.

[26] Soubhik Kumar and Raman Sundrum. Cosmological Collider Physics and the Curvaton. *JHEP*, 04:077, 2020. doi:10.1007/JHEP04(2020)077.

[27] Y. Akrami et al. Planck 2018 results. IX. Constraints on primordial non-Gaussianity. 2019.

[28] Michele Liguori, Emiliano Sefusatti, James R. Fergusson, and E.P.S. Shellard. Primordial non-Gaussianity and Bispectrum Measurements in the Cosmic Microwave Background and Large-Scale Structure. *Adv. Astron.*, 2010:980523, 2010. doi:10.1155/2010/980523.

[29] Juan Martin Maldacena. Non-Gaussian features of primordial fluctuations in single field inflationary models. *JHEP*, 05:013, 2003. doi:10.1088/1126-6708/2003/05/013.

[30] Viviana Acquaviva, Nicola Bartolo, Sabino Matarrese, and Antonio Riotto. Second order cosmological perturbations from inflation. *Nucl. Phys. B*, 667: 119–148, 2003. doi:10.1016/S0550-3213(03)00550-9.

[31] N. Bartolo, E. Komatsu, Sabino Matarrese, and A. Riotto. Non-Gaussianity from inflation: Theory and observations. *Phys. Rept.*, 402:103–266, 2004. doi:10.1016/j.physrep.2004.08.022.

[32] Xingang Chen. Primordial Non-Gaussianities from Inflation Models. *Adv. Astron.*, 2010:638979, 2010. doi:10.1155/2010/638979.

[33] D.S. Salopek and J.R. Bond. Nonlinear evolution of long wavelength metric fluctuations in inflationary models. *Phys. Rev. D*, 42:3936–3962, 1990. doi:10.1103/PhysRevD.42.3936.

[34] Eiichiro Komatsu and David N. Spergel. Acoustic signatures in the primary microwave background bispectrum. *Phys. Rev. D*, 63:063002, 2001. doi:10.1103/PhysRevD.63.063002.

[35] P. A. R. Ade et al. Planck 2015 results. XVII. Constraints on primordial non-Gaussianity. *Astron. Astrophys.*, 594:A17, 2016. doi:10.1051/0004-6361/201525836.

[36] Xingang Chen and Yi Wang. Quasi-Single Field Inflation with Large Mass. *JCAP*, 1209:021, 2012. doi:10.1088/1475-7516/2012/09/021.

[37] Valentin Assassi, Daniel Baumann, and Daniel Green. On Soft Limits of Inflationary Correlation Functions. *JCAP*, 1211:047, 2012. doi:10.1088/1475-7516/2012/11/047.

[38] Emanuela Dimastrogiovanni, Matteo Fasiello, and Marc Kamionkowski. Imprints of Massive Primordial Fields on Large-Scale Structure. *JCAP*, 1602: 017, 2016. doi:10.1088/1475-7516/2016/02/017.

[39] Paolo Creminelli. On non-Gaussianities in single-field inflation. *JCAP*, 0310: 003, 2003. doi:10.1088/1475-7516/2003/10/003.

[40] Hayden Lee, Daniel Baumann, and Guilherme L. Pimentel. Non-Gaussianity as a Particle Detector. *JHEP*, 12:040, 2016. doi:10.1007/JHEP12(2016)040.

[41] Azadeh Moradinezhad Dizgah and Cora Dvorkin. Scale-Dependent Galaxy Bias from Massive Particles with Spin during Inflation. *JCAP*, 1801(01):010, 2018. doi:10.1088/1475-7516/2018/01/010.

[42] Fedor L. Bezrukov and Mikhail Shaposhnikov. The Standard Model Higgs boson as the inflaton. *Phys. Lett. B*, 659:703–706, 2008. doi:10.1016/j.physletb.2007.11.072.

[43] Xingang Chen, Yi Wang, and Zhong-Zhi Xianyu. Standard Model Background of the Cosmological Collider. *Phys. Rev. Lett.*, 118(26):261302, 2017. doi:10.1103/PhysRevLett.118.261302.

[44] Xingang Chen, Yi Wang, and Zhong-Zhi Xianyu. Standard Model Mass Spectrum in Inflationary Universe. *JHEP*, 04:058, 2017. doi:10.1007/JHEP04(2017)058.

[45] P.A.R. Ade et al. Planck 2015 results. XX. Constraints on inflation. *Astron. Astrophys.*, 594:A20, 2016. doi:10.1051/0004-6361/201525898.

[46] Neal Weiner. Unification without Unification. 2001.

[47] Csaba Csaki, Graham D. Kribs, and John Terning. 4-D models of Scherk-Schwarz GUT breaking via deconstruction. *Phys. Rev.*, D65:015004, 2002. doi:10.1103/PhysRevD.65.015004.

[48] J.R. Espinosa, G.F. Giudice, and A. Riotto. Cosmological implications of the Higgs mass measurement. *JCAP*, 05:002, 2008. doi:10.1088/1475-7516/2008/05/002.

[49] Matti Herranen, Tommi Markkanen, Sami Nurmi, and Arttu Rajantie. Spacetime curvature and the Higgs stability during inflation. *Phys. Rev. Lett.*, 113 (21):211102, 2014. doi:10.1103/PhysRevLett.113.211102.

[50] Dario Buttazzo, Giuseppe Degrassi, Pier Paolo Giardino, Gian F. Giudice, Filippo Sala, Alberto Salvio, and Alessandro Strumia. Investigating the near-criticality of the Higgs boson. *JHEP*, 12:089, 2013. doi:10.1007/JHEP12(2013)089.

[51] Malcolm Fairbairn and Robert Hogan. Electroweak Vacuum Stability in light of BICEP2. *Phys. Rev. Lett.*, 112:201801, 2014. doi:10.1103/PhysRevLett.112.201801.

[52] Archil Kobakhidze and Alexander Spencer-Smith. Electroweak Vacuum (In)Stability in an Inflationary Universe. *Phys. Lett. B*, 722:130–134, 2013. doi:10.1016/j.physletb.2013.04.013.

[53] John Kearney, Hojin Yoo, and Kathryn M. Zurek. Is a Higgs Vacuum Instability Fatal for High-Scale Inflation? *Phys. Rev. D*, 91(12):123537, 2015. doi:10.1103/PhysRevD.91.123537.

[54] Jose R. Espinosa, Gian F. Giudice, Enrico Morgante, Antonio Riotto, Leonardo Senatore, Alessandro Strumia, and Nikolaos Tetradis. The cosmological Higgstory of the vacuum instability. *JHEP*, 09:174, 2015. doi:10.1007/JHEP09(2015)174.

[55] C.P. Burgess, Maxim Pospelov, and Tonnis ter Veldhuis. The Minimal model of nonbaryonic dark matter: A Singlet scalar. *Nucl. Phys. B*, 619:709–728, 2001. doi:10.1016/S0550-3213(01)00513-2.

[56] Matthew Gonderinger, Yingchuan Li, Hiren Patel, and Michael J. Ramsey-Musolf. Vacuum Stability, Perturbativity, and Scalar Singlet Dark Matter. *JHEP*, 01:053, 2010. doi:10.1007/JHEP01(2010)053.

[57] Clifford Cheung, Michele Papucci, and Kathryn M. Zurek. Higgs and Dark Matter Hints of an Oasis in the Desert. *JHEP*, 07:105, 2012. doi:10.1007/JHEP07(2012)105.

[58] Mario Kadastik, Kristjan Kannike, Antonio Racioppi, and Martti Raidal. Implications of the 125 GeV Higgs boson for scalar dark matter and for the CMSSM phenomenology. *JHEP*, 05:061, 2012. doi:10.1007/JHEP05(2012)061.

[59] Steven Weinberg. Anthropic Bound on the Cosmological Constant. *Phys. Rev. Lett.*, 59:2607, 1987. doi:10.1103/PhysRevLett.59.2607.

[60] V. Agrawal, Stephen M. Barr, John F. Donoghue, and D. Seckel. Viable range of the mass scale of the standard model. *Phys. Rev. D*, 57:5480–5492, 1998. doi:10.1103/PhysRevD.57.5480.

[61] Nathaniel Craig and Daniel Green. Testing Split Supersymmetry with Inflation. *JHEP*, 07:102, 2014. doi:10.1007/JHEP07(2014)102.

[62] Clifford Cheung, Paolo Creminelli, A. Liam Fitzpatrick, Jared Kaplan, and Leonardo Senatore. The Effective Field Theory of Inflation. *JHEP*, 03:014, 2008. doi:10.1088/1126-6708/2008/03/014.

[63] Steven Weinberg. Quantum contributions to cosmological correlations. *Phys. Rev.*, D72:043514, 2005. doi:10.1103/PhysRevD.72.043514.

[64] Steven Weinberg. *Cosmology, Oxford, UK: Oxford Univ. Pr. (2008) 593 p.* 2008. ISBN 9780198526827. URL http://www.oup.com/uk/catalogue/?ci=9780198526827.

[65] Steven Weinberg. Effective Field Theory for Inflation. *Phys. Rev. D*, 77: 123541, 2008. doi:10.1103/PhysRevD.77.123541.

[66] David Wands, Karim A. Malik, David H. Lyth, and Andrew R. Liddle. A New approach to the evolution of cosmological perturbations on large scales. *Phys. Rev.*, D62:043527, 2000. doi:10.1103/PhysRevD.62.043527.

[67] Steven Weinberg. Adiabatic modes in cosmology. *Phys. Rev.*, D67:123504, 2003. doi:10.1103/PhysRevD.67.123504.

[68] Leonardo Senatore and Matias Zaldarriaga. The constancy of ζ in single-clock Inflation at all loops. *JHEP*, 09:148, 2013. doi:10.1007/JHEP09(2013)148.

[69] Valentin Assassi, Daniel Baumann, and Daniel Green. Symmetries and Loops in Inflation. *JHEP*, 02:151, 2013. doi:10.1007/JHEP02(2013)151.

[70] Paolo Creminelli and Matias Zaldarriaga. Single field consistency relation for the 3-point function. *JCAP*, 0410:006, 2004. doi:10.1088/1475-7516/2004/10/006.

[71] Paolo Creminelli, Guido D'Amico, Marcello Musso, and Jorge Norena. The (not so) squeezed limit of the primordial 3-point function. *JCAP*, 11:038, 2011. doi:10.1088/1475-7516/2011/11/038.

[72] Christian T. Byrnes and Ki-Young Choi. Review of local non-Gaussianity from multi-field inflation. *Adv. Astron.*, 2010:724525, 2010. doi:10.1155/2010/724525.

[73] C.P. Burgess, L. Leblond, R. Holman, and S. Shandera. Super-Hubble de Sitter Fluctuations and the Dynamical RG. *JCAP*, 03:033, 2010. doi:10.1088/1475-7516/2010/03/033.

[74] Xingang Chen, Yi Wang, and Zhong-Zhi Xianyu. Loop Corrections to Standard Model Fields in Inflation. *JHEP*, 08:051, 2016. doi:10.1007/JHEP08(2016)051.

[75] Robert M. Wald. *General Relativity*. Chicago Univ. Pr., Chicago, USA, 1984. doi:10.7208/chicago/9780226870373.001.0001.

[76] Paolo Creminelli, Alberto Nicolis, Leonardo Senatore, Max Tegmark, and Matias Zaldarriaga. Limits on non-gaussianities from wmap data. *JCAP*, 05:004, 2006. doi:10.1088/1475-7516/2006/05/004.

[77] Daniel Babich, Paolo Creminelli, and Matias Zaldarriaga. The Shape of non-Gaussianities. *JCAP*, 08:009, 2004. doi:10.1088/1475-7516/2004/08/009.

[78] Xingang Chen, Yi Wang, and Zhong-Zhi Xianyu. Schwinger-Keldysh Diagrammatics for Primordial Perturbations. *JCAP*, 1712(12):006, 2017. doi:10.1088/1475-7516/2017/12/006.

[79] Mohsen Alishahiha, Eva Silverstein, and David Tong. DBI in the sky. *Phys. Rev.*, D70:123505, 2004. doi:10.1103/PhysRevD.70.123505.

[80] Xingang Chen, Min-xin Huang, Shamit Kachru, and Gary Shiu. Observational signatures and non-Gaussianities of general single field inflation. *JCAP*, 01: 002, 2007. doi:10.1088/1475-7516/2007/01/002.

[81] K. Abe et al. Search for proton decay via $p \to e^+\pi^0$ and $p \to \mu^+\pi^0$ in 0.31 megaton.years exposure of the Super-Kamiokande water Cherenkov detector. *Phys. Rev.*, D95(1):012004, 2017. doi:10.1103/PhysRevD.95.012004.

[82] Pran Nath and Pavel Fileviez Perez. Proton stability in grand unified theories, in strings and in branes. *Phys. Rept.*, 441:191–317, 2007. doi:10.1016/j.physrep.2007.02.010.

[83] Yoshiharu Kawamura. Gauge symmetry breaking from extra space S**1 / Z(2). *Prog. Theor. Phys.*, 103:613–619, 2000. doi:10.1143/PTP.103.613.

[84] Yoshiharu Kawamura. Triplet doublet splitting, proton stability and extra dimension. *Prog. Theor. Phys.*, 105:999–1006, 2001. doi:10.1143/PTP.105.999.

[85] Lawrence J. Hall and Yasunori Nomura. Grand unification in higher dimensions. *Annals Phys.*, 306:132–156, 2003. doi:10.1016/S0003-4916(03)00077-0. [,432(2002)].

[86] Lawrence J. Hall and Yasunori Nomura. Gauge unification in higher dimensions. *Phys. Rev.*, D64:055003, 2001. doi:10.1103/PhysRevD.64.055003.

[87] Alex Kehagias and Antonio Riotto. On the Inflationary Perturbations of Massive Higher-Spin Fields. *JCAP*, 1707(07):046, 2017. doi:10.1088/1475-7516/2017/07/046.

[88] Haipeng An, Michael McAneny, Alexander K. Ridgway, and Mark B. Wise. Quasi Single Field Inflation in the non-perturbative regime. *JHEP*, 06:105, 2018. doi:10.1007/JHEP06(2018)105.

[89] Daniel Baumann, Garrett Goon, Hayden Lee, and Guilherme L. Pimentel. Partially Massless Fields During Inflation. *JHEP*, 04:140, 2018. doi:10.1007/JHEP04(2018)140.

[90] Gabriele Franciolini, Alex Kehagias, and Antonio Riotto. Imprints of Spinning Particles on Primordial Cosmological Perturbations. *JCAP*, 1802(02): 023, 2018. doi:10.1088/1475-7516/2018/02/023.

[91] Nima Arkani-Hamed, Daniel Baumann, Hayden Lee, and Guilherme L. Pimentel. The Cosmological Bootstrap: Inflationary Correlators from Symmetries and Singularities. *JHEP*, 04:105, 2020. doi:10.1007/JHEP04(2020)105.

[92] Nicola Bartolo, Alex Kehagias, Michele Liguori, Antonio Riotto, Maresuke Shiraishi, and Vittorio Tansella. Detecting higher spin fields through statistical anisotropy in the CMB and galaxy power spectra. *Phys. Rev.*, D97(2):023503, 2018. doi:10.1103/PhysRevD.97.023503.

[93] Gabriele Franciolini, Alex Kehagias, Antonio Riotto, and Maresuke Shiraishi. Detecting higher spin fields through statistical anisotropy in the CMB bispectrum. *Phys. Rev.*, D98(4):043533, 2018. doi:10.1103/PhysRevD.98.043533.

[94] Fabian Schmidt, Nora Elisa Chisari, and Cora Dvorkin. Imprint of inflation on galaxy shape correlations. *JCAP*, 1510(10):032, 2015. doi:10.1088/1475-7516/2015/10/032.

[95] Nora Elisa Chisari, Cora Dvorkin, Fabian Schmidt, and David Spergel. Multitracing Anisotropic Non-Gaussianity with Galaxy Shapes. *Phys. Rev.*, D94 (12):123507, 2016. doi:10.1103/PhysRevD.94.123507.

[96] Jérôme Gleyzes, Roland de Putter, Daniel Green, and Olivier Dorè. Biasing and the search for primordial non-Gaussianity beyond the local type. *JCAP*, 1704(04):002, 2017. doi:10.1088/1475-7516/2017/04/002.

[97] Azadeh Moradinezhad Dizgah, Hayden Lee, Julian B. Muñoz, and Cora Dvorkin. Galaxy Bispectrum from Massive Spinning Particles. *JCAP*, 1805 (05):013, 2018. doi:10.1088/1475-7516/2018/05/013.

[98] Azadeh Moradinezhad Dizgah, Gabriele Franciolini, Alex Kehagias, and Antonio Riotto. Constraints on long-lived, higher-spin particles from galaxy bispectrum. *Phys. Rev.*, D98(6):063520, 2018. doi:10.1103/PhysRevD.98.063520.

[99] Giovanni Cabass, Enrico Pajer, and Fabian Schmidt. Imprints of Oscillatory Bispectra on Galaxy Clustering. *JCAP*, 1809(09):003, 2018. doi:10.1088/1475-7516/2018/09/003.

[100] Kazuhiro Kogai, Takahiko Matsubara, Atsushi J. Nishizawa, and Yuko Urakawa. Intrinsic galaxy alignment from angular dependent primordial non-Gaussianity. *JCAP*, 1808(08):014, 2018. doi:10.1088/1475-7516/2018/08/014.

[101] Matteo Biagetti, Emanuela Dimastrogiovanni, and Matteo Fasiello. Possible signatures of the inflationary particle content: spin-2 fields. *JCAP*, 1710(10): 038, 2017. doi:10.1088/1475-7516/2017/10/038.

[102] Haipeng An, Michael McAneny, Alexander K. Ridgway, and Mark B. Wise. Non-Gaussian Enhancements of Galactic Halo Correlations in Quasi-Single Field Inflation. *Phys. Rev.*, D97(12):123528, 2018. doi:10.1103/PhysRevD.97.123528.

[103] Yi Wang, Yi-Peng Wu, Jun'ichi Yokoyama, and Siyi Zhou. Hybrid Quasi-Single Field Inflation. *JCAP*, 1807(07):068, 2018. doi:10.1088/1475-7516/2018/07/068.

[104] Xingang Chen, Yi Wang, and Zhong-Zhi Xianyu. Neutrino Signatures in Primordial Non-Gaussianities. *JHEP*, 09:022, 2018. doi:10.1007/JHEP09(2018)022.

[105] Haipeng An, Mark B. Wise, and Zipei Zhang. De Sitter Quantum Loops as the origin of Primordial Non-Gaussianities. *Phys. Rev. D*, 99(5):056007, 2019. doi:10.1103/PhysRevD.99.056007.

[106] Xingang Chen, Abraham Loeb, and Zhong-Zhi Xianyu. Unique Fingerprints of Alternatives to Inflation in the Primordial Power Spectrum. *Phys. Rev. Lett.*, 122(12):121301, 2019. doi:10.1103/PhysRevLett.122.121301.

[107] A. Vilenkin. Gravitational Field of Vacuum Domain Walls. *Phys. Lett.*, 133B: 177–179, 1983. doi:10.1016/0370-2693(83)90554-3.

[108] J. Ipser and P. Sikivie. The Gravitationally Repulsive Domain Wall. *Phys. Rev.*, D30:712, 1984. doi:10.1103/PhysRevD.30.712.

[109] Nemanja Kaloper and Andrei D. Linde. Inflation and large internal dimensions. *Phys. Rev.*, D59:101303, 1999. doi:10.1103/PhysRevD.59.101303.

[110] Nemanja Kaloper. Bent domain walls as brane worlds. *Phys. Rev.*, D60: 123506, 1999. doi:10.1103/PhysRevD.60.123506.

[111] Lisa Randall and Raman Sundrum. An Alternative to compactification. *Phys. Rev. Lett.*, 83:4690–4693, 1999. doi:10.1103/PhysRevLett.83.4690.

[112] Takeshi Nihei. Inflation in the five-dimensional universe with an orbifold extra dimension. *Phys. Lett.*, B465:81–85, 1999. doi:10.1016/S0370-2693(99)01085-0.

[113] Hang Bae Kim and Hyung Do Kim. Inflation and gauge hierarchy in Randall-Sundrum compactification. *Phys. Rev.*, D61:064003, 2000. doi:10.1103/PhysRevD.61.064003.

[114] Donald Marolf, Mukund Rangamani, and Mark Van Raamsdonk. Holographic models of de Sitter QFTs. *Class. Quant. Grav.*, 28:105015, 2011. doi:10.1088/0264-9381/28/10/105015.

[115] G. W. Gibbons and S. W. Hawking. Cosmological Event Horizons, Thermodynamics, and Particle Creation. *Phys. Rev.*, D15:2738–2751, 1977. doi:10.1103/PhysRevD.15.2738.

[116] Lisa Randall and Raman Sundrum. A Large mass hierarchy from a small extra dimension. *Phys. Rev. Lett.*, 83:3370–3373, 1999. doi:10.1103/PhysRevLett.83.3370.

[117] Walter D. Goldberger and Mark B. Wise. Modulus stabilization with bulk fields. *Phys. Rev. Lett.*, 83:4922–4925, 1999. doi:10.1103/PhysRevLett.83.4922.

[118] Atsushi Higuchi. Forbidden Mass Range for Spin-2 Field Theory in De Sitter Space-time. *Nucl. Phys.*, B282:397–436, 1987. doi:10.1016/0550-3213(87)90691-2.

[119] Andre Lukas, Burt A. Ovrut, and Daniel Waldram. Boundary inflation. *Phys. Rev.*, D61:023506, 2000. doi:10.1103/PhysRevD.61.023506.

[120] Roy Maartens, David Wands, Bruce A. Bassett, and Imogen Heard. Chaotic inflation on the brane. *Phys. Rev.*, D62:041301, 2000. doi:10.1103/PhysRevD.62.041301.

[121] Gian F. Giudice, Edward W. Kolb, Julien Lesgourgues, and Antonio Riotto. Transdimensional Physics and Inflation. *Phys. Rev.*, D66:083512, 2002. doi:10.1103/PhysRevD.66.083512.

[122] Sang Hui Im, Hans Peter Nilles, and Andreas Trautner. Exploring extra dimensions through inflationary tensor modes. *JHEP*, 03:004, 2018. doi:10.1007/JHEP03(2018)004.

[123] Jaume Garriga and Misao Sasaki. Brane world creation and black holes. *Phys. Rev.*, D62:043523, 2000. doi:10.1103/PhysRevD.62.043523.

[124] David Langlois, Roy Maartens, and David Wands. Gravitational waves from inflation on the brane. *Phys. Lett.*, B489:259–267, 2000. doi:10.1016/S0370-2693(00)00957-6.

[125] Andreas Karch and Lisa Randall. Locally localized gravity. *JHEP*, 05:008, 2001. doi:10.1088/1126-6708/2001/05/008. [,140(2000)].

[126] Lorenzo Bordin, Paolo Creminelli, Andrei Khmelnitsky, and Leonardo Senatore. Light Particles with Spin in Inflation. *JCAP*, 1810(10):013, 2018. doi:10.1088/1475-7516/2018/10/013.

[127] Csaba Csaki, Michael L. Graesser, and Graham D. Kribs. Radion dynamics and electroweak physics. *Phys. Rev.*, D63:065002, 2001. doi:10.1103/PhysRevD.63.065002.

[128] Andrei V. Frolov and Lev Kofman. Can inflating brane worlds be stabilized? *Phys. Rev.*, D69:044021, 2004. doi:10.1103/PhysRevD.69.044021.

[129] Uchida Gen and Misao Sasaki. Radion on the de Sitter brane. *Prog. Theor. Phys.*, 105:591–606, 2001. doi:10.1143/PTP.105.591.

[130] Pierre Binetruy, Cedric Deffayet, and David Langlois. The Radion in brane cosmology. *Nucl. Phys.*, B615:219–236, 2001. doi:10.1016/S0550-3213(01)00426-6.

[131] Z. Chacko and Patrick J. Fox. Wave function of the radion in the dS and AdS brane worlds. *Phys. Rev.*, D64:024015, 2001. doi:10.1103/PhysRevD.64.024015.

[132] Zackaria Chacko, Rashmish K. Mishra, and Daniel Stolarski. Dynamics of a Stabilized Radion and Duality. *JHEP*, 09:121, 2013. doi:10.1007/JHEP09(2013)121.

[133] O. DeWolfe, D. Z. Freedman, S. S. Gubser, and A. Karch. Modeling the fifth-dimension with scalars and gravity. *Phys. Rev.*, D62:046008, 2000. doi:10.1103/PhysRevD.62.046008.

[134] Raman Sundrum. Tasi 2004 lectures: To the fifth dimension and back. In *Theoretical Advanced Study Institute in Elementary Particle Physics: Many Dimensions of String Theory (TASI 2005) Boulder, Colorado, June 5-July 1, 2005*, pages 585–630, 2005. [,585(2005)].

[135] Anson Hook, Junwu Huang, and Davide Racco. Minimal signatures of the Standard Model in non-Gaussianities. *Phys. Rev. D*, 101(2):023519, 2020. doi:10.1103/PhysRevD.101.023519.

[136] Anson Hook, Junwu Huang, and Davide Racco. Searches for other vacua. Part II. A new Higgstory at the cosmological collider. *JHEP*, 01:105, 2020. doi:10.1007/JHEP01(2020)105.

[137] Daniel Baumann and Daniel Green. Equilateral Non-Gaussianity and New Physics on the Horizon. *JCAP*, 1109:014, 2011. doi:10.1088/1475-7516/2011/09/014.

[138] Kari Enqvist and Martin S. Sloth. Adiabatic CMB perturbations in pre - big bang string cosmology. *Nucl. Phys.*, B626:395–409, 2002. doi:10.1016/S0550-3213(02)00043-3.

[139] David H. Lyth and David Wands. Generating the curvature perturbation without an inflaton. *Phys. Lett.*, B524:5–14, 2002. doi:10.1016/S0370-2693(01)01366-1.

[140] Takeo Moroi and Tomo Takahashi. Effects of cosmological moduli fields on cosmic microwave background. *Phys. Lett.*, B522:215–221, 2001. doi:10.1016/S0370-2693(02)02070-1, 10.1016/S0370-2693(01)01295-3. [Erratum: Phys. Lett.B539,303(2002)].

[141] Shiyun Lu, Yi Wang, and Zhong-Zhi Xianyu. A Cosmological Higgs Collider. *JHEP*, 02:011, 2020. doi:10.1007/JHEP02(2020)011.

[142] David H. Lyth, Carlo Ungarelli, and David Wands. The Primordial density perturbation in the curvaton scenario. *Phys. Rev.*, D67:023503, 2003. doi:10.1103/PhysRevD.67.023503.

[143] David H. Lyth and Yeinzon Rodriguez. The Inflationary prediction for primordial non-Gaussianity. *Phys. Rev. Lett.*, 95:121302, 2005. doi:10.1103/PhysRevLett.95.121302.

[144] N. Bartolo, S. Matarrese, and A. Riotto. On nonGaussianity in the curvaton scenario. *Phys. Rev.*, D69:043503, 2004. doi:10.1103/PhysRevD.69.043503.

[145] Misao Sasaki, Jussi Valiviita, and David Wands. Non-Gaussianity of the primordial perturbation in the curvaton model. *Phys. Rev.*, D74:103003, 2006. doi:10.1103/PhysRevD.74.103003.

[146] Jihn E. Kim, Hans Peter Nilles, and Marco Peloso. Completing natural inflation. *JCAP*, 0501:005, 2005. doi:10.1088/1475-7516/2005/01/005.

[147] Kiwoon Choi, Hyungjin Kim, and Seokhoon Yun. Natural inflation with multiple sub-Planckian axions. *Phys. Rev.*, D90:023545, 2014. doi:10.1103/PhysRevD.90.023545.

[148] S. H. Henry Tye and Sam S. C. Wong. Helical Inflation and Cosmic Strings. 2014.

[149] Ido Ben-Dayan, Francisco Gil Pedro, and Alexander Westphal. Hierarchical Axion Inflation. *Phys. Rev. Lett.*, 113:261301, 2014. doi:10.1103/PhysRevLett.113.261301.

[150] Yang Bai and Ben A. Stefanek. Natural millicharged inflation. *Phys. Rev.*, D91(9):096012, 2015. doi:10.1103/PhysRevD.91.096012.

[151] Anton de la Fuente, Prashant Saraswat, and Raman Sundrum. Natural Inflation and Quantum Gravity. *Phys. Rev. Lett.*, 114(15):151303, 2015. doi:10.1103/PhysRevLett.114.151303.

[152] B. Allen and C. A. Lütken. Spinor two-point functions in maximally symmetric spaces. *Comm. Math. Phys.*, 106(2):201–210, 1986. URL https://projecteuclid.org:443/euclid.cmp/1104115697.